

CHEMOPREVENTIVE EFFECTS OF ROOT BARK EXTRACT OF *C. PORTORICENSIS* (BENTH.) IN *N-NITROSO-N-METHYLUREA* AND BENZO(A)PYRENE-INDUCED MAMMARY GLAND AND REPRODUCTIVE TOXICITY IN *WISTAR* RATS

BY

ADEFISAN, ADEDOYIN OMOBOLANLE

MATRIC NO: 168161

B.Sc Biochemistry (Ilorin), M.Sc. Biochemistry (Ibadan),

A thesis in the Department of Biochemistry,

Submitted to the Faculty of Basic Medical Sciences,

in partial fulfilment of the requirements for the Degree of

DOCTOR OF PHILOSOPHY

Of the

UNIVERSITY OF IBADAN

FEBRUARY, 2023

Certification Page

I certify that this work was carried out by Miss A.O Adefisan in the Department of Biochemistry, University of Ibadan.

.....
Supervisor

O.A. Adaramoye,

B.Sc (Ilorin), M.Sc (Ibadan), Ph.D. (Ibadan)

Professor, Department of Biochemistry,

University of Ibadan, Nigeria.

DEDICATION

The Almighty God and my loved ones are the inspiration for this research project.

ACKNOWLEDGEMENTS

My deepest thanks and appreciation goes out to the Almighty God, the alpha and omega, the beginning and end, the sufficient and merciful God, for His mercy, faithfulness, grace, and kindness shown to me all throughout my doctoral program. To Him alone be all the glory and honour.

With sincere deepest gratitude and acknowledgment, I want to express my gratitude to Professor Oluwatosin Adekunle Adaramoye, my enormous, good-natured, and warm-hearted supervisor, an eloquent scholar, and a pleasing mentor to emulate, who has permanently brought about a change in the culture that is conducive to the acceptance of academia and ethical researchers in the life sciences. As a result of his academic expertise, I have become more proficient at writing scientific papers and research papers for journals as well as for conferences. I will always be grateful to you, sir, and I will always be indebted to you. May the Lord bless you with a long and healthy life.

My outmost appreciation also goes to Professor E.O Farombi for granting me admission to study M.Sc Biochemistry and his unwavering support at all times. Other Professors in the department- Prof. O.O. Olorunshogo, Prof. Oyeronke O. Odunola, Prof. M.A Gbadegesin, and Prof. C.O.O Olaiya are equally appreciated; may God reward you. I am equally grateful to Dr Amos Abolaji, Dr S.E Owumi, and Dr J.O. Olanlokun for their immense contributions, credible support and words of encouragement. I do not take your assistance and support for granted sirs. God will continue to bless you and yours beyond expectations in Jesus name. Other lecturers in the department Dr I. A. Adedara, Dr Ife Awogbindin, Dr Omolola Adesanoye, thank you all for your love and words of encouragement.

Also, I specially want to appreciate my loving, caring and very supportive father, Mr Lateef Olugbenga and my very sweet, prayerful and loving mother, Mrs Oluwatoyin Florence Adefisan for their unfettered love, unflinching support, unceasing prayers, the frequent words of encouragement, financial support, and most importantly for believing in me against all odds. Thank you daddy and mummy for you are one of the greatest things that have ever happened to me.

My special appreciation also goes to Professor Adekunle Adeniyi for the privilege and opportunity to work in Virology to carry out part of my research. Also, I extend my gratitude to Dr. Moses O. Adewumi's tremendous contribution, great demeanor, and unwavering support, bringing this work to fruition wouldn't have been possible without his support. They both provided the required environment, materials, and equipment to begin and complete the *in vitro* portion of this study. I am deeply grateful to my amiable supervisor for linking me up with these great erudite scholars that has impacted my life and contributed to the successful completion of this research work. God will continue to bless you and yours beyond expectations in Jesus name. I will not fail to thank my senior colleague and a brother, Dr, Ayobami Olajuni for his immense and supportive contribution by providing the *N-Methyl-N-Nitrosurea* used for this research. Efforts of Mr Toluwanimi Akinseye towards the execution of the first stage of my work in virology are thankfully acknowledged. His positive attitude and commitment in putting me through the experiment and data analysis were of huge importance and exemplary.

For his pleasant cooperation and friendship, I would like to thank my colleague and friend Adebayo Olayinka, who was always willing to share and provide unending support. We brainstormed, exchanged ideas, conceptually optimized tests, found some similarities in our different studies, and used our resources to realize our dreams and become the best we can be. For their incredible contributions, support, and words of encouragement, I am also grateful to my senior colleagues Dr. Akanni, Dr. Gbadebo Adeleke, and Mrs. Fausat Adeshola. To other Lab 101 alumni and present members: It has been a pleasure working with you all (Madu Judith, Arowoogun Jeremiah, Kosemani Samson, Olagunju Abolaji, and others) for your significant contributions to the success of this research. I cannot forget the non-academic staff members whose involvement in this research work cannot be overstated; people like Mr Ajiboye, Mr Sambo Eric, Mr Adediran, technologists and other administrative staff. God bless you.

At this junction, I cannot but appreciate the unfeigned love of a mother my doctoral programme gifted me (Mrs Oluwayomi Adaramoye), thousands of tongues cannot just be enough to describe your unflinching support, unceasing prayers, show of love (mother to daughter relationship), loving criticism and corrections and also for trusting

and believing in me. I do not take this motherly love for granted ma. You will forever be appreciated ma. It is my prayer that God continues to bless you and your family beyond any expectations that you or anyone else might have. This appreciation list will not be completed without appreciating my two loving sisters (Oluwafifunmi Adaramoye and Oreofeoluwa Adaramoye), you are an important component of my success story and hold a special place in my heart. God will continue to shower you with undeserved favor in all of your endeavors.

I am also indebted to my siblings Mrs Oladipo Adedayo (a very supportive sister) and Dotun Adefisan (he is always available to give his support to ensure am always in the lab carrying out my analysis). I do not take your assistance and support for granted. Without you two, life would have been meaningless; you will always be precious to me, I love you both. God will continually perfect all that concerns you and grant all your heart desires. My profound gratitude also goes to my in-laws, most especially my mother in love Deaconess Oluwafunmilayo Adawa for her unceasing prayers, support and encouragement (Grandma I do not take your love for granted). May the Lord, in His boundless kindness, continue to lavish you and your family with His blessings and mercies.

Here is where I would like to express my deep gratitude to my number one cheerleader (I call him cheerleader because he is always there to cheer and encourage me when with any academic challenge), my love, God's gift for my life, my support system (ejika ti o je kaso mi ye), ever understanding husband, the most significant part of me, Dr. Temitope Dennis- Adeoye (Adawa); when I was discouraged, He's always there, blowing a gentle breeze and refusing to let me give in. Despite all odds, thank you for sticking with me from the beginning of this program to the present. The bond between us is forever. I would not be able to complete this acknowledgment without expressing my appreciation to my loving children (Olivia Oluwadarasimi Dennis-Adeoye and Jayden Oluwadesire Dennis-Adeoye) that have been so supportive and understanding throughout this process.

I gratefully acknowledged the funding received towards my research work from Thomas Bassir foundation.

Lastly, I want to express my thankfulness to Almighty God for being my source of stability and for bringing me this far via His mercies and favor. May the Lord's name be exalted eternally.

Adedoyin Omobolanle Adefisan.

December, 2022.

ABSTRACT

Breast cancer (BC) remains a disease with high morbidity and mortality. In Nigeria, BC represents about 23% of all cancer cases. Currently available chemotherapeutic interventions are associated with significant adverse effects, hence the need for safer options. *C. portoricensis* (CP) has been applied to manage breast diseases in ethnomedicine. However, there is paucity of scientific basis to justify this claim. In this study, an investigation of the effects of CP on *N-nitroso-N-methylurea* (MNU) and Benzo(a)pyrene (BP)-induced mammary and reproductive organ toxicity in *Wistar* rats was conducted.

A root bark sample of CP was taken from Ikire, Osun State and authenticated at Forest Herbarium Ibadan (FHI:111949). The methanol extract of CP (MCP) was obtained from the powdered root. The MCP was partitioned to obtain *n*-hexane, chloroform, ethylacetate and butanol fractions. The chloroform fraction of CP (CCP) was subjected to biochemical assay using MCF-7 cells. Sixty-four female *Wistar* rats (30-40g) were divided into eight groups (n=8): Vehicle, MNU, [MNU+MCP (100 mg/kg)], [MNU+MCP (200 mg/kg)], [MNU+MCP (300 mg/kg)], MCP (300 mg/kg), [MNU+Vincasar (0.5 mg/kg)] and Vincasar only. In another study, fifty-six female rats were grouped into seven (n=8): Vehicle, [MNU+BP], [MNU+BP+CCP (50 mg/kg)], [MNU+BP+CCP (100 mg/kg)], CCP (100 mg/kg), [MNU+BP+ Vincasar] and Vincasar only. The MNU (50 mg/kg) and BP (50 mg/kg) were administered intraperitoneally at age 7, 10 and 13 weeks. The MCP and CCP were administered orally thrice weekly. Rats were sacrificed; blood and tissues (mammary and uterine) were obtained for analyses. Lactate dehydrogenase (LDH), Superoxide Dismutase (SOD), Catalase, Glutathione-S-Transferase (GST), Glutathione Peroxidase (GPx), malondialdehyde, Nitric Oxide (NO) and Myeloperoxidase were determined by vis-spectrophotometry. Cyclooxygenase-2, inducible Nitric Oxide Synthase (iNOS), B-cell lymphoma-2 (Bcl-2), p53, Interleukins-1 β and 6 (IL-1 β , IL-6), Estrogen and Progesterone receptors (ER⁺, PR⁺) and Epidermal Growth Factor Receptor-2 (EGFR-2) were determined by immunohistochemistry. Micro-section of tissues were subjected to Hematoxylin & Eosin and examined under the light microscope. Data were analysed using ANOVA at $\alpha_{0.05}$.

The CCP decreased levels of IL-1 β (34%), LDH (24%), MPO (74%), malondialdehyde (55%) and increased the activities of SOD (48%) and catalase (49%) in MCF-7 cells. The MNU decreased activities of mammary SOD (22%), uterine CAT (24%) and, GST (25%) relative to Vehicle. The MCP (100 mg/kg) when compared with MNU significantly elevated mammary SOD (18%) and uterine GST (20%). Treatment with CCP (100 mg/kg) when compared with MNU+BP significantly increased the mammary catalase (24.42 \pm 4.86 vs 16.1p6 \pm 2.90), GPx (171.48 \pm 13.97 vs 93.68 \pm 5.06), SOD (25.16 \pm 4.34 vs 16.09 \pm 2.90) and uterine catalase (29.52 \pm 4.83 vs 15.04 \pm 2.41) and SOD (48.56 \pm 4.70 vs 21.42 \pm 0.35), respectively. Additionally, CCP (100 mg/kg) significantly decreased mammary and uterine MPO (73%, 57%), NO (21%, 26%) and malondialdehyde (10%, 31%) when compared with [MNU+BP]-treated rats. The CCP (100 mg/kg) decreased ER⁺, PR⁺, EGFR-2, cyclooxygenase-2, iNOS, IL-6, IL-1 β , Bcl-2 and increased p53 expression in the mammary tissues of [MNU+BP+CCP]-treated rats. Histology of mammary tissues showed atypical epithelia, high nucleocytoplasm and ductal carcinoma in MNU+BP rats, which were reversed in rats given CCP (100 mg/kg).

C. portoricensis demonstrated chemopreventive effects via induction of apoptosis and reduction of inflammatory cytokines.

Keywords: *C. portoricensis*, *N-nitroso-N-methylurea*, Benzo(a)pyrene, Mammary gland

Word count: 498

TABLE OF CONTENTS

Title page	i
Certification	ii
Dedication	iii
Acknowledgements	iv
Abstract	v
Table of Contents	vi
List of Tables	vii
List of Figures	viii
List of Abbreviations	ix

CHAPTER ONE - INTRODUCTION

1.1	Background to the study	1
1.2	Statement of the problem	3
1.3	Rationale of the study	4
1.4	Specific Objectives	4

CHAPTER TWO - LITERATURE REVIEW

2.1	Breast Cancer	7
2.2	Breast	8
2.3	Types of Breast Cancer	9
2.3.1	Non-Intrusive Breast Cancer	9
2.3.2	Intrusive Breast Cancer	9
2.3.3	Common occurrence Breast Cancer	9
2.3.3a	<i>In situ</i> Lobular Cancer (LCIS)	9
2.3.3b	<i>In situ</i> Ductal Carcinoma (DCIS)	9

2.3.3c	Invading Lobular Carcinoma (ILC)	12
2.3.3d	Infiltrating Ductal Carcinoma (IDC)	12
2.3.4	Lesss Frequently Occuring Breast Cancer	12
2.3.4a	Carcinoma of the Medullary Gland	12
2.3.4b	Mutinous Carcinoma	12
2.3.4c	Tubular Carcinoma	12
2.3.4d	Inflammatory Breast Cancer	12
2.3.4e	Paget’s Disease of the Nipple	13
2.3.4f	Phylloides Tumor	13
2.4	Causes of Breast Cancer	13
2.4.1	Having had Breast Cancer in the past	13
2.4.2	Family History	13
2.4.3	Genetic Causes	13
2.4.4	Hormonal Causes	14
2.4.5	Environmental Causes	14
2.5	Signs And Symptoms	14
2.5.1	Early Stage	14
2.5.2	Advanced Stage (Metastasis)	14
2.6	Breast Cancer Diagnosis	14
2.7	Breast Cancer Molecular Subtypes	15
2.7.1	Luminal A- (HR positive / HER-2 negative)	15
2.7.2	Luminal B- (HR positive / HER-2 positive/negative)	15
2.7.3	Triple Negative / Basal Like (HR / HER-2 negative)	16

2.7.4	HER-2 positive / HER-2 enriched	16
2.8	Management of Breast Cancer	16
2.8.1	Surgery	17
2.8.1a	Lumpectomy	17
2.8.1b	Simple or Total Mastectomy	17
2.8.1c	Mastectomy Using a Modified Radical Mastectomy	17
2.8.2	Radiation Therapy	19
2.8.2a	Internal Radiation Therapy	19
2.8.2b	External Beam Radiation	19
2.8.3	Systemic Therapy	19
2.8.3a	Neo-Adjuvant Systemic Therapy	19
2.8.3b	Adjuvant Systemic Therapy	19
2.8.4	Biologic Therapy	20
2.9	Risk Factors	22
2.9.1	Overweight and Obesity	22
2.9.2	Smoking	22
2.9.3	Alcohol	22
2.10	Reproductive Toxicity	23
2.11	<i>N-nitroso-N-methylurea</i> (MNU)	23
2.12	Benzo[a]pyrene (BP)	26
2.13	<i>Calliandra. Portoricensis</i> (CP)	29
2.13.1	Ethnomedicinal Values	29
2.13.2	phytochemical Screening and Composition of CP	29

2.13.3	Anti-microbial and Anti-ulcer Activity of CP	30
2.13.4	Chemical Constituents of CP using GC-MS	30
2.13.5	Anticonvulsant and Analgesic Activity of CP	31
2.13.6	Antioxidant and Anti-venom Properties of CP	31
2.13.7	Anti-proliferative and Cytotoxic Effect of CP	32
2.13.8	Safety and Toxicity of CP	32

CHAPTER THREE - MATERIALS AND METHODS

3.1	Chemicals and Reagents	35
3.2	Plant Material Processing and Extraction	36
3.3	Determination of Reducing Activity of 2,2-Diphenyl-picrylhydrazyl (DPPH)	37
3.4	Assessment of ABTS [2,2-azinobis-(3-ethylbenzothiazolin-6-sulfonic acis)] Reducing Activity	37
3.5	Thin Layer Chromatography of fractions Of <i>Calliandria portoricensis</i>	38
3.6	Assays of Serum Enzymes	38
3.6.1`	Aspartate Aminotransferase (AST) Activity Measurement	38
3.6.2	Alanine Aminotransferase (ALT) Activity Measurement	38
3.6.3	Bilirubin level Measurement	39
3.6.4	Lactate Dehydrogenase (LDH) Activity Measurement	39
3.7	Biochemical Assays: Biomarkers of Oxidative Stress and Inflammation Biomarkers	40
3.7.1	Protein Concentration Measurement	40
3.7.2	Determination of Lipid Peroxidation Product	40

3.7.3	Superoxide Dismutase (SOD) Activity Measurement	41
3.7.4	Catalase Activity Measurement	42
3.7.5	Determination of Glutathione-S-transferase Activity	42
3.7.6	Glutathione Peroxidase Activity Measurement	43
3.7.7	Determination of Reduced Glutathione level	44
3.7.8	Determination of Total Thiol level	45
3.7.9	Nitric Oxide (NO) level Measurement	45
3.7.10	Determination of Myeloperoxidase Activity	46
3.8	Assessment of Urinary Parameters	47
3.9	Immunohistochemistry of Inflammatory and Apoptotic Markers	48
3.10	Assesment of DNA Fragmentation	50
3.11	Methanol extract of <i>C. portoricensis</i> on serum parameters, antioxidants status and hormone receptors in MNU -administered rats.	51
3.12	Assessment of Antioxidative and Radical Scavenging Activities of <i>C. portoricensis</i>	51
3.13	Chloroform Fraction of <i>C. portoricensis</i> on Biochemical Parameters and Hormonal profile in MNU and Benzo[a]pyerene-induced rats.	52
3.14	Assessment of Antiproliferative, Antioxidative and Apoptotic Effects of Chloroform Fraction of <i>C. portoricensis</i> in MCF-7 cells.	52
3.14.1	Biochemecal parameters on cell lysates	53
3.15	Chloroform Fraction of <i>C. portoricensis</i> on MNU and Benzo[a]pyerene - induced mammary toxicity in rats.	53
3.16	Statistical Analysis	54

CHAPTER FOUR - RESULTS

4.1	Protective effect of methanol extract of <i>C. portoricensis</i> on serum parameters, antioxidants status and hormone receptors in MNU-administered rats.	55
4.2	<i>In-vitro</i> Assessment of Antioxidative and Radical Scavenging Activities of <i>C. portoricensis</i>	111
4.3	Chemopreventive Effects of Chloroform Fraction of <i>C. portoricensis</i> on Biochemical Parameters and Hormonal profile in MNU and Benzo[a]pyrene-induced rats.	117
4.4	Assessment of Antiproliferative, Antioxidative and Apoptotic Effects of Chloroform Fraction of <i>C. portoricensis</i> in MCF-7 cells.	202
4.5	Possible Curative Effects of Chloroform Fraction of <i>C. portoricensis</i> on MNU and Benzo[a]pyrene -induced mammary toxicity in rats.	214

CHAPTER FIVE- DISCUSSION

5.1	DISCUSSION	234
-----	------------	-----

CHAPTER SIX - SUMMARY, CONCLUSION AND RECOMMENDATIONS

6.1	SUMMARY	242
6.2	CONCLUSION	243
6.2	RECOMMENDATIONS	245
6.2	CONTRIBUTIONS TO KNOWLEDGE	246
	REFERENCES	247
	APPENDICES	269

LIST OF TABLES

Table 4.1:	Body Weight Changes of Wistar Rats on Exposure to MNU and Treatment with Methanol Fraction of CP and VIN.	56
Table 4.2:	Organ Weight Changes of MNU-Administered Rats Given Methanol Fraction of CP and VIN	57
Table 4.3:	ABTS Radical Scavenging Activity Of <i>C. portoricensis</i>	108
Table 4.4:	DPPH Radical Reducing Activity of <i>C. portoricensis</i>	112
Table 4.5:	Body Weight Changes and Organo-Somatic Weight of MNU and BP-Exposed Rats Given Chloroform Fraction of CP and VIN	114
Table 4.6:	Organs Weight of MNU and BP-Administered Rats Given Chloroform Fraction of CP and VIN	118
Table 4.7:	Urinary Parameters Analysis on MNU and BP-Administered Rats Given Chloroform Fraction of CP and VIN	119
Table 4.8:	Identified Compounds from Chloroform Fraction of <i>C. portoricensis</i>	121
Table 4.9:	Effect of Chloroform fraction of CP And VIN on Cell Growth Inhibition in MCF-7 Cells	200
Table 4.10:	Body Weight Changes of Wistar Rats on Exposure to MNU and BP Given Chloroform Fraction of CP and VIN	203

LISTS OF FIGURES

Figure 1.1:	Normal breast tissue structure	6
Figure 2.1:	Structure of the Breast	9
Figure 2.2:	Breast Tissue structure showing the ducts, lobules and fatty tissue	11
Figure 2.3:	Typical Structure Related to Ductal Carcinoma	12
Figure 2.4:	Various surgery types applied for BC	19
Figure 2.5:	Two theories about how BC starts and progresses	22
Figure 2.6:	Structure of <i>N-nitroso-N-methylurea</i>	26
Figure 2.7:	Structure of Benzo(a)pyrene	28
Figure 2.8:	Metabolism of BP	29
Figure 2.9:	Photograph of <i>C. portoricensis</i>	34
Figure 3.1:	Extraction process of <i>C. portoricensis</i>	36
Figure 4.1:	Effect of methanol extract of <i>C.portoricensis</i> in <i>Wistar</i> rats given <i>MNU</i> on serum alanine aminotransferase activities.	59
Figure 4.2:	Effect of methanol extract of <i>C.portoricensis</i> in <i>Wistar</i> rats given <i>MNU</i> on serum aspartate aminotransferase activities.	60
Figure 4.3:	Effect of methanol extract of <i>C.portoricensis</i> in <i>Wistar</i> rats given <i>MNU</i> on serum total bilirubin levels.	61
Figure 4.4:	Effect of methanol extract of <i>C.portoricensis</i> in <i>Wistar</i> rats given <i>MNU</i> on serum nitric oxide levels.	62
Figure 4.5:	Effect of methanol extract of <i>C.portoricensis</i> in <i>Wistar</i> rats given <i>MNU</i> on serum malondialdehyde levels.	63
Figure 4.6:	Effect of methanol extract of <i>C.portoricensis</i> (CP) in <i>Wistar</i> rats given <i>MNU</i> on serum lactate dehydrogenase activities.	64

Figure 4.7: Effect of methanol extract of <i>C.portoricensis</i> (CP) in <i>Wistar</i> rats given <i>MNU</i> on DNA fragmentation.	65
Figure 4.8: Effect of methanol extract of <i>C.portoricensis</i> in <i>Wistar</i> rats given <i>MNU</i> on mammary Glutathione-S-transferase activities	67
Figure 4.9: Effect of methanol extract of <i>C.portoricensis</i> in <i>Wistar</i> rats given <i>MNU</i> on uterine Glutathione-S-transferase activities.	68
Figure 4.10: Effect of methanol extract of <i>C.portoricensis</i> in <i>Wistar</i> rats given <i>MNU</i> on ovarian Glutathione-S-transferase activities.	69
Figure 4.11: . Effect of methanol extract of <i>C.portoricensis</i> in <i>Wistar</i> rats given <i>MNU</i> on mammary glutathione peroxidase activities.	70
Figure 4.12: Effect of methanol extract of <i>C.portoricensis</i> in <i>Wistar</i> rats given <i>MNU</i> on uterine glutathione peroxidase activities.	71
Figure 4.13: Effect of methanol extract of <i>C.portoricensis</i> in <i>Wistar</i> rats given <i>MNU</i> on ovarian glutathione peroxidase activities.	72
Figure 4.14: Effect of methanol extract of <i>C.portoricensis</i> in <i>Wistar</i> rats given <i>MNU</i> on mammary Catalase activities.	74
Figure 4.15: Effect of methanol extract of <i>C.portoricensis</i> in <i>Wistar</i> rats given <i>MNU</i> on uterine Catalase activities.	75
Figure 4.16: Effect of methanol extract of <i>C.portoricensis</i> in <i>Wistar</i> rats given <i>MNU</i> on ovarian Catalase activities.	76
Figure 4.17: Effect of methanol extract of <i>C.portoricensis</i> in <i>Wistar</i> rats given <i>MNU</i> on mammary Superoxide-dismutase activities.	77
Figure 4.18: Effect of methanol extract of <i>C.portoricensis</i> in <i>Wistar</i> rats given <i>MNU</i> on uterine Superoxide-dismutase activities.	78
Figure 4.19: Effect of methanol extract of <i>C.portoricensis</i> in <i>Wistar</i> rats given <i>MNU</i> on ovarian Superoxide-dismutase activities.	79

Figure 4.20: Effect of methanol extract of <i>C.portoricensis</i> in <i>Wistar</i> rats given <i>MNU</i> on mammary reduced glutathione levels.	81
Figure 4.21: Effect of methanol extract of <i>C.portoricensis</i> in <i>Wistar</i> rats given <i>MNU</i> on uterine reduced glutathione levels.	82
Figure 4.22: Effect of methanol extract of <i>C.portoricensis</i> in <i>Wistar</i> rats given <i>MNU</i> on ovarian reduced glutathione levels.	83
Figure 4.23: Effect of methanol extract of <i>C.portoricensis</i> in <i>Wistar</i> rats given <i>MNU</i> on mammary total sulphhydryl levels.	84
Figure 4.24: Effect of methanol extract of <i>C.portoricensis</i> in <i>Wistar</i> rats given <i>MNU</i> on uterine total sulphhydryl levels.	85
Figure 4.25: Effect of methanol extract of <i>C.portoricensis</i> in <i>Wistar</i> rats given <i>MNU</i> on ovarian total sulphhydryl levels.	86
Figure 4.26: . Effect of methanol extract of <i>C.portoricensis</i> in <i>Wistar</i> rats given <i>MNU</i> on mammary Nitric oxide levels.	88
Figure 4.27: Effect of methanol extract of <i>C.portoricensis</i> in <i>Wistar</i> rats given <i>MNU</i> on uterine Nitric oxide levels.	89
Figure 4.28: Effect of methanol extract of <i>C.portoricensis</i> in <i>Wistar</i> rats given <i>MNU</i> on ovarian Nitric oxide levels.	90
Figure 4.29: Effect of methanol extract of <i>C.portoricensis</i> in <i>Wistar</i> rats given <i>MNU</i> on mammary Myeloperoxidase activities.	91
Figure 4.30: . Effect of methanol extract of <i>C.portoricensis</i> in <i>Wistar</i> rats given <i>MNU</i> on uterine Myeloperoxidase activities .	92
Figure 4.31: Effect of methanol extract of <i>C.portoricensis</i> in <i>Wistar</i> rats given <i>MNU</i> on ovarian Myeloperoxidase activities.	93
Figure 4.32: Effect of methanol extract of <i>C.portoricensis</i> in <i>Wistar</i> rats given <i>MNU</i> on mammary Malondialdehyde levels.	95

Figure 4.33: Effect of methanol extract of <i>C.portoricensis</i> in <i>Wistar</i> rats given <i>MNU</i> on uterine Malondialdehyde levels.	96
Figure 4.34: Effect of methanol extract of <i>C.portoricensis</i> in <i>Wistar</i> rats given <i>MNU</i> on ovarian Malondialdehyde levels.	97
Figure 4.35: Activity of estrogen receptor (ER) in <i>MNU</i> -administered rats given methanol extract of <i>C. portoricensis</i> .	99
Figure 4.36: Activity of progesterone receptor (PR) in <i>MNU</i> -administered rats given methanol extract of <i>C. Portoricensis</i> .	100
Figure 4.37: Activiy of epidermal growth factor receptor-2 (EGFR-2) in <i>MNU</i> -administered rats given methanol extract of <i>C. portoricensis</i> of crude plant extract fraction	101
Figure 4.38: Histopathological alteration of mammary tissues in rats given <i>MNU</i> and methanol extract of CP (M X 400)	103
Figure 4.39: Histopathological alteration of ovary tissues in rats given <i>MNU</i> and methanol extract of CP (M X 400)	104
Figure 4.40: Histopathological alteration of uterus tissues in rats given <i>MNU</i> and methanol extract of CP (M X 400)	105
Figure 4.41: Ultra violet view of spotted thin layer chromatography plates	116
Figure 4.42: Effect of chloroform fraction of <i>C.portoricensis</i> in <i>Wistar</i> rats given <i>MNU</i> and BP on mammary glutathione peroxidase activities of crude plant extract fraction.	123
Figure 4.43: Effect of chloroform fraction of <i>C.portoricensis</i> (CP) in <i>Wistar</i> rats given <i>MNU</i> and BP on mammary reduced glutathione (GSH) levels of crude plant extract fraction.	124
Figure 4.44: Effect of chloroform fraction of <i>C.portoricensis</i> (CP) in <i>Wistar</i> rats given <i>MNU</i> and BP on mammary total sulphhydryl (TSH) levels of crude plant extract fraction.	125

- Figure 4.45: Effect of chloroform fraction of *C.portoricensis* (CP) in *Wistar* rats given *MNU* and BP on mammary Catalase (CAT) activities of crude plant extract fraction. 126
- Figure 4.46: Effect of chloroform fraction of *C.portoricensis* (CP) in *Wistar* rats given *MNU* and BP on mammary superoxide dismutase (SOD) activities of crude plant extract fraction. 127
- Figure 4.47: Effect of chloroform fraction of *C.portoricensis* (4CP) in *Wistar* rats given *MNU* and BP on mammary glutathione-S-transferase (GST) activities of crude plant extract fraction. 128
- Figure 4.48: Effect of chloroform fraction of *C.portoricensis* (CP) in *Wistar* rats given *MNU* and BP on mammary myeloperoxidase (MPO) activities of crude plant extract fraction. 130
- Figure 4.49: Effect of chloroform fraction of *C.portoricensis* (CP) in *Wistar* rats given *MNU* and BP on mammary nitric oxide (NO) levels of crude plant extract fraction. 131
- Figure 4.50: Effect of chloroform fraction of *C.portoricensis* (CP) in *Wistar* rats given *MNU* and BP on mammary malondialdehyde (LPO) levels of crude plant extract fraction. 132
- Figure 4.51: Effect of chloroform fraction of *C.portoricensis* (CP) in *Wistar* rats given *MNU* and BP on uterine glutathione peroxidase (GPx) activities of crude plant extract fraction. 134
- Figure 4.52: Effect of chloroform fraction of *C.portoricensis* (CP) in *Wistar* rats given *MNU* and BP on uterine reduced glutathione (GSH) levels of crude plant extract fraction. 135
- Figure 4.53: Effect of chloroform fraction of *C.portoricensis* (CP) in *Wistar* rats given *MNU* and BP on uterine total sulphhydryl (TSH) levels of crude plant extract fraction. 136

- Figure 4.54: Effect of chloroform fraction of *C.portoricensis* (CP) in *Wistar* rats given *MNU* and BP on uterine and ovarian Catalase (CAT) activities of crude plant extract fraction . 137
- Figure 4.55: Effect of chloroform fraction of *C.portoricensis* (CP) in *Wistar* rats given *MNU* and BP on uterine superoxide dismutase (SOD) activities of crude plant extract fraction. 138
- Figure 4.56: Effect of chloroform fraction of *C.portoricensis* (CP) in *Wistar* rats given *MNU* and BP on uterine glutathione-S-transferase (GST) activities of crude plant extract fraction. 139
- Figure 4.57: Effect of chloroform fraction of *C.portoricensis* (CP) in *Wistar* rats given *MNU* and BP on uterine and ovarian nitric oxide (NO) levels of crude plant extract fraction. 141
- Figure 4.58: Effect of chloroform fraction of *C.portoricensis* (CP) in *Wistar* rats given *MNU* and BP on uterine myeloperoxidase (MPO) activities of crude plant extract fraction. 142
- Figure 4.59: Effect of chloroform fraction of *C.portoricensis* (CP) in *Wistar* rats given *MNU* and BP on uterine malondialdehyde (LPO) levels of crude plant extract fraction. 143
- Figure 4.60: Effect of chloroform fraction of *C.portoricensis* (CP) in *Wistar* rats given *MNU* and BP on ovarian glutathione peroxidase (GPx) activities of crude plant extract fraction. 145
- Figure 4.61: Effect of chloroform fraction of *C.portoricensis* (CP) in *Wistar* rats given *MNU* and BP on ovarian reduced glutathione (GSH) levels. 146
- Figure 4.62: Effect of chloroform fraction of *C.portoricensis* (CP) in *Wistar* rats given *MNU* and BP on ovarian total sulphhydryl (TSH) levels of crude plant extract fraction. 147
- Figure 4.63: Effect of chloroform fraction of *C.portoricensis* (CP) in *Wistar* rats given *MNU* and BP on ovarian Catalase (CAT) activities of crude plant extract fraction. 148

- Figure 4.64: Effect of chloroform fraction of *C.portoricensis* (CP) in *Wistar* rats given *MNU* and BP on ovarian superoxide dismutase (SOD) activities of crude plant extract fraction. 149
- Figure 4.65: Effect of chloroform fraction of *C.portoricensis* (CP) in *Wistar* rats given *MNU* and BP on ovarian glutathione-S-transferase (GST) activities of crude plant extract fraction. 150
- Figure 4.66: Effect of chloroform fraction of *C.portoricensis* (CP) in *Wistar* rats given *MNU* and BP on ovarian uterine nitric oxide (NO) levels of crude plant extract fraction. 152
- Figure 4.67: Effect of chloroform fraction of *C.portoricensis* (CP) in *Wistar* rats given *MNU* and BP on ovarian myeloperoxidase (MPO) activities of crude plant extract fraction. 153
- Figure 4.68: Effect of chloroform fraction of *C.portoricensis* (CP) in *Wistar* rats given *MNU* and BP on ovarian malondialdehyde (LPO) levels of crude plant extract fraction. 154
- Figure 4.69: : Immunohistochemical staining of β -Catenin expression in the mammary tissue of *MNU* and BP rats given chloroform fraction of *C. Portoricensis* (CP) . 156
- Figure 4.70: Immunohistochemical staining of p53 expression in the mammary tissue of *MNU* and BP rats given chloroform fraction of *C. portoricensis* of crude plant extract fraction. 157
- Figure 4.71: . Immunohistochemical staining of Bcl-2 Associated X-protein (BAX) expression in the mammary tissue of *MNU* and BP rats given chloroform fraction of *C. portoricensis*. 158
- Figure 4.72: Immunohistochemical staining of Caspase-9 expression in the mammary tissue of *MNU* and BP rats given chloroform fraction of *C. Portoricensis* (CP). 159

- Figure 4.73: Immunohistochemical staining of Caspase-3 expression in the mammary tissue of *MNU* and BP rats given chloroform fraction of *C. Portoricensis* (CP). 160
- Figure 4.74: Immunohistochemical staining of BCL-2 expression in the mammary tissue of *MNU* and BP rats given chloroform fraction of *C. Portoricensis*. 161
- Figure 4.75: Immunohistochemical staining of interleukin (IL-6) expression in the mammary tissue of *MNU* and BP rats given chloroform fraction of *C. Portoricensis* (CP). 162
- Figure 4.76: Immunohistochemical staining of interleukin (IL-1 β) expression in the mammary tissue of *MNU* and BP rats given chloroform fraction of *C. Portoricensis*(CP). 163
- Figure 4.77: Immunohistochemical staining of cyclooxygenase-2 (COX-2) expression in the mammary tissue of *MNU* and BP rats given chloroform fraction of *C. Portoricensis*. 164
- Figure 4.78: Immunohistochemical staining of inducible nitric oxide synthase (iNOS) expression in the mammary tissue of *MNU* and BP rats given chloroform fraction of *C. Portoricensis*. 165
- Figure 4.79: Immunohistochemical staining of prolactin levels in the mammary tissue of *MNU* and BP rats given chloroform fraction of *C. Portoricensis*. 167
- Figure 4.80: Immunohistochemical staining of follicle stimulating hormone (FSH) levels in the mammary tissue of *MNU* and BP rats given chloroform fraction of *C. Portoricensis*. 168
- Figure 4.81: Immunohistochemical staining of luteinizing hormone (LH) levels in the mammary tissue of *MNU* and BP rats given chloroform fraction of *C. Portoricensis*. 169
- Figure 4.82: Immunohistochemical staining of progesterone levels in the mammary tissue of *MNU* and BP rats given chloroform fraction of *C. Portoricensis* of crude plant extract fraction. 170

Figure 4.83: Mammary gland cyto-architecture of <i>MNU</i> and BP rats given chloroform fraction of <i>C. portoricensis</i> (M X 400) uterine and ovarian of crude plant extract fraction.	172
Figure 4.84: Pictorial section of mammary tumor of the mammary gland	173
Figure 4.85: Photomicrograph of mammary tissues stained with H&E	174
Figure 4.86: Immunohistochemical staining of p53 expression in the ovarian tissue of <i>MNU</i> and BP rats given chloroform fraction of <i>C. Portoricensis</i> of crude plant extract fraction.	176
Figure 4.87: Immunohistochemical staining of Caspase-3 expression in the ovarian tissue of <i>MNU</i> and BP rats given chloroform fraction of <i>C. Portoricensis</i> of crude plant extract fraction.	177
Figure 4.88: Immunohistochemical staining of Bcl-2 Associated X-protein (BAX) expression in the ovarian tissue of <i>MNU</i> and BP rats given chloroform fraction of <i>C. Portoricensis</i> .	178
Figure 4.89: Immunohistochemical staining of inducible nitric oxide synthase (iNOS) expression in the ovarian tissue of <i>MNU</i> and BP rats given chloroform fraction of <i>C. Portoricensis</i> .	179
Figure 4.90: Immunohistochemical staining of BCL-2 expression in the ovarian tissue of <i>MNU</i> and BP rats given chloroform fraction of <i>C. Portoricensis</i> of crude plant extract fraction.	180
Figure 4.91: Immunohistochemical staining of prolactin level in the ovarian tissue of <i>MNU</i> and BP rats given chloroform fraction of <i>C. Portoricensis</i> of crude plant extract fraction.	182
Figure 4.92: Immunohistochemical staining of follicle stimulating hormone (FSH) levels in the ovarian tissue of <i>MNU</i> and BP rats given chloroform fraction of <i>C. Portoricensis</i> .	183
Figure 4.93: Immunohistochemical staining of luteinizing hormone (LH) levels in the ovarian tissue of <i>MNU</i> and BP rats given chloroform fraction of <i>C. Portoricensis</i> (CP).	184

Figure 4.94: Immunohistochemical staining of progesterone levels in the ovarian tissue of <i>MNU</i> and <i>BP</i> rats given chloroform fraction of <i>C. Portoricensis</i> of crude plant extract fraction.	185
Figure 4.95: Ovarian cyto-architecture of <i>MNU</i> and <i>BP</i> rats given chloroform fraction of <i>C. Portoricensis</i> (M X 400).	187
Figure 4.96: Immunohistochemical staining of Caspase-3 expression in the uterine tissue of <i>MNU</i> and <i>BP</i> rats given chloroform fraction of <i>C. Portoricensis</i> of crude plant extract fraction.	189
Figure 4.97: Immunohistochemical staining of BCL-2 expression in the uterine tissue of <i>MNU</i> and <i>BP</i> rats given chloroform fraction of <i>C. Portoricensis</i> of crude plant extract fraction.	190
Figure 4.98: Immunohistochemical staining of prolactin hormone levels in the uterine tissue of <i>MNU</i> and <i>BP</i> rats given chloroform fraction of <i>C. Portoricensis</i> of crude plant extract fraction.	192
Figure 4.99: Immunohistochemical staining of follicle stimulating hormone (FSH) levels in the uterine tissue of <i>MNU</i> and <i>BP</i> rats given chloroform fraction of <i>C. Portoricensis</i> .	193
Figure 4.100: Immunohistochemical staining of lutenizing hormone (LH) levels in the uterine tissue of <i>MNU</i> and <i>BP</i> rats given chloroform fraction of <i>C. Portoricensis</i> of crude plant extract fraction.	194
Figure 4.101: Immunohistochemical staining of progesterone hormone levels in the uterine tissue of <i>MNU</i> and <i>BP</i> rats given chloroform fraction of <i>C. Portoricensis</i> of crude plant extract fraction.	195
Figure 4.102: Uterine cyto-architecture tissues of <i>MNU</i> and <i>BP</i> given chloroform fraction of <i>CP</i> .	197
Figure 4.103: Finger printing chromatograms of <i>C. portoricensis</i> (chloroform fraction) by GCMS.	198
Figure 4.104: Chromatogram of <i>C. portoricensis</i> (chlroform fraction) by GCMS	201

Figure 4.105: Effects of chloroform fraction of <i>C. portoricensis</i> on Caspase-9 activity on MCF-7 cell lysate <i>in vitro</i> .	205
Figure 4.106: Effects of chloroform fraction of <i>C. portoricensis</i> on Caspase-3 levels on MCF-7 cell lysate <i>in vitro</i> .	206
Figure 4.107: Effects of chloroform fraction of <i>C. portoricensis</i> on BAX activity on MCF-7 cell lysate <i>in vitro</i> .	207
Figure 4.108: Effects of chloroform fraction of <i>C. portoricensis</i> on levels of interleukin-1 β (IL-1 β) on MCF-7 cell lysate <i>in vitro</i> .	209
Figure 4.109: Effects of chloroform fraction of <i>C. portoricensis</i> on malondialdehyde (LPO) levels on MCF-7 cell lysate <i>in vitro</i> .	210
Figure 4.110: Effects of chloroform fraction of <i>C. portoricensis</i> on myeloperoxidase (MPO) activities on MCF-7 cell lysate <i>in vitro</i> .	211
Figure 4.111: Effects of chloroform fraction of <i>C. portoricensis</i> on superoxide dismutase (SOD) activities on MCF-7 cell lysate <i>in vitro</i> .	212
Figure 4.112: Effects of chloroform fraction of <i>C. portoricensis</i> on Catalase (CAT) activities on MCF-7 cell lysate <i>in vitro</i> .	213
Figure 4.113: Effect of chloroform fraction of <i>C. portoricensis</i> (CP) on mammary alanine-aminotransferases (ALT) activities in <i>MNU</i> and <i>BP</i> rats of crude plant extract fraction.	217
Figure 4.114: Effect of chloroform fraction of <i>C. portoricensis</i> (CP) on mammary aspartate-aminotransferases (AST) activities in <i>MNU</i> and <i>BP</i> rats of crude plant extract fraction.	218
Figure 4.115: Effect of chloroform fraction of <i>C. portoricensis</i> (CP) on total bilirubin levels (T-BIL) in <i>MNU</i> and <i>BP</i> rats.	219
Figure 4.116: Effect of chloroform fraction of <i>C. portoricensis</i> (CP) on Catalase (CAT) activities in <i>MNU</i> and <i>BP</i> rats.	221

- Figure 4.117: Effect of chloroform fraction of *C. portoricensis* (CP) on mammary glutathione-S-transferases (GST) activities in *MNU* and BP rats of crude plant extract fraction . 222
- Figure 4.118: Effect of chloroform fraction of *C. portoricensis* (CP) on superoxide dismutase (SOD) activities in *MNU* and BP rats. 223
- Figure 4.119: Effect of chloroform fraction of *C. portoricensis* (CP) on glutathione peroxidase (GPx) activities in *MNU* and BP rats. 225
- Figure 4.120: Effect of chloroform fraction of *C. portoricensis* (CP) on mammary reduced glutathione (GSH) levels in *MNU* and BP in rats of crude plant extract fraction. 226
- Figure 4.121: Effect of chloroform fraction of *C. portoricensis* (CP) on mammary half and total sulphhydryl (TSH) levels in *MNU* and BP in rats of crude plant extract fraction. 227
- Figure 4.122: Effect of chloroform fraction of *C. portoricensis* (CP) on mammary malondialdehyde (LPO) levels in *MNU* and BP in the rats of crude plant extract fraction. 229
- Figure 4.123: Effect of chloroform fraction of *C. portoricensis* (CP) on nitric oxide (NO) levels in *MNU* and BP rats. 230
- Figure 4.124: Effect of chloroform fraction of *C. portoricensis* (CP) on mammary myeloperoxidase (MPO) activities in *MNU* and BP in the rats of crude plant extract fraction. 231
- Figure 4.125: Effect of chloroform fraction of *C. portoricensis* (CP) on mammary Nuclear factor kappa B (NF-kB) activity in *MNU* and BP in the rats of crude plant extract fraction. 233
- Figure 4.126: Effect of chloroform fraction of *C. portoricensis* (CP) on mammary inducible nitric oxide synthase (iNOS) activity in *MNU* and BP rats of crude plant extract fraction. 234
- Figure 4.127: Effect of chloroform fraction of *C. portoricensis* (CP) on p53 activity in *MNU* and BP rats. 236

Figure 4.128: Effect of chloroform fraction of <i>C. portoricensis</i> (CP) on Bcl-2 Associated X-protein (BAX) activity in <i>MNU</i> and BP rats.	237
Figure 4.129: Effect of chloroform fraction of <i>C. portoricensis</i> (CP) on Caspase-3 activity in <i>MNU</i> and BP rats.	238
Figure 4.130: Photomicrograph of mammary gland tissues in <i>MNU</i> and BP rats given chloroform fraction of <i>C. portoricensis</i> (M X 400).	240
Figure 4.131: Pictorial section of experimental animal bearing neck tumor before and after CP treatment.	241
Figure 4.132: Photomicrograph of a neck tissue section stained with H&E	242
Figure 4.133: Photomicrograph of neck tumor in <i>MNU</i> and BP rats given chloroform fraction of CP.	243

LISTS OF ABBREVIATIONS

B(a)P:	Benzo(a)pyrene
BAX:	BCL-2 Associated X Protein
BC:	Breast cancer
BCL-2:	B-Cell Lymphoma 2
CCP:	Chloroform Fraction of <i>C. portoricensis</i>
CP:	<i>C. portoricensis</i>
COX-2:	Cyclooxygenase-2
ER:	Estrogen Receptor
EGFR-2:	Epidermal Growth Factor Receptor-2
FSH:	Follicle Stimulating Hormone
GPx:	Glutathione Peroxidase
GSH:	Reduced Glutathione
GST:	Glutathione-S-transferase
HER-2:	Human Epidermal Growth Factor Receptor-2
IL-1 β :	Interleukin-1beta
IL-6:	Interleukin-6
iNOS:	Inducible Nitric Oxide Synthase
ISLC:	In situ Lobular Cancer
ISDC:	In situ Ductal Carcinoma
ILC:	Invading Lobular Carcinoma
IDC:	Infiltrating Ductal Carcinoma
LDH:	Lactate Dehydrogenase

LH:	Luteinizing Hormone
MCP:	Methanol Extract of <i>C. portoricensis</i>
MPO:	Myeloperoxidase
NF-kB:	Nuclear Factor Kappa Beta
MNU:	<i>N-nitroso-N-methylurea</i>
NO:	Nitric Oxide
PR:	Progesterone Receptor
VIN:	Vincasar

CHAPTER ONE

INTRODUCTION

1.1 BACKGROUND TO THE STUDY

Breast cancer (BC) has always been the major leading clinical and societal challenge affecting women globally (Desantis *et al.*, 2014). Several reports have documented BC as the next prominent contributor of cancer related deaths in the world. New BC cases are estimated to be 11.6% globally according to Globacon 2018 (Jemal *et al.*, 2010). Further estimation reported that 30% of all newly diagnosed women cancers in 2020 were BC (Shehata *et al.*, 2012; Esther *et al.*, 2016). BC is more than a single illness, with substantial heterogeneity at both the molecular and clinical level. (Etti *et al.*, 2017; Khalki *et al.*, 2020). Understanding the heterogeneity of BC is critical to the advancement of targeted cancer control and care. (Biau *et al.*, 2016; Saraiva *et al.*, 2020). The clinical course determines the heterogeneity of BC, prognosis as well as the molecular classification into distinct subtypes of Luminal, Basal-like, and HER-2 enriched (Bagheri *et al.*, 2018; Bowers *et al.*, 2019).

Routine biological markers such as estrogen (ER), progesterone (PR), and human epidermal growth factor-2 (HER2) receptors classified BC into different molecular subtypes (Hamed *et al.*, 2018). As indicated by ductal carcinoma *in situ* (DCIS) and different tumor progression routes for each tumor type, these subsets of biological routine biomarkers are maintained throughout tribal groupings (Utage *et al.*, 2018; Jang *et al.*, 2019). The direct aetiology of BC is yet to be uncovered though hormones, lifestyle, genetics, birth history, age, diet, menstrual history and environmental factors have been reported by researchers to upsurge the chance of developing of BC (Kittaneh and Montero, 2013). However, it is not clear how to define the causes of developing cancer. Surgery, chemotherapy, radiotherapy, and hormone therapy are some of the best available treatment options for managing BC (Webb and Kukard, 2020). Resistance to

these available treatment is a major limitation to cancer treatment hence the search for better options with no or little side effect is on going.

Human exposure to environmental toxicants has been on the rise thereby inducing their effects on reproductive functions (Bhardwaj, 2015; Patel *et al.*, 2015). Countless studies have suggested a decline in female reproduction over the decades (Huo *et al.*, 2015; Elvis-offiah *et al.*, 2016; Ziv-Gal and Flaws, 2016). These declines may be attributed to cultural changes such as increased use of birth control in women, delay in child bearing, although, mother, father or fetus exposures to environmental toxicants may also contribute to these changes (Zama and Uzumcu, 2010; Schwab *et al.*, 2014). It is therefore crucial to periodically examine the known or expected effects of environmental factors such as carcinogens on the reproductive capacity of the experimental animals as well as humans (De Coster and Van Larebeke, 2012; Gaskins and Mínguez-Alarcón, 2018; Ma *et al.*, 2019). Examples of these environmental toxicants include but not limited to aflatoxin, cadmium, arsenic, MNU and BP (Rudel *et al.*, 2011; Uri, 2014; Gray *et al.*, 2017).

The MNU is a high degree distinct breast gland carcinogen as well as complete potent and direct alkylating agent which does not require metabolic activation (Oishi *et al.*, 2000; Thordason *et al.*, 2001). It has been proven and widely accepted as a human mutagen and toxic. This is founded on sufficient proof of carcinogenicity through the use of experimental animals (Etten *et al.*, 2005). Also, benzo[a]pyrene (BP) has been suggested to be capable of initiating and promoting carcinogenesis (Taylor *et al.*, 2006). The biotransformation of BP requires a metabolic activation by cytochrome P₄₅₀ (CYP 1A1 and CYP 1B1) into a more reactive compound BP-7,8-dihydrodiol-9-10-epoxide which come in contact with DNA to form DNA adduct (IARC, 2020).

Alternative medicines is recently gaining tremendous interest and becoming popular in treating cancer and infertility worldwide (Ou-yang *et al.*, 2019; Kurubanjerdjit, 2020). One of the natural products that is gaining attention lately is *C. portoricensis* (CP). CP is a multifaceted herb with mutiple therapeutic benefits. It has white scented and globose flower that looks like small snow ball (Ogbole *et al.*, 2018). It is also known as powder puff. Over 200 species of CP have been identified, with the majority of them located in

Asia, Africa, and America's tropical and subtropical climates. It is called 'Tude' in Yoruba, 'Ule' in Igbo, and 'Oga' in Hausa in Nigeria. (Oyebo *et al.*, 2019).

CP stands out as the most popular traditionally employed remedy in south western part of Nigeria for treating breast engorgement and other related diseases (Onyeama *et al.*, 2012; Ogbole *et al.*, 2017). Parts of the plant used and treatment methods varies from one locality to another. For example, the root decoction used in one locality may be different from the stem and leaf decoction used in another locality, thus, effectiveness of all the plant parts have been proven (Onyeama *et al.*, 2012; Oyebo *et al.*, 2019). CP herbs have been established as a high-polyphenol source. It has anti-inflammatory (Adaramoye *et al.*, 2017), antimicrobial (Oguegbulu *et al.*, 2020) antioxidative (Adefisan *et al.*, 2019), anti-proliferative (Adaramoye *et al.*, 2015), anti-convulsant (Root, 1988) as well as analgesic (Aguwa and Lawal, 1988; Agunu *et al.*, 2005) properties.

1.2 STATEMENT OF THE PROBLEM

Several decades back, different combinations of cytotoxic agents were proposed and tested. In metastatic and adjuvant settings, combination chemotherapy became the standard method of BC treatment (Sledge *et al.*, 2014). Doxorubicin was first used in clinical trials in the late 1960s and early 1970s, and it was thought to be a very effective therapy against BC, followed by anthracycline-based combos and cyclophosphamide. The frequent use of combination therapy in malignant BC patients has been called into doubt (Veronesi *et al.*, 2005). This is because several randomised trials carried out in comparing single agent doxorubicin to single agent paclitaxel as well as the merging of both agents stipulated that the combination of the two agents generated a higher degree of response and a longer time to therapeutic failure, but no difference in survival rates.(Bray *et al.*, 2004).

This findings as well as other trials put a set-back on the use of combination chemotherapy while sequential use of single-agent chemotherapy was accepted as the standard of care (Sledge *et al.*, 2014). On the contrary, combination therapy clinical trials as well as successive back-to-back therapy was interminable which gives rise to third generation of adjuvant chemotherapy trials since most of the headway in BC treatment ensue due to the development of adjuvant chemotherapy (Jones, 2008).

BC that has receptor for estrogen (ER+) is one of the most often diagnosed cancers around the globe, however, anti-estrogen have globally impacted treatment intervention in cancer medicine (Aiyer and Gupta, 2011; Anderson *et al.*, 2014; Parodi *et al.*, 2017). The use of selective estrogen receptor modulator tamoxifen or aromatase inhibitor as therapy for five years enhances overall survival and lower BC reapparence in patients diagnosed with first phase ER-positive BC and is widely accepted as standard of care . However, there is still insistent risk of tumor reoccurrence beyond five years of treatment despite the use of adjuvant therapy with endocrine agents (Arzi *et al.*, 2020). Nonetheless, resistance to combination and endocrine therapies remains a clinical and scientific threat.

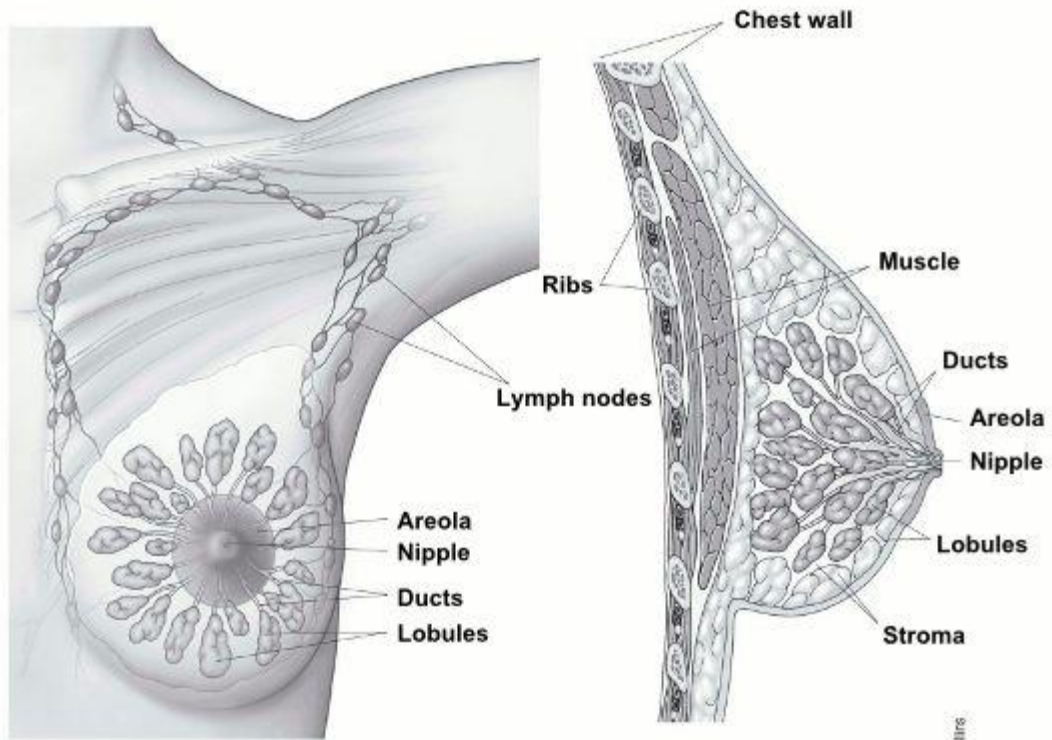
1.3 RATIONALE FOR THE STUDY

Due to anticancer drug resistance, which leads to recurrence, anticancer medications' harsh and non-selective effects, and the aggressive nature of breast tumors, lesser output in BC treatment has been achieved (Lantz *et al.*, 2007). In addition, medical approach against female reproductive dysfunction has been less successful (Elvis *et al.*, 2016). On prostate cancer cells, anti-oxidants and polyhenolic chemicals in CP are said to have anti-oxidative and cytotoxic effects (Adaramoye *et al.*, 2015). The promise in cancer treatment and reproductive dysfunction by phytochemicals has become crucial due to the limits of current therapy options. The main objective of this study is to investigate the protective effects of fractions of *C. portoricensis* on MNU-induced mammary and reproductive toxicities.

1.4 SPECIFIC OBJECTIVES

- To investigate the protective effect of methanol extract of CP on serum parameters, antioxidants status, and hormone receptors in MNU-administered rats.
- To assess the most potent fraction of root bark of CP *in vitro* using antioxidants methods.
- To examine the chemopreventive impact of the most potent fraction of CP on serum biochemical indices, hormonal profile, antioxidants status, apoptotic, and inflammatory biomarkers in MNU and BP-induced rats.
- To investigate possible anti-proliferative, antioxidative, and apoptotic effects of the most potent fraction of CP on MCF-7 cell line and cell lysates.

- To examine the possible curative impact of the most potent fraction of CP on antioxidant parameters, apoptotic, and inflammatory indices in MNU and BP-induced rats.



Normal breast tissue

© Sam and Amy Collins

Figure 1.1: Normal breast tissue structure (Sims *et al.*, 2007)

CHAPTER TWO

LITERATURE REVIEW

2.1 BREAST CANCER

Cancer is a term that refers to a group of diseases that cause cell mutation and uncontrolled growth (Jaglanian, 2020). Almost all kinds of cancer cells literally form a lump known as tumor (Webb and Kukard, 2020)). These tumors are named after the body parts they originate from. BC can therefore be referred to as uncontrolled proliferated cells originating from the breast tissues (Prakash *et al.*, 2019). Generally, cancer cells are known to be similar to the organism cells they originate from with similar DNA and RNA but not identical. This is the reason why the immune system (especially weakened immune system) can not detect most cancer cells at the initial stage (Acosta-casique *et al.*, 2018). RNA and DNA modifications in normal cells give rise to cancer cells. These alterations may be induced by factors such as radiations, viruses, bacteria, fungi, tissue inflammation and irritation, heat, free radicals, environmental chemicals, and DNA and RNA ageing (Kurubanjerdjit, 2020). All these agents can bring about alterations that may initiate cancer (Knickle *et al.*, 2018). Also, unfavourable conditions such as unhealthy environment, genetic predisposition to mutations, poor diets, and old age often results to high rate of DNA and RNA mutations (Kittaneh nd Montero, 2013).

Breast cancer has been the major leading cancer in women around the world, both in industrialized and emerging nations (Ediriweera *et al.*, 2020; Taka *et al.*, 2021). The existence of BC has been reported around the globe with high income countries having higher incidence rate which varies based on race and ethnicity (Desantis *et al.*, 2014). Despite remarkable approach in diagnosing and treating BC, there are still unresolved clinical and scientific mystery (Illiano *et al.*, 2018; Alehaideb *et al.*, 2020) . In 2020, WHO reported BC as the 5th major cause of cancer deaths around the globe with approximately 685,000 mortality ascribed to it. In Nigeria, increase in urbanisation and

lifestyle changes have contributed to increase in BC cases which are historically low until the recent development in lifestyle expectancy and adjustments (Scully *et al.*, 2012).

2.2 BREAST

The two types of tissues that make up the breast include:

- Secretory tissues (Glandular)
- Supporting tissues (Stromal)

Glandular tissues- Glandular tissues contain lobules and the ducts (i.e the milk-producing secretory vessel and the milk passage). The ducts are the tubes that connect the lobules to the nipple.

Stromal tissues- This includes the breast's adipose and threadlike connective tissues.

Lymphatic tissue-immune system of the breast helps to remove cellular fluids and debris. (Saldara *et al.*, 2014).

Different tumour types may emanate from different areas of the breast. Generally, non-cancerous (benign) changes that occur within the breast results into larger percent of developed breast tumours (Kerdelhu *et al.*, 2016; Kai *et al.*, 2018). Examples includes developed cyst which consists of packets of accumulated fluids, fibrosis, breast pain and lumpiness and thickening areas (Akram *et al.*, 2017). The cells lining the ducts are where the majority of breast tumors begin (ductal cancers). Some cancers start in the cells that line the lobules (lobule cancer), whereas others start elsewhere (Jemal *et al.*, 2010).

The majority of lumps are benign, meaning they will not spread to other regions of the body or kill the patient (Shindikar *et al.*, 2016). Almost all cancers at this stage are curable, since some breast cancers are limited within the ducts or breast lobules and certain breast tumors are *in situ* (Utage *et al.*, 2018). Furthermore, most malignant breast tumours are invasive, entering the breast surrounding tissues through the duct and glandular walls (Weber *et al.*, 2014). The extent to which BC cells invade surrounding tissues is determined by the stage of the disease (Wang, 2017; Jaglanian, 2020).

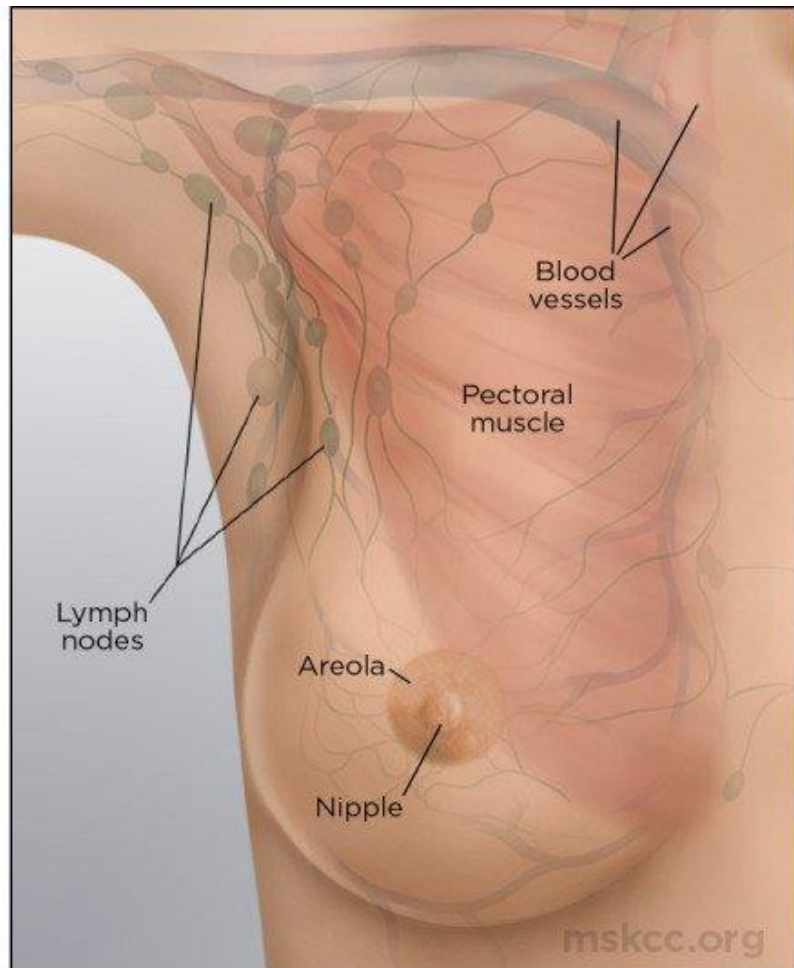
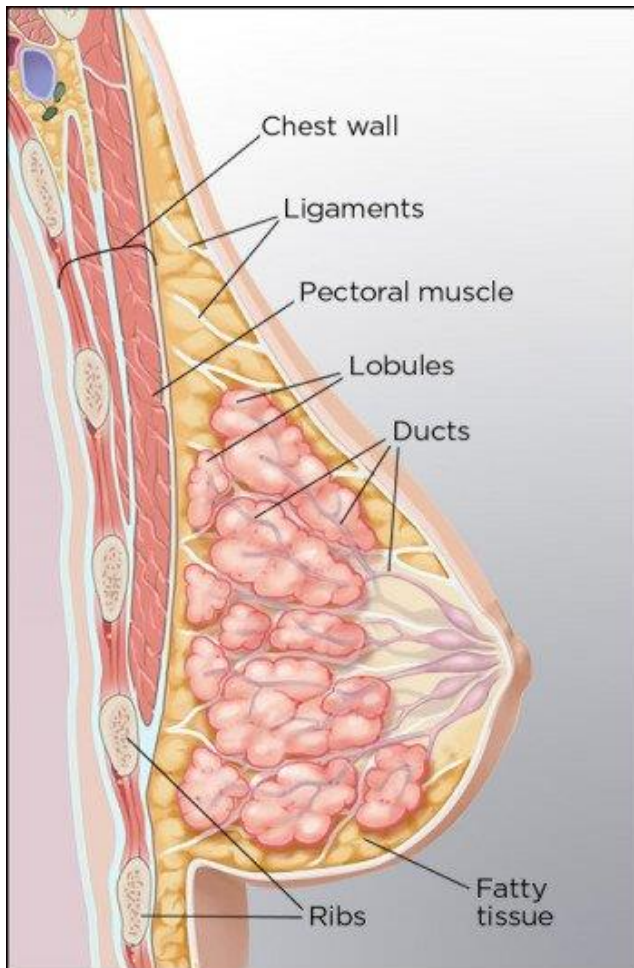


Figure 2.1: Structure of the Breast (Benson and Jatoi, 2012)

2.3 TYPES OF BREAST CANCER

2.3.1 Non-Intrusive Breast Cancer- These are cells that only reside in the tubes and so don't spread throughout the breast's connective and fatty tissues. Ductal carcinoma *in situ* (DCIS) is now the most prevalent kind of non-intrusive breast cancer, which accounts for about 90% of all cases (Weigelt *et al.*, 2010). Despite the fact that lobular carcinoma *in situ* (LCIS) is not as prevalent as DCIS. It is one of the most significant BC risk factors.

2.3.2 Intrusive Breast Cancer- These are invading cells that penetrate the connective and fatty tissues of the breast by breaking through the duct and lobular walls. Cancer cells can be intrusive even if they haven't progressed to the lymph nodes or other organs (Bray *et al.*, 2004).

2.3.3 Common Occurrence in Breast Cancer

2.3.3a *In situ* lobular cancer (LCIS)

Cancer cells that have not gone beyond the initial formed area are referred to be '*in situ*'. LCIS is defined by a considerable spike in cells number in the breast lobules.

2.3.3b *In situ* ductal carcinoma (DCIS)

Most of the prevalent forms of non-invasive BC occur when the breast duct becomes restricted.

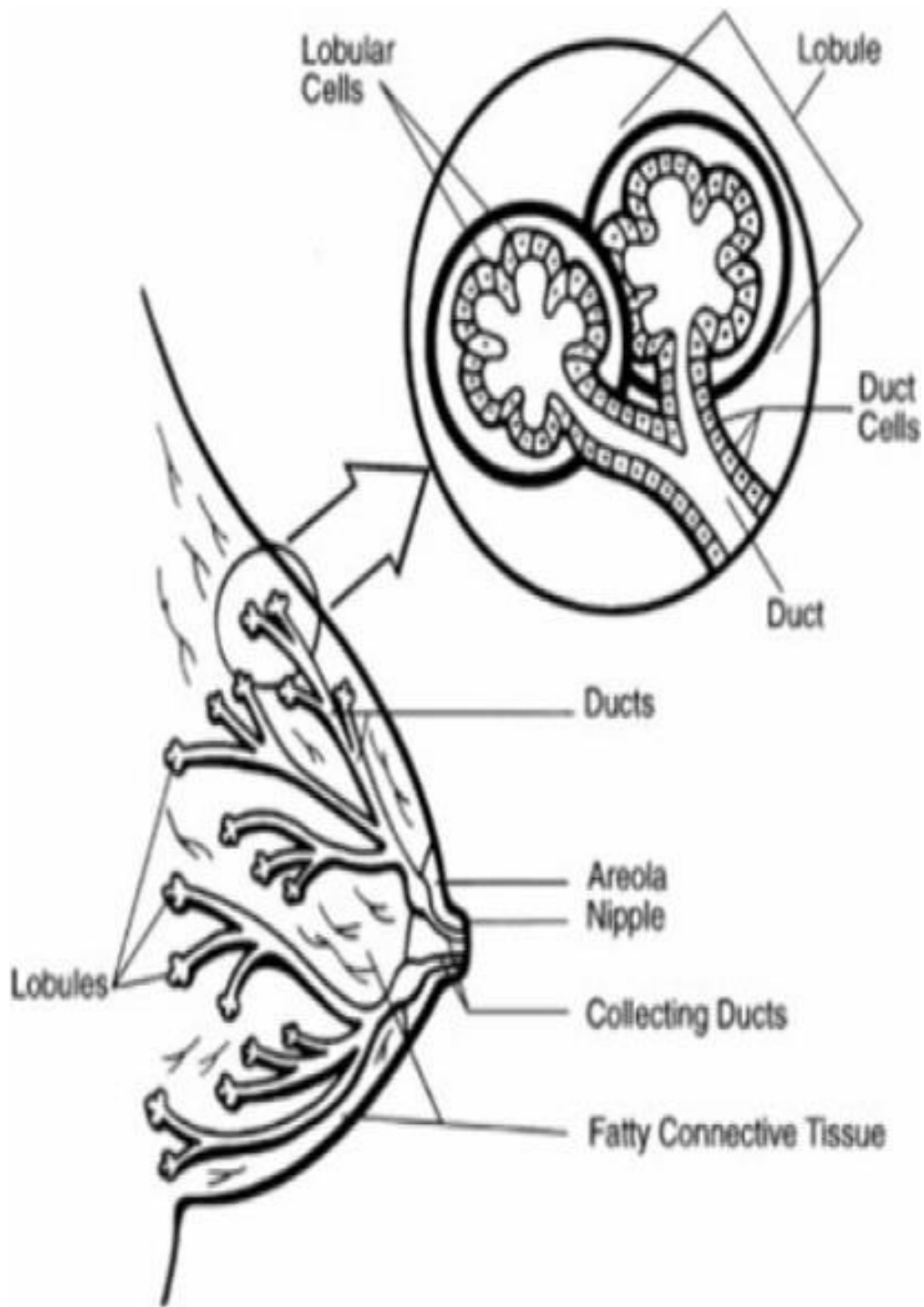


Figure 2.2: Breast Tissue structure showing the ducts, lobules, and fatty tissue (Veronesi *et al.*, 2005)

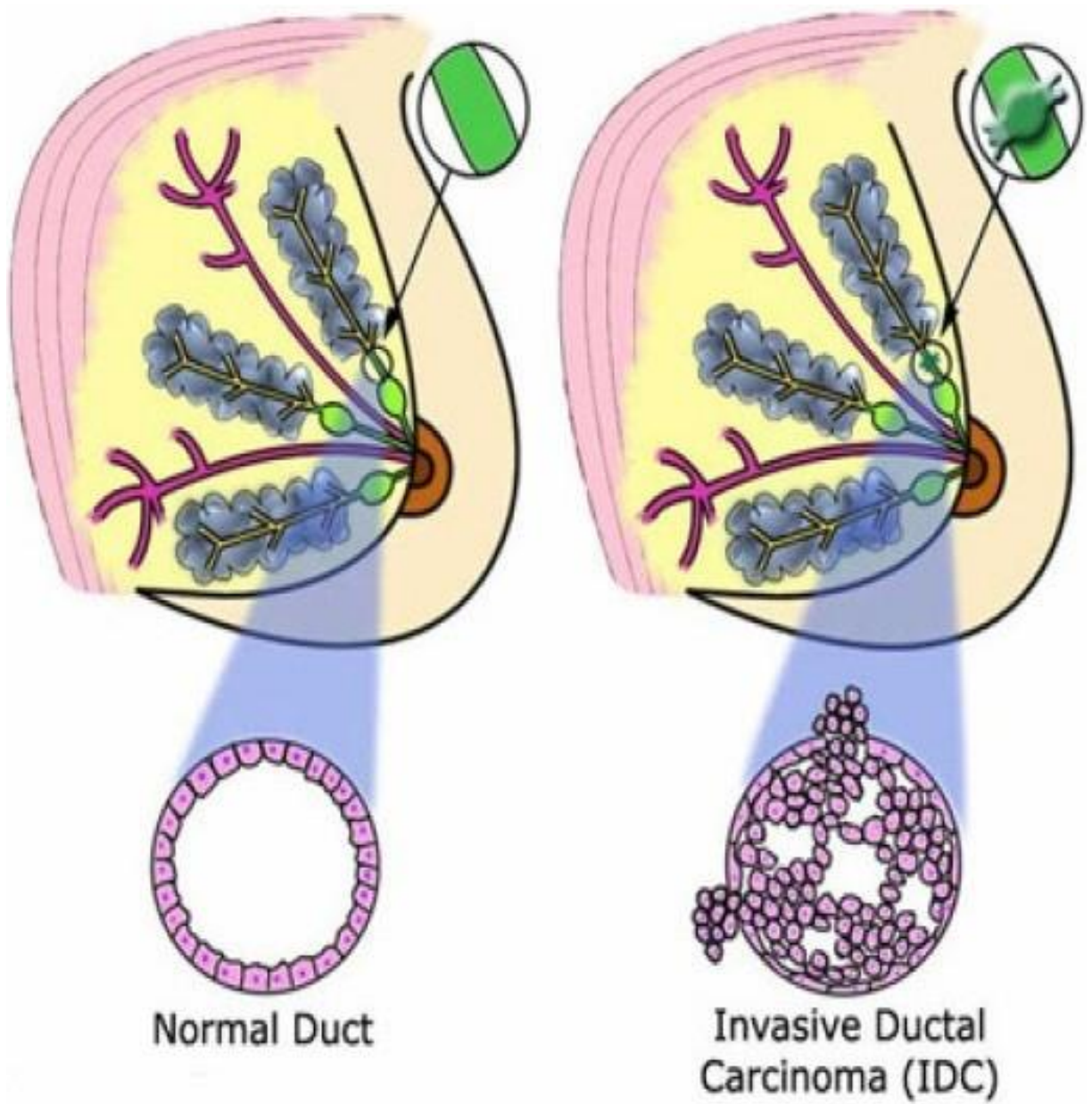


Figure 2.3: Typical Structure Related to Ductal Carcinoma (Veronesi *et al.*, 2005)

2.3.3c Infiltrating lobular carcinoma (ILC)

Infiltrating lobular carcinoma (ILC) commence from the lobules (milk secretory vessels) of the breast and extends to other body parts. A significant proportion of BCs are caused by it (Cedolini *et al.*, 2014).

2.3.3d Infiltrating ductal carcinoma (IDC)

Intrusive ductal carcinoma is another name for IDC. Breast milk ducts are the first to develop IDC, which spreads through the duct wall, into connective, fatty, and other body tissues. It is responsible for more than 80% of all female cancers (Jones, 2008).

2.3.4 Less frequently occurring breast cancer

2.2.4a Carcinoma of the medullary gland

Medullary carcinoma is a tumor that has created a distinct barrier between normal and malignant tissue (an invasive BC). This form of cancer makes up 5% of all BC cases (Taylor *et al.*, 2010).

2.3.4b Mucinous Carcinoma

Colloid carcinoma is another name for mucinous carcinoma. Mucinous carcinoma diagnosed patients have higher chances of better prognosis than patients diagnosed with regular invasive carcinoma (Kittaneh and Montero, 2013). It is known to be generated by mucus-producing cells in the breast.

2.3.4c Tubular Carcinoma

Invading breast carcinoma is uncommon. Invasive carcinoma patients have a worse prognosis than tubular carcinoma patients. This only accounts for about 2% BC diagnoses (Hamed *et al.*, 2018).

2.3.4d Inflammatory Breast Cancer

As a result of cancer cells clogging lymph arteries, red and hot appearance of an inflammatory breast with dimples and thick ridges appears (Lantz *et al.*, 2007). It is very aggressive because it is an unusual type of tumor accounting for 1% of all cases.

(invasive). Inflammatory breast cancer is considered an aggressive and unusual cancer because it grows quickly, more likely to have spread at the time it's found, and is more likely to come back after treatment than other types of breast cancer.

2.3.4e Paget's disease of the nipple

This is an infrequent tumor type that starts in the duct and progresses to nipple area and breast areola. It is an unusual cases that accounts for only 1% of BC cases (Cedolini *et al.*, 2014).

2.3.4f Phylloides Tumor

Phylloides tumor which is either cancerous or non-cancerous begins in the breast connective tissues. It can be treated through surgical procedures. Phylloides tumors are special cases of about 2% mortality in women yearly. It is also spelled as 'phyllodes' (Stephen, 2008).

2.4 CAUSES OF BREAST CANCER

2.4.1 Having had BC in the past

Women suffering from BC history likely to get cancer in other parts of the breast (Shah *et al.*, 2014).

2.4.2 Family history

The risk of BC developing in women is higher if they have a family history of the disease, especially if their mother, daughter, or sister originally developed it (Biau *et al.*, 2016). If more than one members of the family has had BC before, the risk is significantly higher, and it is even higher if the relative was younger at the time of diagnosis (Dai *et al.*, 2018).

2.4.3 Genetic Causes

In genetic predisposition, both paternal and maternal genetic composition contributes to the risk factor. According to a previous study, defects in BC vulnerability genes BRCA1 and BRCA2 are accountable for 5% to 10% of breast tumor cases. (Sanguinetti *et al.*, 2015). Women with BRCA mutations are expected to develop BC at a rate of 57% as they get older (Jemal *et al.*, 2014).

2.4.4 Hormonal Causes

Incidence of BC increases with changes or imbalance in hormone levels. Alteration in hormone levels could be as a result of use of contraceptive pills, irregularity in menstrual cycle, early age pregnancy etc (Wang, 2017).

2.4.5 Environmental Causes

Women who work in industrial locations, are exposed to environmental contaminants, have long-term low-dose radiation exposure, or have undergone intense radiation treatment at younger age in the chest, are at increased chance of developing breast tumor (Gray *et al.*, 2017).

2.5 SIGNS AND SYMPTOMS

When the tumor is small enough to be treated, BC usually has no symptoms (Lantz *et al.*, 2007).

2.5.1 Early Stage

The presence of lumps in the breast or armpit is early onset of BC. Early look out for presence of lumps can be achieved by consistent breast self-examination (BSE) either by self or through the help of second party. This makes it easier to recognize breast size, texture, changes and condition. Basic alarming traits to look out for in the breast are swelling in the breast (lump), swelling armpits (lymph nodes), nipple abnormalities, unusual discomfort in the breast, discharge from the nipple which could either be clear or bloody discharge, nipple pains and scaly nipple (Fatima *et al.*, 2017).

2.5.2 Advanced Stage (Metastasis)

Shortness of breath (lung metastasis), bone pain (bone metastasis), low appetite, weakness, unexplained weight loss (liver metastasis) and headaches are all indications of breast metastasis (Lantz *et al.*, 2007; Scully *et al.*, 2012)

2.6 BREAST CANCER DIAGNOSIS

Early stage diagnosing in cancer treatment is important to BC patients. The screening can be done from a variety of diagnostic platforms. One of the main diagnostic ways for

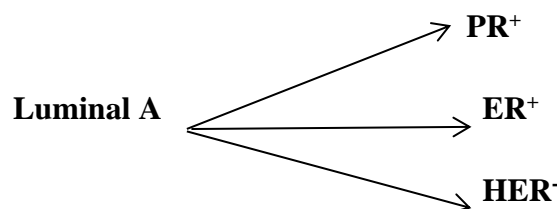
collecting relevant data from patients with BC is to use imaging tools such as Mammography, magnetic resonance imaging (MRI) etc. (Hamed *et al.*, 2018).

2.7 BREAST CANCER MOLECULAR SUBTYPES

The vast molecular and clinical heterogeneity of BC may be separated into four distinct subtypes, each of which is defined in part by the hormone receptor (HR) and other types of proteins associated in each tumour (Fatima *et al.*, 2017). Healthy breast cells usually have estrogen and progesterone as well as a protein called HER-2 which promotes normal cell proliferation (Khalki *et al.*, 2020). Two out of every three women diagnosed with BC had estrogen and progesterone receptors (Bagheri *et al.*, 2018). Also, about 20-30% of BCs have too many HER-2 proteins (Anderson *et al.*, 2014). BC that has receptors for estrogen (ER+) or progesterone (PR+) can be given hormone therapy. However, BC with excessive HER-2 expression, on the other hand, can be given anti-HER-2 targeted therapy medications like trastuzumab, perjeta, Tykerb, Nerlynx and Kadcyla (Anderson *et al.*, 2014). Hormone therapy is not an option for people with triple negative BC as well as medicines that block HER-2, since they lack receptors for estrogen, progesterone, or HER-2. Chemotherapy, radiation treatment, and non-HER-2 targeted therapy are all options for treating triple negative breast cancer (Scully *et al.*, 2012).

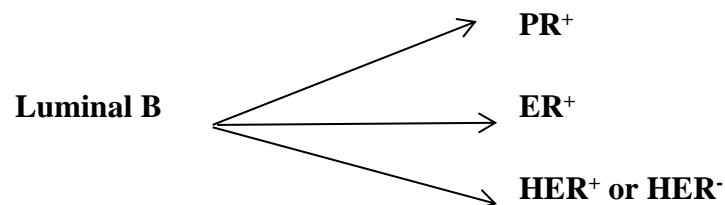
2.7.1 Luminal A- (HR positive / HER2-negative)

It is also referred to as HER-2 negative (Human Epidermal growth factor receptor-2). Luminal A is a common molecular subgroup of BC, and it grows more slowly than other cancer types. ER⁺ or PR⁺ people have positive hormone receptors. This subgroup has a low amount of Ki-67 (a proliferative marker in breast cancer), a protein that controls how quickly cancer cells multiply.



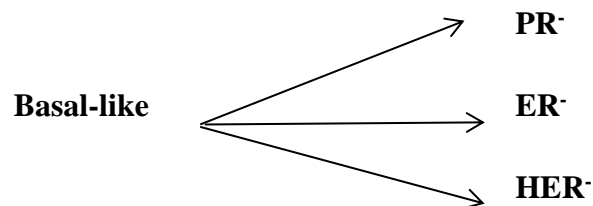
2.7.2 Luminal B- (HR positive / HER2-positive/negative)

This particular subtype depicts both HER positive and HER negative due to overexpression of HER-2. Luminal B cancer cells proliferate more quickly than Luminal A cancer cells and are therefore regarded more aggressive (Prakash *et al.*, 2019). They have greater levels of Ki-67 and are positive for hormone receptors.



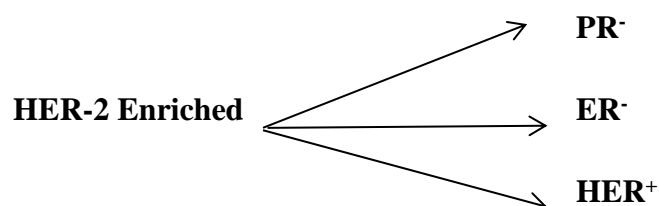
2.7.3 Triple-negative / Basal-like (HR / HER2-negative)

The cells in this kind of cancer lack estrogen, progesterone or HER-2 receptors. BC that begins in the breast ducts is frequently invasive (Alessandra *et al.*, 2018; Arzi *et al.*, 2020). This is usually observed in women with BRCA 1 gene mutations.



2.7.4 HER-2 positive / HER-2 enriched

HER-2 is found in one out of every five invasive BCs. Cancers that are HER-2 positive are also ER⁻, PR⁻ and HER-2 positive (Li *et al.*, 2019). This BC subgroup has an excess of HER-2 gene copies, resulting in the presence of HER-2 protein receptors on breast cells. In ordinary situations, Her-2 sensors control how a healthy breast cell forms, proliferate, and fixes itself (Shehata *et al.*, 2012). When the cells proliferate, on the other hand, the receptors instruct the cells to divide and grow uncontrollably as a result of excessive absorption of HER-2.



2.8 MANAGEMENT OF BREAST CANCER

The patient and physician choose the finest treatment options according to the tumor grade. The biological properties of the tumor, the patient's age and interests, as well as the advantages and disadvantages of possible treatment also must be addressed before treatment begins (Gallego-ortega and Ormandy, 2014). Surgery is commonly used to treat BC patients and it is frequently combined with additional treatments such as chemotherapy, hormone therapy, radiation therapy, or biologic therapy (Gallego-ortega and Ormandy, 2014).

2.8.1 SURGERY

Based on the stage and nature of tumor, surgery may be required to remove cancer from the breast. Different surgical procedures include:

2.8.1a Lumpectomy

It entails the excision of malignant tissue as well as a rim of normal tissue that is eliminated entirely.

2.8.1b Simple or Total Mastectomy

The entire breast is surgically removed during this operation.

2.8.1c Mastectomy using a Modified Radical Mastectomy

The complete breast and underarm lymph nodes must be removed, but not the surrounding chest wall muscle. Because of the proven efficacy of less invasive and disfiguring procedures, radical mastectomy is less commonly utilized or recommended (Bray *et al.*, 2004).

Depending on the surgical type chosen by both the patient and physician, both lumpectomy and mastectomy is frequently followed by lymph node removal from the armpit to see if the cancer has spread to other body parts (Scully *et al.*, 2012). The detection of cancer cells in the lymphoid tissue will indicates whether or not more therapy is necessary, as well as the process to be followed. However, lumpectomy is often followed by radiation therapy.

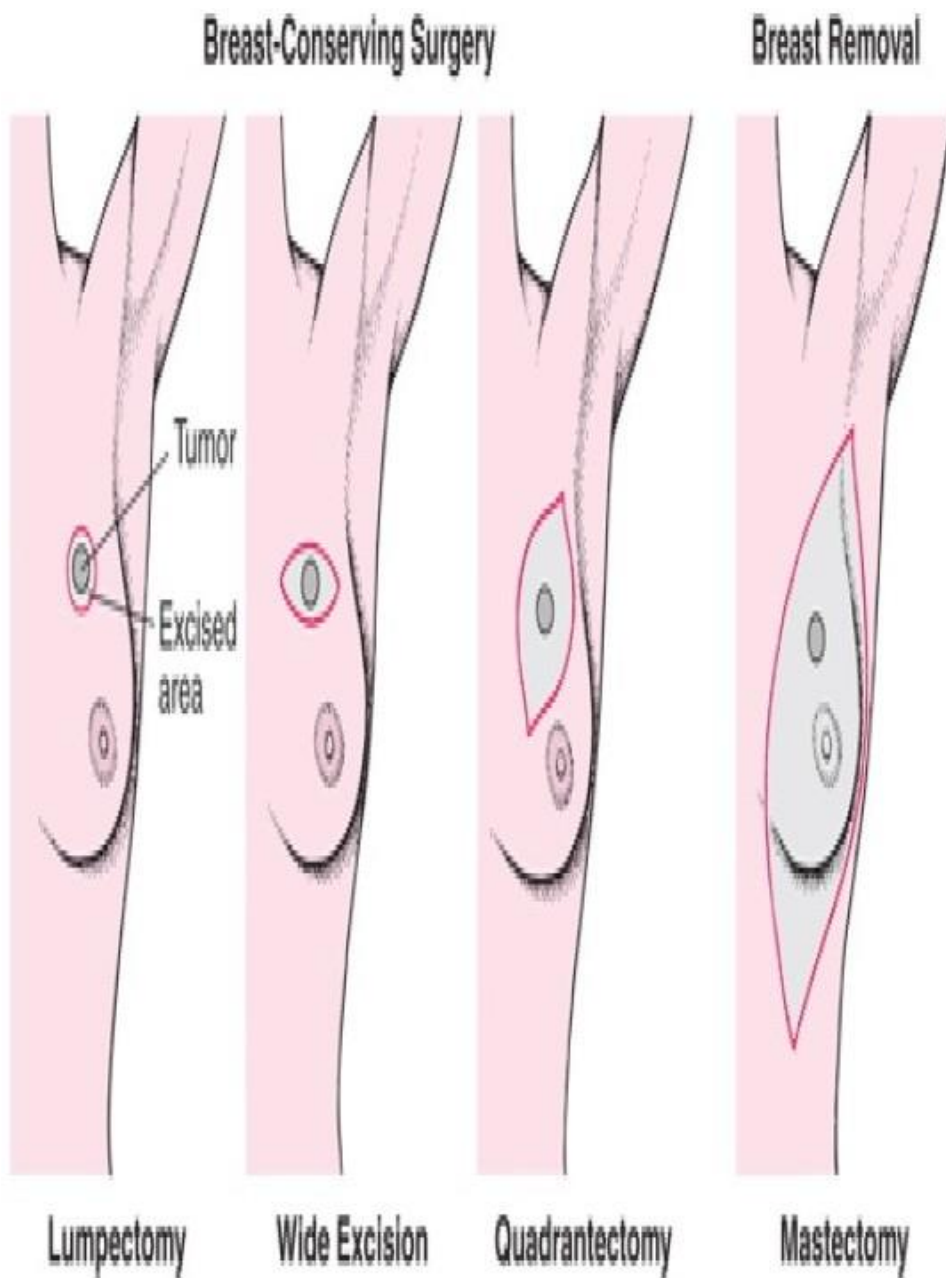


Figure 2.4: Varieties of surgical procedures used in BC (Mamounas *et al.*, 2014)

2.8.2 RADIATION THERAPY

Radiation therapy is used to slow tumor growth before surgery and to destroy cancerous cells which persist after surgery in the breast, chest wall, or armpit. This procedure involves focusing radiation on the cancer-affected areas, which include the entire breast and other affected areas (Webb and Kukard, 2020). The sort of radiation therapy used is determined by the type, stage, and site of the tumor being treated (Lulu, 2017). Radiation therapy is divided into two categories;

2.8.2a Internal Radiation Therapy

This is also known as brachy-therapy. It entails the use of radioactive substance contained in catheters, needles, or wires that are inserted into the cancer directly (Wahba and El-Hadaad, 2015).

2.8.2b External Beam Radiation

Radiation therapy is normally given over five to seven weeks period. It is frequently prescribed, after a lumpectomy and in rare situations after a mastectomy.

2.8.3 SYSTEMIC THERAPY

As part of systemic therapy, anti-cancer drugs can be given intravenously or consumed orally. It can be recommended both before and after surgery. This therapy process includes chemotherapy, hormone therapy, and biologic therapy.

2.8.3a Neo-adjuvant Systemic Therapy

Adjuvant therapy given before the main treatment is called neo-adjuvant therapy. This type of adjuvant therapy can also decrease the chance of the cancer coming back, and it's often used to make the primary treatment such as an operation or radiation treatment easier or more effective. It is a term for the treatment offered to a patient before surgery. It is usually recommended before surgery. It helps to shrink tumor size by making surgical removal process possible, easy and also allow for less extensive surgery. This

process helps patients needed to undergo mastectomy otherwise opt for breast-conserving surgery.

2.8.3b Adjuvant Systemic Therapy

It is a term for the treatment offered to a patient following surgery. After all obvious and detectable malignancy has been eliminated; it is commonly employed to destroy hidden cancerous cells that have invaded other body parts. Since surgical removal of the complete cancer cell is impossible in metastatic breast cancer, systemic therapy is frequently advised. As a result, one of the most commonly suggested therapy alternatives is systematic therapies. Adjuvant treatment is intended to eliminate or delay the appearance of occult micro-metastatic disease, which is believed to be responsible for distant treatment failures after local therapy. Adjuvant chemotherapy has been used in an attempt to reduce recurrence and to improve long-term survival.

2.8.4 BIOLOGIC THERAPY

HER2/neu growth-promoting proteins are over expressed in about 15%-30% of BC cases (Tuli *et al.*, 2019). They tend to grow faster and are most like likely to reccur than tumors that do not over expressed HER2. However, a monoclonal antibody, trastuzumab, helps to directly combat the HER2 over expression in breast tumors, by improving survival benefit in women with metastatic breast cancer (Diermeier-Daucher *et al.*, 2012). Short comings of breast cancer treatment that affect quality of life results in brief and prolonged side effects which includes fatigue, psychological distress, hormonal symptoms etc. Physical activity, on the other hand, has been proven to help alleviate some of the negative effects of BC and its therapy in various studies (Kantarjian *et al.*, 2017; Stein *et al.*, 2018 and Schuster *et al.*, 2019).

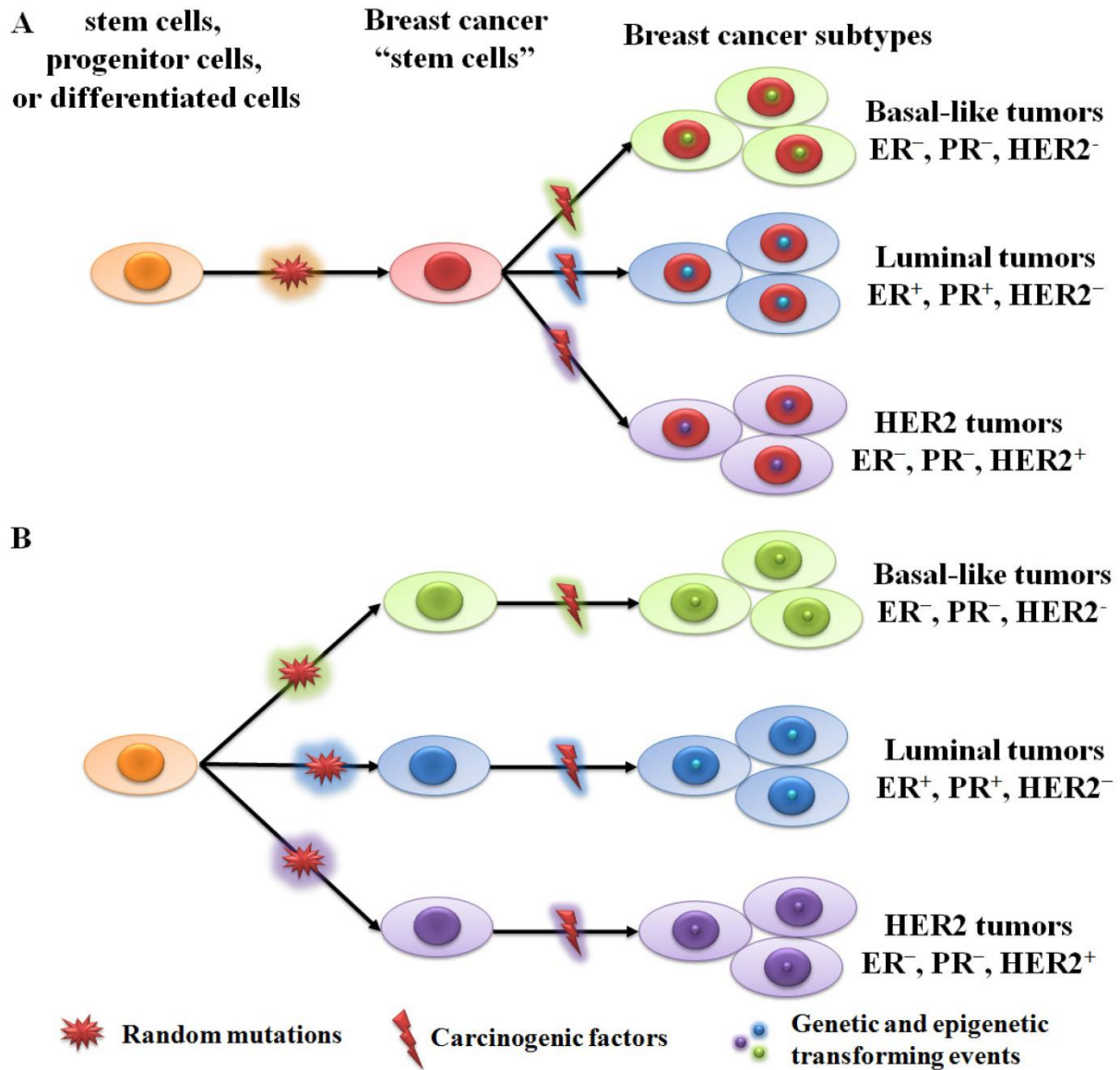


Figure 2.5: Two theories about how breast cancer starts and progresses (Taylor *et al.*, 2010)

- A- All tumor subtypes are made out of the same stem cells or progenitor cells.
- B- Each tumor subtype develops from a single type of cell (stem cell, progenitor cell or differentiated cell).

2.9 RISK FACTORS

Risks are divided into changeable and non-modifiable categories.

The following are the key modifiable risk factors for BC

2.9.1 Overweight and Obesity

Obese older women who have had their first menstrual cycle early and have already entered menopause are known to have an increased risk of BC. Numerous studies have connected obesity to BC (Kai *et al.*, 2018). It has been discovered that high amounts of insulin and insulin-like factors in response to obesity can stimulate cancer cell development (Horgan *et al.*, 2019; Jaglanian, 2020).

2.9.2 Smoking

Active smokers, both post-menopausal and prenatal, have an increased risk of getting BC (Umthong *et al.*, 2011). Passive smoking is also connected to the development of BC (Akram, 2017).

2.9.3 Alcohol

Overindulging in alcoholic beverages can increase the risk of BC. Romieu and colleagues, reported a correlation between alcohol intake and hormone receptor-positive and negative cancers (Sun *et al.*, 2017).

2.10 Reproductive Toxicity

Human exposure to environmental toxicants has recently been on the rise thereby inducing their impacts on reproductive functions (Hunt *et al.*, 2016; Sifakis *et al.*, 2017). Examples of these toxicants includes aflatoxin, cadmium, BP, MNU etc (Dyer, 2014; Louis *et al.*, 2016; Ma *et al.*, 2019). Cadmium and benzo[a]pyrene have been demonstrated to be very poisonous to humans and animals (Shah *et al.*, 2014). Industrial use of these toxicants contributes to its accumulation in the environment (Knez, 2013; Bhardwaj, 2015). Following acute poisoning, they have been demonstrated to target several organs, resulting in reproductive toxicity, nephrotoxicity, carcinogenicity, teratogenicity, endocrine and immune toxicity (Luccio-camelo and Prins, 2011; Miyagawa *et al.*, 2011; Uzumcu and Zama, 2016).

The female reproductive system is known to play a major physiological function to produce ovum necessary for healthy progeny (Diamanti-Kandarakis *et al.*, 2009; Zama and Uzumcu, 2010; Smarr *et al.*, 2016) . Ovum formation and other reproductive activities are aided by the ovarian steroid hormones (Craig and Wang, 2011; Béranger *et al.*, 2012). Hormones released by the brain and pituitary control the ovary's and endometrium's cyclical changes (Smarr *et al.*, 2016). Cadmium, BP, MNU have been documented to target ovary and the uterus by suppressing the production of hormones (Mamounas *et al.*, 2012). Oxidative stress has been linked to the etiology of infertility in both male and female reproductive organs. Approximately 50% of infertility cases are as a result of male reproductive pathologies which are either acquired or congenital thereby impairing spermatogenesis as well as fertility (Elvis *et al.*, 2016; Ziv-Gal and Flaws, 2016; Vander and Wyns, 2018; Ma *et al.*, 2019). Since sperm count and motility are the most important determinants of fertilization strength, men with high levels of oxidative stress or DNA damaged sperm are likely to become infertile (Knez, 2013; Uloma *et al.*, 2016). On the contrary, oxidative stress in female infertility as a result of environmental toxicants continues to be a hot topic because various research have presented inconclusive information about oxidative stress impact on female reproductive organs (Kristini *et al.*, 2014; Ziv-Gal and Flaws, 2016; Vander and Wyns, 2018) .

2.11 *N-nitroso-N-methylurea*

Chemical carcinogens have been used to create tumors in many organs in experimental animals for several decades (Knez, 2013). MNU is a well-known mammary carcinogen and direct alkylating chemical that requires no metabolic activation (Kinoshita *et al.*, 2016). On the basis of substantial evidence of carcinogenicity in experimental animals, MNU has been proven and widely regarded to be a human carcinogen and toxicant (Tueche *et al.*, 2018).

Pharmaceutical items, cosmetics, and other small exposure sources include diet (smoked and fried fish, beer), profession (beautician, plastics, steel, and farming), societal habits (cigarette inhalation), laboratory use, and small contact causes etc (Raj *et al.*, 2003). Accumulation of this chemical in food is linked to processing circumstances including pickled foods kept in humidified condition, smoked in nitrogen rich air, cooked with elevated heat and given nitrate or nitrite (Stuff *et al.*, 2009).

In rats, mice and fishes, MNU may act as a carcinogen, causing cancer to grow in the breast, uterus, ovary, prostate, liver and intestine (Faustino-Rocha *et al.*, 2015). The development of lesions in various tissues is dependent on the animal species, strain, age, MNU dose, and method of administration. In humans, acute exposure to MNU can cause irritation of the eyes and skin, nausea, migraines, and diarrhea (Sledge *et al.*, 2014; Faustino *et al.*, 2015). This model, according to Gullino and colleagues, is the most straight forward method for inducing mammary cancer cells in rats, which have many similarities to humans in terms of tumor origin, connection with steroids hormones and the appearance of their receptors, aggressiveness, modifications in the Wnt/Beta-catenin pathway, and expression of several genes. (p53, caspases etc) in human mammary carcinogenesis (Faustino *et al.*, 2015).

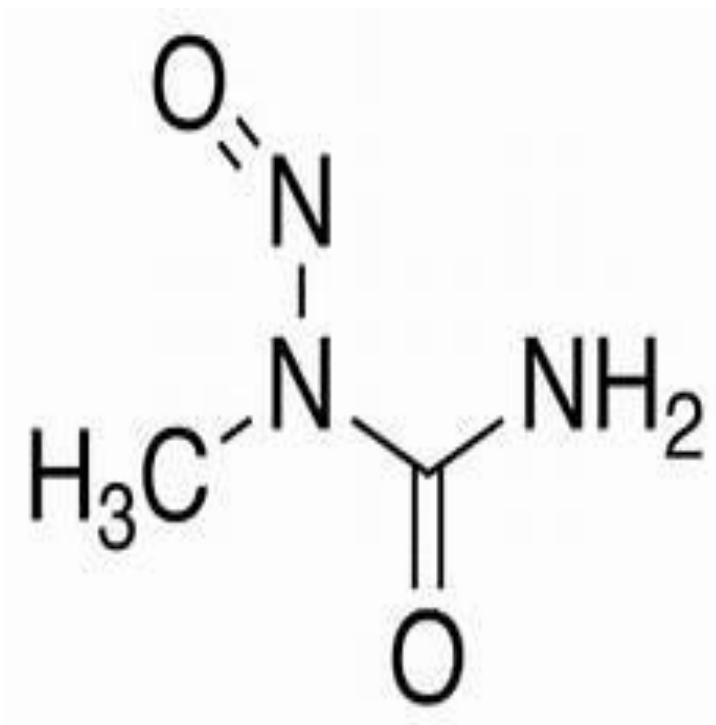


Figure 2.6: *N-nitroso-N-methylurea* (Narayanan *et al.*, 2003)

2.12 Benzo[a]pyrene

The environmental pollutant benzo[a]pyrene (BP) is generated by incomplete combustion, pyrolysis of organic materials, which initiates and promotes cancer development (Alessandra-Perini *et al.*, 2018; Knickle *et al.*, 2018). Except near their sources, these compounds can be found in trace amounts in water, soils, air, and sediments (Cambridge *et al.*, 2006). They are also found in a variety of foods and a few pharmaceuticals. By initiating skin carcinogenesis in mice, BP was found to have both a local and systemic carcinogenic effect, as well as being carcinogenic in single-dose tests (Pugalendhi *et al.*, 2011). Cytochrome P₄₅₀ (CYP1A1) and (CYP1B1) has been identified as the major catalyst in the metabolism of BP and other polycyclic aromatic hydrocarbons (Nguyen *et al.*, 2019). Several findings have documented CYP1A1 as the enzyme with the highest affinity for BP metabolism (Remani, 2019).

When cytochrome P₄₅₀, particularly CYP1A1 and CYP1B1, metabolically activates BP, more reactive molecules are produced. such as BP-7,8-dihydrodiol-9,10-epoxide which react with DNA to produce DNA adducts (Whitsett *et al.*, 2006). The synthesis of benzo[a]pyrene -7,8-epoxide, catalyzed by CYP450 1A1, is the initial step in BP bioactivation, followed by epoxide hydrolase to generate the BP-7,8-dihydrodiol metabolite. Cytochrome P₄₅₀ 1A1 converts this to the BP-7,8-dihydrodiol-9,10-epoxide species also known as diol epoxide (Arumugam *et al.*, 2014). Sources of exposures to BP includes tobacco smoke, cigarette smoke, industrial emission, motor vehicle exhaust, cooking and residential and commercial heating of organic fuel (Nvau *et al.*, 2020).

Findings have reported sides stream cigarette smoke to be three times higher in BP concentration than mainstream smoker (Jemal *et al.*, 2010). Meats that have been barbecued, grilled, or smoked, fried meals that have been processed at high temperatures, bread and grains are all sources of polycyclic aromatic hydrocarbons in the diet (Taylor *et al.*, 2006). Occupational exposures primarily occur through skin contact and inhalation (Raj *et al.*, 2003). BP induces tumors such as lung tumours, skin tumours, liver tumours, forestomach tumours, as well as mammary gland tumours in many species (Whitsett *et al.*, 2006). Human exposures to BP are linked with series of cancers such as in coke production: lung; coal gasifications: bladder, lung etc (Taylor *et al.*, 2006)

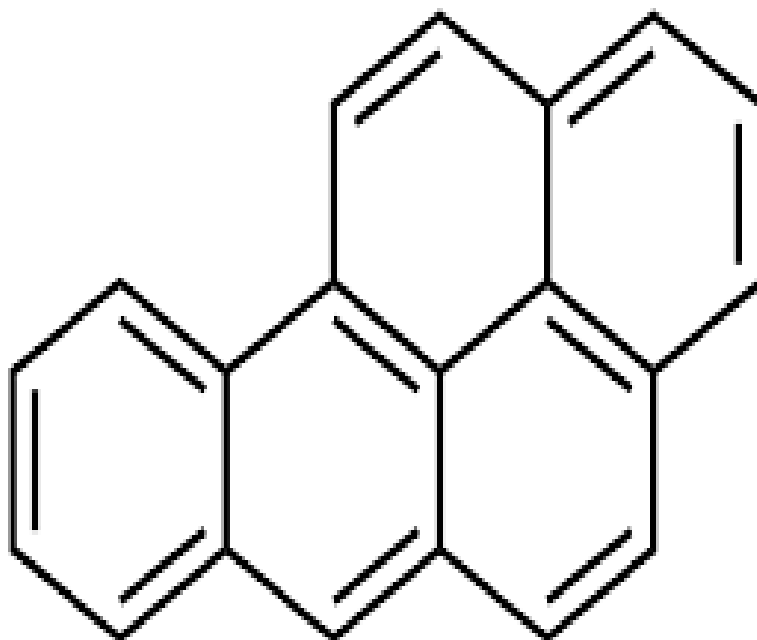


Figure 2.7: Structure of Benzo[a]pyrene (Schwarz *et al.*, 2001)

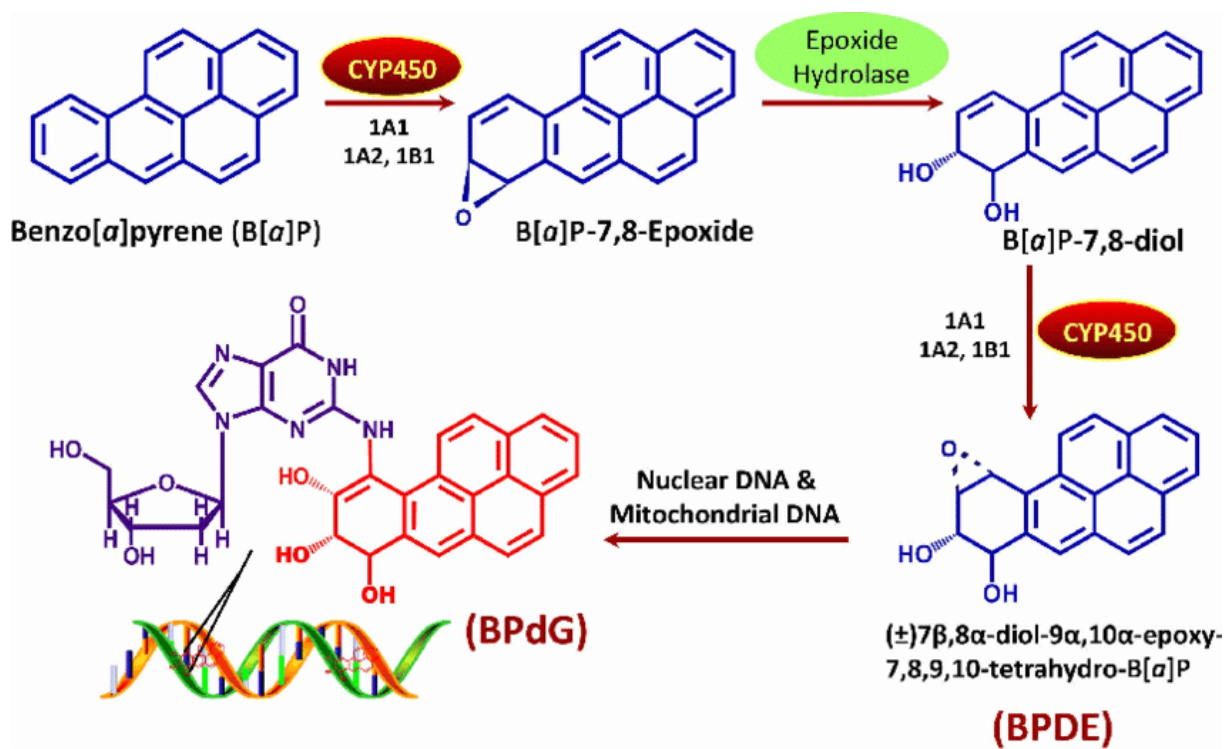


Figure 2.8: Metabolism of Benzo[a]pyrene (Kim *et al.*, 1998).

2.13 *C. portoricensis*

2.13.1 ETHNOMEDICINAL VALUES

C. portoricensis (CP) is a multifaceted plant with a wide range of therapeutic applications. Powder puff, sometimes called CP, is a leguminosae (legume family) permanent shrub (Olorunsogo, 2018 and Oyebode et al., 2019). It blooms with white fragrant flowers that resemble snowballs. It is known as 'Tude' in Yoruba, 'Ule' in Igbo, and 'Oga' in Hausa in Nigeria. In distribution, there are over 200 species of CP distributed across tropical and sub-tropical areas of America, Asia and Africa. Species of *Calliandra* includes *C. eriophylla*, *C. anomala*, *C. haematocephala*, *C. portoricensis* among others (Peter *et al.*, 2012). The CP is traditionally used in Nigeria herbal homes for treating breast engorgement and other related diseases.

In South eastern and South western Nigeria, traditional herbal homes have successfully explored CP extracts to treat snake bites, diarrhoea, pain relief and for managing sickle cell crisis (Amujoyegbe *et al.*, 2014). It is also used as worm expeller, for treating toothache, coated tongue and enlarged tonsil. Rahaman Onike, 2010 equally reported that a book entitled 'A textbook of Medicinal Plants' documented the use of CP in treating fever, stomach disorder, amenorrhoea, and lumbago. In Ghana, it was reported that the root bark of CP when mixed with pepper can be used for treating gonorrhoea, headache relief, promoting sneezing and in ophthalmic preparation (Agunu *et al.*, 2005). Also, traditionally, its concoctions are used for treating snakebites by grounding the roots into powder or squeezing the leaves juice into alcoholic beverage (Onyeama *et al.*, 2013). Despite its numerous advantages, nothing is known regarding its impact on BC and reproductive dysfunction.

2.13.2 PHYTOCHEMICAL SCREENING AND COMPOSITION OF *C. portoricensis*

Onyeama *et al.*, (2012) qualitatively evaluated CP extract for alkaloids, saponins, tannins, flavonoids, polyphenols, reducing chemicals, glycosides, phlobatanins, anthraquinones and hydroxymethyl groups (Onyeama *et al.*, 2013; Mileo *et al.*, 2019). His findings showed the phytochemical screening of CP extract confirmed the absence of tannins, phlobatannins, anthraquinones and hydroxymethyl anthraquinones in both fresh and dry samples (Gbadamosi, 2012). In addition, he reported the presence of alkaloids

and glycosides (Tiwari and Rai, 2016). He also stated that alkaloids functions and importance in plants metabolism are arguable because most alkaloids are known to be very toxic. Furthermore, flavonoids, steroids, polyphenols, glycosides, saponins and reducing chemicals were discovered in the phytochemical screening of CP (Orishadipe *et al.*, 2010; Onyeama *et al.*, 2012; 2013).

2.13.3 ANTIMICROBIAL AND ANTI-ULCER ACTIVITIES OF *C. portoricensis*

Aguwa and Lawal, (1988), were the first to report on the antibacterial properties of CP, utilizing ethanol and aqueous plant extracts. However, Orishadipe *et al* (2010) and Oguegbulu *et al.*, (2020) both demonstrated the antimicrobial activity of CP using nine human pathogens including fungi, gram positive and negative bacteria namely *Staphylococcus aureus*, *Escherichia coli*, *Bacillus subtilis*, *Klebsiella pneumonia*, *Streptococcus fecalis*, *Candisa albican*, *Samonella gallinallum*, *Pseudomonas aeruginosa*, and *Aspergillus nigar* (Orishadipe *et al.*, 2010). According to Oguegbulu *et al.*, (2020) the leaf and root extracts of CP had antibacterial and antifungal activity against a variety of human infections, with the leaf extract having lower antibacterial and antifungal characteristics than the root extract.

Similarly, Orishadipe *et al.*, (2010) equally demonstrated that the *n*-hexane extract of CP was active against *S. aureus*, *E.coli* and *S. gallinallum* while no activity was reported for *K. pneumonia*, *B. subtilis*, and *P. aeruginosa* respectively (Aguwa and Lawal, 1988; Orishadipe *et al.*, 2010). Also, Aguwa and Lawal reported the anti-ulcer activity of ethanol and aqueous extract of CP by using indomethacin-induced ulcers model (Aguwa and Lawal, 1988; Lin and Tan, 1994). Their findings documented that both extracts exhibited ulcerogenic effects (Ukwe, 2008). It was also stated that aqueous extract of CP were more effective compared to ethanol extract confirming the ulcer-protective activity of CP leaf extracts (Lin and Tan, 1994).

2.13.4 CHEMICAL CONSTITUENTS OF *C. portoricensis* USING GC-MS

Orishadipe *et al.*, (2010) investigated the chemical contents of CP using GC-MS, and their findings documented the existence of the following identified chemicals in the hexane fraction of *C. portoricensis* root bark; undecane, dodecane, decenal, 4-ethyoxycyclohexanone, 3,7-dimethylundecane, tetradecane, 2-methyltetradecane,

tetradecanoic acid methyl ester, 9-hexadecenoic acid methyl ester, 14-methylpentadecanoic acid methyl ester, hexadecanoic acid, hexadecanoic acid ethyl ester and 14-methylhexadecanoic acid methyl ester. Some of the compounds that were not identified according to his report were as a result of low concentration which is less than 2% as required by the gas chromatography-mass spectrometry machine. NIST 62 library was employed to compare the mass spectrum of each identified compound (Orishadipe *et al.*, 2010).

2.13.5 ANTICONVULSANT AND ANALGESIC ACTIVITIES OF *C. portoricensis*

C. portoricensis has been widely used traditionally by Southern part of Nigeria for treating convulsions and gastrointestinal problems. The anticonvulsant property of CP was first reported by Adesina and Akinwumi, (1988). However, Akah *et al.*, (1987) equally demonstrated anticonvulsant activity of CP using pentylenetetrazole and electroshock-induced convulsion model. His findings demonstrated that the aqueous extracts of both CP root and stem proffered protection against PTZ- and electroshock-induced convulsions in mice, thus, possessing anticonvulsant activity when administered intraperitoneally (Aguwa and Lawal, 1988).

Using acetic acid-induced squirming and formalin distress provocation tests, Agunu *et al.*, (2005) assessed the analgesic activity effectiveness of CP root and leaf methanol extracts in mice and rats. Their finding suggested that the root and leaf extracts of CP have analgesic property by subduing abdomoinal cramping induced by acetic acid as well as the abdominal pains triggered by the formalin test (Correa *et al.*, 1993; Amujoyegbe *et al.*, 2014)

2.13.6 ANTIOXIDANT AND ANTI-VENOM PROPERTIES OF *C. portoricensis*

Traditional herbalists over the years have explored the use of ethanol extract of CP by squeezing out the juicy part of the plants specifically as anti-haemotoxin of snakebites. However, studies have corroborated the use of CP traditionally in South eastern part of Nigeria for treating snake bites and oxidative stress generated in envenomed rats (Pe *et al.*, 2012; Onyeama *et al.*, 2013). Onyeama and collaborators clearly stated that the viperian venom overwhelmed the naturally-existing antioxidant defense enzymes in experimental rats. Also, their findings further suggested that the ethanol and methanol

extract of CP may be useful in alleviating and reversing the haemotoxin-induced haemotoxicity in *Wistar* rats as a result of an increase in haemoglobin concentration following co-administration of CP. In addition, CP methanol extract also stimulated antioxidant defenses in male *Wistar* rats, according to Pe *et al.*, (2012). Furthermore, Adaramoye *et al.*, (2015) equally established the antioxidative capacity of CP methanol extract *in vitro* by displaying strong reducing activities.

2.13.7 ANTI-PROLIFERATIVE AND CYTOTOXIC EFFECTS OF *C. portoricensis*

Adaramoye *et al.*, (2015) examined the anti-proliferative effects of *C. portoricensis* on LNCaP and PC-3 cells and discovered that PC-3 growth was inhibited in a concentration-dependent way. In addition, their studies confirmed CP's anti-angiogenic action in CAMs, with the results indicating a considerable reduction in vessel size in CAMs (Adaramoye *et al.*, 2015; Oyebode *et al.*, 2019, 2018) . Furthermore, Oyebode *et al.*, (2018; 2019) also found that the methanol portion of CP suppressed the proliferation of LNCaP, DU-145, lung cancer and healthy VERO cells respectively.

2.13.8 SAFETY AND TOXICITY OF *C. portoricensis*

Chronic treatment of *C. portoricensis* root and leaf extract to mice and rats may affect gastrointestinal and pancreas function (Ofusori *et al.*, 2011). The lethal dose acute toxicity of the CP was demonstrated by Onyeama *et al.*, (2013). They reported that administration of the CP extract at 39mg/kg, 625mg/kg and 10,000mg/kg resulted in high mortality in the last two groups except in the first that received 39mg/kg where there was only one death after 24hrs.



Figure 2.9: Photograph of *C. portoricensis* (Amujoyegbe *et al.*, 2014)

CHAPTER THREE

MATERIALS AND METHODS

3.1 CHEMICALS AND REAGENTS

N-nitroso-*N*-methylurea, Benzo[a]pyrene, Dithiobis-(2-dinitrobenzoic acid) (DTNB), Sulphosalicylic acid, Hydrogen peroxide, Potassium dichromate, Sodium azide, 1-chloro-2,4-dinitrobenzene (CDNB), Trichloroacetic acid, Adrenalin, Sodium hydroxide (NaOH), Thiobarbituric acid (TBA), Phosphoric acid (H₃PO₄), Sulfazilamide, Reduced glutathione (GSH), Alanine aminotransferase (ALT), Aspartate aminotransferase (AST), Bilirubin, Naphthylene dihydroxide, Phosphoric acid, 2,2-Diphenyl-1-picrylhydrazyl (DPPH), 2,2-azinobis (3-ethylbenzothiazoline-6-sulfonic acid), Ammonium sulphate (NH₄SO₄), Ethylene diethylamine (EDTA), Triton-X100, kits for Interleukin-1 β (IL-1 β), BAX, Caspase-3, Caspase-9, Immunochemical staining of β -catenin, BAX, p53, Caspase-3, Caspase-9, Interleukins (-6 and 1 β), iNOS and COX-2 proteins. Other chemicals and reagents were of a high analytical quality.

3.2 PLANT MATERIAL PROCESSING AND EXTRACTION

C. portoricensis (CP) was obtained fresh from Odofin Agbegi village, Ikire, Osun State. Forest Herbarium Ibadan (FHI) number 111949 was used to validate the CP. The roots were cleaned, stripped and dried in the laboratory for two weeks before being pulverized and weighed. Cold extraction was used to extract the powdered roots with *n*-hexane and methanol. The methanol extract was evaporated to dryness (40°C). The methanol extracts was partitioned to get the chloroform, butanol, and ethyl-acetate fractions of CP. Below is the extraction flow chat of the CP.

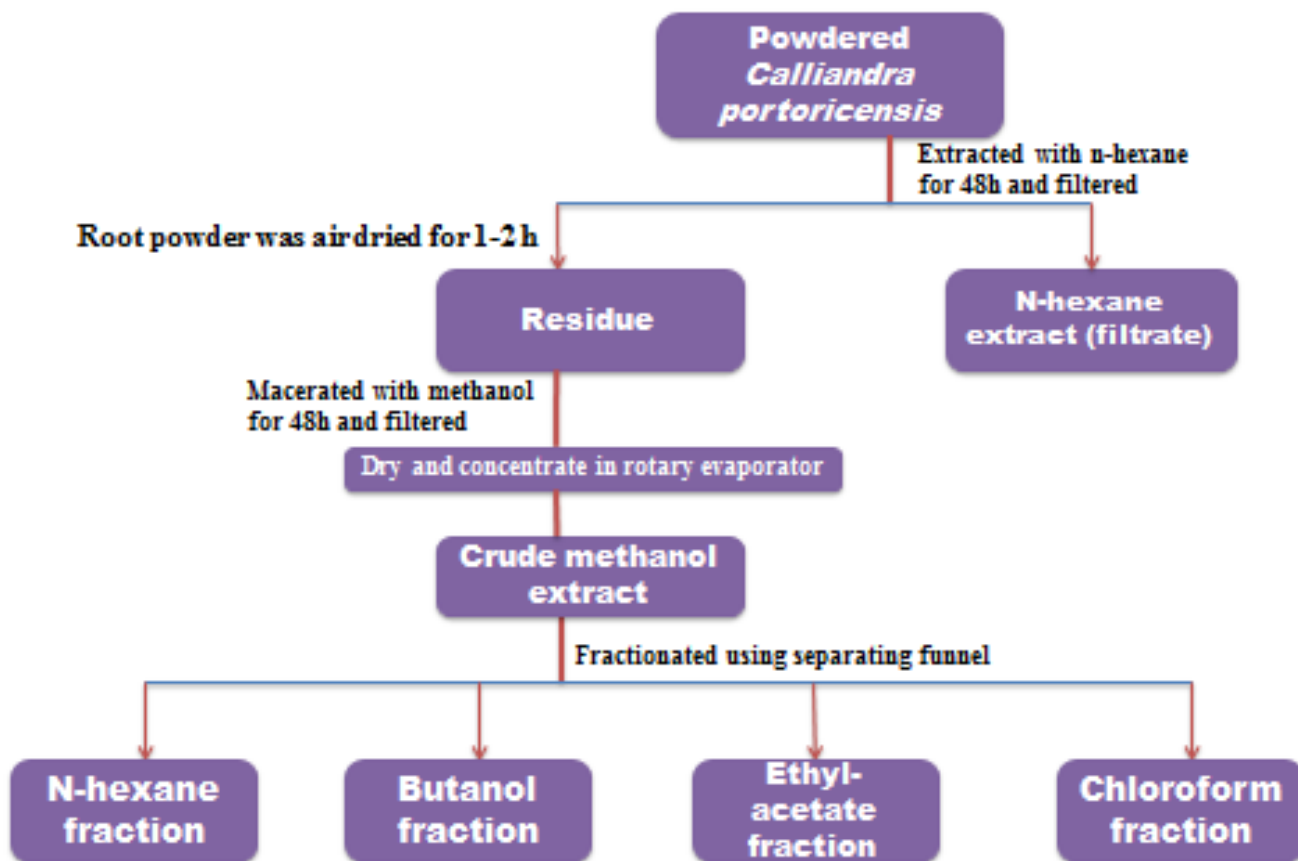


Figure 3.1: Extraction process of *C. portoricensis*

3.3 DETERMINATION OF REDUCING ACTIVITY OF 2,2-DIPHENYL-1-PICRYLHYDRAZYL (DPPH)

The DPPH activity was carried out as stated by Menezes *et al.*, (2001).

Principle

The highest optical density of freshly synthesized DPPH is 517 nm, resulting in a rich purple color solution. Addition of antioxidants alleviate DPPH by reducing the purple colour to an oxidized product 2,2-diphenyl-1-hydrazine thereby resulting into a reduction in optical density. The dissolution of the DPPH radical by the antioxidants can be assessed using spectrophotometer and expressed as radical scavenging ability.

Preparation of Reagents; See Apendix 1

Procedure

40 µg -2000 µg extract was prepared in 4mL distilled water into six different test tubes. 1 mL from each test tube was dispensed into another three separate test tubes (triplicates). To each of the triplicate, 1mL of DPPH was added and was allowed to stand for 30 minutes at 37°C before reading at 517 nm. Catechin was used as standard.

Calculation

$$\% I = [(A_{\text{Control}} - A_{\text{sample}}) / A_{\text{Control}}] \times 100 \quad \dots\dots\dots \text{EQU 3.3}$$

A_{control} - control optical density with no test compound, A_{sample} denotes the test compound optical density, and % I denotes the proportion inhibition of the DPPH oxidants.

3.4 ASSESSMENT OF ABTS [2,2-azinobis- (3-ethylbenzothiazolin-6-sulfonic acid)] REDUCING ACTIVITY

ABTS activity was carried out as stated by Roberta *et al.*, (1999).

Principle

The interaction between ABTS (7 mM) in H₂O and K₂S₂O₈ (potassium persulphate; 2.45 mM) kept in the dark at 37°C for 12 hours generates the ABTS⁺ cation radical. The mixture was mixed with ethanol before use to get absorbance of 0.70 ± 0.025 at 734 nm.

Preparation of Reagents; See Appendix 2

Procedure

ABTS and potassium persulfate solution was mixed together in the dark and allowed to stand for 12-16 hours before use. At 12 hours 2mL of ABTS working solution was diluted with about 65-70 mL of acetate buffer (pH 0.5) to get a working solution at (0.700 ± 0.025) using spectrophotometer preceding the reagent use. 500 μ L of ABTS mixture was introduced into microcuvette and the extracts was added at varying concentrations starting from 50 μ L, 100 μ L, 200 μ L, 300 μ L and 400 μ L respectively. An absorbance measurement was conducted for 6 minutes at 734 nm.

3.5 THIN LAYER CHROMATOGRAPHY ASSESMENT OF FRACTIONS OF *Calliandria portoricensis*

The origin and solvent front is marked using a pencil on a TLC plate. To spot the plate, a capillary tube is used to spot different fractions of CP on the marked TLC plate a couple of times to ensure the presence of the sample for smooth separation. Once the CP fractions have been spotted on the plate, it is then gently placed in a small glass capillary chamber filled with the mobile phase (ethylacetate-chloroform) and ensuring the origin spot are not below the solvent level in the chamber. The solvent is then allowed to run within a centimeter of the top of the plate and remove it with tweezers. Using a pencil, a line is immediately draw across the plate where the solvent front can be seen. The proper location of this solvent front line is important for calculations. The separated spots is observed under the UV light.

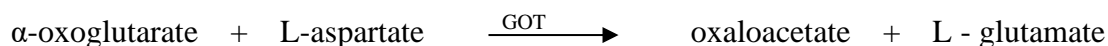
$$\text{Rf value} = \frac{\text{Distance moved by spot}}{\text{Distance moved by solvent}}$$

3.6 ASSAYS OF SERUM ENZYMES

3.6.1 Aspartate Aminotransferase (AST) Activity Measurement

The activity of AST was carried out as stated by Reitman and Frankel (1957).

Concept



AST was tested using the amount of oxaloacetate hydrazone generated by 2, 4-dinitrophenylhydrazine.

Reagents; See Appendix 3

Procedure

Phosphate buffer (100 mmol/L, pH 7.4), L-aspartate (100 mmol/L) and α -oxoglutarate (2 mmol/L) were mixed with the diluted sample (0.1 mL) and incubated at 37°C (30 minutes duration). In the reaction mixture, 2, 4-dinitrophenylhydrazine (0.5 mL; 2 mmol/L) was added and allowed to stand at 25°C for exactly 20 minutes. After 5 minutes, the optical density was recorded at 546nm against the reagent blank using NaOH (5.0 mL; 0.4 mol/L)

3.6.2 Alanine Aminotransferase (ALT) Activity Measurement

The activity of ALT was carried out as stated by Reitman and Frankel (1957).

Concept



Alanine aminotransferase was tested using the amount of pyruvate hydrazone generated by 2, 4-dinitrophenylhydrazine.

Preparation of Reagents; See Appendix 4

Procedure

Phosphate buffer (100 mmol/L, pH 7.4), L-alanine (100 mmol/L) and α -oxoglutarate (2 mmol/L) were mixed with diluted sample (0.1 mL) and incubated at 37°C (30 minutes duration). The reaction mixture was given 2, 4-dinitrophenylhydrazine (0.5 mL; 2 mmol/L) and allowed to stand at 25°C for exactly 20 minutes. After 5 minutes, the optical density was measured at 546 nm against blank.

3.6.3 Bilirubin level Measurement

The level of bilirubin was determined using the principle provided by (Jendrassik and Grof, (1991).

Principle

An alkaline solution of diazotised sulphanilic acid reacts with conjugated (direct) bilirubin to produce a blue-colored complex.

Preparation of Reagents; See Appendix 5

Procedures

As prescribed by the bilirubin kit, a drop of R2 was added to 0.2 mL of sample and 1 mL of R3 for 10 minutes at 20-25°C. Thereafter, 1 mL of R4 was introduced into the reaction mixture which was then incubated at 25°C for 5-30 minutes. Absorbance readings was taken at 578 nm. R1 was added to replace the sample, which served as sample blank.

3.6.4 Lactate dehydrogenase (LDH) Activity Measurement

The activity of LDH was determined using the principle provided by Weissnar and Colleagues, (2014).

Principle

Lactate dehydrogenase is an oxidoreductase which catalyses the interconversion of lactate and pyruvate. The non-radioactive colorimetric LDH assay is based on the reduction of tetrazolium salt MTT in a NADH-coupled enzymatic reaction to a reduced form of MTT which exhibits an absorption maximum at 565 nm. The intensity of the purple color formed is directly proportional to the enzyme activity. LDH is most often measured to evaluate the presence of tissue or cell damage.



Preparation of Reagents; See Appendix 6

Procedure

The sample (0.02 mL) was pipetted into the cuvette after substrate (1.0 mL) and buffer was pipetted. At 37°C, mixture was mixed and incubated. At 340 nm, absorbance were measured and recorded for 3 minutes at 1 minute intervals.

Calculation

By multiplying the change in absorbance by 8095, the LDH activity is calculated in Unit per litre (U/L).

$$\text{LDH activity (U/L)} = 4127 \times \Delta A_{340} \text{ nm/min} \dots\dots\dots \text{EQU 3.5.4}$$

3.7 BIOCHEMICAL ASSAYS: OXIDATIVE STRESS AND INFLAMMATION BIOMARKERS

3.7.1 Protein Concentration Measurement

The protein concentrations in mammary, uterine, and ovarian homogenates, were determined using the Biuret method (Sánchez, 1951).

Concept

The assay relies on the production of a blue compound with a 540 nm optical density. When Cu^{2+} and proteins reacts under alkaline circumstances. Copper sulphate, potassium iodide and sodium titrate make up the Biuret reagent. A bovine serum albumin (BSA) standard curve is commonly used to calibrate this method.

BSA Standard Curve Calibration

0.05-0.5 mg of protein/mL of BSA stock solution was serially diluted in normal saline. Each protein (1 mL) standard solution received 4 mL of Biuret reagent which was left for 30 minutes at 37°C. The absorbance was measured at 540 nm , and an absorbance graph was generated against BSA concentrations.

Reagents Preparation; See Appendix 7

Protein Concentration Measurement in Samples

Distilled water was used to dilute the homogenates (mammary, uterus, and ovary). This was required to decrease the protein sample to Biuret method's sensitivity range. Biuret (1 mL) was introduced to the samples (diluted), and reaction were permitted to stand at 37°C for 30 minutes before recording the optical density at 540 nm. To acquire the actual concentration of sample's protein, the concentration of protein in the extrapolated samples were multiplied by the dilution factor after calibration with BSA.

3.7.2 Determination of Lipid Peroxidation Product

The TBARS formed during LPO were measured to determine lipid peroxidation product, as stated by (Susana *et al.*, 2001).

Principle

The interaction between TBA and MDA, an end product of LPO, is the basis for this approach. The product turns pink when heated in an acidic pH environment, absorbs maximum at 532nm, and may be extracted into organic solvents like butanol. The amount of free MDA produced is commonly used to calibrate this test, and the results are given in $\mu\text{M}/\text{mg}$ protein.

Preparation of Reagents; See Appendix 8

Procedure

Aliquot sample (0.4 mL) was combined with Tris-KCl (1.6 mL) buffer and 10% TCA (0.5 mL). After that, 0.75 % TBA (0.5 mL) was introduced and the mixture was incubated at 80°C for 45 minutes. After cooling in ice, then the mixture is centrifuged for 10 minutes at 3000 rpm. The optical density of the clear pink solution was recorded at 532nm against a H₂O blank. The MDA level was estimated using the Todorova *et al.*, technique (2005). Using molar extinction coefficient of $1.56 \times 10^5 \text{M}^{-1}\text{cm}^{-1}$, lipid peroxidation in units /mg protein or gram tissue was calculated.

3.7.3 Superoxide Dismutase (SOD) Activity Measurement

The activity of SOD was determined using the principle provided by Misra and Fridovich, (1972).

Principle

In SOD assay, superoxide anions are produced by the action of xanthine oxidase. Superoxide dismutase catalyzes the dismutation of superoxide anion into H₂O₂ and O₂. Superoxide anion acts on WST-1 (tetrazolium salt) to produce a water-soluble formazan dye which can be detected by the increase in absorbance at 450 nm. The greater the activity of superoxide dismutase in the sample, the less formazan dye is produced.

Preparation of Reagents; See Appendix 9

Procedure

In a cuvette, sample (50 μ L) was mixed with carbonate buffer (2.5 mL, 0.05M at pH 10.2) and epinephrine (0.3 mL) via inversion. An absorbance at 480 nm was taken over the course of 2.5 minutes.

Calculation

$$\text{Change in optical density per minute} = \frac{A_f - A_i}{2.5}$$

A_i = initial optical density

A_f = final optical density

$$\% \text{ Inhibition} = \left(\frac{\text{Increase in sample optical density}}{\text{Increase in blank optical density}} \right) \times 100 \dots\dots\dots \text{EQU 3.6.3}$$

The amount of superoxide dismutase required to block the oxidation of adrenalin by at least 50% is defined as a unit of superoxide dismutase activity.

3.7.4 Catalase Activity Measurement

Claiborne *et al* technique was used to determine catalase activity (1984).

Principle

The reduction of absorbance recorded at 240nm as catalase breaks down hydrogen peroxide is the basis for this approach. The extinction coefficient was calculated using the method described by Noble and Gibson (1970).

Preparation of Reagent; See Appendix 10

Procedure

In a 1 cm quartz cuvette, sample (50 μ l) was pipetted into 19 mM hydrogen peroxide (2.95 mL) mixture and inverted to mix. The readings were taken every 5 minutes at 240nm. .

3.7.5 Glutathione-S-Transferase (GST) Activity Measurement

GST activity was measured using Habig *et al* technique (1974).

Principle

When using 1-chloro-2,4-dinitrobenzene as the second substrate, glutathione-S-transferases have relatively high activity. As the substance is conjugated with reduced glutathione, its maximum absorption wavelength shifts. The new 340nm wavelength's at increased absorption enables for a direct assessment of the enzyme process.

Reagents preparation; See Appendix 11

Procedure

The estimation medium consisted of 30 mL of reduced glutathione (0.1 M) added to 150 mL of 20 mM of 1-chloro- 2, 4-dinitrobenzene (CDNB), followed by 2.82 mL of 0.1 M Phosphate buffer (pH 6.5) and 30 mL of Cytosol/Microsomes. Before the absorbance was measured at 340 nm against a blank, the reaction was run for 60 seconds each time. The temperature was kept at almost 30°C. The optical density was recorded.

3.7.6 Glutathione Peroxidase (GPx) Activity Measurement

The GPx activity was measured using Rotruck *et al* technique's (1973).

Principle

Glutathione peroxidase catalyzes the conversion of GSH to GSSG by hydrogen peroxide. When GSH and DTNB come together, they generate 5-thio-2-nitrobenzoic acid (TNB), which has a spectrophotometric absorbance at 412nm (Anderson *et al.*, 1985).

Procedure

NaN₃ (0.1 mL), GSH (0.2 mL), H₂O₂ (0.1 mL), sample (0.5 mL), and dH₂O (0.6 mL) were added to 0.5 mL Phosphate buffer. TCA (0.5 mL) was added after 3 minutes of incubation at 37°C, and the mixture was centrifuged for 5 minutes at 3000 rpm. K₂HPO₄ (2 mL)and DTNB (1 mL) were added to supernatant (1 mL each), and the readings was recorded at 412 nm against a blank.

Reagents preparation; See Appendix 12

3.7.7 Determination of Reduced Glutathione (GSH) Level

Beutler *et al* technique was used to measured GSH level (1963)

Principle

In most cases, GSH contains the majority of cellular non-protein sulfhydryl groups. The idea for this technique came from the appearance of a markedly stable (yellow) color when sulfhydryl compounds were exposed to 5,5'-dithiobis-(2-nitrobenzoic acid) (Ellman's reagent). Ellman's reagent interacts with GSH to yield 2-nitro-5-thiobenzoic acid, a chromophoric product with a 412 nm molar absorption. This compound's optical density at 412 nm is proportional to the sample's reduced glutathione stage.

Reagents Preparation; See Appendix 13

Procedure

To make 1 in 10 dilutions, the test sample (0.1 mL) was diluted with H₂O (0.9 mL). To deproteinize the diluted test sample, 4 % sulphosalicylic acid solution (3 mL precipitating solution) was introduced. At 3,000 g, the mixture was centrifuged for 10 minutes. After that, the supernatant (0.5 mL) was mixed with phosphate buffer (0.1 M; 4 mL), then Ellman's Reagent (4.5 mL) was added. A blank was made using 0.1 M phosphate buffer (4 mL), 0.5 mL of the diluted precipitating solution (adding 3 mL of precipitating solution to 2 mL of dH₂O), and Ellman's Reagent mixture (4.5 mL). All readings were taken at 412 nm within 5 minutes of introducing Ellman's Reagent since the color developed is not stable. The absorbance at 412 nm is proportional to reduced glutathione, GSH.

3.7.8 Determination of Total Thiol (TSH) Level

The total thiol level was assayed for according to the method of Ellman (1951).

Principle

The reduced form of glutathione and other protein with sulphhydryl are available in cellular pro-oxidant and antioxidant system in tissues. This method is based on the development of a relatively stable (yellow) color when Ellman's (5,5'-dithiobis-(2-nitro-benzoic acid) is added to sulphhydryl compounds. The chromophoric product

resulting from the reaction of Ellman's reagent with the reduced sulphhydryl groups which is 2-nitro-5-thiobenzoic acid possess a molar absorption at 412 nm.

Procedure

An aliquot of the sample supernatant was added to Ellman's reagent and read at absorbance of 412 nm at 30 minuted incubation time.

3.7.9 Nitrite (Nitric Oxide) Measurement

During the metabolism of nitric oxide (NO[•]), the end product nitrite (NO₂⁻) reacts with hypochlorous acid (HOCl) or myeloperoxidase, it rapidly accelerates tyrosine nitration by creating nitryl chloride (NO₂Cl) and nitrogen dioxide (NO₂[•]). Myeloperoxidase-dependent processes convert NO₂⁻ to NO₂Cl and NO₂[•] in activated polymorphonuclear neutrophils. NO₂ can affect inflammatory processes *in vivo* through oxidative mechanisms such as tyrosine nitration and chlorination. Nitric oxide (NO[•]) generation, the nitrite (NO₂⁻) concentration of tissues was determined. To quantify the results, the Griess reaction was used (Dimitrios Tsikas, 2005).

Principle

Tissue nitrite combines with a diazotizing agent like sulfanilamide (SA) to create a temporary diazonium salt in acidic environments. This intermediate is then allowed to react with N-naphthyl-ethylenediamine (NED), a coupling reagent, to provide a stable azo product. Before reacting with nitrite, SA and NED can be combined in an acid medium. A high-sensitivity nitrite assay can detect nitrite concentrations as low as 0.5M due to the product's vibrant pink-purple color. The nitrite concentration in the sample is linearly related to the optical density at 540 nm.

Preparation of Reagents; See Appendix 14

Procedure

The number of nitrite in serum was deduced by incubating a sample (0.5 mL) with Griess reagent [0.5 mL; 0.1 % N-(1-naphthyl) ethylenediamine dihydrochloride; 1 percent sulfanilamide in 5 % phosphoric acid] at 37°C for 20 minutes after undergoing Griess reaction. The OD 550 (absorbance at 550 nm) was measured. The concentration

of sodium nitrite was determined by comparing the OD 550 of a reference solution to known sodium nitrite concentrations.

Calibration curve

Calibrator was created by diluting stock NaNO₂ solutions (20 mmol/L) with distilled water at various strengths. The dilution of nitrate callibrator with glycine buffer was done the same way the samples was diluted. A linear range of nitrate between 0 and 100 mol/L was plotted to create the calibration curve.

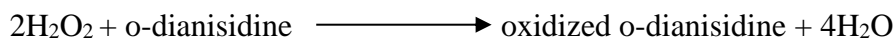
3.7.10 Determination of Myeloperoxidase Activity (MPO)

The activity of myeloperoxidase (MPO), a marker of polymorphonuclear leukocyte accumulation, was measured using a modified version of Trush's method (1994)

Principle

The lysosomal enzyme myeloperoxidase (MPO) is only found in neutrophils and monocytes which is found in the azurophilic granules of polymorphonuclear leukocytes (PMNs). MPO oxidizes a variety of aromatic compounds with H₂O₂ produced by neutrophils, providing bacterial activity with substrate radicals (Hampton *et al.*, 1998). This enzyme can also generate hypochlorous acid, a potent non-radical oxidant (HOCl) by oxidizing chloride ions. Neutrophils produces HOCl which is one of the most powerful bactericidal chemical. However, excessive generation of free radicals can lead to tissue damage and oxidative stress.

Using o-dianisidine (Sigma-Aldrich) and hydrogen peroxide, MPO activity was evaluated spectrophotometrically in this work. According to the following overall process, the oxidation of o-dianisidine to an oxidized o-dianisidine is catalyzed by MPO (a brown-colored product) in the presence of H₂O₂ with a minimum absorbance at 470 nm.



Reagents preparation; See Appendix 15

Procedure

In duplicate, to 7 μL of sample homogenate, an aliquot of o-dianisidine (200 μL) and of diluted H_2O_2 (50 μL) was added. With an extinction value of 11.3 mM/cm and a specific activity of IU/mg protein, one unit of MPO is defined as that which causes a 0.001 per minute increase in absorbance. The absorbance was taken at 460nm for 3 minutes

3.8 Assessment of Urinary Parameters

Urine Reagent Strips are firm plastic strips onto which several separate reagent areas are affixed. The test is for the qualitative and semi-quantitative detection of one or more analytes in urine. It can be used in general evaluation of health, and aids in the diagnosis and monitoring of metabolic or systemic diseases that affect kidney function, endocrine disorders and diseases or disorders of the urinary tract.

Specimen Collection And Preparation

A urine specimen was collected in a clean, dry container using metabolic cage over night and tested for urobilinogen, albumin, protein, bilirubin, glucose, ascorbic acid, ketone, nitrite, creatinine, pH and blood.

Procedure

Remove the strip from the closed canister and use as soon as possible. Close tightly the canister after removing the strip and completely immerse the reagent areas of the strip in fresh, well mixed urine and immediately remove the strip to avoid dissolving the reagents in the urine. While removing the strip from the urine, run the edge of the strip against the rim of the urine container to remove excess urine. Hold the strip in a horizontal position and bring the edge of the strip into contact with an absorbent material (e.g. a paper towel) to avoid mixing chemicals from adjacent reagent areas and/or soiling hands with urine. Compare the reagent areas to the corresponding color blocks on the canister label. Hold the strip close to the color blocks and match carefully.

3.9 Immunohistochemistry of Inflammatory and Apoptotic Markers

The immunohistochemical analysis was determined using the principle provided by Chakravarthi and colleagues (2010).

Principle

This is centered on the manufacturer's specification of a 1:100 dilution of a primary antibody binding to specified antigens.

Procedure

Immunohistochemical labeling of formalin-fixed tissue slices from the breast, uterus, and ovary was employed to investigate expression of the selected proteins. A secondary enzyme-conjugated antibody is then given the antibody-antigen combination. In the presence of substrate and chromogen, the enzyme works on the substrate to produce colored deposits at the locations of antibody-antigen contact, which were observed using a binocular microscope. Positive antigen locations in the cell cytoplasm, cell membrane, and nuclei were well-defined in color when compared to controls. Xylene was used to deparaffinize tissue slides (twice; 5 minutes each). After that, the tissue slides were examined. After that, the tissue slides were washed twice in ethanol at varying concentrations for 3 minutes each time (ethanol: 100 % , 95 % and 70 %). The slides were rinsed with PBS for 5 minutes (0.01 M; pH 7.4). The antigens were retrieved by heating the slides to 97°C for 5 minutes in sodium citrate buffer (0.05 M; pH 6.0), then cooling them in the retrieval buffer for 20 minutes before being rinsed twice with wash buffer for 5 minutes each time. Before incubation, the slides were soaked in 10% BSA in PBS (blocking buffer) for 15 minutes at 37°C in a humidified environment, then washed with wash buffer. After that, the primed tissue slides were probed with diluted primary antibody and incubated for an hour at room temperature in a temperature controlled environment. The biotinylated + streptavidine HRP secondary was diluted and applied to the segments on the slides, then incubated for the time specified after the slides had been rinsed twice with wash buffer for 5 minutes (polymer-single layer for 30 minutes). After washing the slides with wash buffer, the slide sections were incubated for further 15 minutes with 130 L of diluted Sav-HRP conjugates. For color development, the tissue pieces were painted with a freshly made DAB substrate solution (130 L) until the appropriate color strength was achieved. The slides were washed three times for two minutes each time under running water.. Hematoxylin was used to counterstain the nuclei for 20 seconds before rinsing, Dehydrated with 95 % , 95 % , 100 % and 100 % ethanol for 5 minutes after being rinsed under running water for 10 minutes. Before being mounted with a cover slip and mounting solution, the slides were

xylene-cleared three times. The color of the antibody staining on the tissue slides was viewed and photographed using an inverted fluorescence microscope (A Brunel Microscope Limited SP-98-FL) with an attached camera (Canon EOS 1100D, Japan).

Scoring of slides:

Depending on the antigenic sites, brown color cells in the cytoplasm, cell membrane, or nuclei were considered positive. Hematoxylin staining was used to score the cells. There is no staining if there is less than 5% staining, weak staining if there is 6-24% staining (light yellow), moderate staining if there is 25-49 % staining (yellow-brown), strong staining if there is 50-74 % staining (brown), and very strong staining if there is 75-100 % staining (dark brown).

3.10 DNA Fragmentation Assay

The DPA (diphenylamine) colorimetric approach is used to identify cell death in resting cells or other cell types when DNA labeling is either impossible or difficult. Procedure for DNA fragmentation was carried out in line with the manufacturer's instructions, Waterborg and Matthew, (1956) and Arzi *et al* (2018).

Principle

A $\text{Ca}^{++}/\text{Mg}^{++}$ -dependent endonuclease cleaves DNA in the linker region between nucleosome cores, resulting in the production of a series of multiplsets of a 180 bp subunit within the nucleus. This approach is based on the idea that centrifugal sedimentation can separate substantially fragmented double-stranded DNA from chromosomal DNA. Following cell lysis and nuclear DNA release, two fractions (corresponding to intact and fragmented DNA, respectively) are centrifuged; DNA is precipitated, hydrolyzed, and colorimetrically measured after staining with deoxyribose-binding diphenylamine (DPA).

Reagents preparation; See Appendix 16

Procedure

To extract cell lysate, the mammary tissue was mechanically homogenized in 400 μL hypotonic lysis buffer (10 mM-1 mM EDTA, pH 7.5, 0.2 % (v/v) Triton-X-100). The cell lysate was centrifuged for 15 minutes at 13,800 g. The supernatant, which contained

small DNA fragments, was immediately separated. The diphenylamine (DPA) assay was performed on the supernatant as well as a pellet containing significant fragments of DNA.

Both the supernatant and the pellet were utilized in the DPA test after acid extraction of DNA. Large bits of DNA and cell debris were found in the pellet, which was resuspended in 400 L hypotonic lysis buffer. Both the remaining half of the supernatant and the re-suspended pellet received 400 µL of 10% trichloroacetic acid (TCA). The tubes were centrifuged for 10 minutes at 2000 rpm. The precipitate was resuspended in 400 µL of 5% TCA solution. For 30 minutes, the tubes were incubated at 80°C. The isolated DNA supernatant was allowed to cool at room temperature. One volume of extracted DNA was mixed with two volumes of color reagent (freshly produced DPA reagent). The samples were kept at 40°C for 48 hours to generate a blue tint. A spectrophotometer was used to colorimetrically measure the blue color at 578/600 nm. The following formula was used to calculate the percentage of DNA fragmentation:

$$\% \text{ DNA fragmentation} = \text{O.D. of supernatant} / (\text{O.D. of supernatant} + \text{O.D. of pellet}) \times 100$$

3.11 Assessment of Chemopreventive Effects of Methanol Extract of *C. portoricensis* on Serum Parameters, Antioxidants Status and Hormone Receptors in *N-nitroso-N-methylurea*-Administered Rats.

Procedure

Sixty-four female *Wistar* rats (30-40g) were divided into eight different groups at random (n=8): Two weeks prior to the experiment, the animals were acculturated. Normal saline was given to Group 1 as a control, while MNU (50mg/kg) was given to Group 2. MNU (50mg/kg) and CP (100mg/kg) were given to Group 3, MNU (50mg/kg) and CP (200mg/kg) to Group 4, MNU (50mg/kg) and CP (300mg/kg) to Group 5, and 300mg/kg CP solely to Group 6. MNU (50 mg/kg) and vincasar (0.5 mg/kg) were given to group 7, while vincasar only was given to group 8. At ages 7, 10, and 13, the MNU was administered intraperitoneally in a single dose for a period of 10 weeks. For the duration of the experiment, three times a week, CP was administered orally, and twice a week, vincasar was administered intraperitoneally for the period of 10 weeks. Blood was

collected, mammary glands, uterus, and ovary tissues were retrieved for biochemical and immunohistochemical investigations.

3.12 Assessment of Antioxidative and Radical Scavenging Activities of *C. portoricensis*

Procedure

The DPPH was dissolved in methanol and filled up to 100 mL. Different concentrations of extract were dissolved in 4 mL of distilled water into 6 different test tubes. 1 mL each from a test tube was dispensed into three separate test tubes (triplicates). To each of the triplicate, DPPH (1 mL each) was added to the test tube and allowed to stand at 37°C for 30 mins before reading at 517 nm. Also, ABTS and potassium per sulphate was weighed and dissolved in distilled water. Both solution (ABTS and potassium per sulphate) was mixed together in the dark and allowed to stand for 12-16 hours before use. To make a working standard solution, 2 mL of ABTS working solution was diluted with 70 mL of acetate buffer after 12 hours. 500 µL of ABTS mixture was added into micro cuvette and the extracts was added at varying concentrations starting from 50 µL, 100 µL, 200 µL, 300 µL and 400 µL respectively.

3.13 Assessment of Chemopreventive Effects of Chloroform Fraction of *C. portoricensis* (CCP) on Biochemical Parameters and Hormonal profile in *N-nitroso-N-methylurea* and Benzo[a]pyrene-induced rats.

Procedure

Fifty-six *Wistar* rats (female; 30-40g) were splitted into seven groups (n=8) according to their weights in the following manner; rats were acculturated for two weeks before the experiment began. Corn oil (vehinacle) was given to Group 1, whereas MNU (50mg/kg) and BP (50mg/kg) were given to Group 2. MNU (50mg/kg), BP (50mg/kg), and CCP (50mg/kg) were given to Group 3, MNU (50mg/kg), BP (50mg/kg), and CCP (100mg/kg) were given to Group 4, CCP only (100mg/kg) was given to Group 5, MNU (50mg/kg), BP (50mg/kg), and vincasar (0.5mg/kg) were given to Group 6 while Group 7 received vincasar only. MNU was injected via-intraperitoneal in a single dose at age 7, 10 and 13 weeks for the period pf 10 weeks. CCP was administered orally thrice weekly while vincasar was injected via-intraperitoneal twice weekly for the period of 10 weeks. Cervical dislocation was used to sacrifice the animals, and blood was taken. Mammary

glands, uterus and ovary tissues were obtained for biochemical and immunohistochemical analyses.

3.14 Assessment of Antiproliferative, Antioxidative, and Apoptotic Effects of Chloroform Fraction of *C. portoricensis* in MCF-7 cells.

Procedure

Cells viability was determined using (3-[4,5-dimethylthiazol-2-yl]-2,5 diphenyl tetrazolium bromide) MTT assay. Dulbecco's modified Eagle medium (DMEM) was used to grow the MCF-7 cells. Cells were cultured after introducing into 96-well plates (density of 5×10^3 cells per well). Following 24-hour incubation period, the cells were given various doses of chloroform fraction of CP (5, 25, 50, and 100 $\mu\text{g/mL}$) for 72 hours. For 4 hours, the MTT (thiazolyl blue tetrazolium bromide), 7% FCS, and penicillin/streptomycin in PBS were introduced and incubated. The dye was solubilized with DMSO after incubation. The concentration of MTT-formazan product dissolved in DMSO was determined using a microplate reader set to 550 nm.

3.14.1 Assessment of Biochemical parameters on MCF-7 cell lysates

MCF-7 cells were seeded in 96-well plates to study the effect of chloroform fraction of CP on biochemical parameters. Following 24 hours incubation, the cells were given 49.3 $\mu\text{g/mL}$ (IC_{50}) of CP for another 24 hours. The cells were rinsed three times with wash buffer, thereafter, lytic buffer was added to lyse the cells, incubated for 30 minutes and placed in a centrifuge tube. To separate the supernatant from the cell debris, the obtained cell lysates were centrifuged for 10 minutes at 10,000 x g. The cell lysate supernatant was used to measure biochemical parameters and apoptotic markers.

3.15 Assessment of Curative Effects of Chloroform Fraction of *C. portoricensis* (CCP) on *N-nitroso-N-methylurea* and Benzo[a]pyrene-induced mammary toxicity in rats.

Procedure

A total of thirty-two female rats were divided into four groups, each with eight rats. Prior to the experiment, the animals were given a fourteen-days acclimatization period.

Group 1 received normal saline (vehicle), group 2 received MNU (50mg/kg) and BP (50mg/kg), group 3 received MNU (50mg/kg), BP(50mg/kg) and given CCP(100mg/kg) while group 4 received MNU (50mg/kg), BP(50mg/kg) and vincasar (0.5mg/kg) respectively. The rats were given a single dosage of MNU and BP (50 mg/kg) intraperitoneally at ages 7, 10, and 13 weeks (three weeks interval) for a period of 10 weeks. The CCP (orally) and vincasar (intraperitoneally) were administered for another period of two weeks respectively. Animals were sacrificed through cervical dislocation, blood was collected, neck and mammary tissues were obtained for biochemical and immunohistochemical analyses.

3.16 Statistical Analysis

Values (mean \pm SDev) are based on eight rats per group. The data in this study were analyzed using One-Way Analysis of Variance, and statistical significance was determined at less than .05.

CHAPTER FOUR

RESULTS

4.1 Chemopreventive effect of methanol extract of *C. portoricensis* on serum parameters, antioxidants status, and hormone receptors in *N-nitroso-N-methylurea* administered rats.

Results from table 4.1 and table 4.2 depict that administration of MNU caused reduction in body weight gained by 21% relative to vehicle. On the contrary, the mammary gland's weight and organo-somatic weight increased by 67% and 52%, respectively, in the MNU-treated groups (pless than .05). Similarly, MNU induced a drastic (pless than .05) increase in ovarian weight without any noticeable effect on uterine weight. The ovarian organo-somatic weights rose by 15.4%, but the uterine organo-somatic weights differed slightly ($p>0.05$). Co-treatment with CP specifically at 200mg/kg and 300mg/kg restored the body weight gained, mammary gland and uterus organo-somatic weight drastically (pless than .05).

Table 4.1: Weight changes in rats given *N-nitroso-N-methylurea* and methanol extract of *C. portoricensis*

	WEIGHT (g)			MAMMARY	TISSUE
	Original	Terminal	Body mass	Body mass (g)	Organ-body
	Body mass (g)	Body mass (g)	Gained (g)		mass ^a
VEHICLE	52.63±3.93	157.25±9.97	104±7.14	0.45±0.12	0.33±0
MNU	62.88±3.23	145.15±2.84	82.27±4.51	0.75±0.08*	0.50±0.08
MNU+CP 1	63.63±5.40	154.25±3.23	89.75±1.20	0.91±0.01*	0.61±0.05*
MNU+CP 2	61.13±3.14	160.55±1.34	99.42±7.71	0.67±0.19***	0.43±0.09***
MNU+CP 3	67.38±5.73	146.35±7.28	78.97±1.91	0.55±0.06***	0.38±0.02***
CP 3 ONLY	52.25±6.39	139.10±2.95	86.65±3.46	0.69±0.16	0.50±0.11
MNU + VIN	68.63±3.70	125.6±1.70	57.10±8.06	0.89±0.13	0.68±0.15
VIN ONLY	77.00±4.63	134.25±1.10	57.25±9.16	0.65±0.20	0.56±0.19

MNU= *N-nitroso-N-methylurea*; CP= *C. portoricensis*; VIN= Vincasar; a= % body weight. CP 1 =100 mg/kg, CP 2= 200 mg/kg and CP 3= 300 mg/kg.

* = p less than .05 in contrast to vehicle. ** = p less than .05 in contrast to untreated group. Values (mean±SDev) are based on 5-8 rats per group.

TABLE 4.2: Organ weight changes of *N-nitroso-N-methylurea*-administered rats given methanol extract of *C. portoricensis* and Vincasar

	UTERUS		OVARY	
	Body mass(g)	Organ- body mass ^a	Body mass (g)	Organ- body mass ^a
VEHICLE	0.11±0.04	0.08±0.01	0.17±0.06	0.13±0.00
MNU	0.11±0.04	0.06±0.01	0.23±0.02*	0.15±0.01*
MNU+CP 1	0.09±0.01	0.06±0.00	0.16±0.02**	0.11±0.02**
MNU+CP 2	0.14±0.02	0.08±0.00	0.17±0.05**	0.11±0.02**
MNU+CP 3	0.14±0.01	0.09±0.00	0.15±0.01**	0.10±0.00**
CP 3 ONLY	0.10±0.04	0.06±0.01	0.14±0.04	0.10±0.03
MNU + VIN	0.07±0.01	0.05±0.00	0.14±0.01	0.11±0.00
VIN ONLY	0.10±0.02	0.07±0.00	0.16±0.04	0.14±0.06

MNU= *N-nitroso-N-methylurea*; CP= *C. portoricensis*; VIN= Vincasar. CP 1 =100 mg/kg, CP 2= 200 mg/kg and CP 3= 300 mg/kg. * = p less than .05 in contrast to vehicle. ** = p less than .05 in contrast to untreated group. Values (mean±SDev) are based on 5-8 rats per group.

Activity of aspartate aminotransferases (AST) and total bilirubin (T-BIL) level was drastically (pless than .05) elevated in MNU-administered rats while alanine aminotransferase (ALT) activity was slightly elevated in MNU-exposed group relative to vehinle. Serum lactate dehydrogenase activity and nitric oxide level increased significantly in MNU-treated groups. In addition, a slight increase in serum malondialdehyde (LPO) level was observed in rats exposed to MNU. However, co-administration with CP at all doses tested significantly mitigated MNU-induced alterations across CP-treated groups.

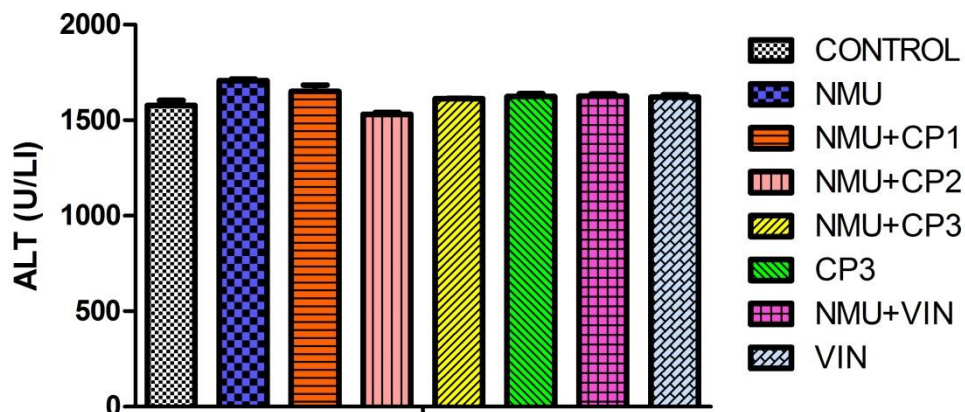


Figure 4.1: Effect of methanol extract of *C. portoricensis* (CP) in Wistar rats given *N*-nitroso-*N*-methylurea (MNU) on serum alanine aminotransferase activities (ALT). MNU= *N*-nitroso-*N*-methylurea; CP= *C. portoricensis*; VIN= Vincasar. CP 1 =100 mg/kg, CP 2= 200 mg/kg and CP 3= 300 mg/kg. Values (mean±SDev) are based on 5-8 rats per group.



Figure 4.2: Effect of methanol extract of *C. portoricensis* (CP) in Wistar rats given *N-nitroso-N-methylurea* (MNU) on serum aspartate aminotransferase activities (AST). MNU= *N-nitroso-N-methylurea*; CP= *C. portoricensis*; VIN= Vincasar. CP 1 =100 mg/kg, CP 2= 200 mg/kg and CP 3= 300 mg/kg. * = p less than .05 in contrast to vehicle. ** = p less than .05 in contrast to untreated group. Values (mean±SDev) are based on 5-8 rats per group.

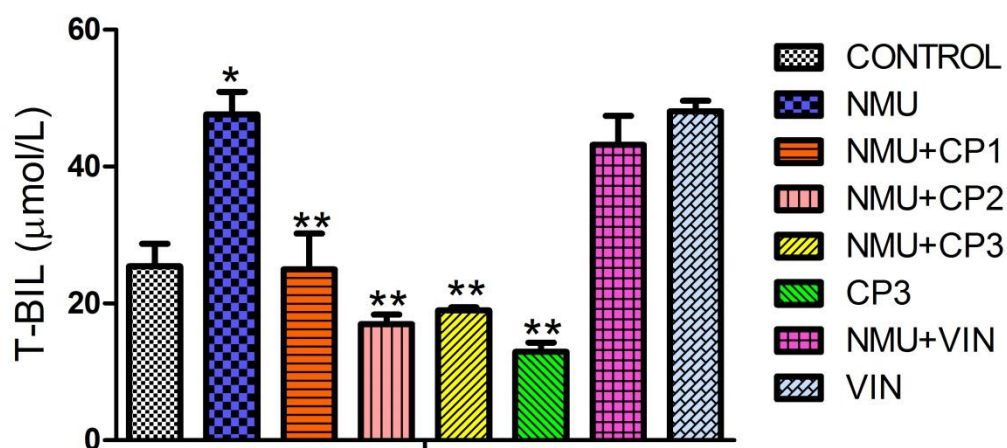


Figure 4.3: Effect of methanol extract of *C. portoricensis* (CP) in Wistar rats given *N-nitroso-N-methylurea* (MNU) on serum total bilirubin (T-BIL) levels. MNU= *N-nitroso-N-methylurea*; CP= *C. portoricensis*; VIN= Vincasar. CP 1 =100 mg/kg, CP 2= 200 mg/kg and CP 3= 300 mg/kg. * = p less than .05 in contrast to vehicle. ** = p less than .05 in contrast to untreated group. Values (mean±SDev) are based on 5-8 rats per group.



Figure 4.4: Effect of methanol extract of *C. portoricensis* (CP) in Wistar rats given *N-nitroso-N-methylurea* (MNU) on serum nitric oxide (NO) levels. MNU= *N-nitroso-N-methylurea*; CP= *C. portoricensis*; VIN= Vincasar. CP 1 =100 mg/kg, CP 2= 200 mg/kg and CP 3= 300 mg/kg. * = p less than .05 in contrast to vehicle. ** = p less than .05 in contrast to untreated group. Values (mean±SDev) are based on 5-8 rats per group.

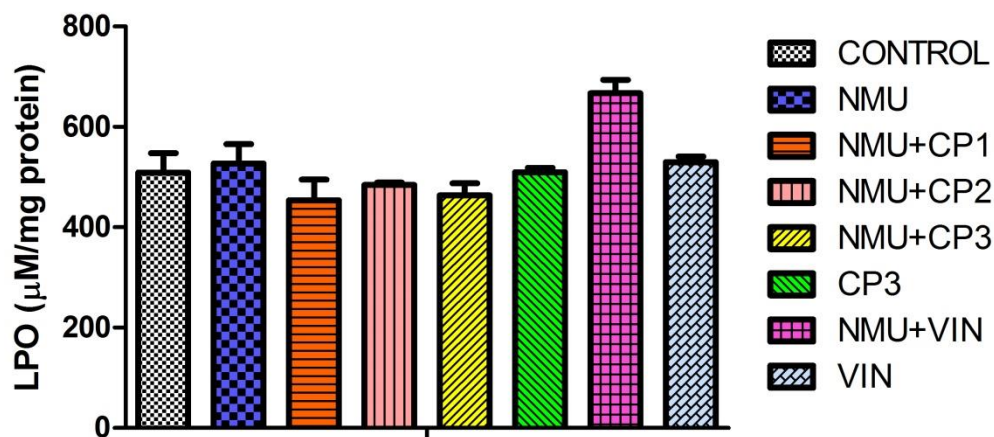


Figure 4.5: Effect of methanol extract of *C. portoricensis* (CP) in Wistar rats given *N-nitroso-N-methylurea* (MNU) on serum malondialdehyde (LPO) levels. MNU= *N-nitroso-N-methylurea*; CP= *C. portoricensis*; VIN= Vincasar. CP 1 =100 mg/kg, CP 2= 200 mg/kg and CP 3= 300 mg/kg. Values (mean±SDev) are based on 5-8 rats per group.

MNU and BP administration significantly increased lactate dehydrogenase activity when compared to vehicle group. In addition, DNA fragmentation levels slightly decreased in MNU and BP-treated rats relative to vehicle. However, co-treatment with CP and VIN drastically decreased lactate dehydrogenase activities across the treated groups while CP and VIN treatment slightly increased DNA fragmentation levels

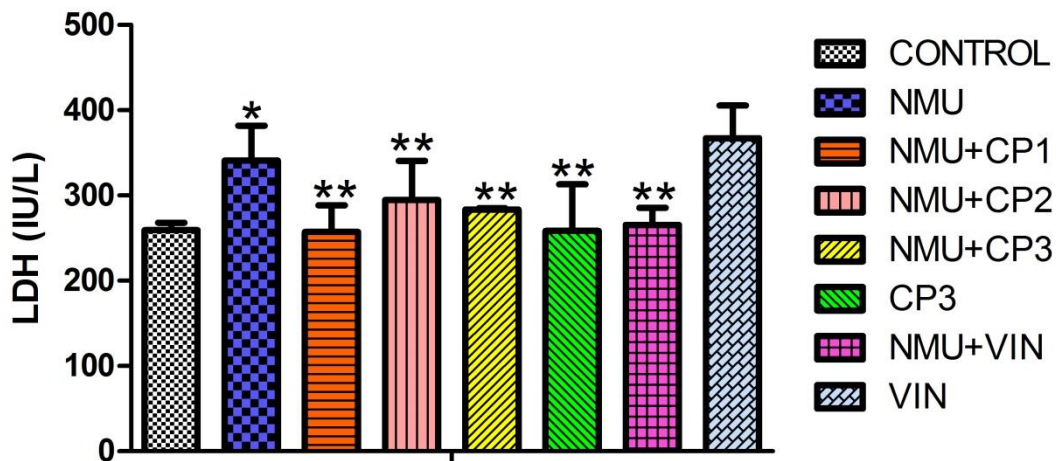


Figure 4.6: Effect of methanol extract of *C. portoricensis* (CP) in Wistar rats given *N-nitroso-N-methylurea* (MNU) on serum lactate dehydrogenase (LDH) activities. MNU= *N-nitroso-N-methylurea*; CP= *C. portoricensis*; VIN= Vincasar. CP 1 =100 mg/kg, CP 2= 200 mg/kg and CP 3= 300 mg/kg. * = p less than .05 in contrast to vehicle. ** = p less than .05 in contrast to untreated group. Values (mean±SDev) are based on 5-8 rats per group.

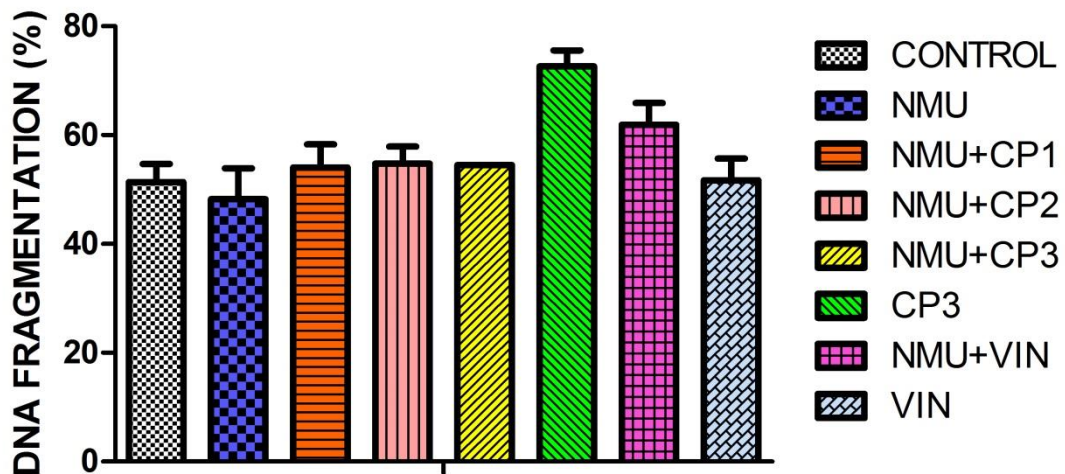


Figure 4.7: Effect of methanol extract of *C.portoricensis* (CP) in Wistar rats given *N-nitroso-N-methylurea* (MNU) on DNA fragmentation. MNU= *N-nitroso-N-methylurea*; CP= *C. portoricensis*; VIN= Vincasar. CP 1 =100 mg/kg, CP 2= 200 mg/kg and CP 3= 300 mg/kg. Values (mean±SDev) are based on 5-8 rats per group.

Mammary, uterine, and ovarian GPx and GST activities were drastically decreased in MNU-treated rats when compared to vehicle. Precisely, mammary GPx and GST decreased by 32% and 6.02%, ovarian GPx and GST decreased by 38.7% and 9.64% while uterine GPx and GST decreased by 23.34% and 9.75% respectively. Co-treatment with CP significantly elevated GPx and GST activities.

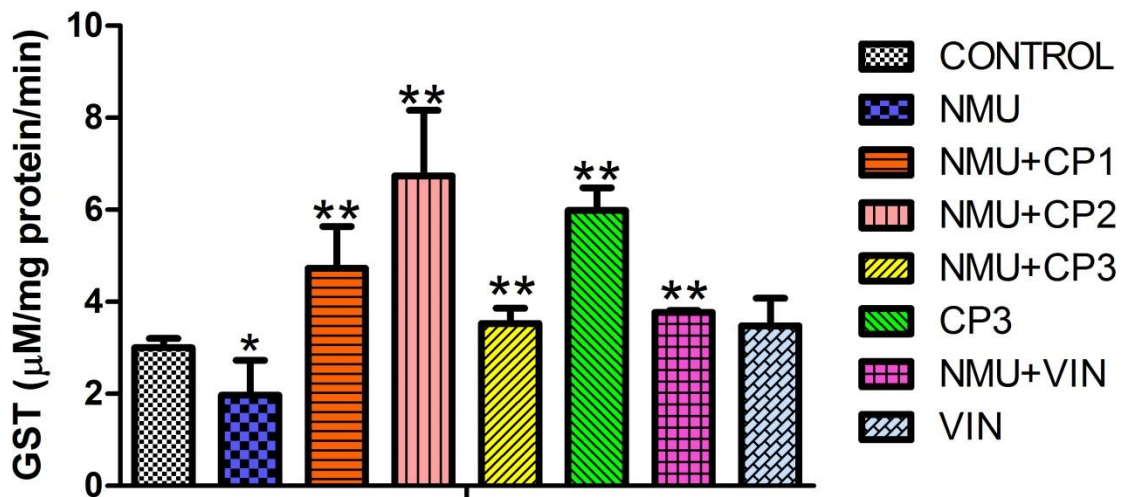


Figure 4.8: Effect of methanol extract of *C. portoricensis* (CP) in Wistar rats given *N-nitroso-N-methylurea* (MNU) on mammary Glutathione-S-transferase (GST) activities. MNU= *N-nitroso-N-methylurea*; CP= *C. portoricensis*; VIN= Vincasar. CP 1 =100 mg/kg, CP 2= 200 mg/kg and CP 3= 300 mg/kg. * = p less than .05 in contrast to vehicle. ** = p less than .05 in contrast to untreated group. Values (mean±SDev) are based on 5-8 rats per group.

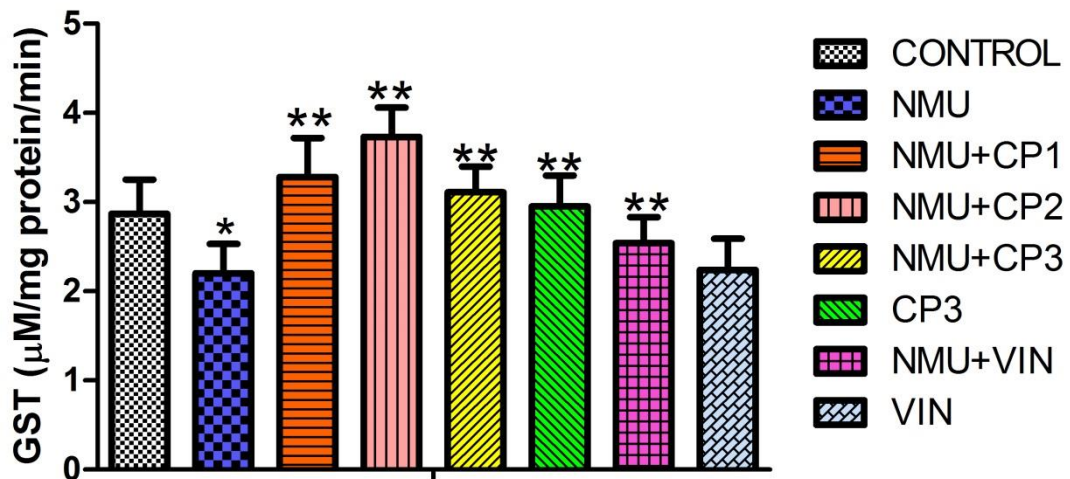


Figure 4.9: Effect of methanol extract of *C. portoricensis* (CP) in Wistar rats given *N*-nitroso-*N*-methylurea (MNU) on uterine Glutathione-S-transferase (GST) activities. MNU= *N*-nitroso-*N*-methylurea; CP= *C. portoricensis*; VIN= Vincasar. CP 1 =100 mg/kg, CP 2= 200 mg/kg and CP 3= 300 mg/kg. * = p less than .05 in contrast to vehicle. ** = p less than .05 in contrast to untreated group. Values (mean±SDev) are based on 5-8 rats per group.



Figure 4.10: Effect of methanol extract of *C. portoricensis* (CP) in Wistar rats given *N-nitroso-N-methylurea* (MNU) on ovarian Glutathione-S-transferase (GST) activities. MNU= *N-nitroso-N-methylurea*; CP= *C. portoricensis*; VIN= Vincasar. CP 1 =100 mg/kg, CP 2= 200 mg/kg and CP 3= 300 mg/kg. * = p less than .05 in contrast to vehicle. ** = p less than .05 in contrast to untreated group. Values (mean±SDev) are based on 5-8 rats per group.

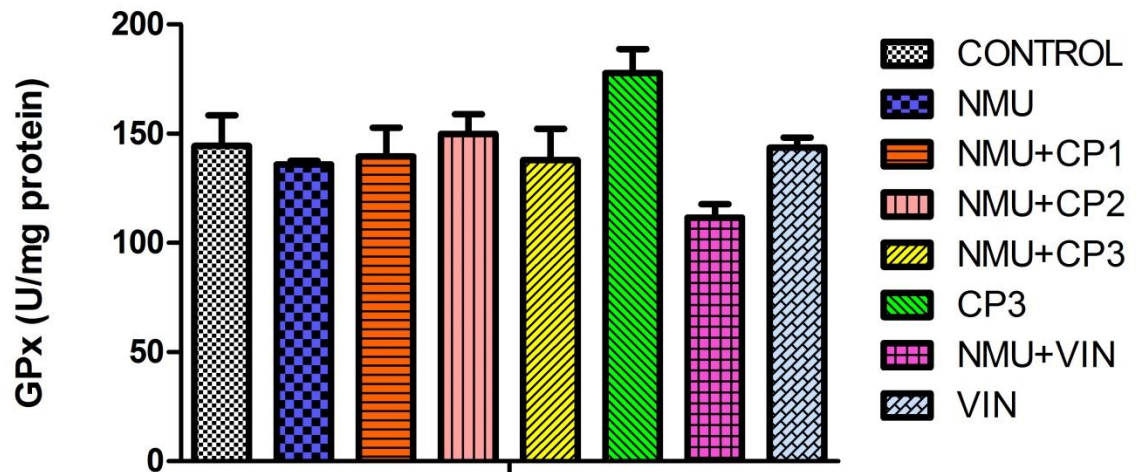


Figure 4.11: Effect of methanol extract of *C. portoricensis* (CP) in Wistar rats given *N-nitroso-N-methylurea* (MNU) on mammary glutathione peroxidase (GPx) activities. MNU= *N-nitroso-N-methylurea*; CP= *C. portoricensis*; VIN= Vincasar. CP 1 =100 mg/kg, CP 2= 200 mg/kg and CP 3= 300 mg/kg. Values (mean±SDev) are based on 5-8 rats per group.

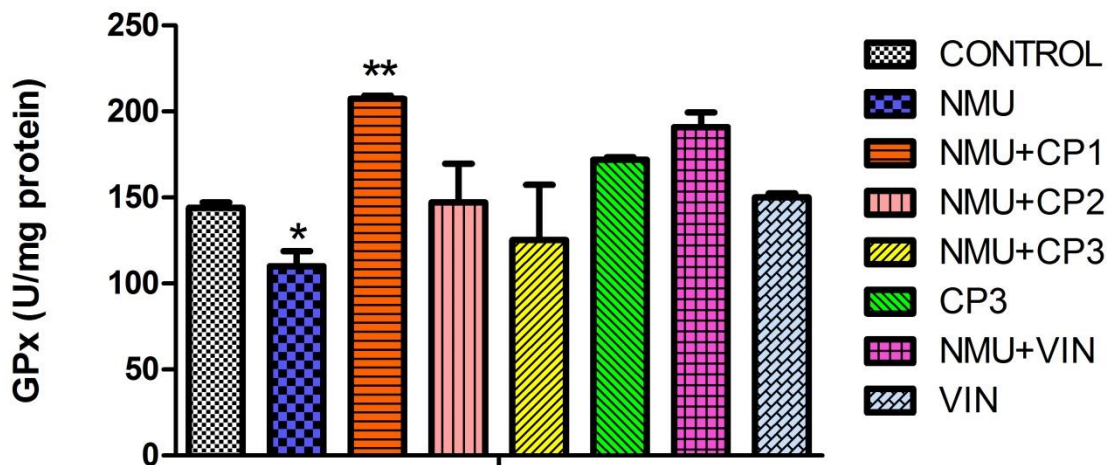


Figure 4.12: Effect of methanol extract of *C. portoricensis* (CP) in Wistar rats given *N-nitroso-N-methylurea* (MNU) on uterine glutathione peroxidase (GPx) activities. MNU= *N-nitroso-N-methylurea*; CP= *C. portoricensis*; VIN= Vincasar. CP 1 =100 mg/kg, CP 2= 200 mg/kg and CP 3= 300 mg/kg. * = p less than .05 in contrast to vehicle. ** = p less than .05 in contrast to untreated group. Values (mean±SDev) are based on 5-8 rats per group.

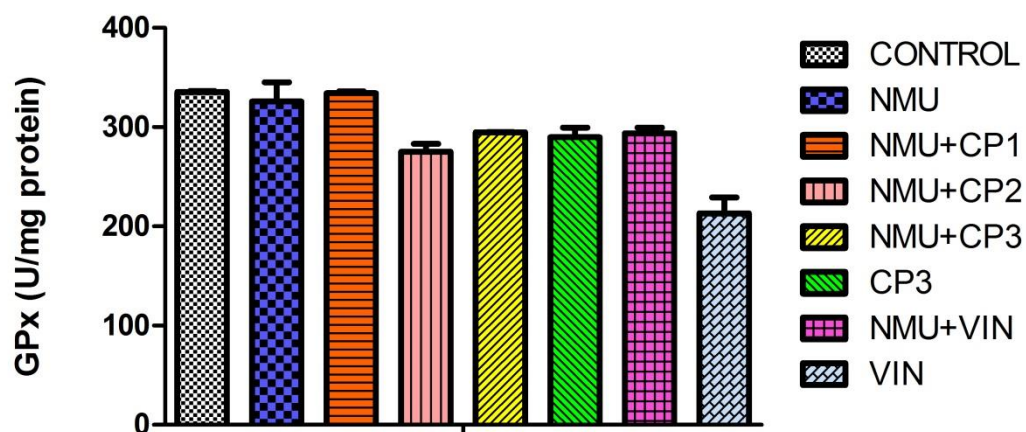


Figure 4.13: Effect of methanol extract of *C. portoricensis* (CP) in Wistar rats given *N*-nitroso-*N*-methylurea (MNU) on ovarian glutathione peroxidase (GPx) activities. MNU= *N*-nitroso-*N*-methylurea; CP= *C. portoricensis*; VIN= Vincasar. CP 1 =100 mg/kg, CP 2= 200 mg/kg and CP 3= 300 mg/kg. Values (mean±SDev) are based on 5-8 rats per group.

Activities of catalase (CAT) and superoxide dismutase (SOD) were depleted in the mammary, uterine and ovarian tissues of MNU-exposed groups. Co-administration with CP restored the antioxidant enzymes activities when compared to MNU-treated groups.

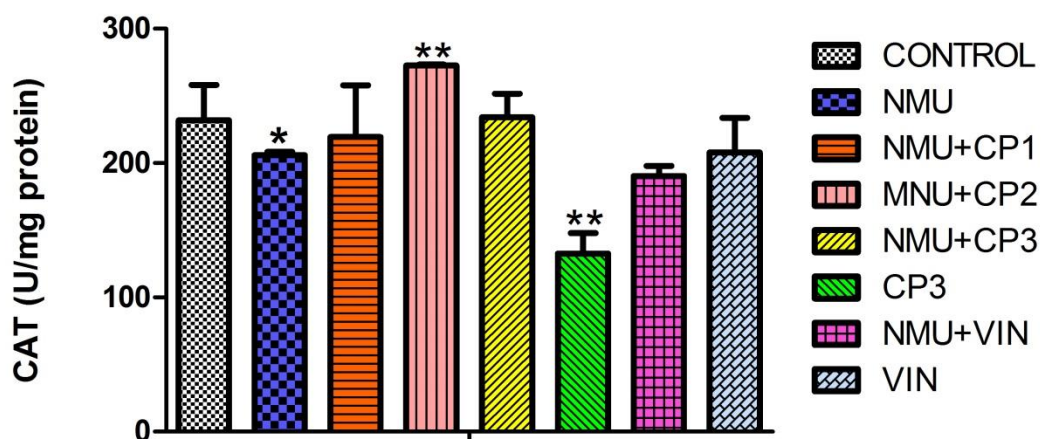


Figure 4.14: Effect of methanol extract of *C. portoricensis* (CP) in Wistar rats given *N-nitroso-N-methylurea* (MNU) on mammary Catalase (CAT) activities. MNU= *N-nitroso-N-methylurea*; CP= *C. portoricensis*; VIN= Vincasar. CP 1 =100 mg/kg, CP 2= 200 mg/kg and CP 3= 300 mg/kg. * = p less than .05 in contrast to vehicle. ** = p less than .05 in contrast to untreated group. Values (mean±SDev) are based on 5-8 rats per group.

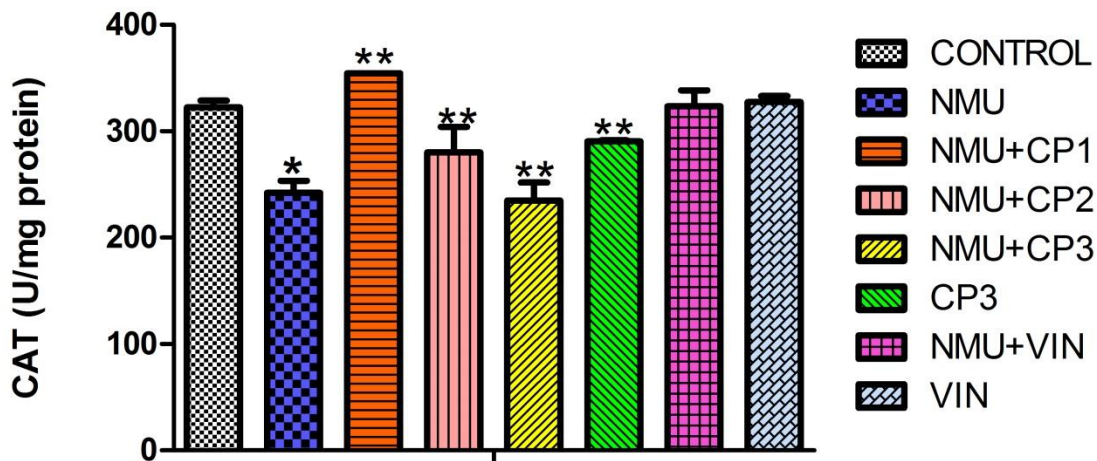


Figure 4.15: Effect of methanol extract of *C. portoricensis* (CP) in Wistar rats given *N-nitroso-N-methylurea* (MNU) on uterine Catalase (CAT) activities. MNU= *N-nitroso-N-methylurea*; CP= *C. portoricensis*; VIN= Vincasar. CP 1 =100 mg/kg, CP 2= 200 mg/kg and CP 3= 300 mg/kg. * = p less than .05 in contrast to vehicle. ** = p less than .05 in contrast to untreated group. Values (mean±SDev) are based on 5-8 rats per group.

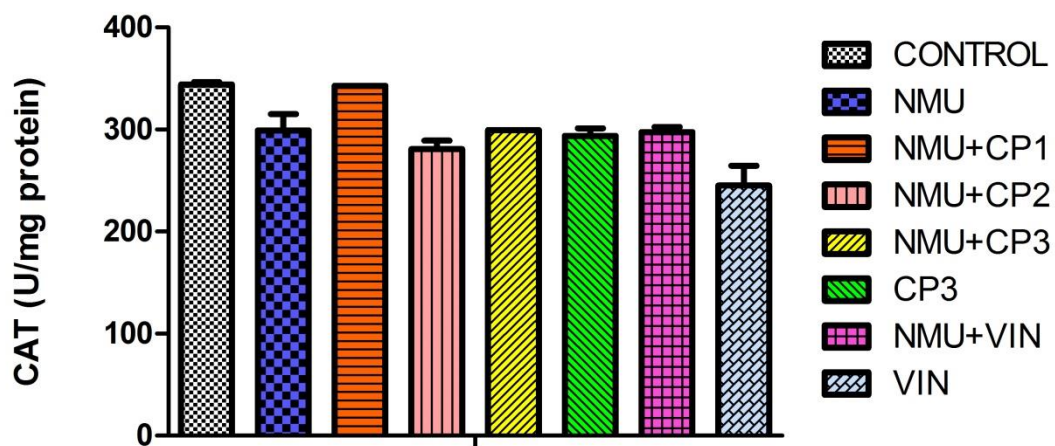


Figure 4.16: Effect of methanol extract of *C. portoricensis* (CP) in Wistar rats given *N*-nitroso-*N*-methylurea (MNU) on ovarian Catalase (CAT) activities. MNU= *N*-nitroso-*N*-methylurea; CP= *C. portoricensis*; VIN= Vincasar. CP 1 =100 mg/kg, CP 2= 200 mg/kg and CP 3= 300 mg/kg. Values (mean±SDev) are based on 5-8 rats per group.

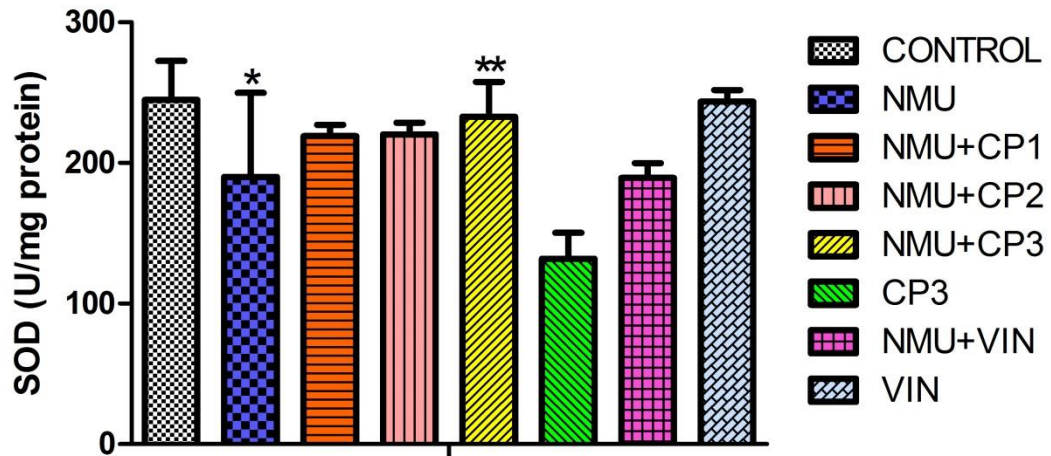


Figure 4.17: Effect of methanol extract of *C. portoricensis* (CP) in Wistar rats given *N-nitroso-N-methylurea* (MNU) on mammary Superoxide-dismutase (SOD) activities. MNU= *N-nitroso-N-methylurea*; CP= *C. portoricensis*; VIN= Vincasar. CP 1 =100 mg/kg, CP 2= 200 mg/kg and CP 3= 300 mg/kg. * = p less than .05 in contrast to vehicle. ** = p less than .05 in contrast to untreated group. Values (mean±SDev) are based on 5-8 rats per group.

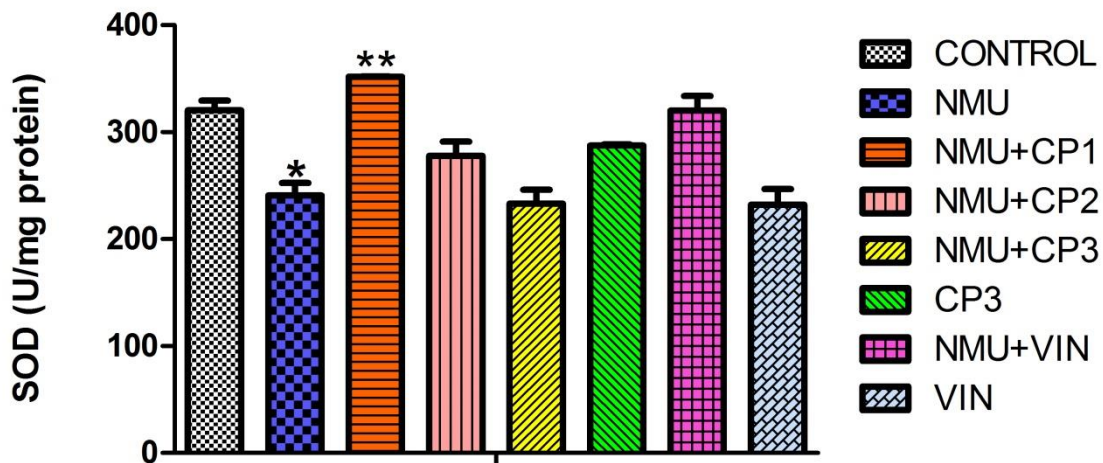


Figure 4.18: Effect of methanol extract of *C. portoricensis* (CP) in Wistar rats given *N-nitroso-N-methylurea* (MNU) on uterine Superoxide-dismutase (SOD) activities. MNU= *N-nitroso-N-methylurea*; CP= *C. portoricensis*; VIN= Vincasar. CP 1 =100 mg/kg, CP 2= 200 mg/kg and CP 3= 300 mg/kg. * = p less than .05 in contrast to vehicle. ** = p less than .05 in contrast to untreated group. Values (mean±SDev) are based on 5-8 rats per group.

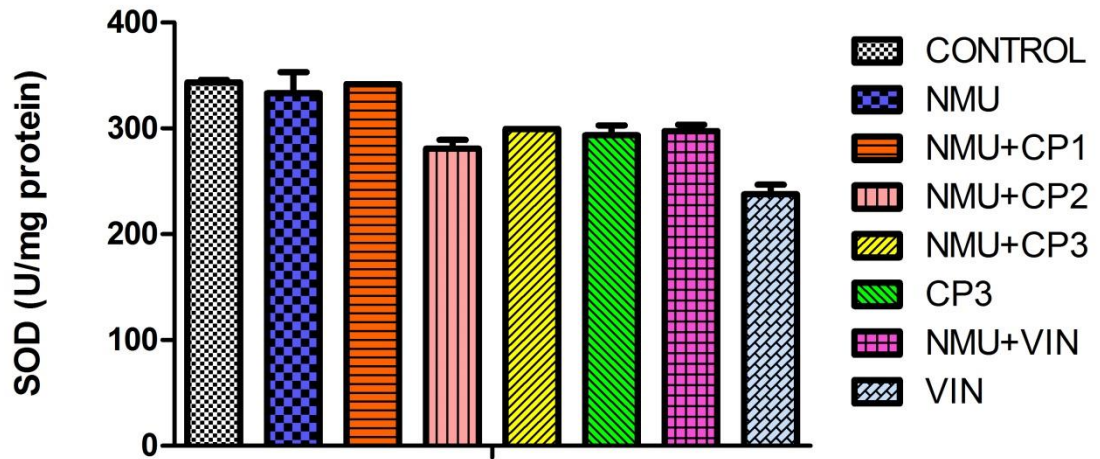


Figure 4.19: Effect of methanol extract of *C. portoricensis* (CP) in Wistar rats given *N-nitroso-N-methylurea* (MNU) on ovarian Superoxide-dismutase (SOD) activities. MNU= *N-nitroso-N-methylurea*; CP= *C. portoricensis*; VIN= Vincasar. CP 1 =100 mg/kg, CP 2= 200 mg/kg and CP 3= 300 mg/kg. Values (mean±SDev) are based on 5-8 rats per group.

Administration of MNU caused drastic reduction in mammary, uterine, and ovarian GSH and TSH levels while treatment with CP across treated groups significantly attenuated GSH level in a dose-dependent way. In addition, there was no drastic difference in TSH level following co-treatment with CP.

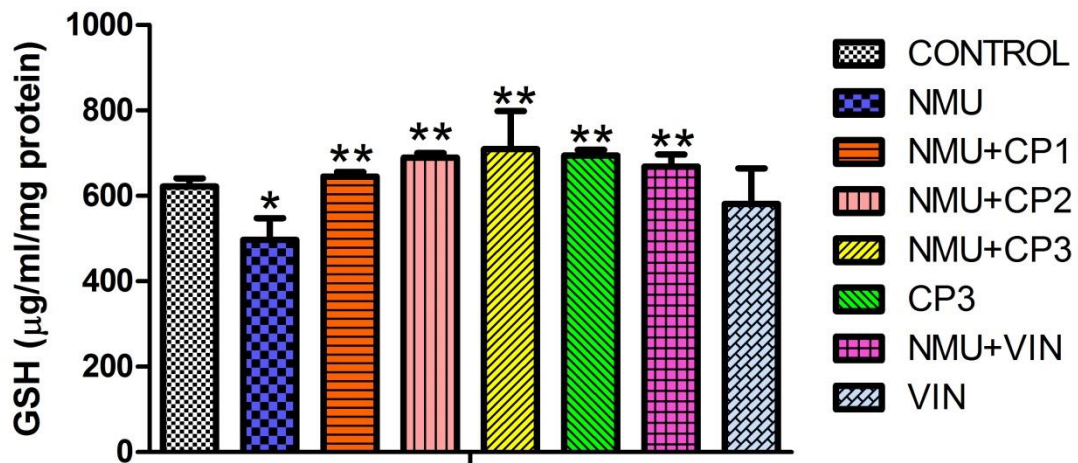


Figure 4.20: Effect of methanol extract of *C. portoricensis* (CP) in Wistar rats given *N-nitroso-N-methylurea* (MNU) on mammary reduced glutathione (GSH) levels. MNU= *N-nitroso-N-methylurea*; CP= *C. portoricensis*; VIN= Vincasar. CP 1 =100 mg/kg, CP 2= 200 mg/kg and CP 3= 300 mg/kg. * = p less than .05 in contrast to vehicle. ** = p less than .05 in contrast to untreated group. Values (mean±SDev) are based on 5-8 rats per group.

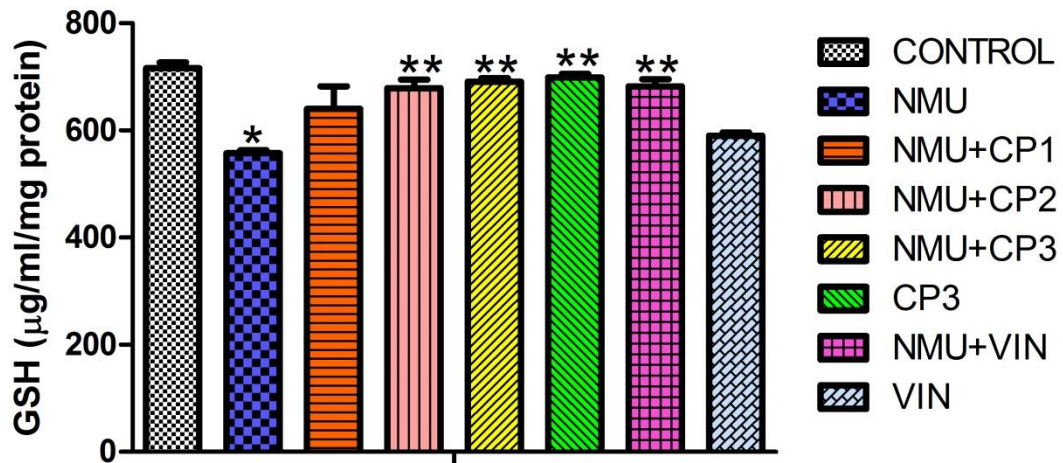


Figure 4.21: Effect of methanol extract of *C. portoricensis* (CP) in Wistar rats given *N*-nitroso-*N*-methylurea (MNU) on uterine reduced glutathione (GSH) levels. MNU= *N*-nitroso-*N*-methylurea; CP= *C. portoricensis*; VIN= Vincasar. CP 1 =100 mg/kg, CP 2= 200 mg/kg and CP 3= 300 mg/kg. * = p less than .05 in contrast to vehicle. ** = p less than .05 in contrast to untreated group. Values (mean±SDev) are based on 5-8 rats per group.

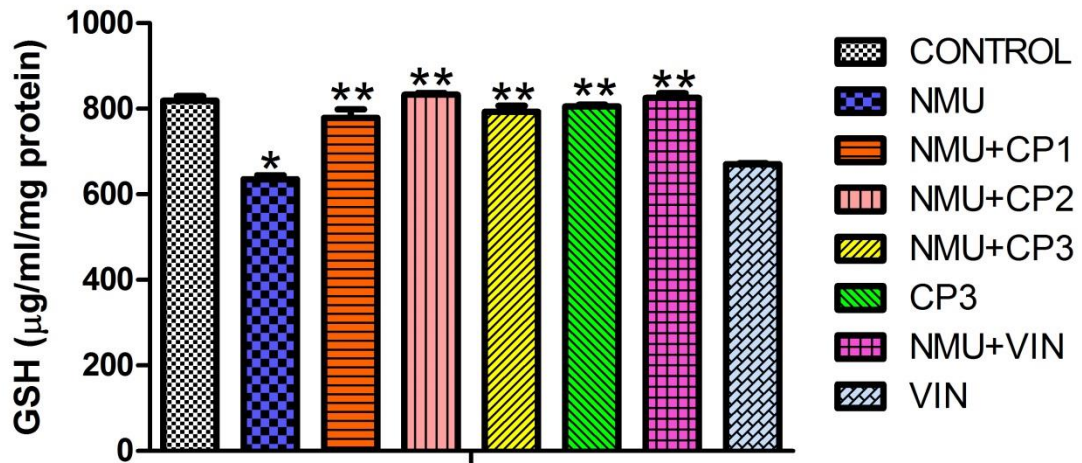


Figure 4.22: Effect of methanol extract of *C. portoricensis* (CP) in Wistar rats given *N-nitroso-N-methylurea* (MNU) on ovarian reduced glutathione (GSH) levels. MNU= *N-nitroso-N-methylurea*; CP= *C. portoricensis*; VIN= Vincasar. CP 1 =100 mg/kg, CP 2= 200 mg/kg and CP 3= 300 mg/kg. * = p less than .05 in contrast to vehicle. ** = p less than .05 in contrast to untreated group. Values (mean±SDev) are based on 5-8 rats per group.

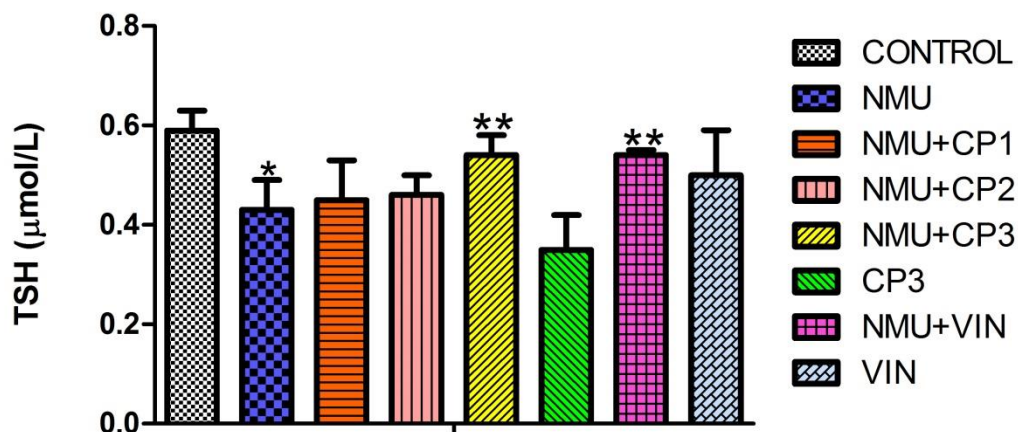


Figure 4.23: Effect of methanol extract of *C. portoricensis* (CP) in Wistar rats given *N*-nitroso-*N*-methylurea (MNU) on mammary total sulphhydryl (TSH) levels. MNU= *N*-nitroso-*N*-methylurea; CP= *C. portoricensis*; VIN= Vincasar. CP 1 =100 mg/kg, CP 2= 200 mg/kg and CP 3= 300 mg/kg* = p less than .05 in contrast to vehicle. ** = p less than .05 in contrast to untreated group. Values (mean±SDev) are based on 5-8 rats per group.

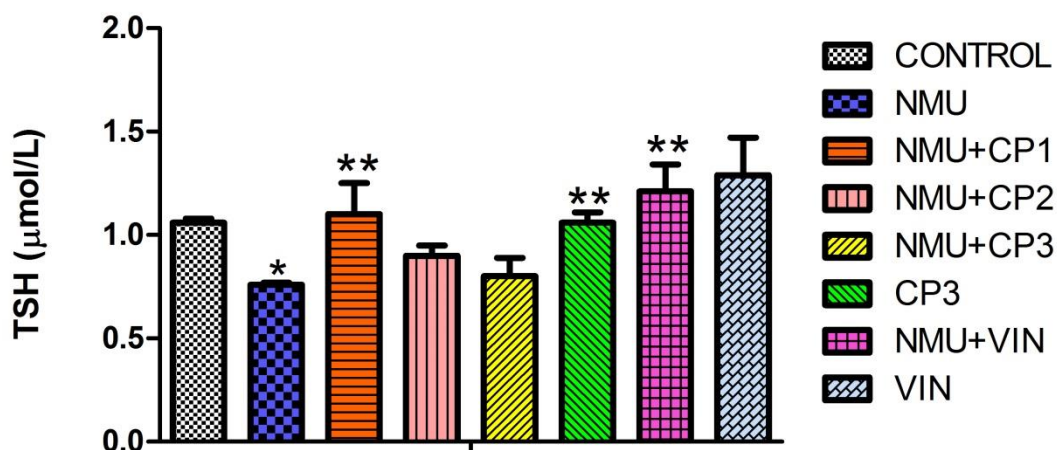


Figure 4.24: Effect of methanol extract of *C. portoricensis* (CP) in Wistar rats given *N-nitroso-N-methylurea* (MNU) on uterine total sulphhydryl (TSH) levels. MNU= *N-nitroso-N-methylurea*; CP= *C. portoricensis*; VIN= Vincasar. CP 1 =100 mg/kg, CP 2= 200 mg/kg and CP 3= 300 mg/kg. * = p less than .05 in contrast to vehicle. ** = p less than .05 in contrast to untreated group. Values (mean±SDev) are based on 5-8 rats per group.

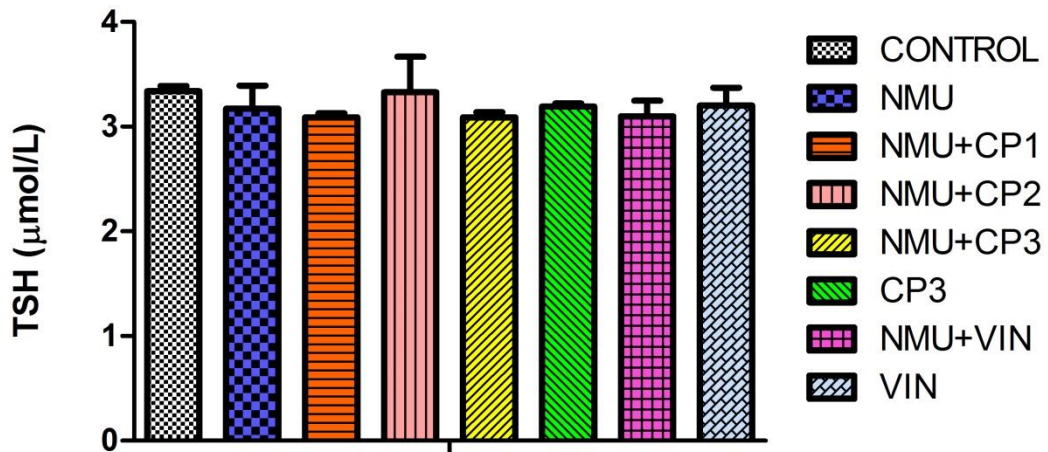


Figure 4.25: Effect of methanol extract of *C. portoricensis* (CP) in Wistar rats given *N-nitroso-N-methylurea* (MNU) on ovarian total sulphhydryl (TSH) levels. MNU= *N-nitroso-N-methylurea*; CP= *C. portoricensis*; VIN= Vincasar. CP 1 =100 mg/kg, CP 2= 200 mg/kg and CP 3= 300 mg/kg. Values (mean±SDev) are based on 5-8 rats per group.

Co-administration of CP slightly decreased NO levels in mammary by 1.03%, 1.14% and 1.17%; ovarian by 3.36%, 2.64%, and 1.38% and uterine by 6.6%, 3.05% and 1.3% in a dose-dependent manner at 100mg/kg, 200mg/kg and 300mg/kg respectively. Also, CP reduced MPO activities both in uterine and ovarian tissues. Correspondingly, CP shows a dose-dependent inhibition of MPO activity notably in the uterus.

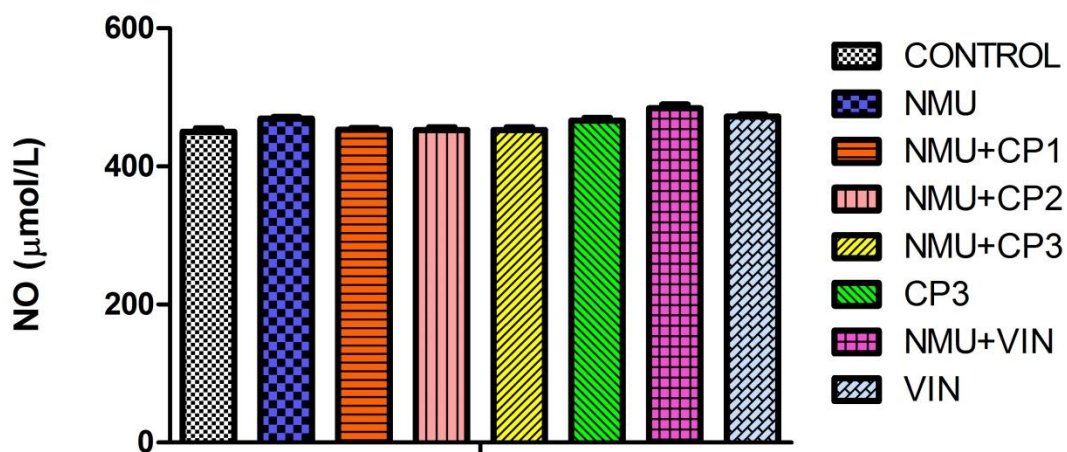


Figure 4.26: Effect of methanol extract of *C. portoricensis* (CP) in Wistar rats given *N-nitroso-N-methylurea* (MNU) on mammary Nitric oxide (NO) levels. MNU= *N-nitroso-N-methylurea*; CP= *C. portoricensis*; VIN= Vincasar. CP 1 =100 mg/kg, CP 2= 200 mg/kg and CP 3= 300 mg/kg. Values (mean±SDev) are based on 5-8 rats per group.

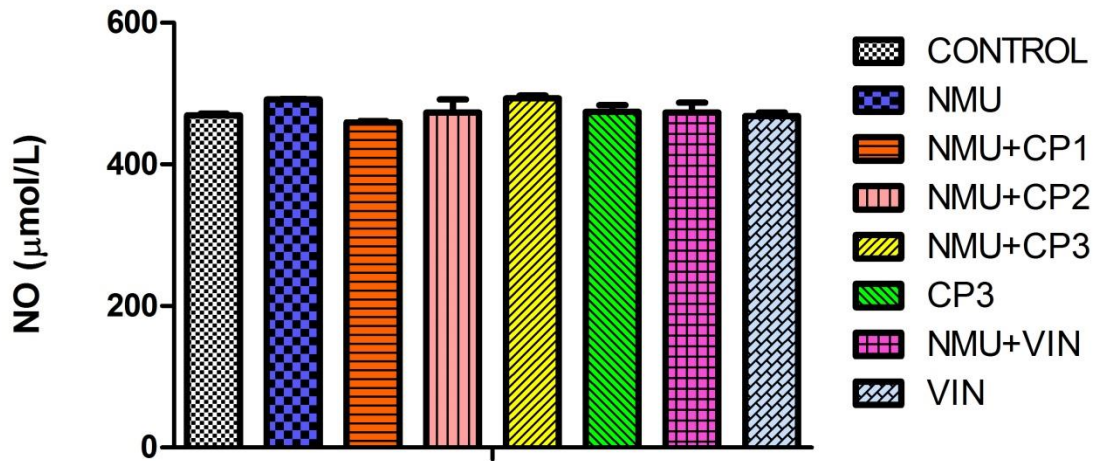


Figure 4.27: Effect of methanol extract of *C. portoricensis* (CP) in Wistar rats given *N-nitroso-N-methylurea* (MNU) on uterine Nitric oxide (NO) levels. MNU= *N-nitroso-N-methylurea*; CP= *C. portoricensis*; VIN= Vincasar. CP 1 =100 mg/kg, CP 2= 200 mg/kg and CP 3= 300 mg/kg. Values (mean±SDev) are based on 5-8 rats per group.

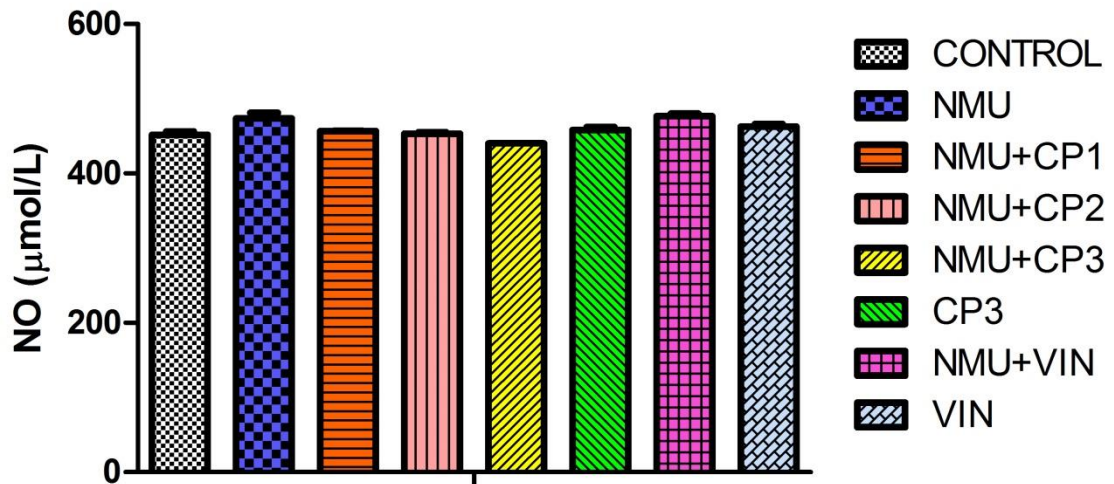


Figure 4.28: Effect of methanol extract of *C. portoricensis* (CP) in Wistar rats given *N*-nitroso-*N*-methylurea (MNU) on ovarian Nitric oxide (NO) levels. MNU= *N*-nitroso-*N*-methylurea; CP= *C. portoricensis*; VIN= Vincasar. CP 1 =100 mg/kg, CP 2= 200 mg/kg and CP 3= 300 mg/kg. Values (mean±SDev) are based on 5-8 rats per group.



Figure 4.29: Effect of methanol extract of *C. portoricensis* (CP) in Wistar rats given *N-nitroso-N-methylurea* (MNU) on mammary Myeloperoxidase (MPO) activities. MNU= *N-nitroso-N-methylurea*; CP= *C. portoricensis*; VIN= Vincasar. CP 1 =100 mg/kg, CP 2= 200 mg/kg and CP 3= 300 mg/kg. * = p less than .05 in contrast to vehicle. ** = p less than .05 in contrast to untreated group. Values (mean±SDev) are based on 5-8 rats per group.

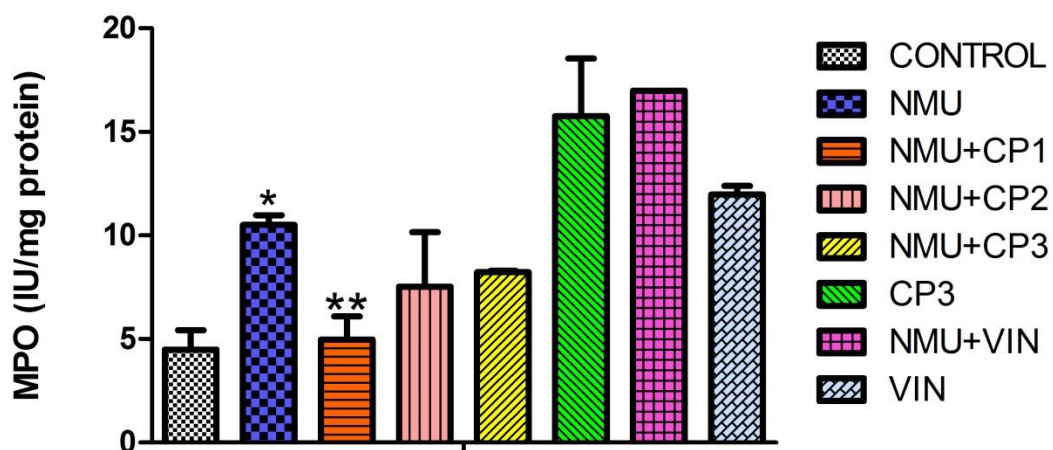


Figure 4.30: Effect of methanol extract of *C. portoricensis* (CP) in Wistar rats given *N-nitroso-N-methylurea* (MNU) on uterine Myeloperoxidase (MPO) activities. MNU= *N-nitroso-N-methylurea*; CP= *C. portoricensis*; VIN= Vincasar. CP 1 =100 mg/kg, CP 2= 200 mg/kg and CP 3= 300 mg/kg. * = p less than .05 in contrast to vehicle. ** = p less than .05 in contrast to untreated group. Values (mean±SDev) are based on 5-8 rats per group.

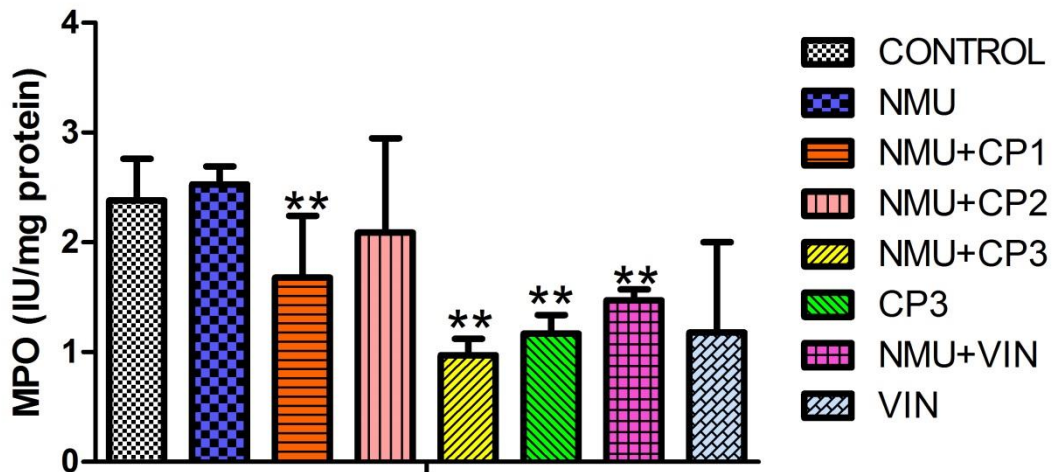


Figure 4.31: Effect of methanol extract of *C. portoricensis* (CP) in Wistar rats given *N*-nitroso-*N*-methylurea (MNU) on ovarian Myeloperoxidase (MPO) activities. MNU= *N*-nitroso-*N*-methylurea; CP= *C. portoricensis*; VIN= Vincasar. CP 1 =100 mg/kg, CP 2= 200 mg/kg and CP 3= 300 mg/kg. ** = p less than .05 in contrast to untreated group. Values (mean±SDev) are based on 5-8 rats per group.

Mammary, uterine and ovarian LPO levels were elevated in MNU treated rats by 16.8%, 17.9% and 167%, respectively relative to vehicles. The LPO levels in these tissues decreased drastically (pless than .05) following CP treatment (Figure 4.32- figure 4.34).

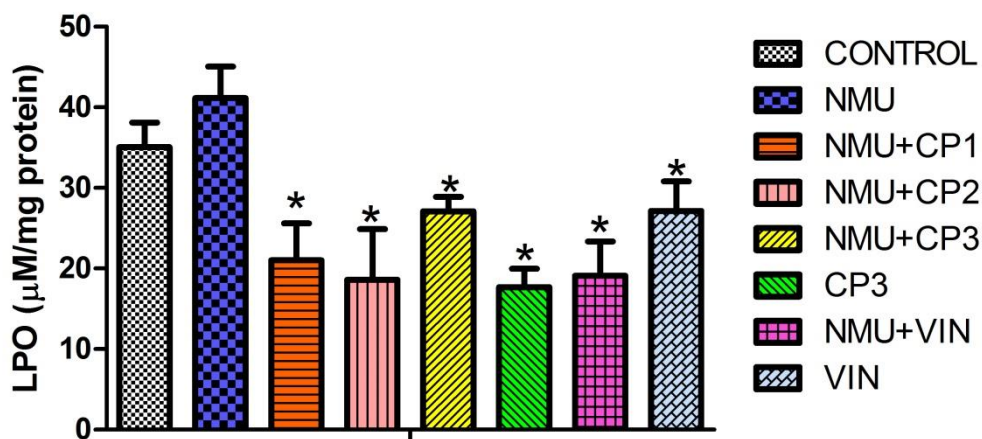


Figure 4.32: Effect of methanol extract of *C. portoricensis* (CP) in Wistar rats given *N*-nitroso-*N*-methylurea (MNU) on mammary Malondialdehyde (LPO) levels. MNU= *N*-nitroso-*N*-methylurea; CP= *C. portoricensis*; VIN= Vincasar. CP 1 =100 mg/kg, CP 2= 200 mg/kg and CP 3= 300 mg/kg. * = p less than .05 in contrast to untreated group. Values (mean±SDev) are based on 5-8 rats per group.



Figure 4.33: Effect of methanol extract of *C. portoricensis* (CP) in Wistar rats given *N*-nitroso-*N*-methylurea (MNU) on uterine Malondialdehyde (LPO) levels. MNU= *N*-nitroso-*N*-methylurea; CP= *C. portoricensis*; VIN= Vincasar. CP 1 =100 mg/kg, CP 2= 200 mg/kg and CP 3= 300 mg/kg. ** = p less than .05 in contrast to untreated group. Values (mean±SDev) are based on 5-8 rats per group.



Figure 4.34: Effect of methanol extract of *C. portoricensis* (CP) in Wistar rats given *N*-nitroso-*N*-methylurea (MNU) on ovarian Malondialdehyde (LPO) levels. MNU= *N*-nitroso-*N*-methylurea; CP= *C. portoricensis*; VIN= Vincasar. CP 1 =100 mg/kg, CP 2= 200 mg/kg and CP 3= 300 mg/kg. * = p less than .05 in contrast to vehicle. ** = p less than .05 in contrast to untreated group. Values (mean±SDev) are based on 5-8 rats per group.

Expression of ER⁺, PR⁺ and EGFR-2 was presented in figures 4.35, 4.36 and 4.37. MNU-treated rats exhibit elevated ER⁺, PR⁺, and EGFR-2 activities, whereas treatment with CP at all doses markedly reduced (pless than .05) activities of ER⁺, PR⁺ and EGFR-2 across the CP treated groups.

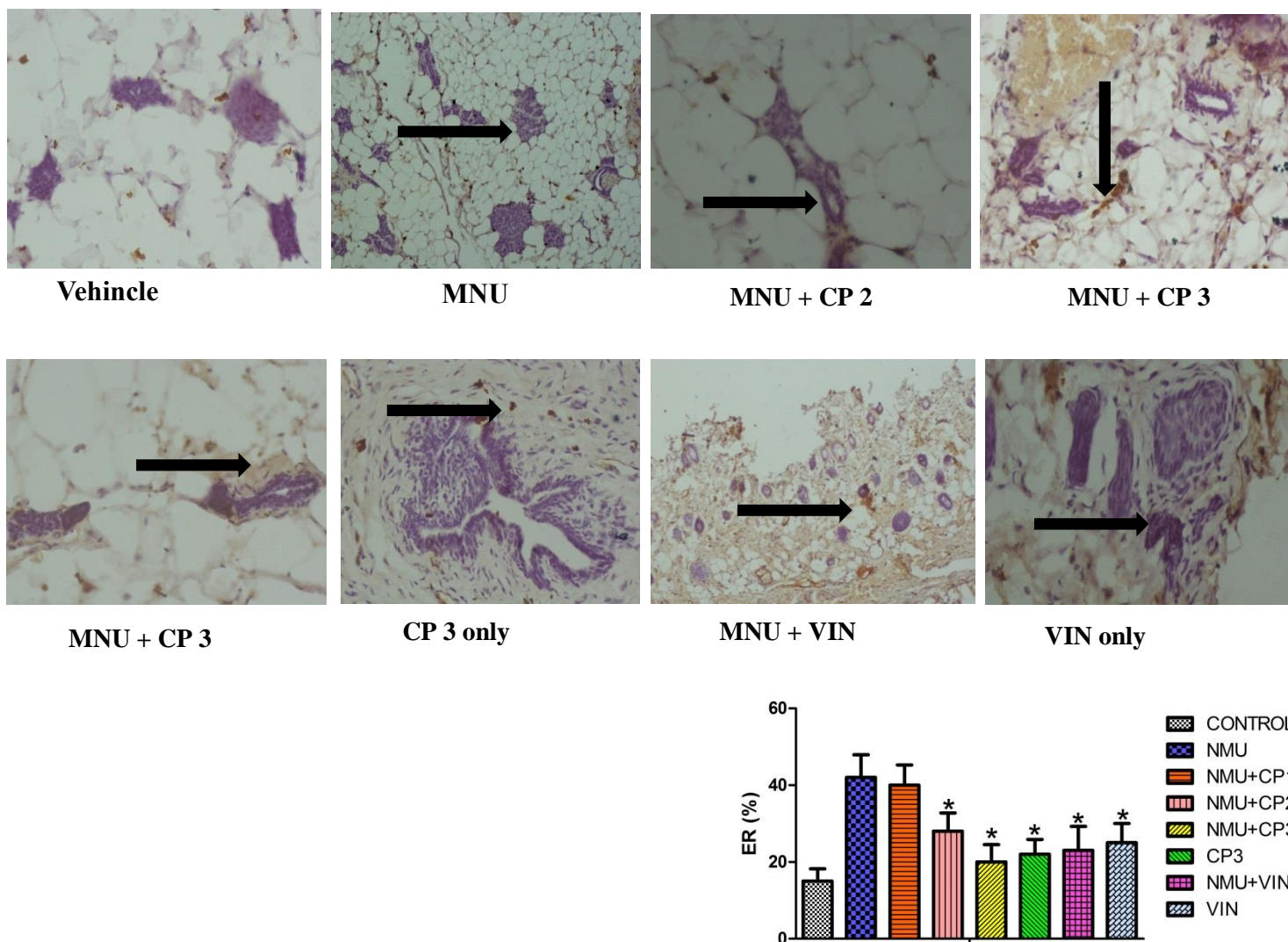


Figure 4.35: Activity of estrogen receptor (ER) in *N-nitroso-N-methylurea* (MNU)-administered rats given methanol extract of *C. portoricensis* (CP). MNU= *N-nitroso-N-methylurea* CP= *C. portoricensis*; VIN= Vincasar. CP 1 =100 mg/kg, CP 2= 200 mg/kg and CP 3= 300 mg/kg. The black arrows showing the expression of estrogen receptors

* = p less than .05 in contrast to untreated group. Values (mean±SDev) are based on 5-8 rats per group.

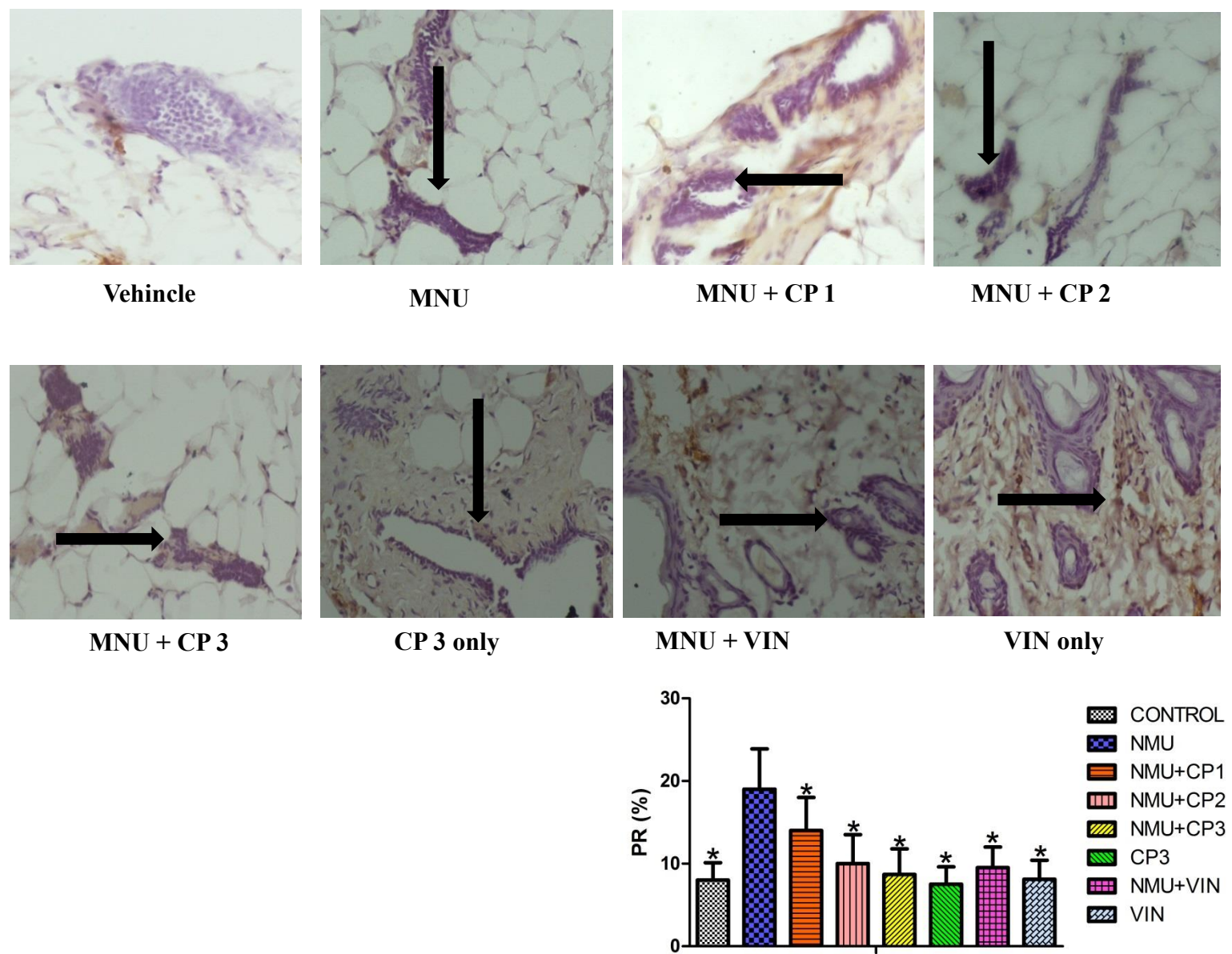


Figure 4.36: Activity of progesterone receptor (PR) in *N-nitroso-N-methylurea* (MNU)-administered rats given methanol extract of *C. portoricensis* (CP). MNU= *N-nitroso-N-methylurea*; CP= *C. portoricensis*; VIN= Vincasar. CP 1 =100 mg/kg, CP 2= 200 mg/kg and CP 3= 300 mg/kg. The black arrows showing the expression of progesterone receptors. * = p less than .05 in contrast to untreated group. Values (mean±SDev) are based on 8 rats per group.

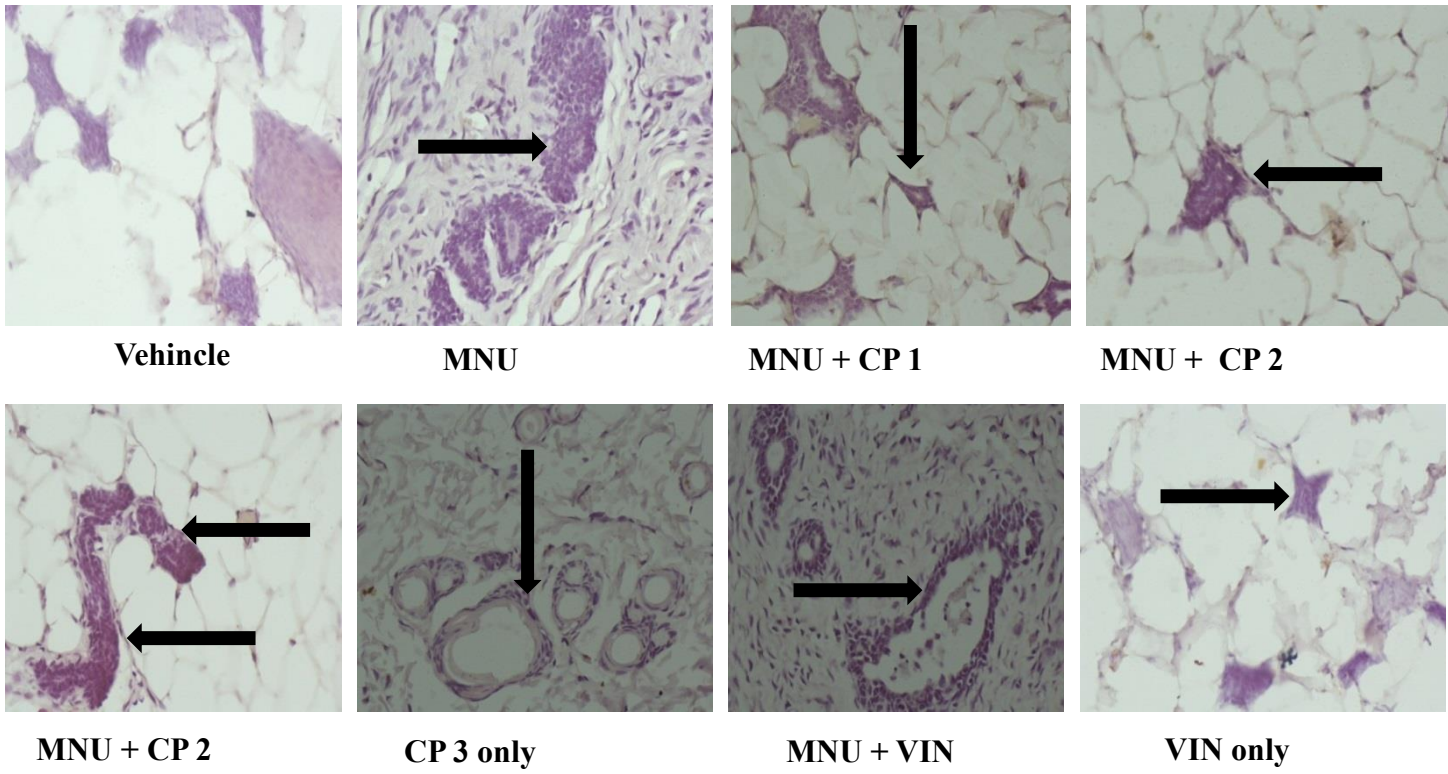


Figure 4.37: Activiy of epidermal growth factor receptor-2 (EGFR-2) in *N-nitroso-N-methylurea* (MNU)-administered rats given methanol extract of *C. portoricensis* (CP). MNU= *N-nitroso-N-methylurea*; CP= *C. portoricensis*; VIN= Vincasar. CP 1 =100 mg/kg, CP 2= 200 mg/kg and CP 3= 300 mg/kg. The black arrows showing the expression of epidermal growth factor receptors. * = pless than .05 in contrast to untreated group. Values (mean±SDev) are based on 8 rats per group.

The cyto-architecture of mammary gland appeared normal showing normal stroma and mammary adipose tissue while MNU-exposed group revealed increase in periductal fibrous tissues along with benign fibroid adenoma (figure 4.38a). Also, the uterine and ovarian tissues appeared normal showing normal uterine endometrial gland and ovarian theca cells layers while MNU-administered groups revealed inflamed uterine stroma cells as well as ovarian stroma with fibrosis (figure 4.38a and figure 4.38b). However co-treatment with CP at all doses attenuated MNU-induced cyto-architecture alterations across the treated groups. Histological analysis of the uterus and ovary revealed that the high dose of CP, specifically 300mg/kg, caused substantial alterations similar to the vehicle group while CP at low dose (100mg/kg) showed mild changes in both uterine and ovarian tissues.

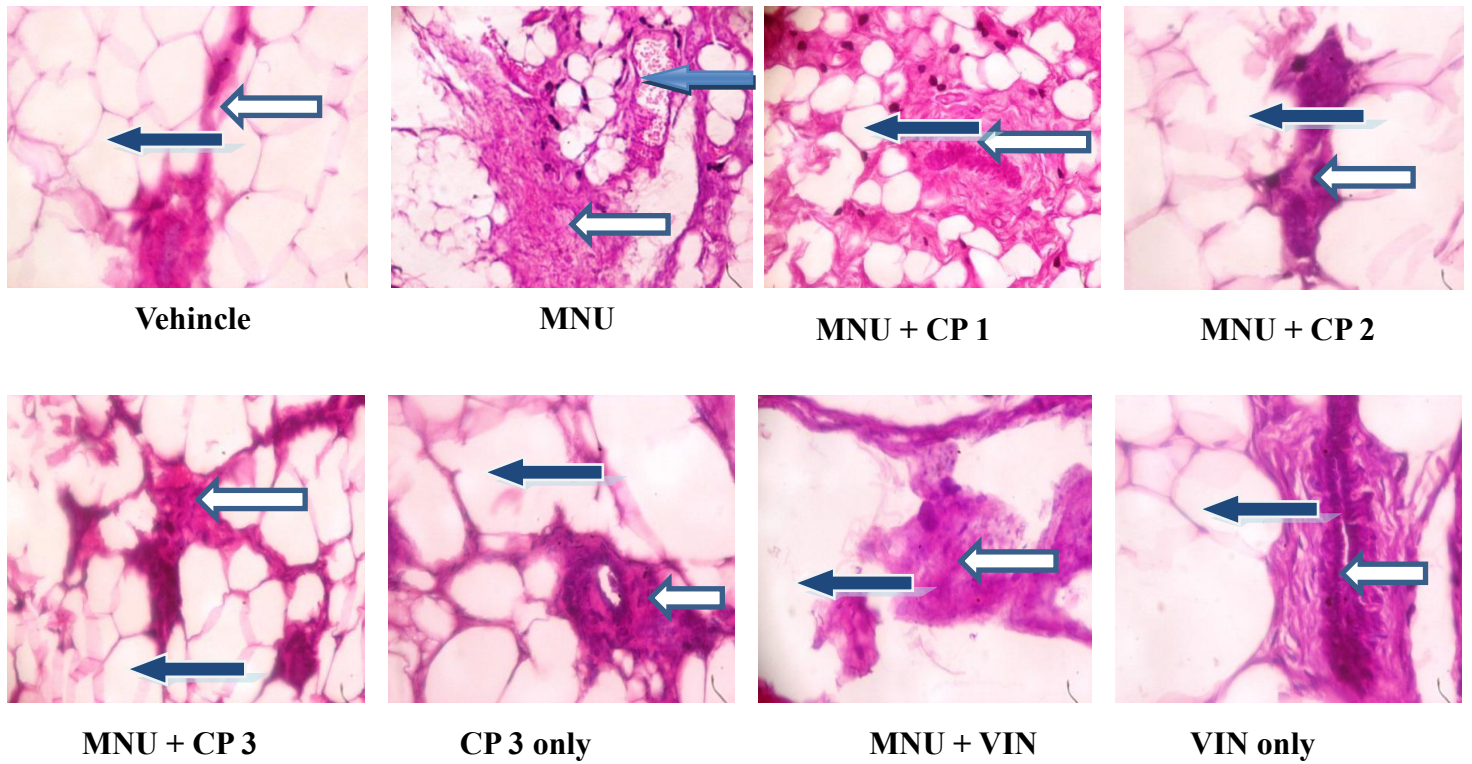
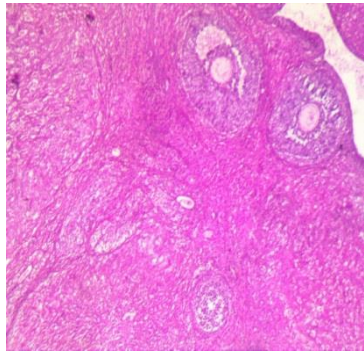
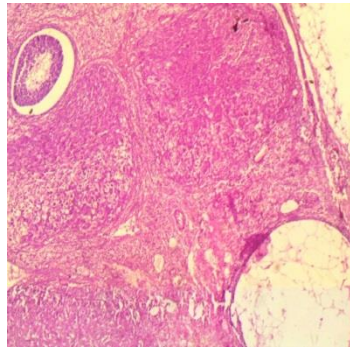


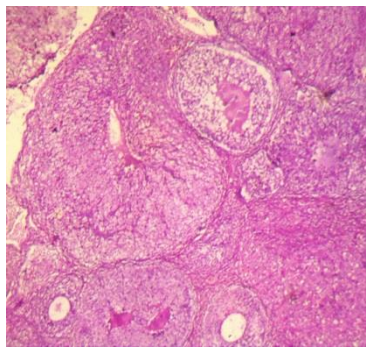
Figure 4.38a: Histopathological alteration of mammary tissues in rats given *N*-nitroso-*N*-methylurea and methanol extract of *C. portoricensis* (M X 400)



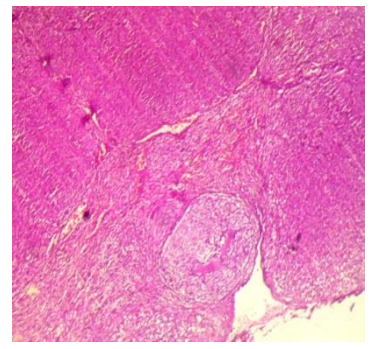
Vehicle



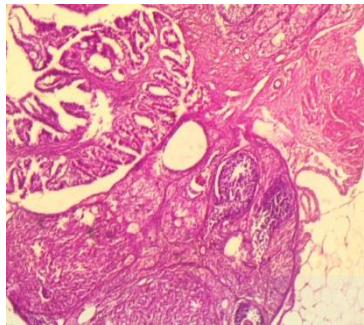
MNU



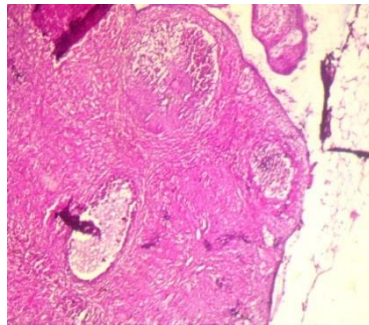
MNU + CP1



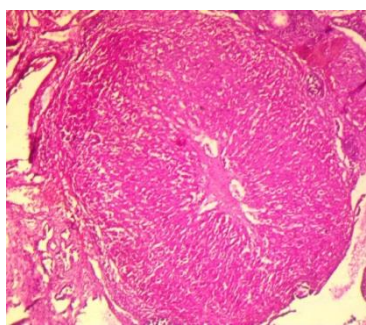
MNU + CP2



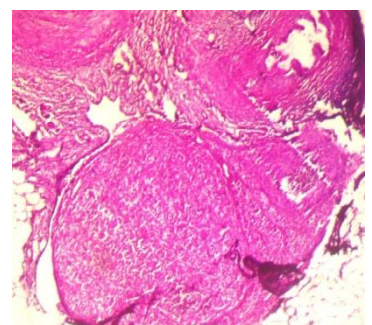
MNU + CP3



CP3 ONLY



MNU + VIN



VIN ONLY

Figure 4.38b: Histopathological alteration of ovary tissues in rats given *N-nitroso-N-methylurea* and methanol extract of *C. portoricensis* (M X 400)

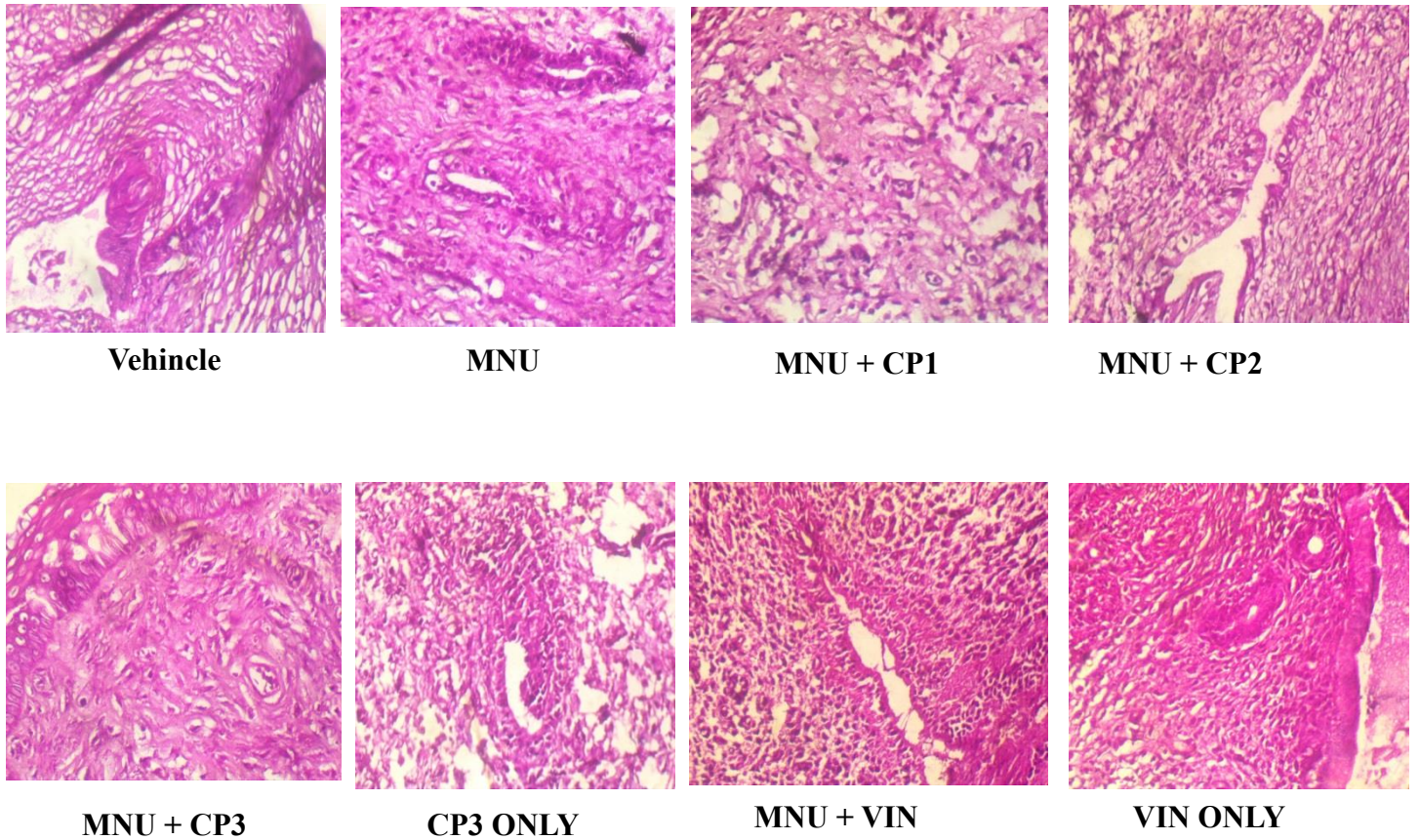


Figure 4.38c: Histopathological alteration of uterus tissues in rats given *N-nitroso-N-methylurea* and methanol extract of *C. portoricensis* (M X 400)

4.2: *In-vitro* Assessment of Antioxidative and Radical Scavenging Activities of *C. portoricensis*

According to table 4.4, CP extracts reduced the ABTS cation radicals in a concentration-dependent manner. Butanol, ethyl acetate and chloroform fractions of CP showed concentration-dependent increase in reducing ABTS cation radical. The chloroform fraction of CP at 50 μ L - 400 μ L showed the highest reducing potential by scavenging ABTS cation radical in a concentration-dependent way relative to catechin. Specifically, the percentage ABTS reducing activity of the chloroform fraction are 27.0%, 34.2%, 35.3%, 36.7% and 38.2% respectively. Also, the ABTS radical scavenging percentages of crude methanol, n-hexane, and ethyl acetate were 10.6%, 21.7%, 27.2%, 26.4% and 30.9% (crude methanol extract); 7.12%, 8.72%, 14.8%, 19.2%, 21.6% (*n*-hexane) 12.6%, 28.5%, 36.15%, 36.9% and 37.6% (ethyl acetate).

TABLE 4.4: THE ABTS RADICAL SCAVENGING ACTIVITY OF *C. portoricensis* In Vitro

CP EXTRACT CONC.	50 (µL/mL)	100 (µL/mL)	200 (µL/mL)	300 (µL/mL)	400 (µL/mL)
ABTS Radical Scavenging (%)					
CATECHIN	27.08±1.32	28.38±2.99	29.42±2.82	33.3±1.71	35.85±2.24
CRUDE METHANOL	10.6±0.17*	21.65±0.38*	27.17±0.39*	26.43±0.42	30.90±1.36*
N-HEXANE FRACTION	7.12±2.29*	8.72±2.68*	14.77±1.32*	19.15±0.85*	21.6±0.39*
BUTANOL FRACTION	25.65±3.59	22.65±3.71	26.37±0.79	24.43±0.43	31.07±0.53
ETHYL-ACE FRACTION	12.58±0.26*	28.53±0.73*	36.15±1.21*	36.87±1.03*	37.6±1.40*
CHF FRACTION	27.03±1.29*	34.17±0.41*	35.33±0.88*	36.72±0.39*	38.15±1.22*

ABTS= (2,2-azinobis-(3-ethylbenzothiazolin-6-sulfonic acid); ETHYL-ACE= Ethylacetate; CHF = Chloroform; *= Concentration-dependent increase in ABTS radical scavenging (%)

Results from table 4.5 shows that CP extracts had a substantial (pless than .05) and concentration-dependent increase in DPPH reducing activity. There was dose-dependent increase in reducing DPPH radical activity in butanol extract, ethyl acetate extract and chloroform fraction. Specifically, the chloroform fraction at 0.0078mg/ml-0.25mg/ml revealed the highest scavenging ability relative to standard catechin in a dose-dependent way. Also, the chloroform fraction, butanol extract, and ethyl acetate extracts all had a percentage DPPH lowering action; 72.5%, 74.4%, 79.1%, 90.5%, 100.8% and 121.0% (chloroform fraction); 53.0%, 52.9%, 53.0%, 55.7%, 55.9%, 57.9%, and 59.8% (butanol extract) and 55.3%, 55.8%, 55.6%, 60.4%, 64.5% and 74.0% (ethyl-acetate extract) respectively.

TABLE 4.5: THE DPPH REDUCING ACTIVITY OF *C. portoricensis* In Vitro

EXTRACT	0.0078	0.0156	0.03125	0.0625	0.125	0.25
CONC	($\mu\text{L}/\text{mL}$)	($\mu\text{L}/\text{mL}$)	($\mu\text{L}/\text{mL}$)	($\mu\text{L}/\text{mL}$)	($\mu\text{L}/\text{mL}$)	($\mu\text{L}/\text{mL}$)
DPPH Radical Scavenging (%)						
CATECHIN	104.90 \pm 4.87	136.57 \pm 2.64	140.66 \pm 2.43	137.89 \pm 4.36	137.67 \pm 2.61	137.90 \pm 3.33
METHANOL	49.05 \pm 2.77	52.77 \pm 3.23	48.52 \pm 3.00	50.41 \pm 3.82	50.55 \pm 8.45	51.85 \pm 6.68
N-HEXANE	76.74 \pm 4.48*	74.48 \pm 4.58*	75.64 \pm 3.82*	78.74 \pm 5.62*	82.75 \pm 2.43*	90.94 \pm 10.99
BUTANOL	52.99 \pm 3.61*	53.02 \pm 2.99*	55.69 \pm 3.76*	55.90 \pm 2.86*	57.89 \pm 3.00*	59.76 \pm 3.86*
ETYL-ACE	55.29 \pm 5.35	55.79 \pm 5.08*	55.64 \pm 6.21*	60.40 \pm 4.23	64.53 \pm 3.13	79.02 \pm 4.34*
CHF	72.46 \pm 3.19*	74.39 \pm 4.38*	79.14 \pm 3.79*	90.51 \pm 3.79*	100.83 \pm 4.28*	21.03 \pm 3.12*

DPPH= 2,2-Diphenyl-1-Picrylhydrazyl; ETYL-ACE= Ethylacetate; CHF = Chloroform; *= Concentration-dependent increase in DPPH radical scavenging (%)

Results from figure 4.41 showed the chloroform fraction of CP have five distinct spot on the TLC plate. Out of the spots separated, spot one which is more visible and

distinct than the other spots have retention value of 0.44. Also, the distinct spot from the chloroform fraction is also present on the ethylacetate fraction but not as distinct as the chloroform fraction. The amount of visible compound present in chloroform fraction of CP compared to the ethylacetate fraction may probably be responsible for the effective activity of the chloroform fraction of CP. In addition, the last fifth spot on CP chlororm fraction may also contribute to the effective activity of chloroform fraction of CP, when compared to the four spots on ethylacetate fraction.

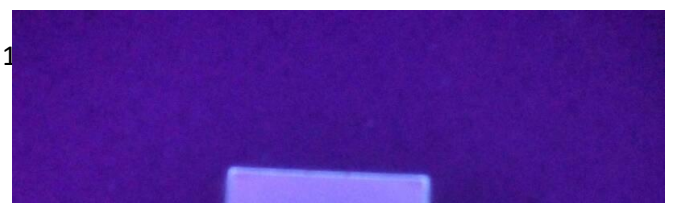


Figure 4.41: Ultra violet view of spotted thin layer chromatography plates

A. TLC plate spotted with different fractions of *C. portoricensis* (H=hexane fraction, C=chloroform fraction, E=ethylacetate fraction, B=butanol fraction and M=methanol fraction)

B. TLC plate spotted with only chloroform fraction of *C. portoricensis*

4.3: Chemopreventive Effects of Chloroform Fraction of *C. portoricensis* on Biochemical Parameters and Hormone Profile in *N-nitroso-N-methylurea* and Benzo[a]pyrene-induced rats

Body weights and organo-somatic weights changes of rats exposed to MNU and BP as well as chloroform fraction of CP was evaluated in tables 4.6 and 4.7. Administration of MNU and BP drastically decreased the animals' body weight gained by 32% when compared to vehicle group. Contrary to this, organo-somatic weights in the uterus, ovary and mammary tissues significantly increased by 2.3 folds, 1.4 fold and 37% respectively in rats exposed to MNU and BP. Co-treatment with chloroform fraction of CP restored body weight gained and organo-somatic weights relative to MNU and BP exposed groups.

Table 4.6: Body weight changes and organo-somatic weight of MNU and BP-exposed rats given chloroform fraction of CP.

	BODY WEIGHT (g)			MAMMARY	TISSUE
	Original	Terminal	Body mass	Body mass (g)	Organ-body
	Body mass (g)	Body mass (g)	Gained (g)		mass(a)
VEHICLE	51.32±2.87	144.97±4.48	93.65±1.45	0.64±0.09	0.49±0.03
MNU+BP	63.83±1.51	141.13±6.00	77.30±6.54*	1.27±0.29*	0.67±0.18
MNU+BP+CP1	68.89±2.68	167.00±2.34	103.1±2.76**	0.71±0.02**	0.46±0.05**
MNU+BP+CP2	73.09±4.25	151.08±4.48	77.99±5.63	0.89±0.20**	0.58±0.17**
CP 2	54.84±2.01	136.38±3.94	81.54±2.71	1.03±0.08	0.66±0.16
MNU+BP+VIN	80.44±5.56	165.8±4.59	85.36±8.82**	0.60±0.09	0.40±0.06**
VIN ONLY	66.02±2.47	141.25±8.80	75.23±3.97	0.49±0.13	0.39±0.13

MNU= *N-nitroso-N-methylurea*; BP= Benzo[a]pyrene; CP= *C. portoricensis*; VIN= Vincasar; a= % body weight. CP 1 =50 mg/kg and CP 2= 100 mg/kg. * = p less than .05 in contrast to vehicle. ** = p less than .05 in contrast to untreated group. Values (mean±SDev) are based on 5-8 rats per group.

TABLE 4.7: Organs weight of MNU and BP-administered rats given chloroform fraction of *C. portoricensis*

	UTERUS		OVARY	
	Body mass (g)	Organ- body mass ^a	Body mass (g)	Organ- body mass ^a
VEHICLE	0.17±0.03	0.11±0.01	0.11±0.02	0.07±0.02
MNU + BP	0.24±0.08	0.22±0.03*	0.14±0.02	0.10±0.02
MNU+BP+CP1	0.22±0.06	0.23±0.03	0.14±0.03	0.09±0.02
MNU+BP+CP2	0.16±0.03	0.15±0.02	0.13±0.02	0.05±0.01**
CP 2	0.21±0.06	0.18±0.01	0.13±0.01	0.08±0.02
MNU + VIN	0.12±0.02	0.08±0.01	0.18±0.01	0.06±0.00
VIN ONLY	0.14±0.03	0.15±0.04	0.13±0.01	0.09±0.00

MNU= *N-nitroso-N-methylurea*; BP= Benzo[a]pyrene; CP= *C. portoricensis*; VIN= Vincasar; a= % body weight. CP 1 =50 mg/kg and CP 2= 100 mg/kg. * = p less than .05 in contrast to vehicle. ** = p less than .05 in contrast to untreated group. Values (mean±SDev) are based on 5-8 rats per group.

The urinary parameters of MNU and BP administered rats were investigated in table 4.8 and the results showed moderate presence of bilirubin levels whereas, a 100 mg/kg dose of CP reduced bilirubin levels in urine samples.

Table 4.8: Urinary parameters of MNU and BP-administered rats given chloroform fraction of *C. portoricensis*

Treatment	Protein	Glucose	Bilirubin	pH	Ketone	Urobilinogen	Nitrite	Ascorbic Acid
Vehicle	+	-	-	6.3	-	+++	-	++
MNU+BP	+	-	++	7.3	-	+++	-	-
MNU+BP+CP1	+	-	++	6	-	+++	-	-
MNU+BP+CP2	-	-	+	6.3	-	+++	-	-
CP2	+	-	Absence	6.5	-	+++	-	++
MNU+VIN	+	-	++	7	-	+++	-	-
VIN	+	-	++	7	-	+++	-	++

MNU= *N-nitroso-N-methylurea*; BP= Benzo[a]pyrene; CP= *C. portoricensis*; VIN= Vincasar. CP 1 =50mg/kg and CP 2= 100 mg/kg.

+ = Mild; - =Negative; ++ = Moderate; +++ = Normal

MNU and BP administration caused remarkable reduction in mammary superoxide dismutase (SOD), catalase (CAT), glutathione-S-transferase (GST), total sulphhydryl (TSH) and glutathione peroxidase (GPx) activities by 46%, 38%, 47%, 50% and 49%, respectively when compared to vehicle (Figures 4.41-4.46). However, co-administration with chloroform fraction of CP at both doses of 50mg/kg and 100 mg/kg interestingly mitigated SOD, CAT, GST, TSH and GPx activities statistically similar to vehicle values.

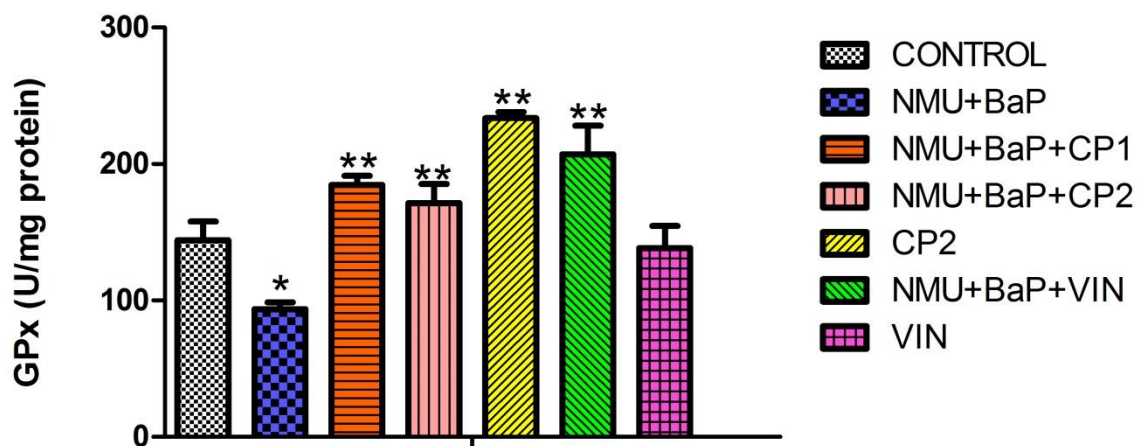


Figure 4.42: Effect of chloroform fraction of *C. portoricensis* (CP) in Wistar rats given MNU and BP on mammary glutathione peroxidase (GPx) activities. MNU= *N*-nitroso-*N*-methylurea; BP= Benzo[a]pyrene; CP= *C. portoricensis*; VIN= Vincasar. CP 1 =50 mg/kg and CP 2= 100 mg/kg. * = p less than .05 in contrast to vehicle. ** = p less than .05 in contrast to untreated group. Values (mean±SDev) are based on 5-8 rats per group.

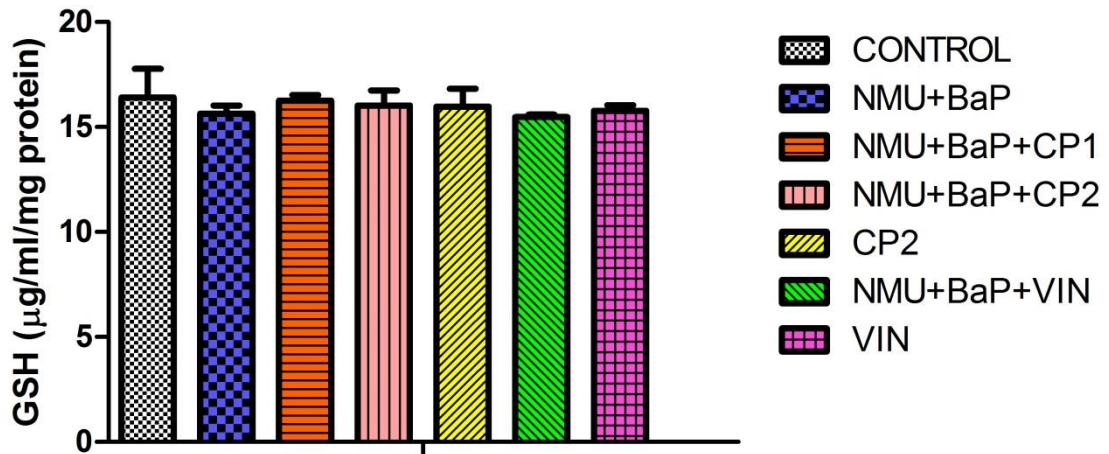


Figure 4.43: Effect of chloroform fraction of *C. portoricensis* (CP) in Wistar rats given *MNU* and *BP* on mammary reduced glutathione (GSH) levels. *MNU*= *N*-nitroso-*N*-methylurea; *BP*= Benzo[*a*]pyrene; *CP*= *C. portoricensis*; *VIN*= Vincasar. *CP* 1 =50 mg/kg and *CP* 2= 100 mg/kg.

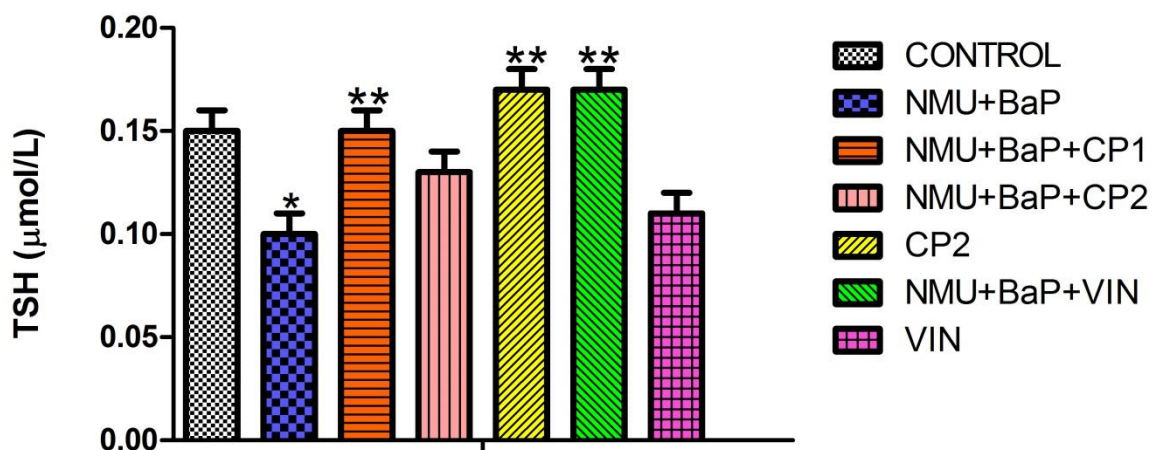


Figure 4.44: Effect of chloroform fraction of *C. portoricensis* (CP) in Wistar rats given MNU and BP on mammary total sulphydryl (TSH) levels. MNU= *N*-nitroso-*N*-methylurea; BP= Benzo[a]pyrene; CP= *C. portoricensis*; VIN= Vincasar. CP 1 =50 mg/kg and CP 2= 100 mg/kg. * = p less than .05 in contrast to vehicle. ** = p less than .05 in contrast to untreated group. Values (mean±SDev) are based on 5-8 rats per group.

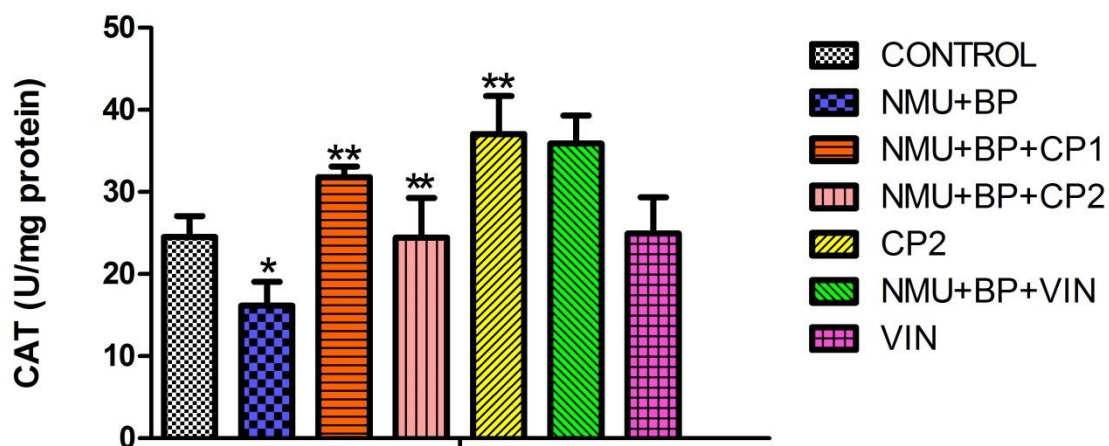


Figure 4.45: Effect of chloroform fraction of *C. portoricensis* (CP) in Wistar rats given *MNU* and *BP* on mammary Catalase (CAT) activities. *MNU*= *N-nitroso-N-methylurea*; *BP*= Benzo[a]pyrene; *CP*= *C. portoricensis*; *VIN*= Vincasar. CP 1 =50 mg/kg and CP 2= 100 mg/kg. * = p less than .05 in contrast to vehicle. ** = p less than .05 in contrast to untreated group. Values (mean±SDev) are based on 5-8 rats per group.

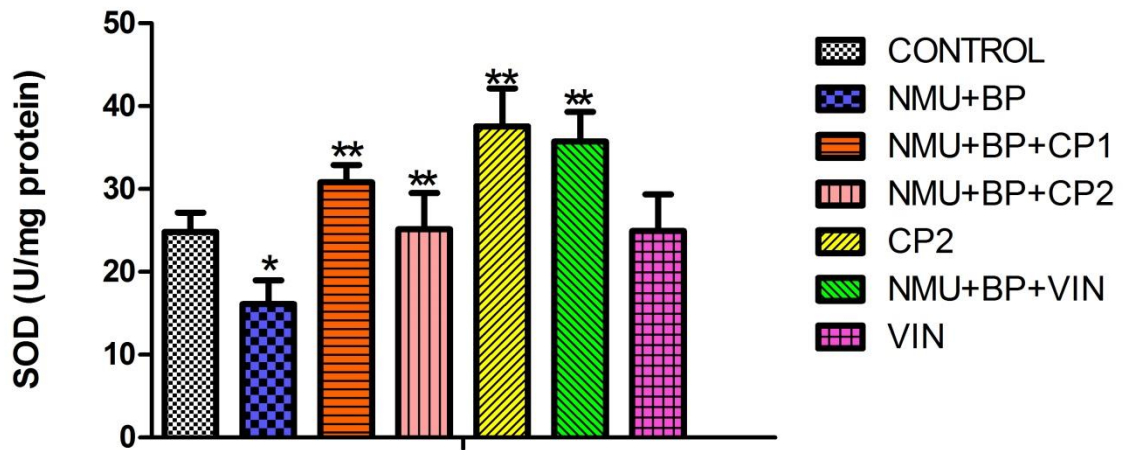


Figure 4.46: Effect of chloroform fraction of *C. portoricensis* (CP) in Wistar rats given MNU and BP on mammary superoxide dismutase (SOD) activities. MNU= *N*-nitroso-*N*-methylurea; BP= Benzo[a]pyrene; CP= *C. portoricensis*; VIN= Vincasar. CP 1 =50 mg/kg and CP 2= 100 mg/kg. * = p less than .05 in contrast to vehicle. ** = p less than .05 in contrast to untreated group. Values (mean±SDev) are based on 5-8 rats per group.

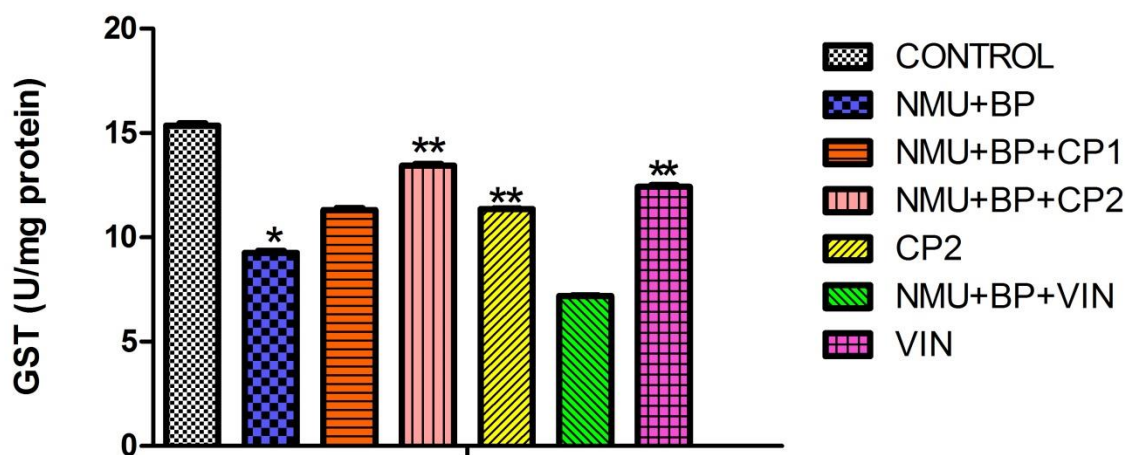


Figure 4.47: Effect of chloroform fraction of *C. portoricensis* (CP) in Wistar rats given MNU and BP on mammary glutathione-S-transferase (GST) activities. MNU= *N*-nitroso-*N*-methylurea; BP= Benzo[a]pyrene; CP= *C. portoricensis*; VIN= Vincasar. CP 1 =50 mg/kg and CP 2= 100 mg/kg. * = p less than .05 in contrast to vehicle. ** = p less than .05 in contrast to untreated group. Values (mean±SDev) are based on 5-8 rats per group.

Mammary malondialdehyde (MDA; index of oxidative stress) level increased drastically in MNU and BP-treated rats by 2.6 folds. Comparably, nitric oxide (NO) level and myeloperoxidase (MPO) activity were significantly elevated by 2.6 folds and 1.7 folds; respectively in the mammary tissues of MNU and BP groups. Whereas co-treatment with CP at both doses significantly (pless than .05) attenuated mammary LPO, NO and MPO in relation to MNU and BP groups.



Figure 4.48: Effect of chloroform fraction of *C. portoricensis* (CP) in Wistar rats given *MNU* and *BP* on mammary myeloperoxidase (MPO) activities. *MNU*= *N-nitroso-N-methylurea*; *BP*= Benzo[*a*]pyrene; *CP*= *C. portoricensis*; *VIN*= Vincasar. *CP* 1 =50 mg/kg and *CP* 2= 100 mg/kg. * = *p* less than .05 in contrast to vehicle. ** = *p* less than .05 in contrast to untreated group. Values (mean±SDev) are based on 5-8 rats per group.

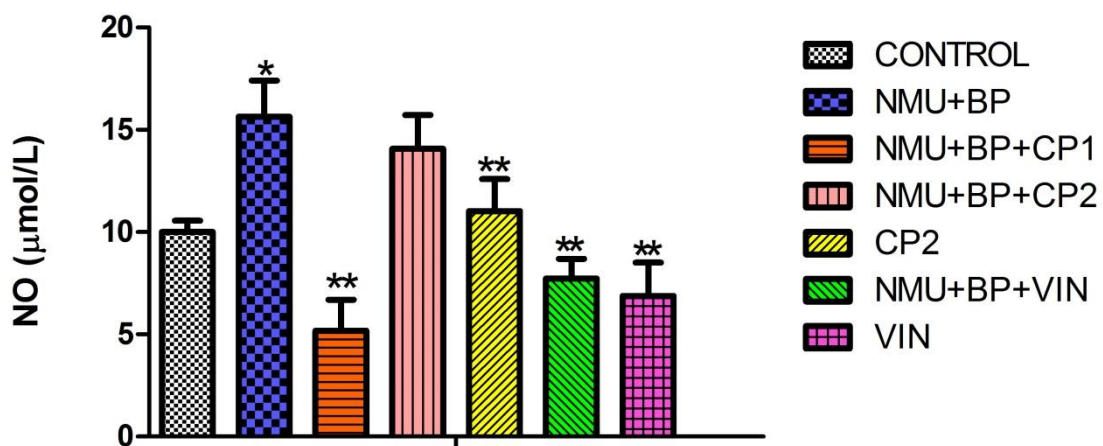


Figure 4.49: Effect of chloroform fraction of *C. portoricensis* (CP) in Wistar rats given *MNU* and *BP* on mammary nitric oxide (NO) levels. *MNU*= *N-nitroso-N-methylurea*; *BP*= Benzo[*a*]pyrene; *CP*= *C. portoricensis*; *VIN*= Vincasar. *CP* 1 =50 mg/kg and *CP* 2= 100 mg/kg. * = *p* less than .05 in contrast to vehicle. ** = *p* less than .05 in contrast to untreated group. Values (mean±SDev) are based on 5-8 rats per group.

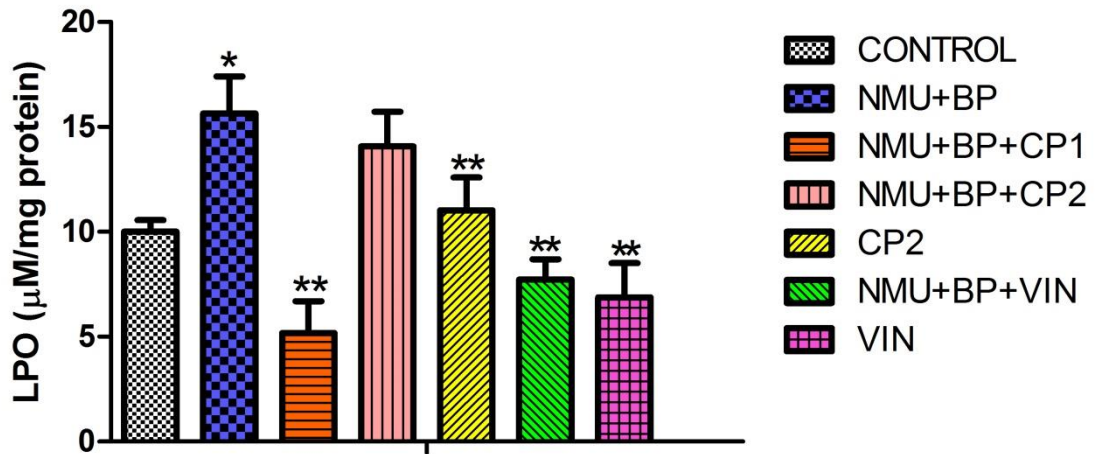


Figure 4.50: Effect of chloroform fraction of *C. portoricensis* (CP) in Wistar rats given MNU and BP on mammary malondialdehyde (LPO) levels. MNU= *N*-nitroso-*N*-methylurea; BP= Benzo[a]pyrene; CP= *C. portoricensis*; VIN= Vincasar. CP 1 =50 mg/kg and CP 2= 100 mg/kg. * = p less than .05 in contrast to vehicle. ** = p less than .05 in contrast to untreated group. Values (mean±SDev) are based on 5-8 rats per group.

Administration of MNU and BP significantly reduced uterine CAT, GST, GPx, and TSH compared to vehicles. While in uterine SOD and GSH, there were no significant variations. However, co-treatment with CP at both doses mitigated the antioxidants activities across the treated groups.

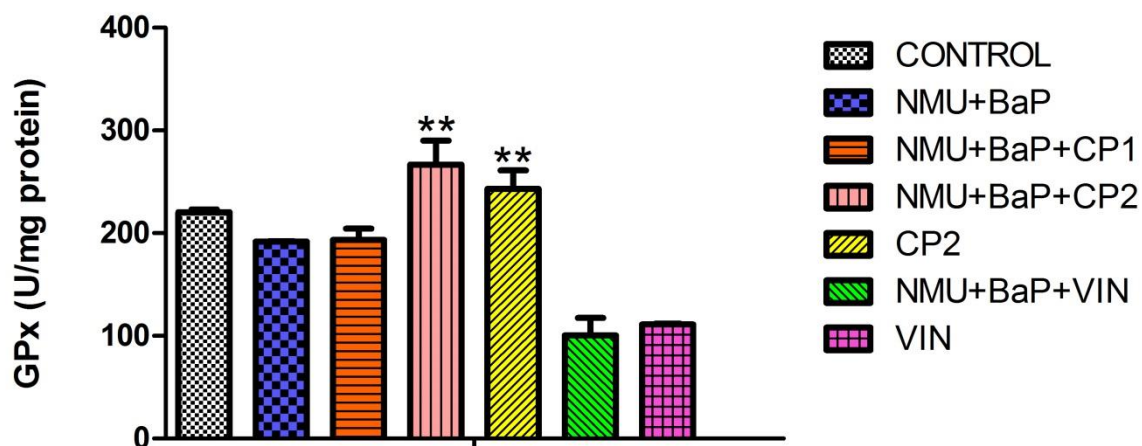


Figure 4.51: Effect of chloroform fraction of *C. portoricensis* (CP) in Wistar rats given *MNU* and *BP* on uterine glutathione peroxidase (GPx) activities. *MNU*= *N*-nitroso-*N*-methylurea; *BP*= Benzo[*a*]pyrene; *CP*= *C. portoricensis*; *VIN*= Vincasar. *CP* 1 =50 mg/kg and *CP* 2= 100 mg/kg. ** = *p* less than .05 in contrast to untreated group. Values (mean±SDev) are based on 5-8 rats per group.

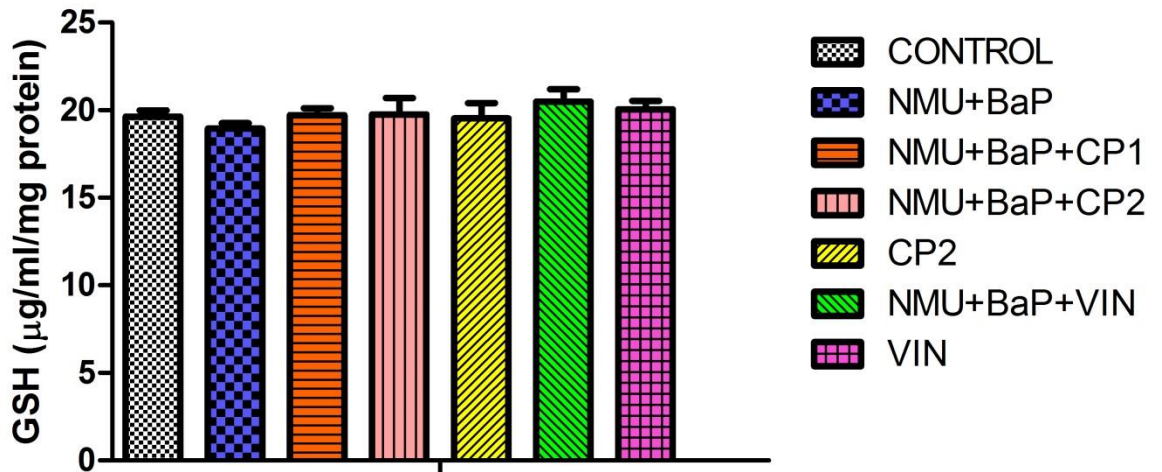


Figure 4.52: Effect of chloroform fraction of *C. portoricensis* (CP) in *Wistar* rats given *MNU* and *BP* on uterine reduced glutathione (GSH) levels. MNU= *N*-nitroso-*N*-methylurea; BP= Benzo[a]pyrene; CP= *C. portoricensis*; VIN= Vincasar. CP 1 =50 mg/kg and CP 2= 100 mg/kg.

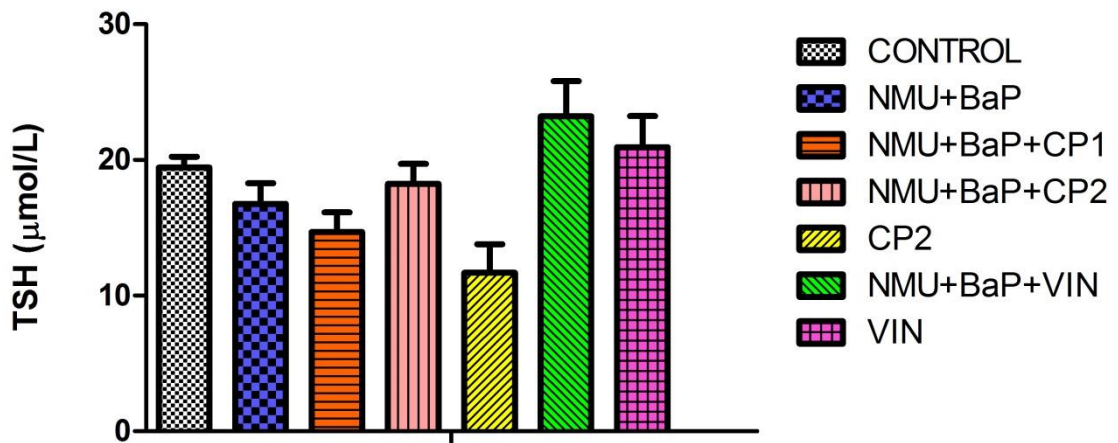


Figure 4.53: Effect of chloroform fraction of *C. portoricensis* (CP) in Wistar rats given MNU and BP on uterine total sulphydryl (TSH) levels. MNU= *N*-nitroso-*N*-methylurea; BP= Benzo[a]pyrene; CP= *C. portoricensis*; VIN= Vincasar. CP 1 =50 mg/kg and CP 2= 100 mg/kg



Figure 4.54: Effect of chloroform fraction of *C. portoricensis* (CP) in Wistar rats given MNU and BP on uterine Catalase (CAT) activities. MNU= *N*-nitroso-*N*-methylurea; BP= Benzo[a]pyrene; CP= *C. portoricensis*; VIN= Vincasar. CP 1 =50 mg/kg and CP 2= 100 mg/kg. * = p less than .05 in contrast to vehicle. ** = p less than .05 in contrast to untreated group. Values (mean±SDev) are based on 5-8 rats per group.

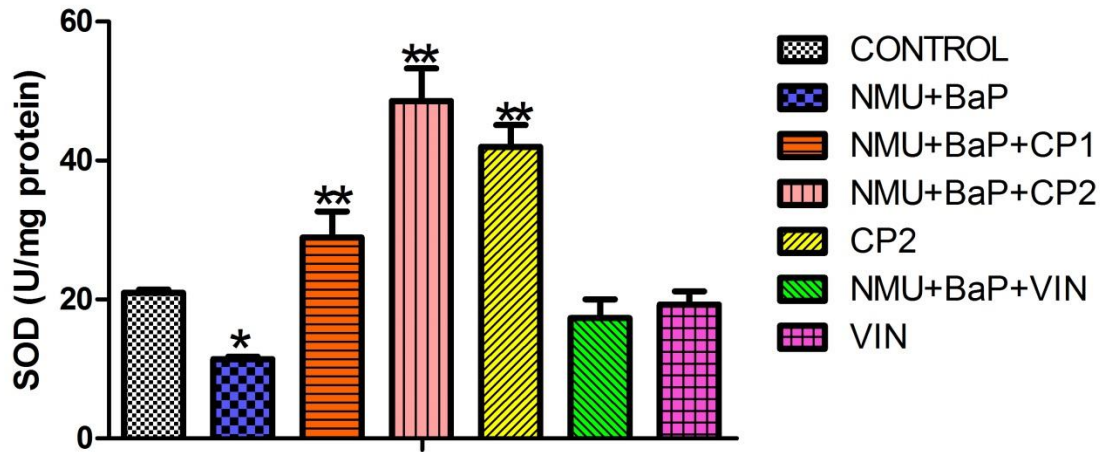


Figure 4.55: Effect of chloroform fraction of *C. portoricensis* (CP) in *Wistar* rats given *MNU* and *BP* on uterine superoxide dismutase (SOD) activities. MNU= *N-nitroso-N-methylurea*; BP= Benzo[a]pyrene; CP= *C. portoricensis*; VIN= Vincasar. CP 1 =50 mg/kg and CP 2= 100 mg/kg * = p less than .05 in contrast to vehicle. ** = p less than .05 in contrast to untreated group. Values (mean±SDev) are based on 5-8 rats per group.



Figure 4.56: Effect of chloroform fraction of *C. portoricensis* (CP) in Wistar rats given *MNU* and *BP* on uterine glutathione-S-transferase (GST) activities. MNU= *N*-nitroso-*N*-methylurea; BP= Benzo[a]pyrene; CP= *C. portoricensis*; VIN= Vincasar. CP 1 =50 mg/kg and CP 2= 100 mg/kg. * = p less than .05 in contrast to vehicle. ** = p less than .05 in contrast to untreated group. Values (mean±SDev) are based on 5-8 rats per group.

Uterine malondialdehyde level increased in MNU and BP-treated rats by 2.9%. Also, nitric oxide (NO) level and myeloperoxidase (MPO) activity were markedly increased by 18% and 4 folds respectively in uterine tissues of MNU and BP groups. Whereas co-treatment with CP at both doses significantly (pless than .05) attenuated uterine LPO, NO and MPO in relation to MNU and BP groups.

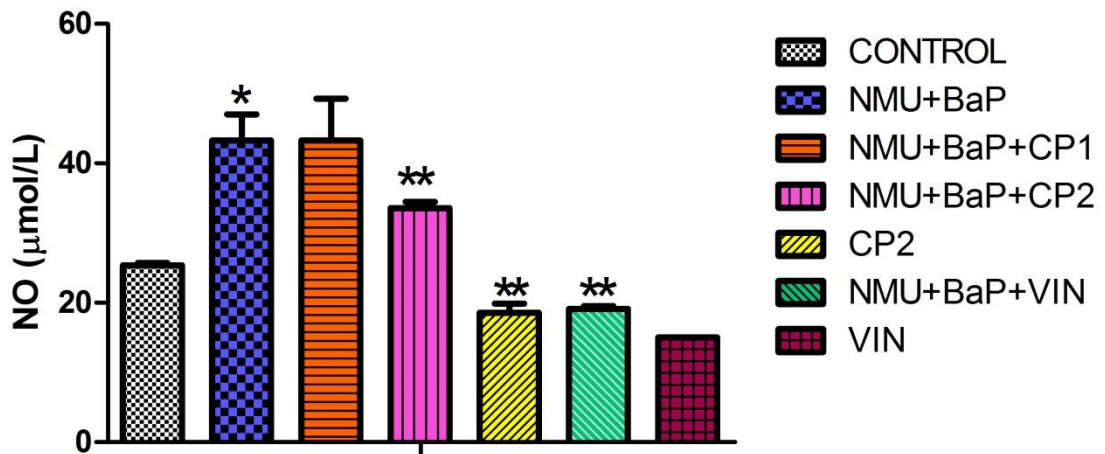


Figure 4.57: Effect of chloroform fraction of *C. portoricensis* (CP) in Wistar rats given MNU and BP on uterine nitric oxide (NO) levels. MNU= *N-nitroso-N-methylurea*; BP= Benzo[a]pyrene; CP= *C. portoricensis*; VIN= Vincasar. CP 1 =50 mg/kg and CP 2= 100 mg/kg. * = p less than .05 in contrast to vehicle. ** = p less than .05 in contrast to untreated group. Values (mean±SDev) are based on 5-8 rats per group.



Figure 4.58: Effect of chloroform fraction of *C. portoricensis* (CP) in Wistar rats given MNU and BP on uterine myeloperoxidase (MPO) activities. MNU= *N*-nitroso-*N*-methylurea; BP= Benzo[a]pyrene; CP= *C. portoricensis*; VIN= Vincasar. CP 1 =50 mg/kg and CP 2= 100 mg/kg. * = p less than .05 in contrast to vehicle. ** = p less than .05 in contrast to untreated group. Values (mean±SDev) are based on 5-8 rats per group.

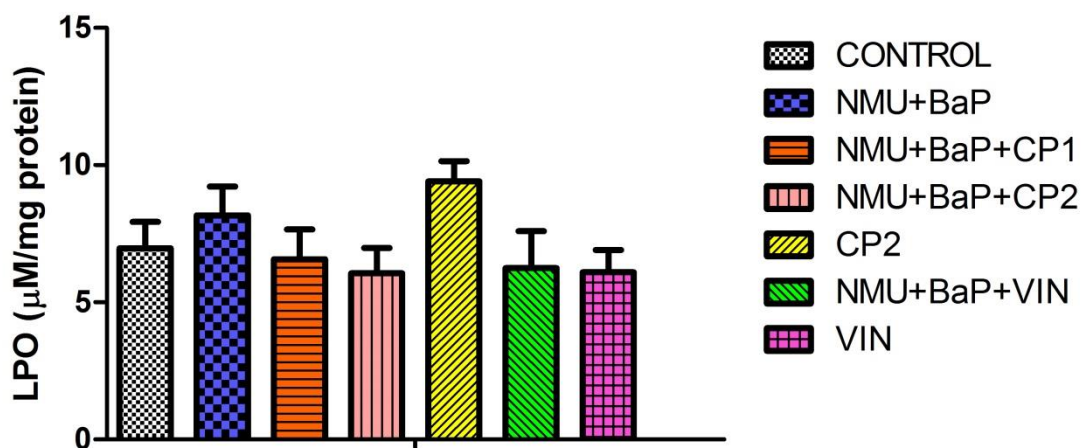


Figure 4.59: Effect of chloroform fraction of *C. portoricensis* (CP) in Wistar rats given *MNU* and *BP* on uterine malondialdehyde (LPO) levels. *MNU*= *N*-nitroso-*N*-methylurea; *BP*= Benzo[a]pyrene; *CP*= *C. portoricensis*; *VIN*= Vincasar. CP 1 =50 mg/kg and CP 2= 100 mg/kg.

The activities of ovarian GST, CAT, GPx and TSH levels depleted in MNU and BP exposed rats when compared to vehincls. In addition, the MNU and BP-treated groups, shows a modest decrease in ovarian SOD activity and GSH level in relation to vehincls group. However, co-treatment with chloroform fraction of CP at both doses of 50mg/kg and 100 mg/kg mitigated the antioxidants activities statistically similar to vehincls values.

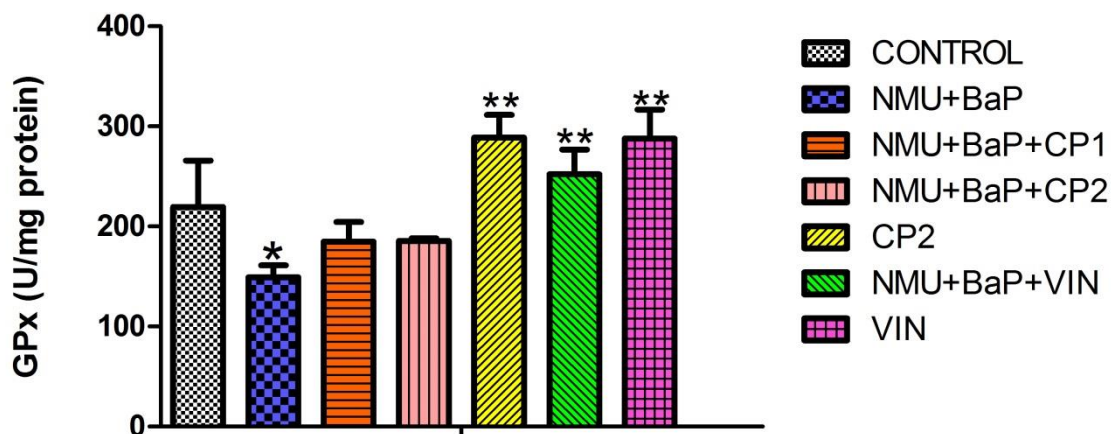


Figure 4.60: Effect of chloroform fraction of *C. portoricensis* (CP) in Wistar rats given MNU and BP on ovarian glutathione peroxidase (GPx) activities. MNU= *N*-nitroso-*N*-methylurea; BP= Benzo[a]pyrene; CP= *C. portoricensis*; VIN= Vincasar. CP 1 =50 mg/kg and CP 2= 100 mg/kg. * = p less than .05 in contrast to vehicle. ** = p less than .05 in contrast to untreated group. Values (mean±SDev) are based on 5-8 rats per group.

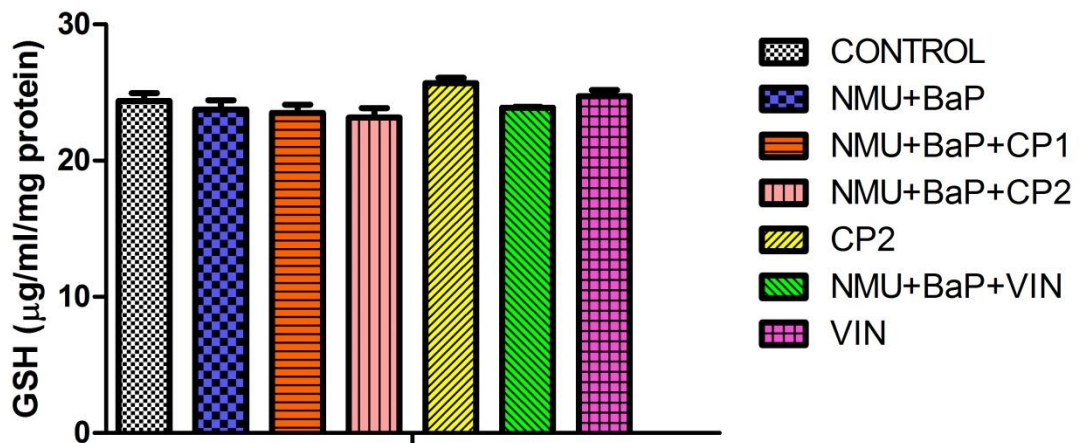


Figure 4.61: Effect of chloroform fraction of *C. portoricensis* (CP) in Wistar rats given MNU and BP on ovarian reduced glutathione (GSH) levels. MNU= *N*-nitroso-*N*-methylurea; BP= Benzo[a]pyrene; CP= *C. portoricensis*; VIN= Vincasar. CP 1 =50 mg/kg and CP 2= 100 mg/kg.

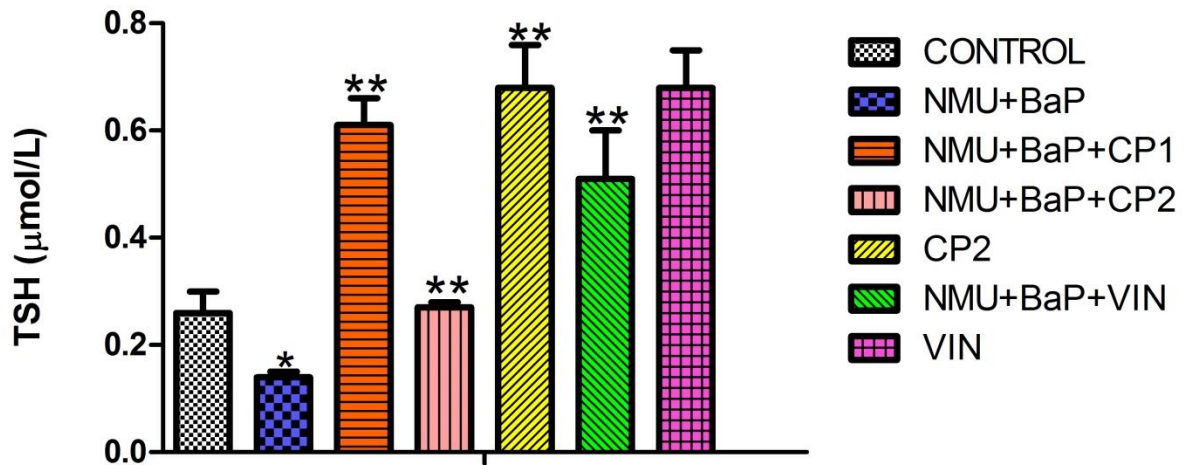


Figure 4.62: Effect of chloroform fraction of *C. portoricensis* (CP) in Wistar rats given MNU and BP on ovarian total sulphhydryl (TSH) levels. MNU= *N-nitroso-N-methylurea*; BP= Benzo[a]pyrene; CP= *C. portoricensis*; VIN= Vincasar. CP 1 =50 mg/kg and CP 2= 100 mg/kg. * = p less than .05 in contrast to vehicle. ** = p less than .05 in contrast to untreated group. Values (mean±SDev) are based on 5-8 rats per group.

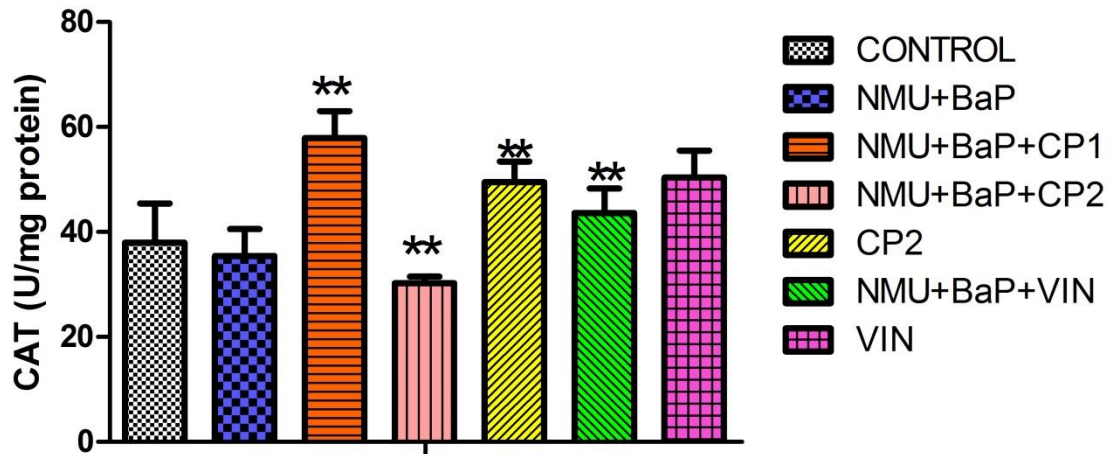


Figure 4.63: Effect of chloroform fraction of *C. portoricensis* (CP) in Wistar rats given MNU and BP on ovarian Catalase (CAT) activities. MNU= *N*-nitroso-*N*-methylurea; BP= Benzo[a]pyrene; CP= *C. portoricensis*; VIN= Vincasar. CP 1 =50 mg/kg and CP 2= 100 mg/kg. **= p less than .05 in contrast to untreated group. Values (mean±SDev) are based on 5-8 rats per group.

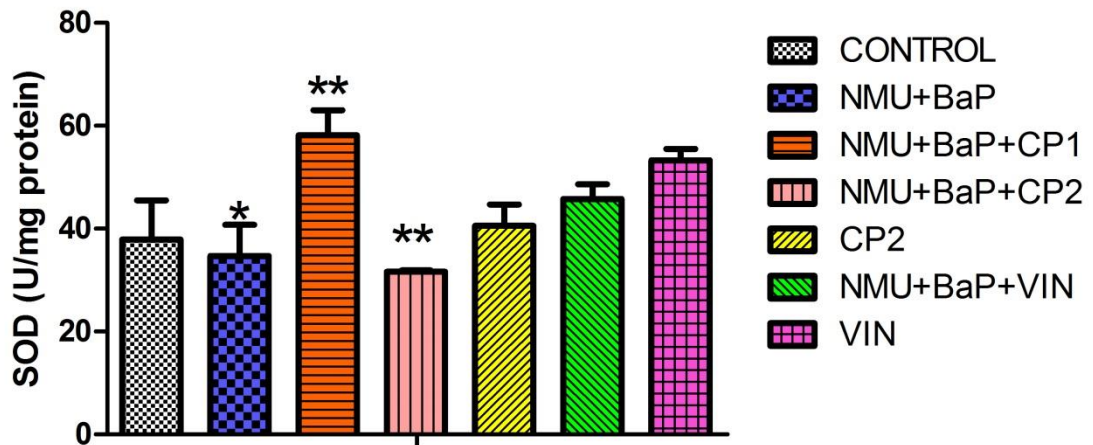


Figure 4.64: Effect of chloroform fraction of *C. portoricensis* (CP) in Wistar rats given MNU and BP on ovarian superoxide dismutase (SOD) activities. MNU= *N*-nitroso-*N*-methylurea; BP= Benzo[a]pyrene; CP= *C. portoricensis*; VIN= Vincasar. CP 1 =50 mg/kg and CP 2= 100 mg/kg. * = p less than .05 in contrast to vehicle. ** = p less than .05 in contrast to untreated group. Values (mean±SDev) are based on 5-8 rats per group.

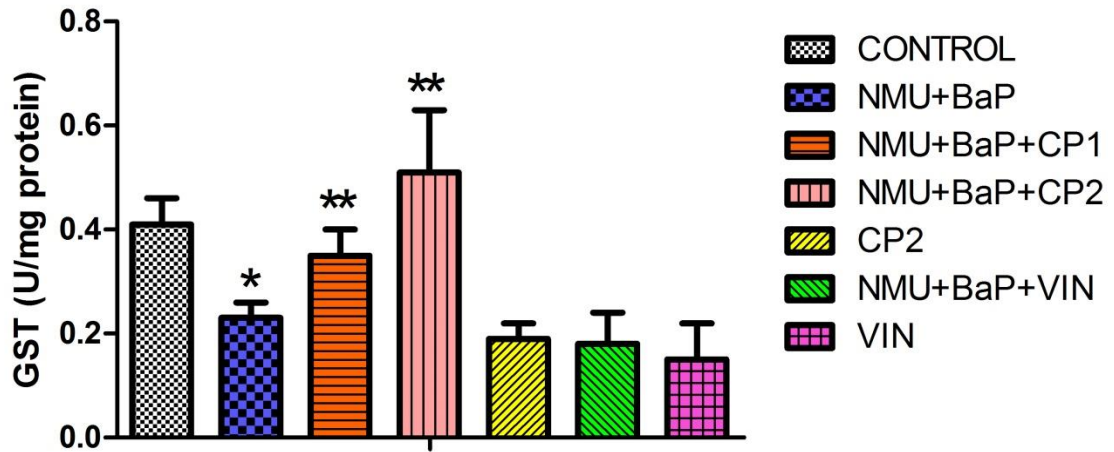


Figure 4.65: Effect of chloroform fraction of *C. portoricensis* (CP) in Wistar rats given MNU and BP on ovarian glutathione-S-transferase (GST) activities. MNU= *N*-nitroso-*N*-methylurea; BP= Benzo[a]pyrene; CP= *C. portoricensis*; VIN= Vincasar. CP 1 =50 mg/kg and CP 2= 100 mg/kg. * = p less than .05 in contrast to vehicle. ** = p less than .05 in contrast to untreated group. Values (mean±SDev) are based on 5-8 rats per group.

Ovarian malondialdehyde level was significantly elevated in MNU and BP-treated rats by 58% when compared to vehicle group. Comparably, nitric oxide (NO) level and myeloperoxidase (MPO) activity were drastically increased by 2 folds and 38.9%, respectively, in ovarian tissues of MNU and BP groups. Whereas co-treatment with CP at both doses significantly (p less than .05) ameliorated ovarian LPO, NO and MPO in relation to MNU and BP groups.

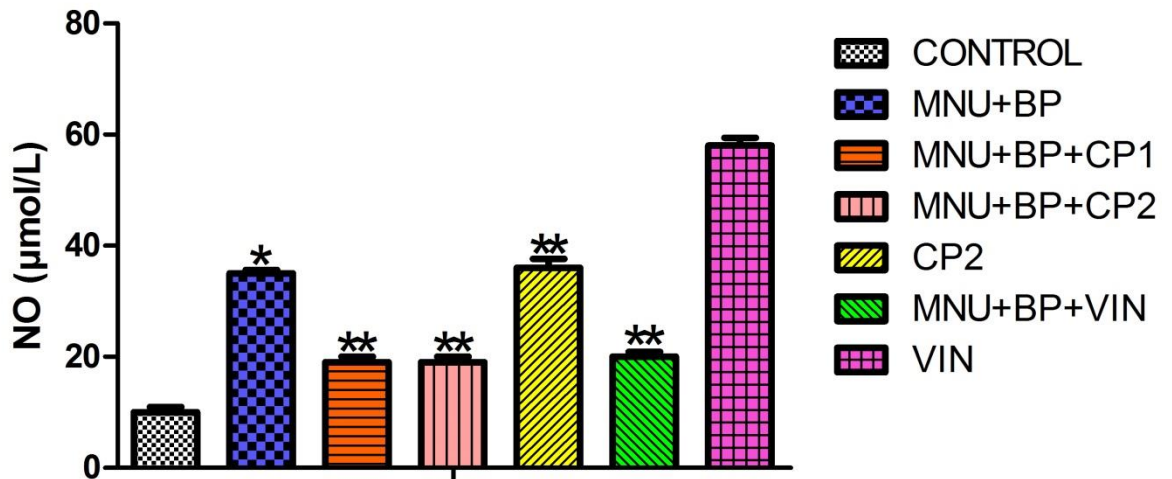


Figure 4.66: Effect of chloroform fraction of *C. portoricensis* (CP) in Wistar rats given MNU and BP on ovarian nitric oxide (NO) levels. MNU= *N*-nitroso-*N*-methylurea; BP= Benzo[a]pyrene; CP= *C. portoricensis*; VIN= Vincasar. CP 1 =50 mg/kg and CP 2= 100 mg/kg. * = p less than .05 in contrast to vehicle. ** = p less than .05 in contrast to untreated group. Values (mean±SDev) are based on 5-8 rats per group.



Figure 4.67: Effect of chloroform fraction of *C. portoricensis* (CP) in *Wistar* rats given MNU and BP on ovarian myeloperoxidase (MPO) activities. MNU= *N*-nitroso-*N*-methylurea; BP= Benzo[a]pyrene; CP= *C. portoricensis*; VIN= Vincasar. CP 1 =50 mg/kg and CP 2= 100 mg/kg. * = p less than .05 in contrast to vehicle. ** = p less than .05 in contrast to untreated group. Values (mean±SDev) are based on 5-8 rats per group.

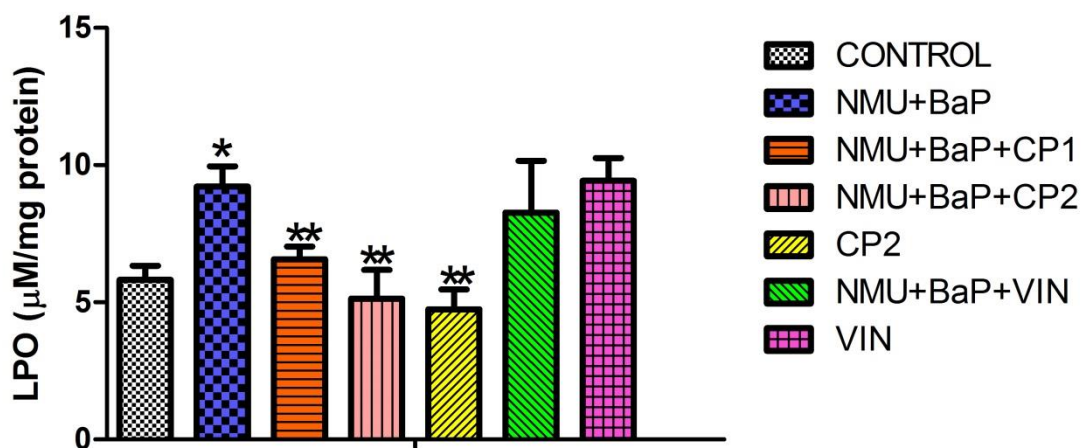


Figure 4.68: Effect of chloroform fraction of *C. portoricensis* (CP) in Wistar rats given MNU and BP on ovarian malondialdehyde (LPO) levels. MNU= *N-nitroso-N-methylurea*; BP= Benzo[a]pyrene; CP= *C. portoricensis*; VIN= Vincasar. CP 1 =50 mg/kg and CP 2= 100 mg/kg. * = p less than .05 in contrast to vehicle. ** = p less than .05 in contrast to untreated group. Values (mean±SDev) are based on 5-8 rats per group.

Proteins expression; Caspase-3, caspase-9, p53, BAX, IL- 1 β , IL- 6, iNOS, COX-2, BCL-2 and beta-catenin are presented in figures 4.68- 4.77. MNU and BP treatment caused down-regulation in mammary caspase-3, caspase-9 and BAX activities in relation to the Vehicle groups. Contrary to the vehicle, MNU and BP treatment increased the activity of beta-catenin, COX-2, and iNOS in the mammary gland. In the same manner, administration of MNU and BP demonstrates strong expression in mammary interleukins (1 β and 6) as well as BCL-2 activities.

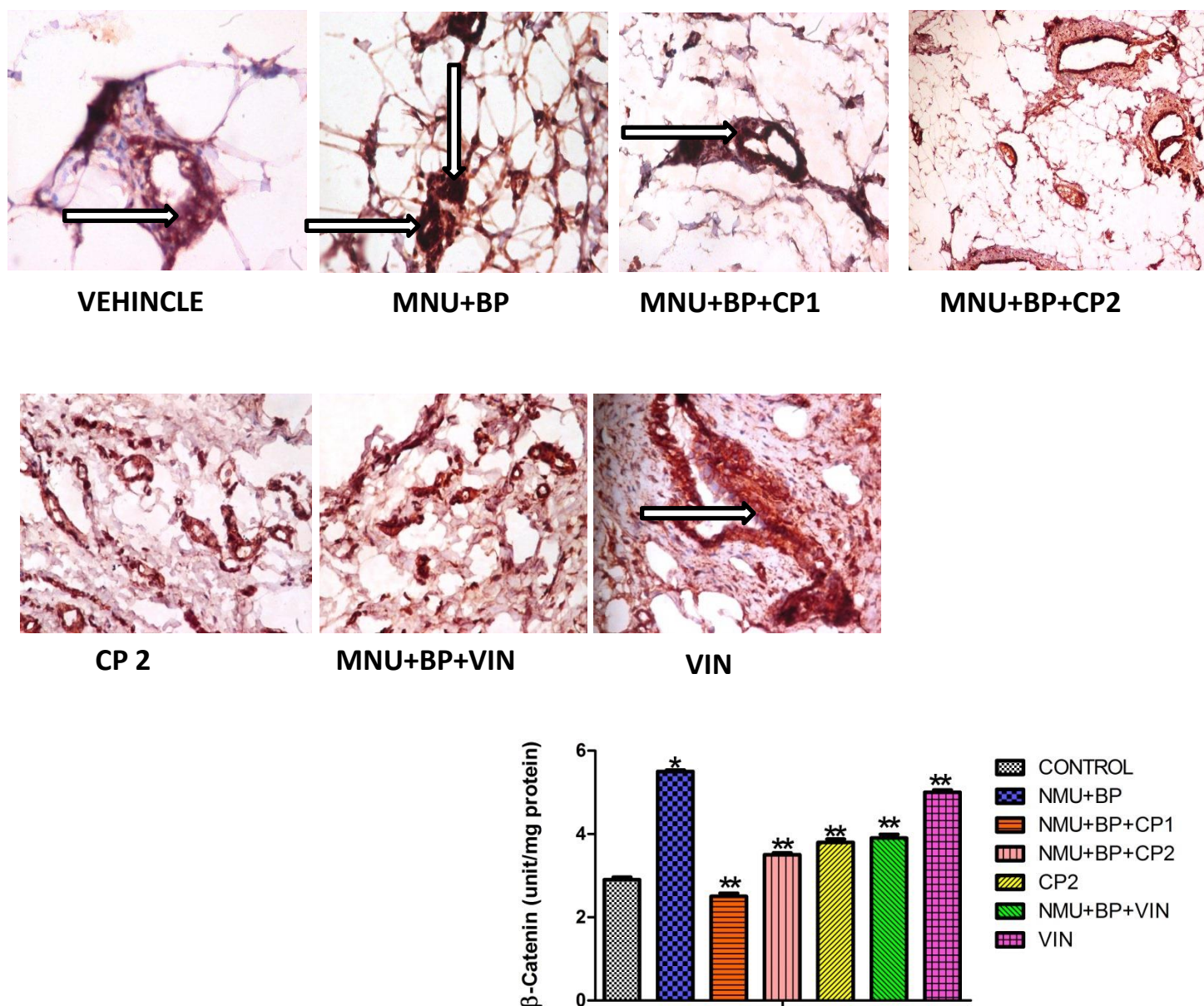


Figure 4.69: Immunohistochemical staining of beta-Catenin expression in the mammary tissue of MNU and BP rats given chloroform fraction of *C. portoricensis*. MNU= *N-nitroso-N-methylurea*; BP= Benzo[a]pyrene; CP= *C. portoricensis*; VIN= Vincasar. CP 1 =50 mg/kg and CP 2= 100 mg/kg. The white arrows showing the expression of beta-Catenin. * = p less than .05 in contrast to vehicle. ** = p less than .05 in contrast to untreated group. Values (mean±SDev) are based on 5-8 rats per group.

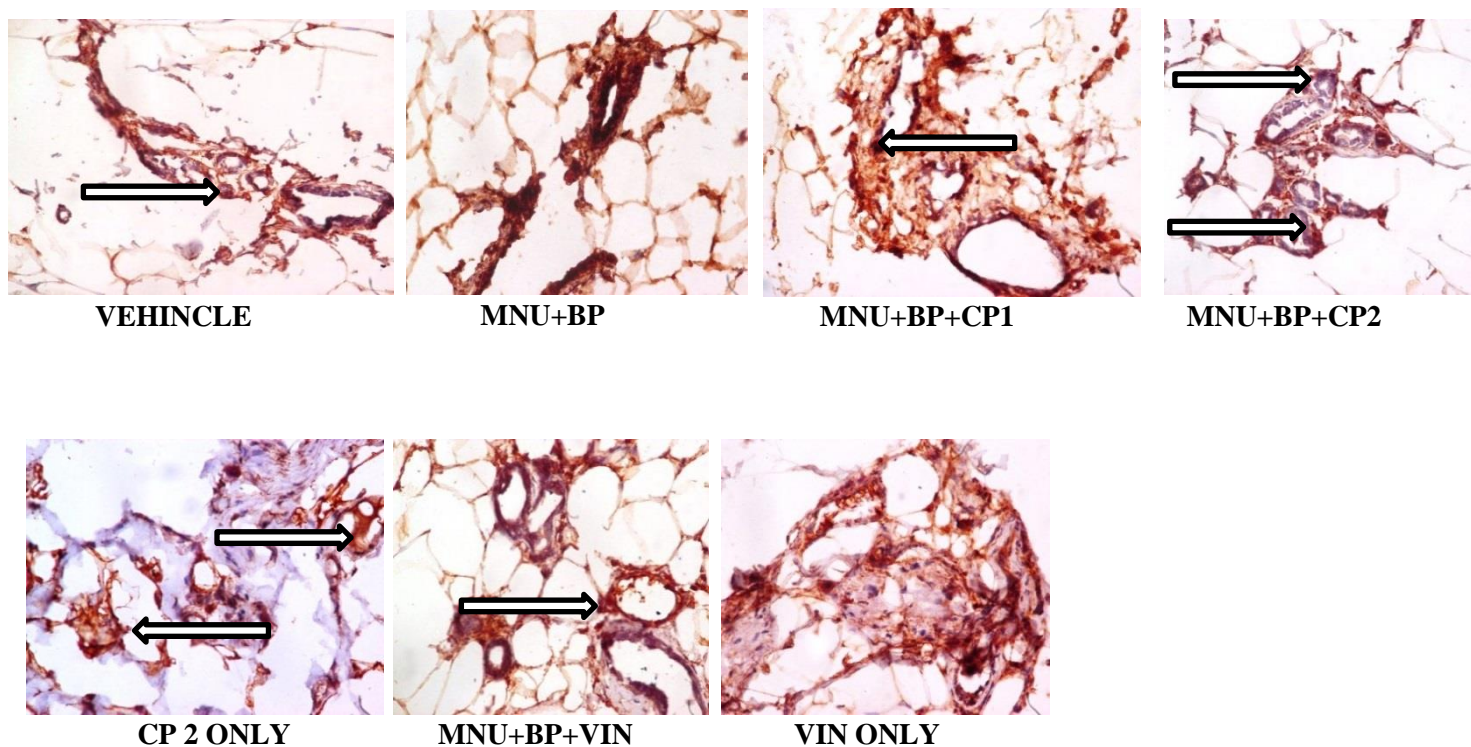


Figure 4.70: Immunohistochemical staining of p53 expression in the mammary tissue of MNU and BP rats given chloroform fraction of *C. portoricensis*. MNU= *N*-nitroso-*N*-methylurea; BP= Benzo[a]pyrene; CP= *C. portoricensis*; VIN= Vincasar. CP 1 =50 mg/kg and CP 2= 100 mg/kg. The white arrows showing the expression of p53. * = p less than .05 in contrast to vehicle. ** = p less than .05 in contrast to untreated group. Values (mean±SDev) are based on 5-8 rats per group.

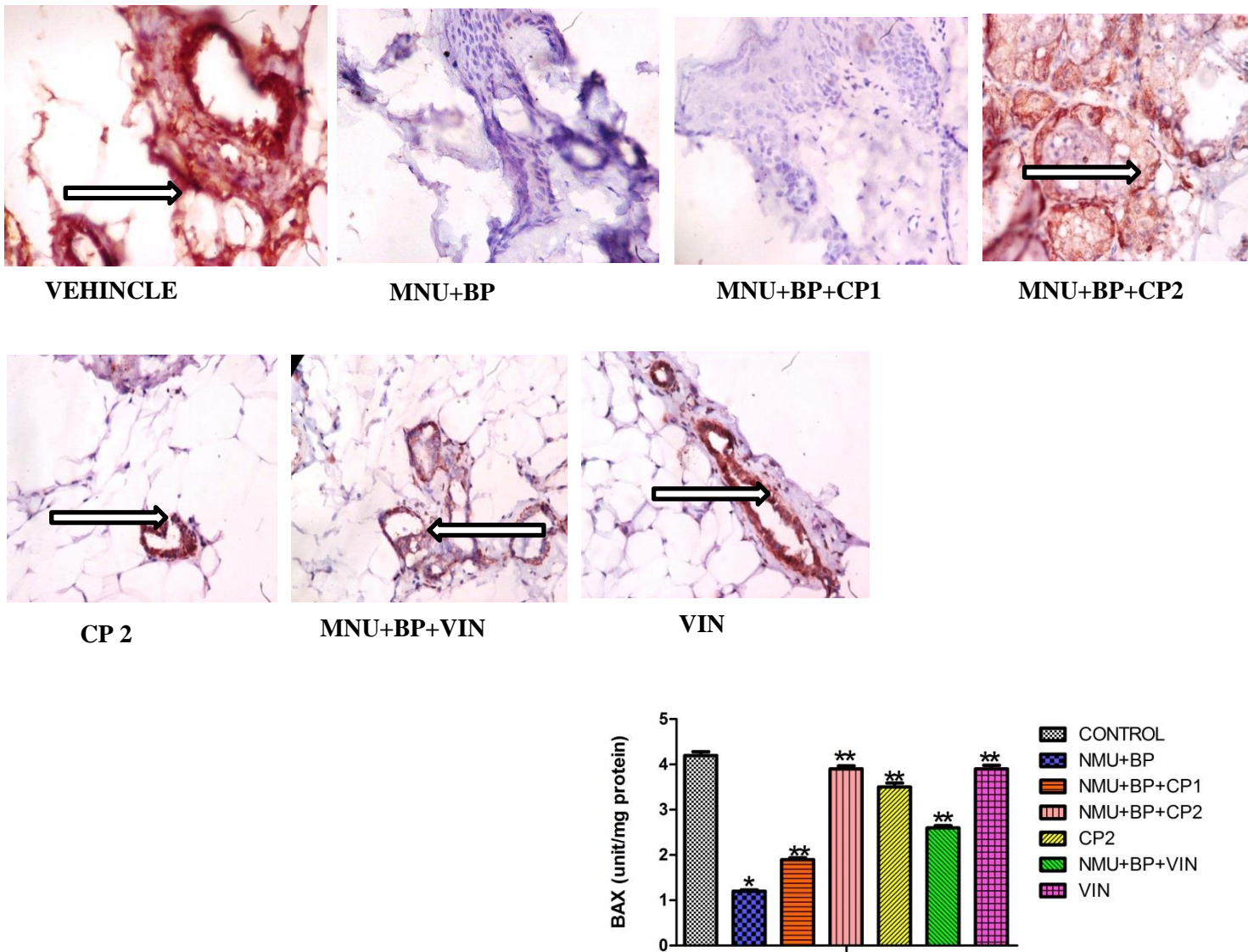


Figure 4.71: Immunohistochemical staining of Bcl-2 Associated X-protein (BAX) expression in the mammary tissue of MNU and BP rats given chloroform fraction of *C. portoricensis*. MNU= *N-nitroso-N-methylurea*; BP= Benzo[a]pyrene; CP= *C. portoricensis*; VIN= Vincasar. CP 1 =50 mg/kg and CP 2= 100 mg/kg. The white arrows showing the expression of BAX. * = p less than .05 in contrast to vehicle. ** = p less than .05 in contrast to untreated group. Values (mean±SDev) are based on 5-8 rats per group.

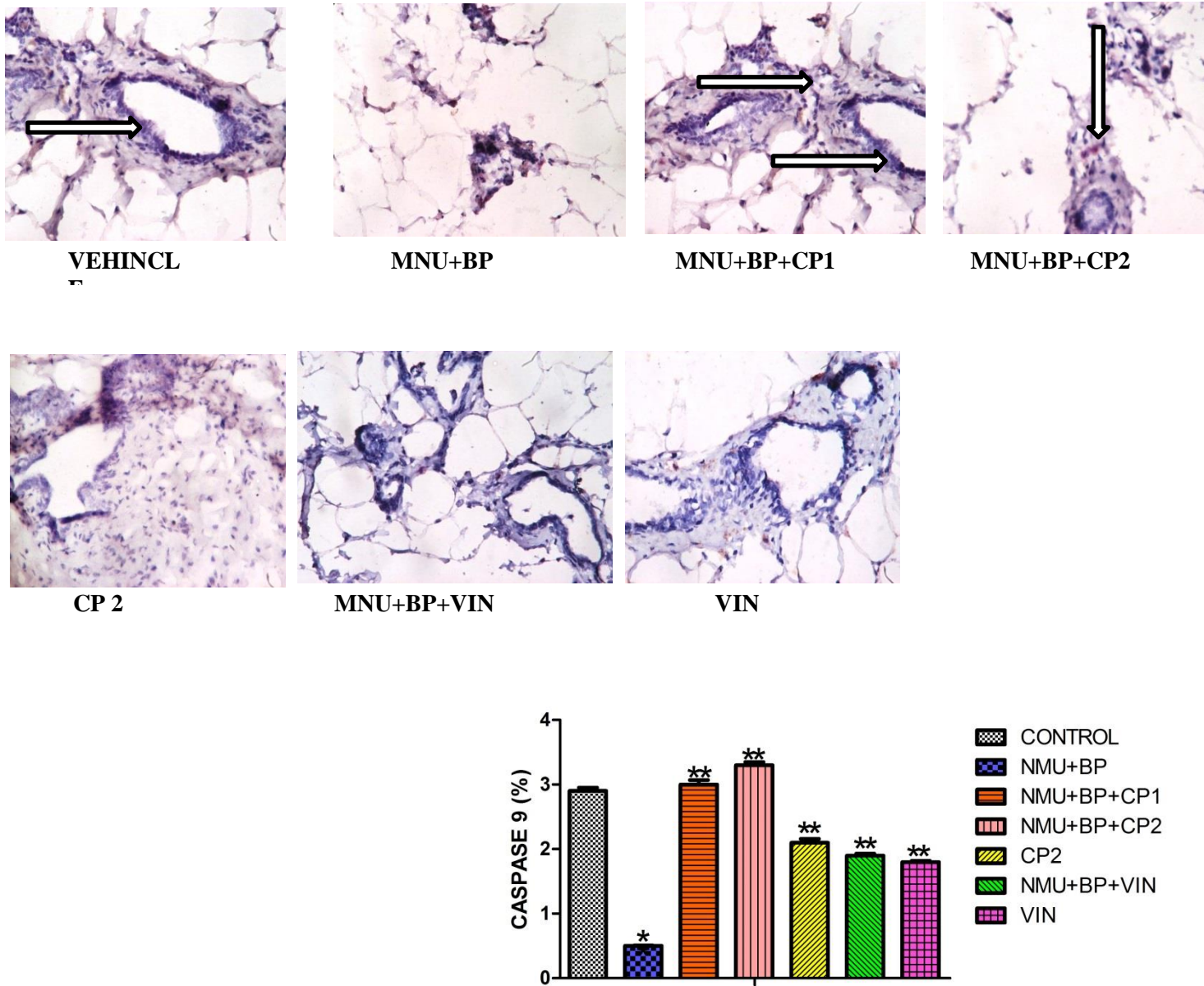


Figure 4.72: Immunohistochemical staining of Caspase-9 expression in the mammary tissue of MNU and BP rats given chloroform fraction of *C. portoricensis*. MNU= *N-nitroso-N-methylurea*; BP= *Benzo[a]pyrene*; CP= *C. portoricensis*; VIN= *Vincasar*. CP 1 =50 mg/kg and CP 2= 100 mg/kg. The white arrows showing the expression of caspase-9. * = p less than .05 in contrast to vehinle. ** = p less than .05 in contrast to untreated group. Values (mean±SDev) are based on 5-8 rats per group.

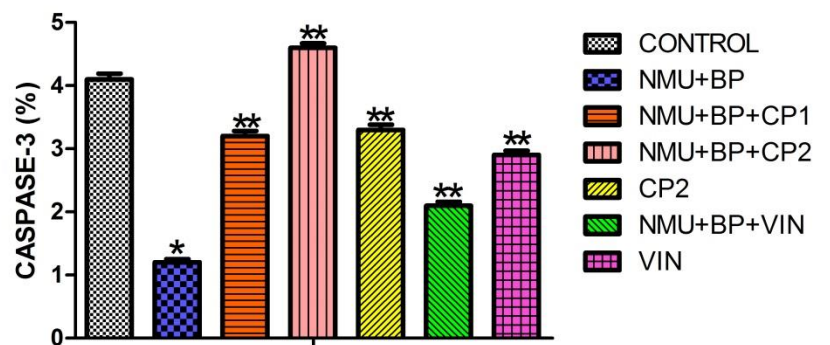
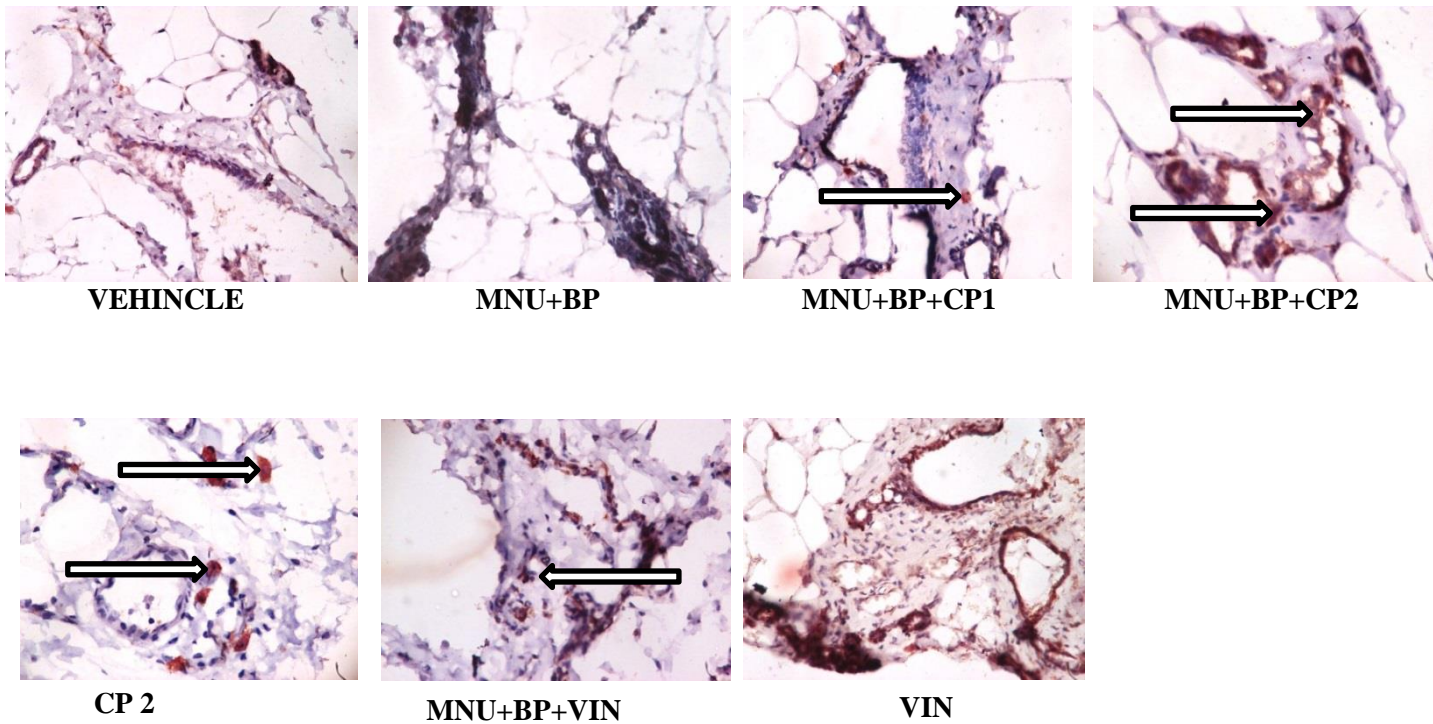


Figure 4.73: Immunohistochemical staining of Caspase-3 expression in the mammary tissue of MNU and BP rats given chloroform fraction of *C. Portoricensis*. MNU= *N-nitroso-N-methylurea*; BP= *Benzo[a]pyrene*; CP= *C. portoricensis*; VIN= *Vincasar*. CP 1 =50 mg/kg and CP 2= 100 mg/kg. The white arrows showing the expression of caspase-3. * = p less than .05 in contrast to vehiclle. ** = p less than .05 in contrast to untreated group. Values (mean±SDev) are based on 5-8 rats per group.

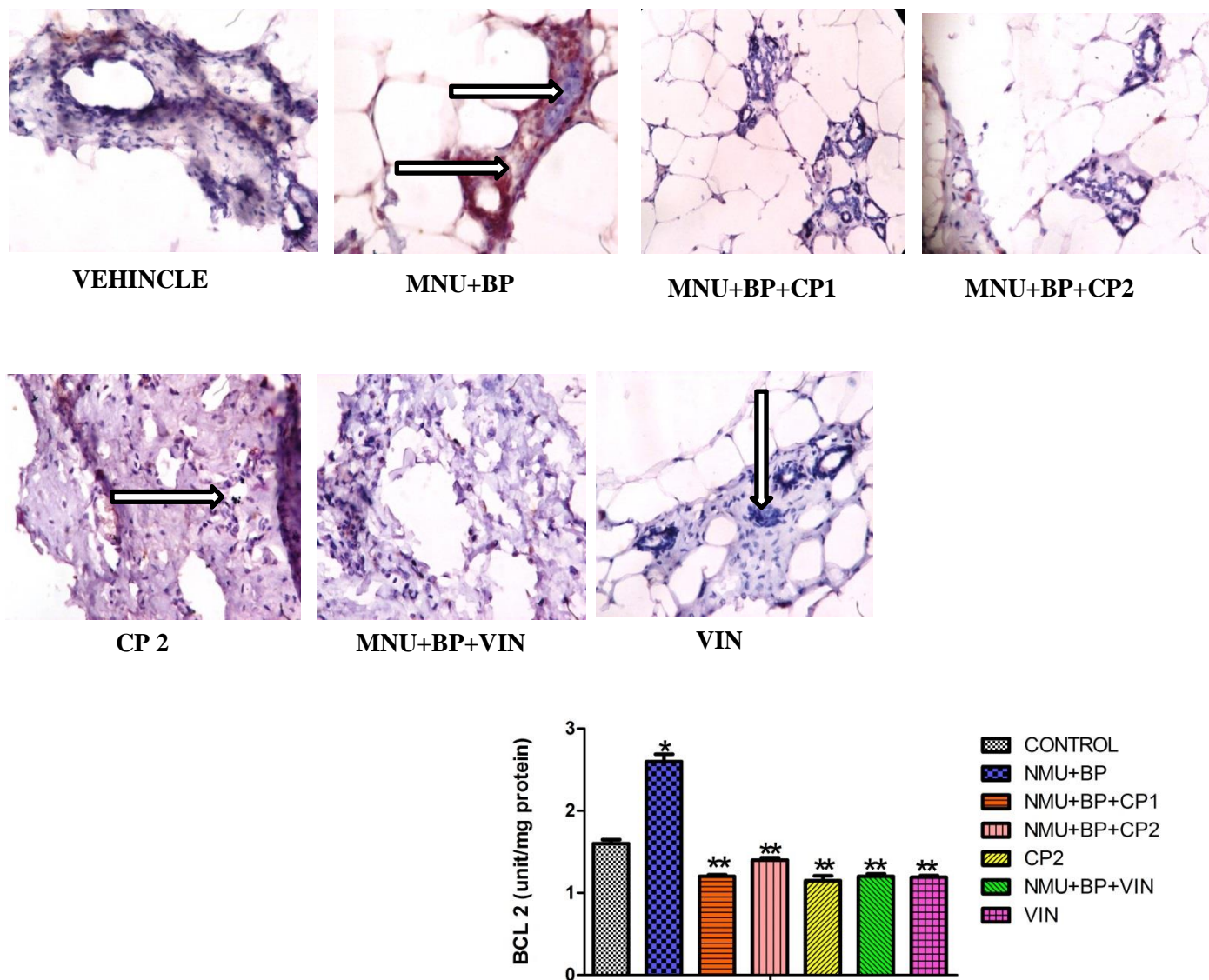


Figure 4.74: Immunohistochemical staining of BCL-2 expression in the mammary tissue of MNU and BP rats given chloroform fraction of *C. Portoricensis*. MNU= *N-nitroso-N-methylurea*; BP= Benzo[a]pyrene; CP= *C. portoricensis*; VIN= Vincasar. CP 1 =50 mg/kg and CP 2= 100 mg/kg. The white arrows showing the expression of BCL-2. * = p less than .05 in contrast to vehicle. ** = p less than .05 in contrast to untreated group. Values (mean±SDev) are based on 5-8 rats per group.

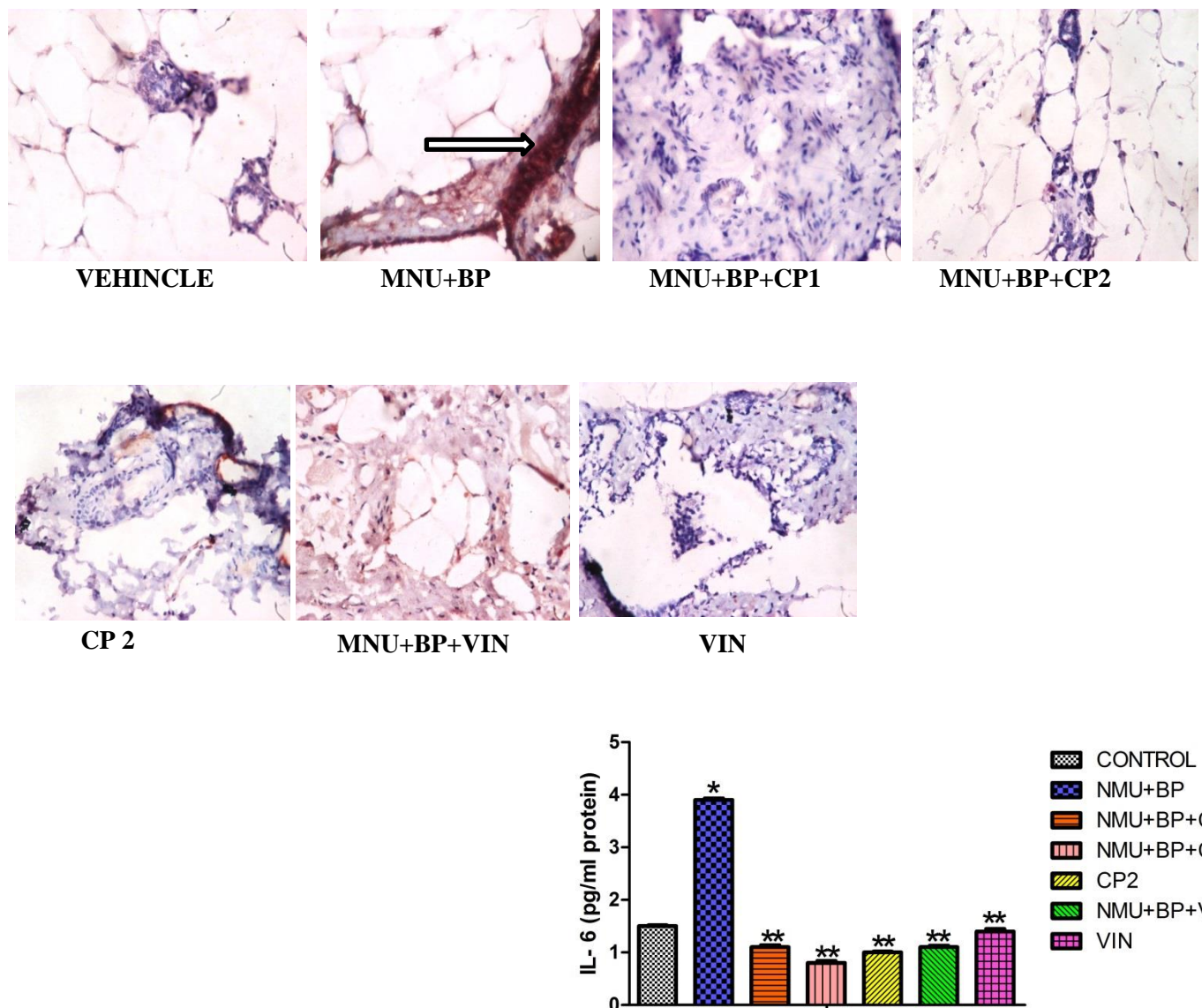


Figure 4.75: Immunohistochemical staining of interlukin (IL-6) expression in the mammary tissue of MNU and BP rats given chloroform fraction of *C. Portoricensis*. MNU= *N-nitroso-N-methylurea*; BP= *Benzo[a]pyrene*; CP= *C. portoricensis*; VIN= *Vincasar*. CP 1 =50 mg/kg and CP 2= 100 mg/kg. The white arrows showing the expression of IL-6. * = p less than .05 in contrast to vehicle. ** = p less than .05 in contrast to untreated group. Values (mean±SDev) are based on 5-8 rats per group.

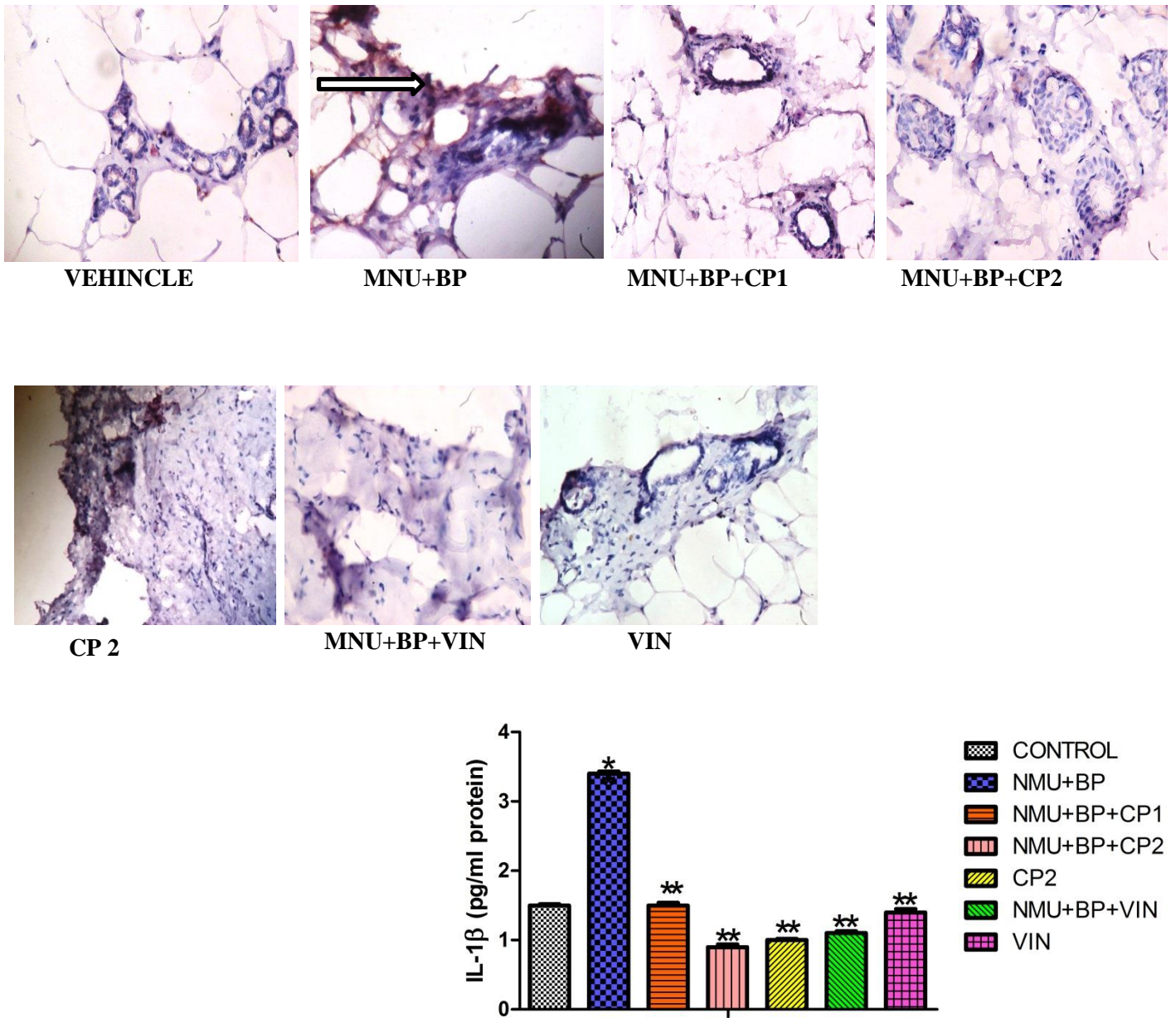


Figure 4.76: Immunohistochemical staining of interleukin (IL-1 β) expression in the mammary tissue of MNU and BP rats given chloroform fraction of *C. Portoricensis*. MNU= *N*-nitroso-*N*-methylurea; BP= Benzo[a]pyrene; CP= *C. portoricensis*; VIN= Vincasar. CP 1 =50 mg/kg and CP 2= 100 mg/kg. The white arrows showing the expression of IL-1 β . * = p less than .05 in contrast to vehicle. ** = p less than .05 in contrast to untreated group. Values (mean \pm SDev) are based on 5-8 rats per group.

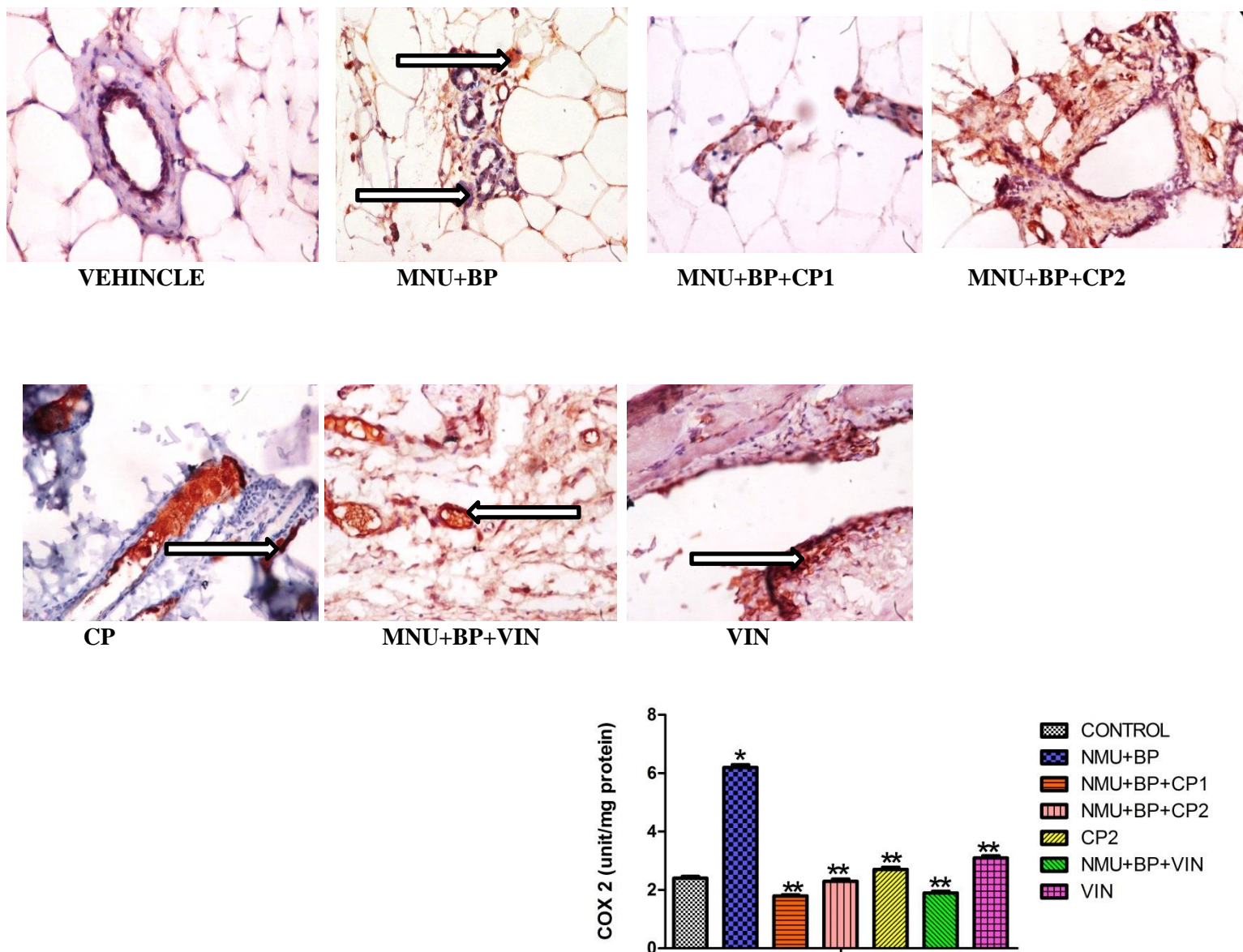


Figure 4.77: Immunohistochemical staining of cyclooxygenase-2 (COX-2) expression in the mammary tissue of MNU and BP rats given chloroform fraction of *C. Portoricensis*. MNU= *N*-nitroso-*N*-methylurea; BP= Benzo[a]pyrene; CP= *C. portoricensis*; VIN= Vincasar. CP 1 =50 mg/kg and CP 2= 100 mg/kg. The white arrows showing the expression of COX-2. * = p less than .05 in contrast to vehicle. ** = p less than .05 in contrast to untreated group. Values (mean±SDev) are based on 5-8 rats per group.

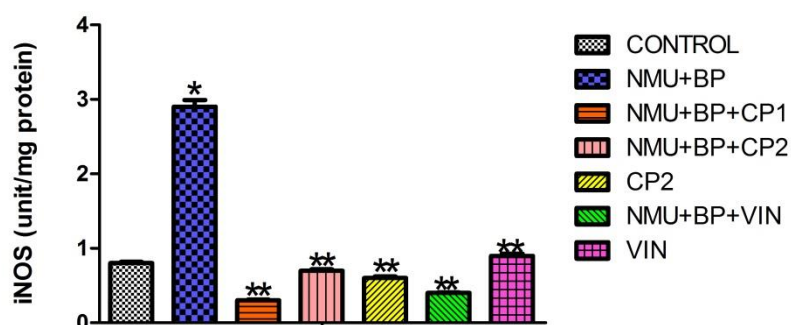
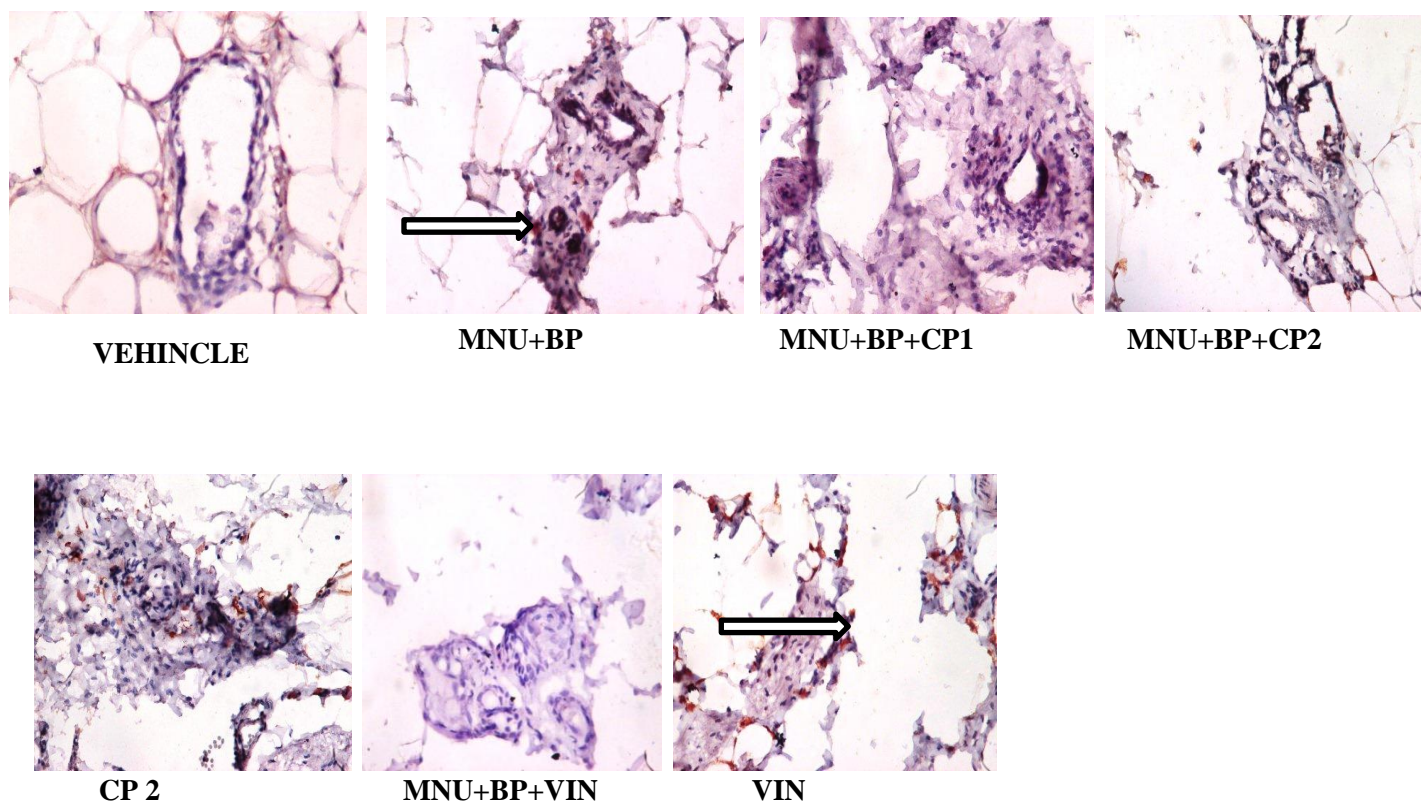


Figure 4.78: Immunohistochemical staining of inducible nitric oxide synthase (iNOS) expression in the mammary tissue of MNU and BP rats given chloroform fraction of *C. Portoricensis*. MNU= *N-nitroso-N-methylurea*; BP= Benzo[a]pyrene; CP= *C. portoricensis*; VIN= Vincasar. CP 1 =50 mg/kg and CP 2= 100 mg/kg. The white arrows showing the expression of iNOS. * = p less than .05 in contrast to vehinle. ** = p less than .05 in contrast to untreated group. Values (mean±SDev) are based on 5-8 rats per group.

MNU and BP-treated rats had significant (p less than .05) higher levels of FSH, LH, and progesterone in their mammary tissues when compared to vehicles (figures 4.79-4.81). In addition, mammary prolactin level increased in MNU and BP-administered rats but not significantly expressed (figure 4.78). Following co-administration with chloroform fraction of CP, elevated prolactin, FSH, LH and progesterone were significantly (p less than .05) reduced at both doses.

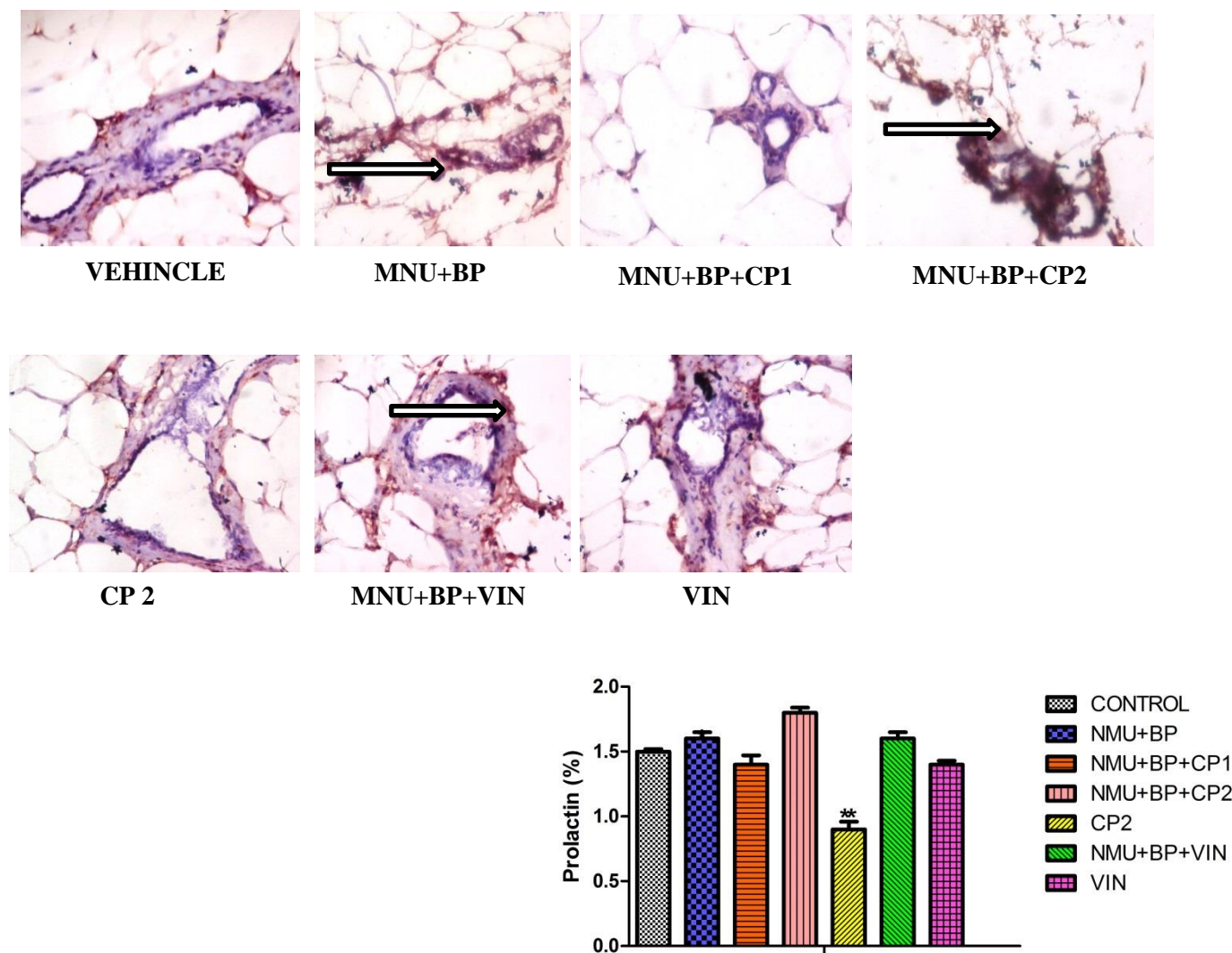


Figure 4.79: Immunohistochemical staining of prolactin levels in the mammary tissue of MNU and BP rats given chloroform fraction of *C. Portoricensis*. MNU= *N-nitroso-N-methylurea*; BP= Benzo[a]pyrene; CP= *C. portoricensis*; VIN= Vincasar. CP 1 =50 mg/kg and CP 2= 100 mg/kg. The white arrows showing expression of prolactin. * = p less than .05 in contrast to vehicle. ** = p less than .05 in contrast to untreated group. Values (mean±SDev) are based on 5-8 rats per group.

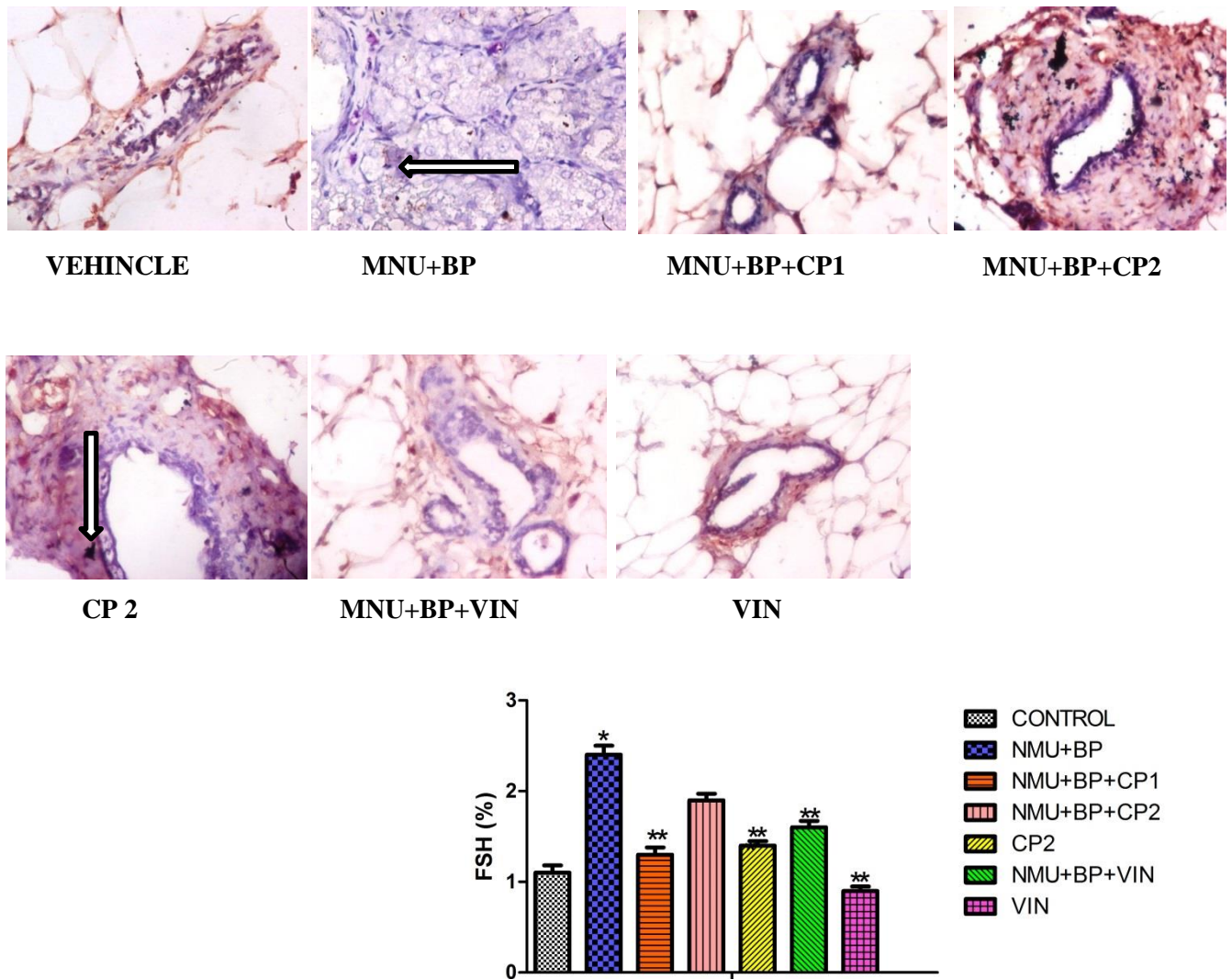


Figure 4.80: Immunohistochemical staining of follicle stimulating hormone (FSH) levels in the mammary tissue of MNU and BP rats given chloroform fraction of *C. Portoricensis*. MNU= *N-nitroso-N-methylurea*; BP= Benzo[a]pyrene; CP= *C. portoricensis*; VIN= Vincasar. CP 1 =50 mg/kg and CP 2= 100 mg/kg. The white arrows showing expression of follicle stimulating hormones. * = p less than .05 in contrast to vehicle. ** = p less than .05 in contrast to untreated group. Values (mean±SDev) are based on 5-8 rats per group.

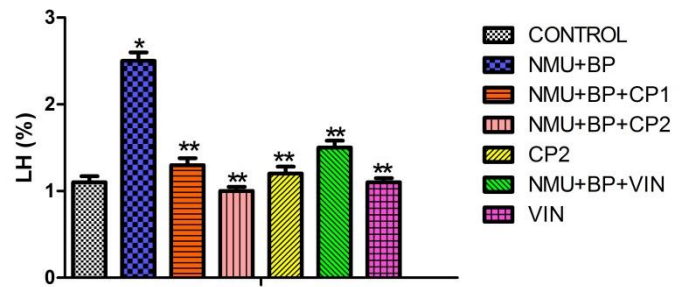
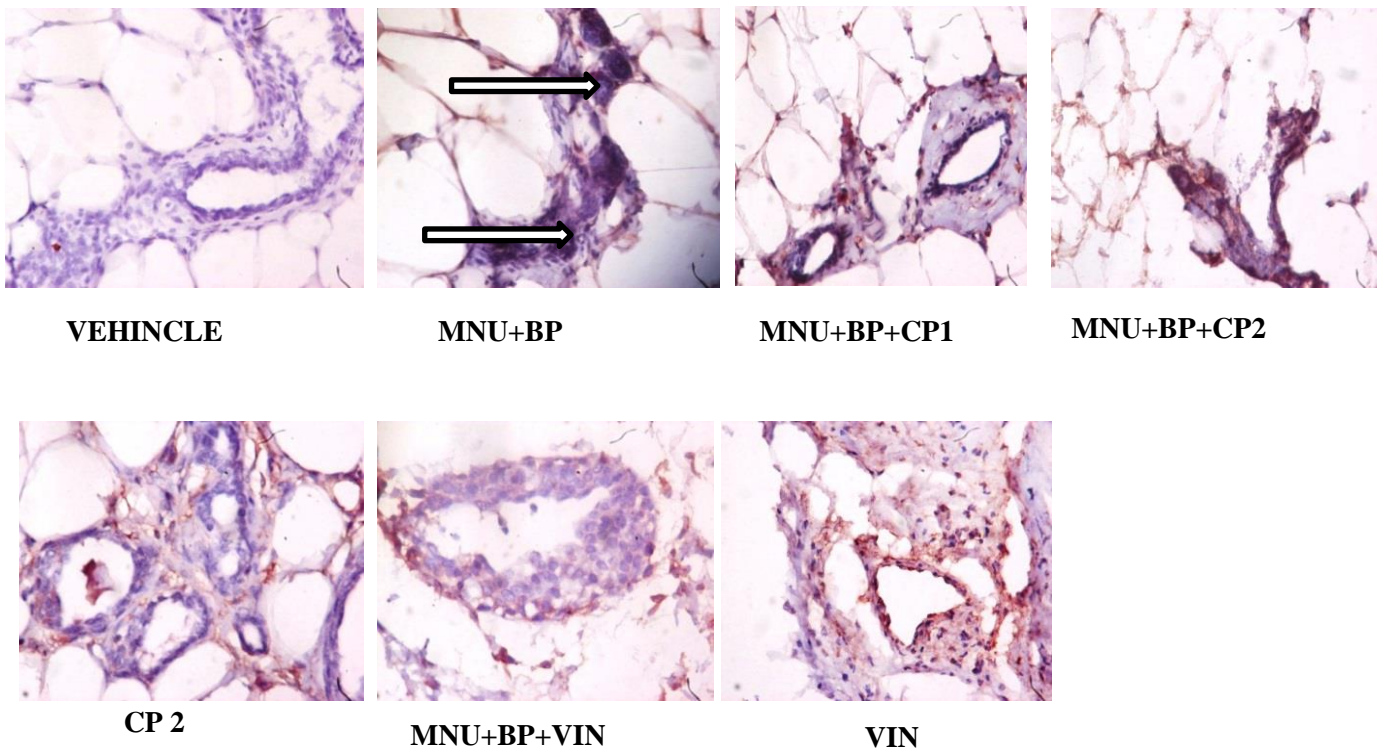


Figure 4.81: Immunohistochemical staining of luteinizing hormone (LH) levels in the mammary tissue of MNU and BP rats given chloroform fraction of *C. Portoricensis*. MNU= *N-nitroso-N-methylurea*; BP= *Benzo[a]pyrene*; CP= *C. portoricensis*; VIN= *Vincasar*. CP 1 =50 mg/kg and CP 2= 100 mg/kg. * = p less than .05 in contrast to vehicle. ** = p less than .05 in contrast to untreated group. Values (mean±SDev) are based on 5-8 rats per group. The white arrows showing expression of luteinizing hormones.

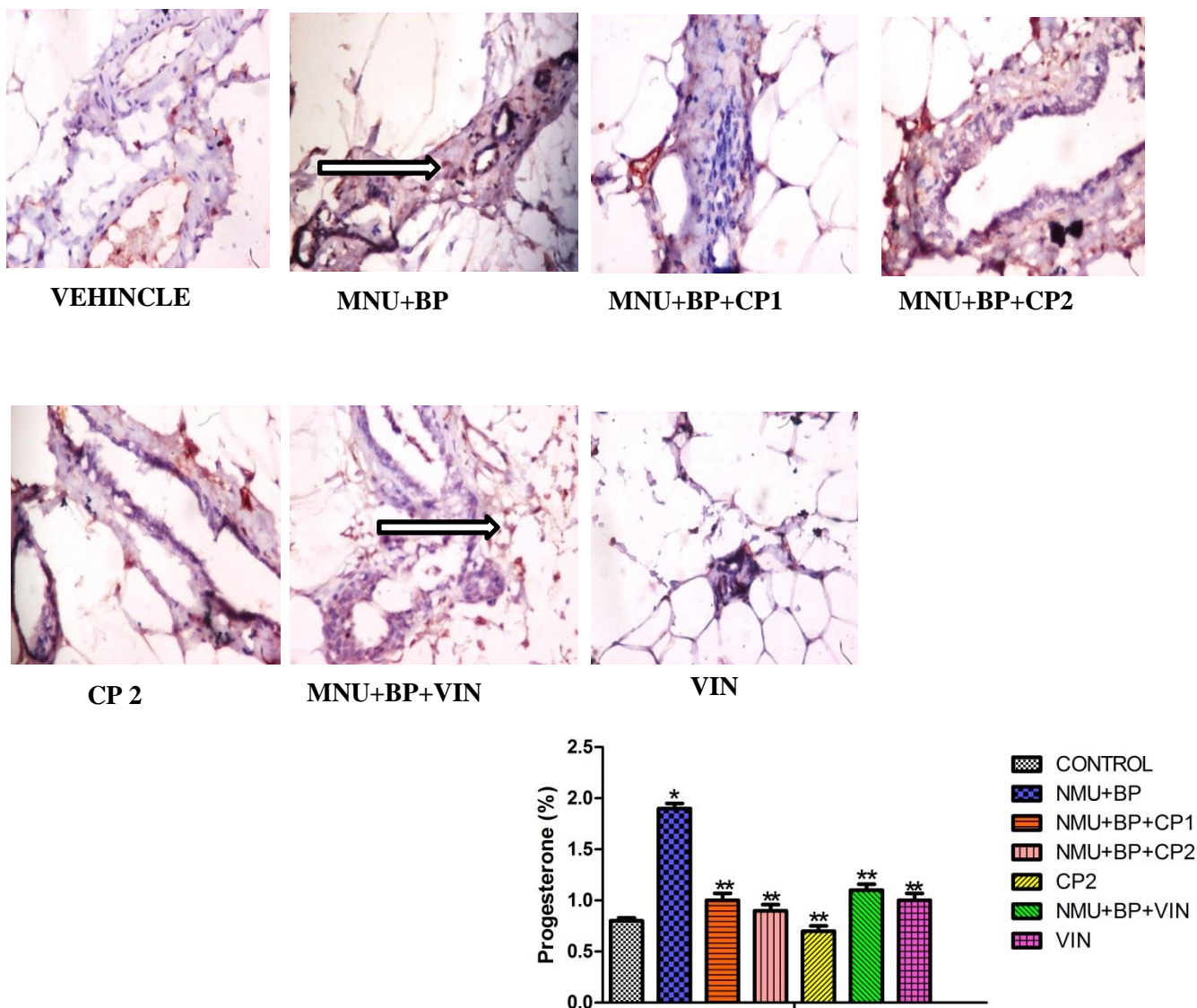


Figure 4.82: Immunohistochemical staining of progesterone levels in the mammary tissue of MNU and BP rats given chloroform fraction of *C. Portoricensis*. MNU= *N-nitroso-N-methylurea*; BP= Benzo[a]pyrene; CP= *C. portoricensis*; VIN= Vincasar. CP 1 =50 mg/kg and CP 2= 100 mg/kg. * = p less than .05 in contrast to vehinacle. ** = p less than .05 in contrast to untreated group. Values (mean±SDev) are based on 5-8 rats per group. The white arrows showing expression of progesterone hormones.

The cyto-architecture of mammary tissues was examined in figure 4.82. The Vehicle of the mammary tissue bared normal stroma and epithelial cells while MNU and BP-treatment affirmed the presence of ductal adenocarcinoma in the mammary tissue. Co-treatment with chloroform fraction of CP attenuated MNU and BP altered mammary tissues cyto-architecture when compared to vehincls.

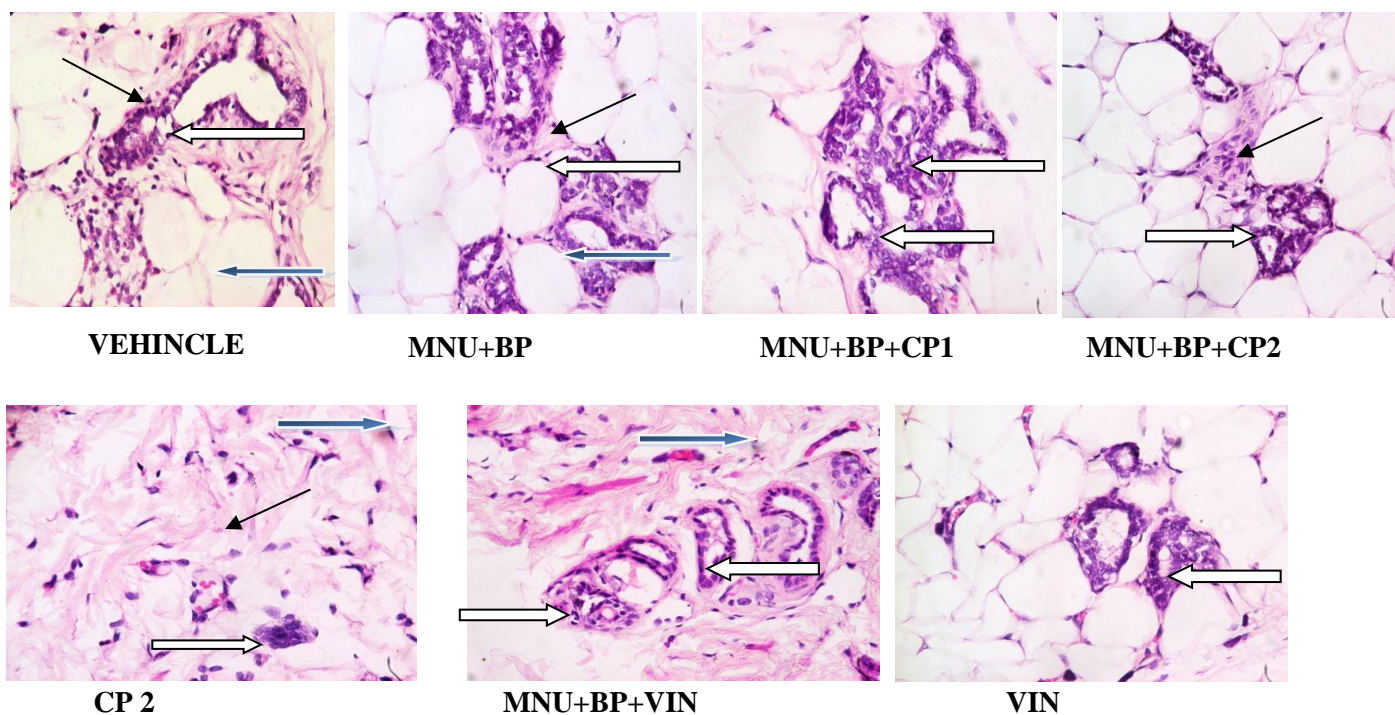


Figure 4.83: Mammary gland cyto-architecture of MNU and BP rats given chloroform fraction of *C. portoricensis* (M X 400). MNU= *N*-nitroso-*N*-methylurea; BP= Benzo[a]pyrene; CP= *C. portoricensis*; VIN= Vincasar. CP 1 =50 mg/kg, CP 2= 100 mg/kg.

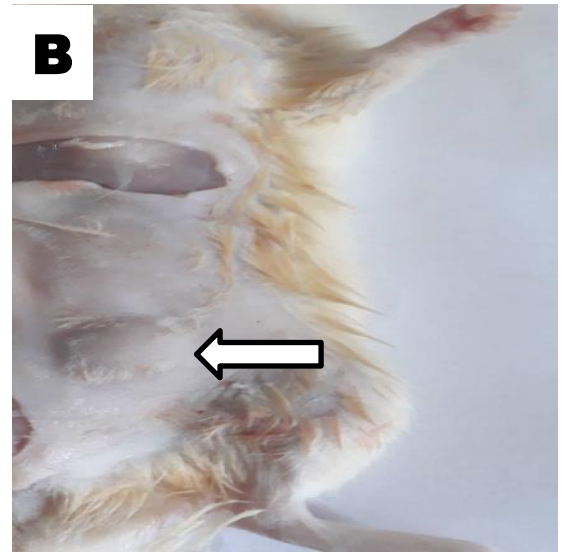
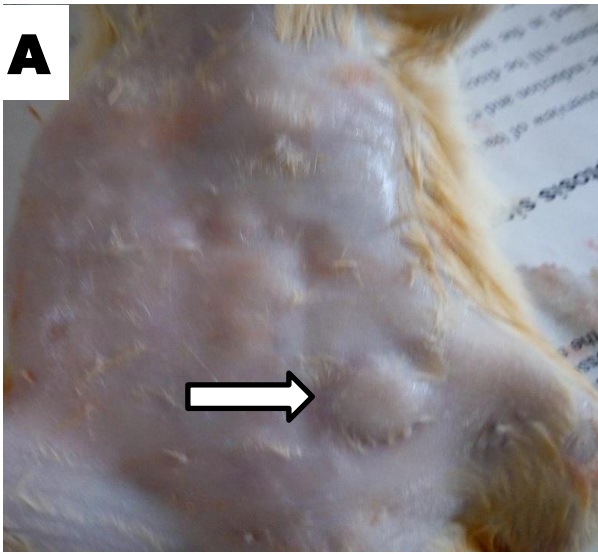
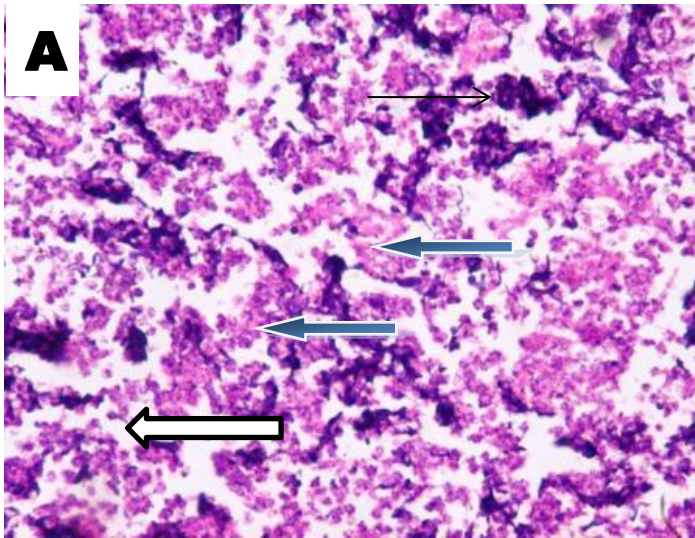
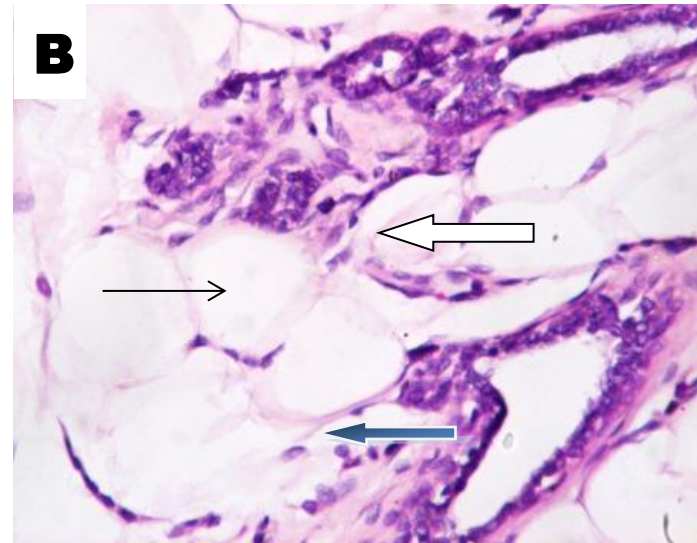


Figure 4.84: Pictorial section of mammary tumor of the mammary gland



Tumor 1



Tumor 2

Figure 4.85: **Tumor 1**- Photomicrograph of mammary tissues stained with Haematoxylin and Eosin showing large cystic tumour (white arrow), there are necrotic tissues (blue arrow) and suppurated inflammatory cells seen (slender arrow).

Tumor 2: Photomicrograph of a mammary tissue stained by Haematoxylin and Eosin showing the glands with ductal carcinoma, the epithelium contains atypical epithelial cells that have darkly pigmented nuclei and high nucleocytoplasmic contents (white arrow), normal stroma consisting of a mixture of fibrous connective tissue (slender arrow) and normal mammary adipose tissue (blue arrow).

MNU and BP-administration strongly up-regulated ovarian BCL-2 and iNOS activities in figures 4.87 and 4.88 respectively. On the contrary, ovarian p53, caspase-3 and BAX activities (figures 4.85 - 4.87) were mildly down-regulated in MNU and BP-treated rats. However, p53, BAX and caspase-3 were impressively up-regulated following co-treatments with chloroform fraction of CP at both doses.

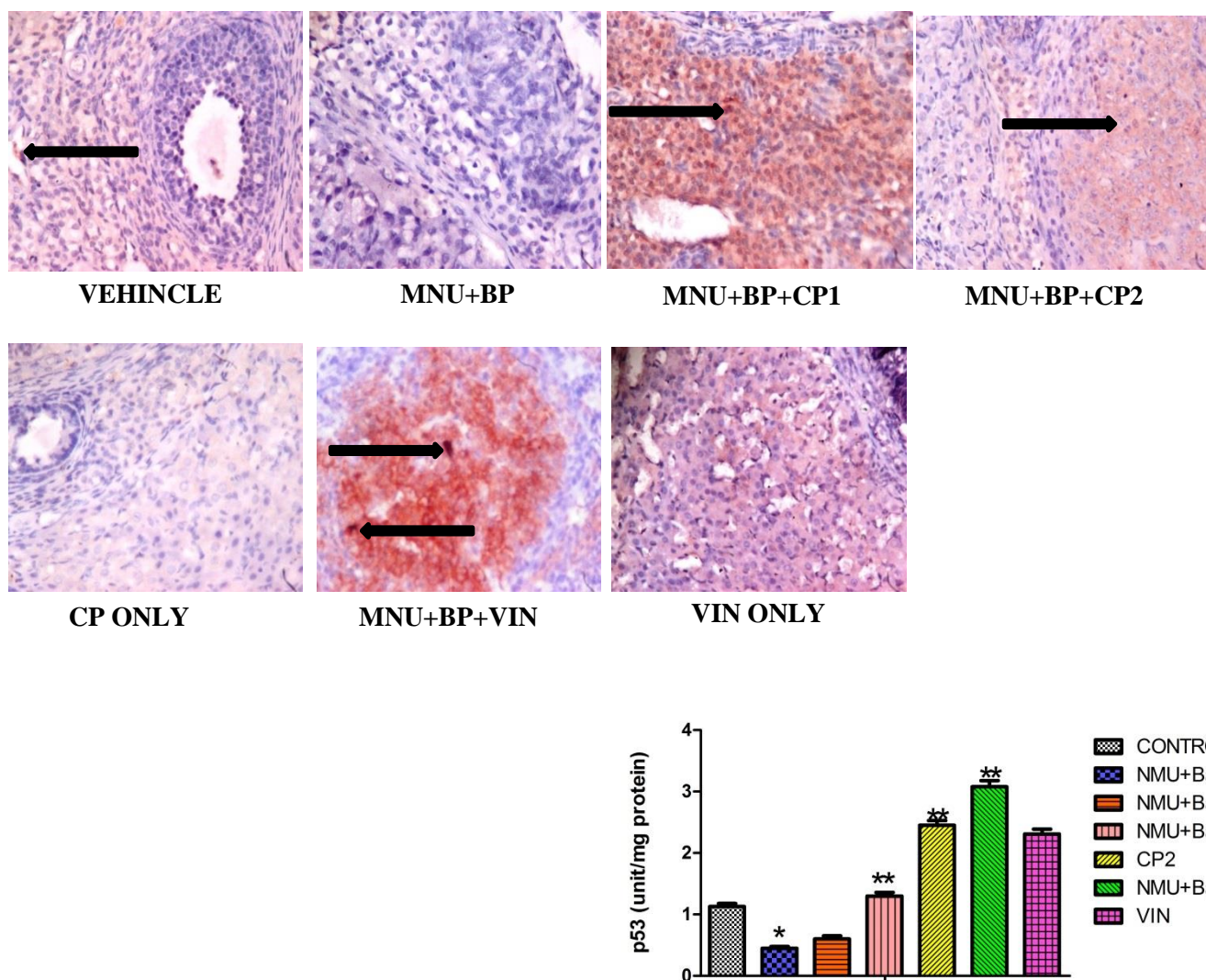


Figure 4.86: Immunohistochemical staining of p53 expression in the ovarian tissue of MNU and BP rats given chloroform fraction of *C. Portoricensis*. MNU= *N-nitroso-N-methylurea*; BP= Benzo[a]pyrene; CP= *C. portoricensis*; VIN= Vincasar. CP 1 =50 mg/kg and CP 2= 100 mg/kg. * = p less than .05 in contrast to vehinacle. ** = p less than .05 in contrast to untreated group. Values (mean±SDev) are based on 5-8 rats per group. The white arrows showing expression of p53.

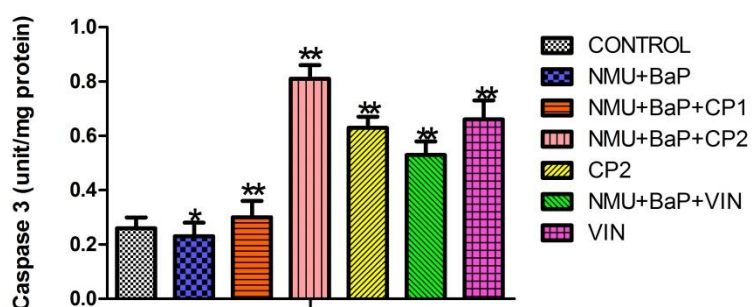
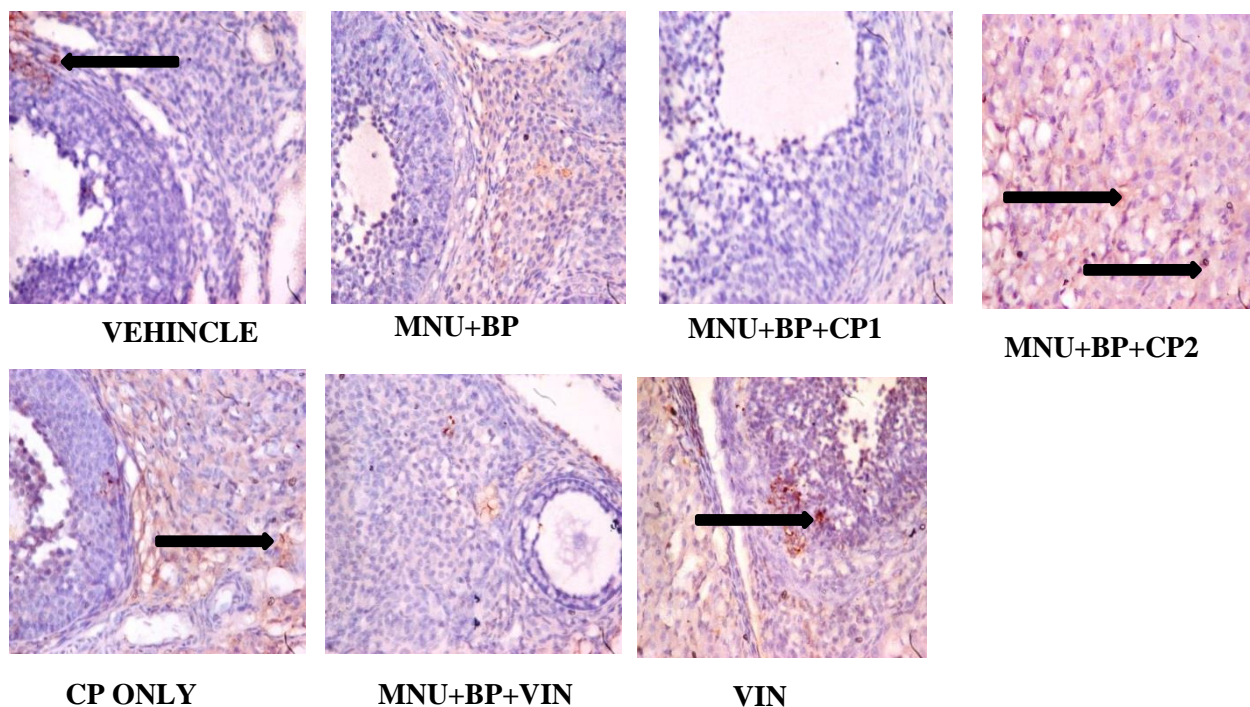


Figure 4.87: Immunohistochemical staining of Caspase-3 expression in the ovarian tissue of MNU and BP rats given chloroform fraction of *C. Portoricensis*. MNU= *N-nitroso-N-methylurea*; BP= *Benzo[a]pyrene*; CP= *C. portoricensis*; VIN= *Vincasar*. CP 1 =50 mg/kg and CP 2= 100 mg/kg. * = p less than .05 in contrast to vehicle. ** = p less than .05 in contrast to untreated group. Values (mean±SDev) are based on 5-8 rats per group. The white arrows showing expression of caspase-3.

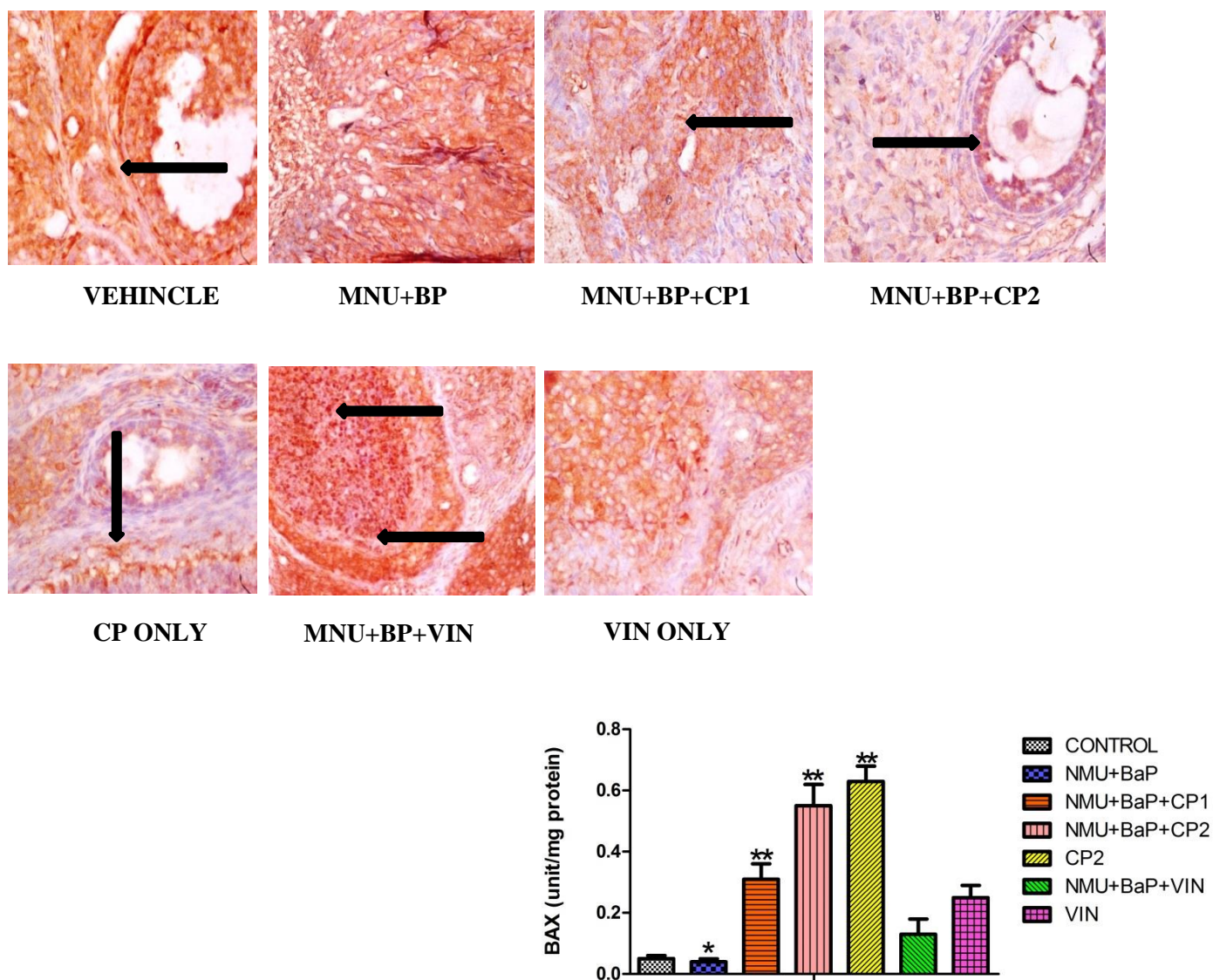


Figure 4.88: Immunohistochemical staining of Bcl-2 Associated X-protein (BAX) expression in the ovarian tissue of MNU and BP rats given chloroform fraction of *C. Portoricensis*. MNU= *N-nitroso-N-methylurea*; BP= *Benzo[a]pyrene*; CP= *C. portoricensis*; VIN= *Vincasar*. CP 1 =50 mg/kg and CP 2= 100 mg/kg. * = p less than .05 in contrast to vehinicle. ** = p less than .05 in contrast to untreated group. Values (mean±SDev) are based on 5-8 rats per group. The white arrows showing expression of BAX.

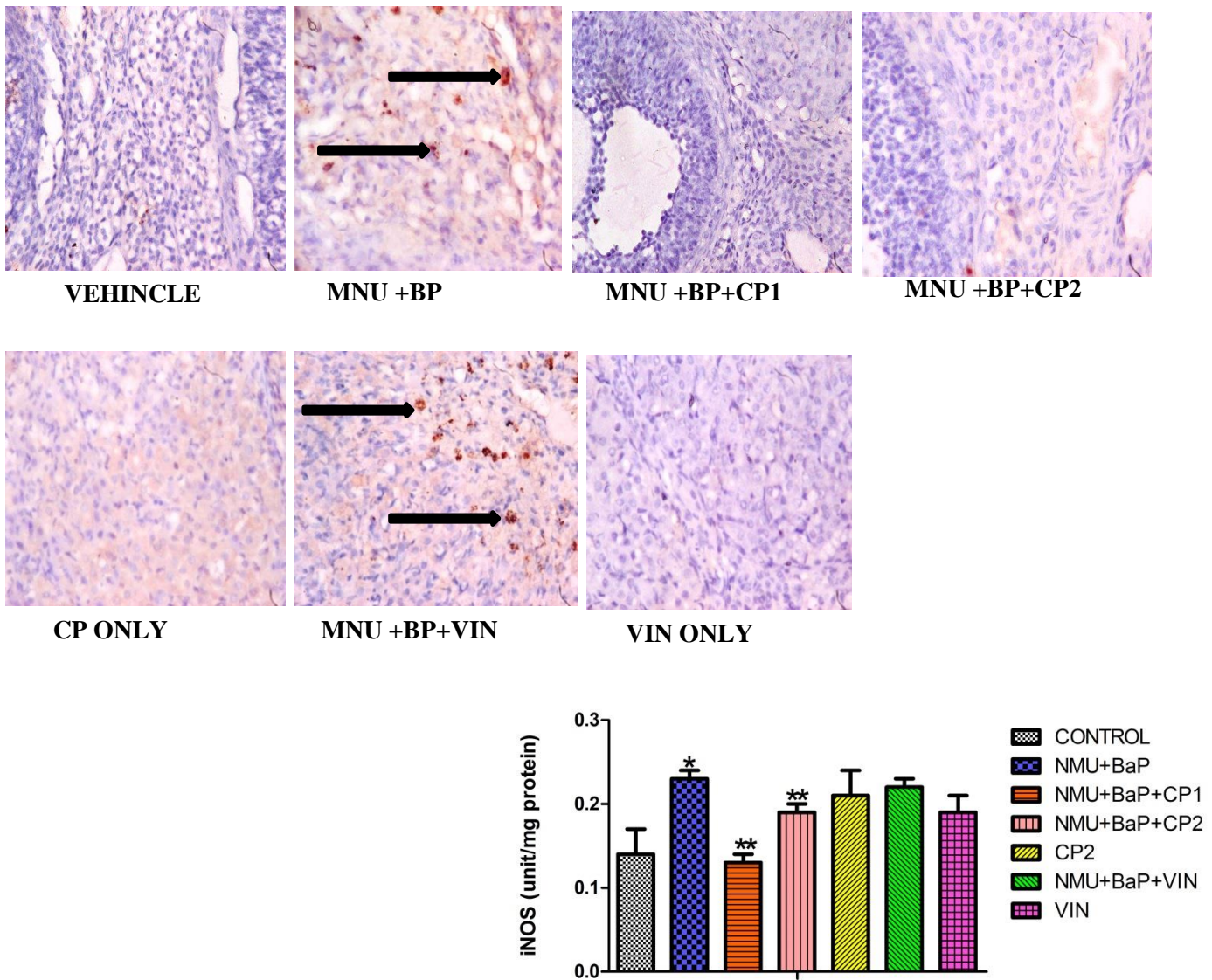


Figure 4.89: Immunohistochemical staining of inducible nitric oxide synthase (iNOS) expression in the ovarian tissue of MNU and BP rats given chloroform fraction of *C. Portoricensis*. MNU= *N-nitroso-N-methylurea*; BP= Benzo[a]pyrene; CP= *C. portoricensis*; VIN= Vincasar. CP 1 =50 mg/kg and CP 2= 100 mg/kg. * = p less than .05 in contrast to vehinicle. ** = p less than .05 in contrast to untreated group. Values (mean±SDev) are based on 5-8 rats per group. The white arrows showing expression of iNOS.

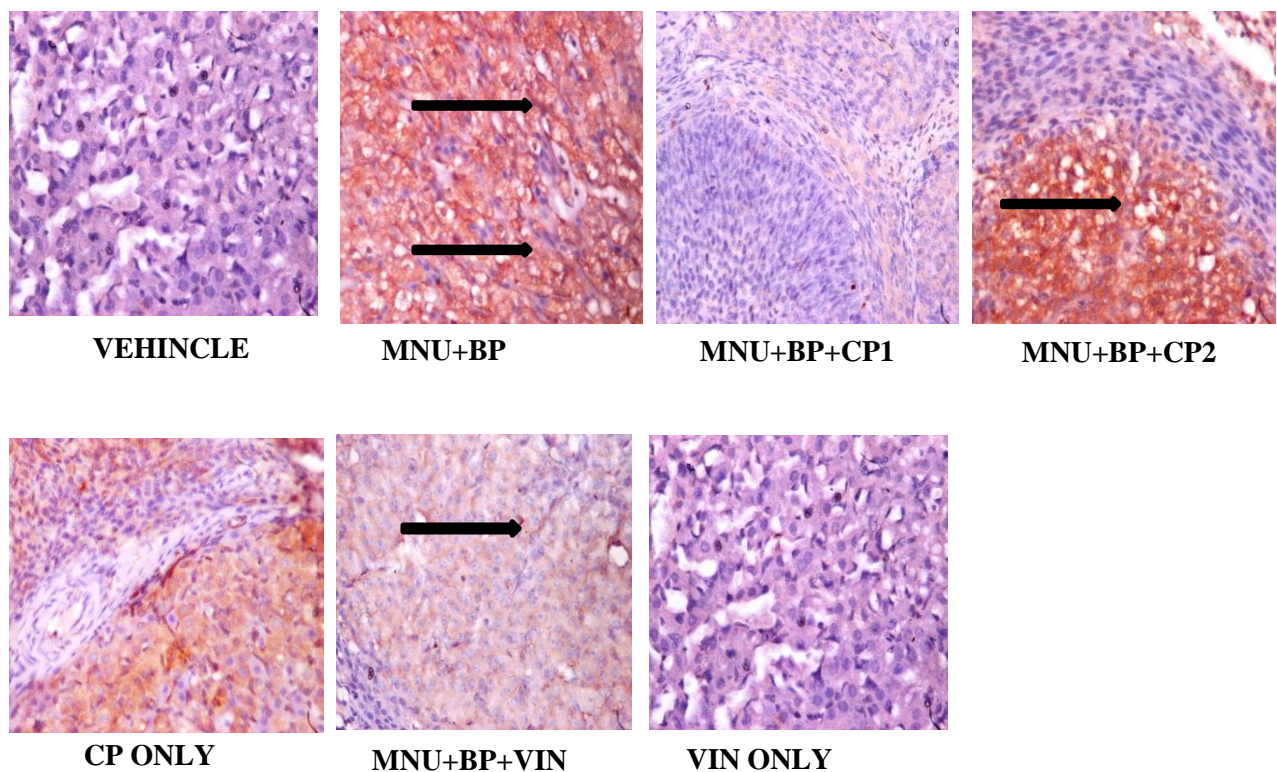


Figure 4.90: Immunohistochemical staining of BCL-2 expression in the ovarian tissue of MNU and BP rats given chloroform fraction of *C. Portoricensis*. MNU= *N*-nitroso-*N*-methylurea; BP= Benzo[a]pyrene; CP= *C. portoricensis*; VIN= Vincasar. CP 1 =50 mg/kg and CP 2= 100 mg/kg. * = p less than .05 in contrast to vehinicle. ** = p less than .05 in contrast to untreated group. Values (mean±SDev) are based on 5-8 rats per group. The white arrows showing expression of BCL-2.

Ovarian prolactin, FSH, LH and progesterone levels were drastically increased in MNU and BP-treated groups (figures 108-111 and figures 4.90 - 4.92). However, following co-administration with chloroform fraction of CP, elevated prolactin, FSH, LH and progesterone were significantly (pless than .05) reduced at both doses.

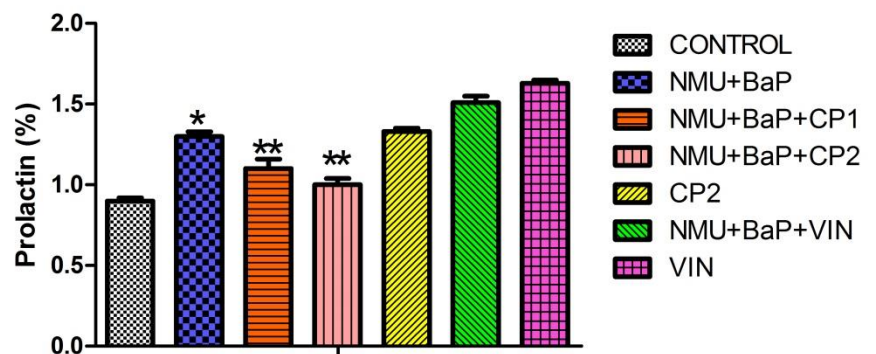
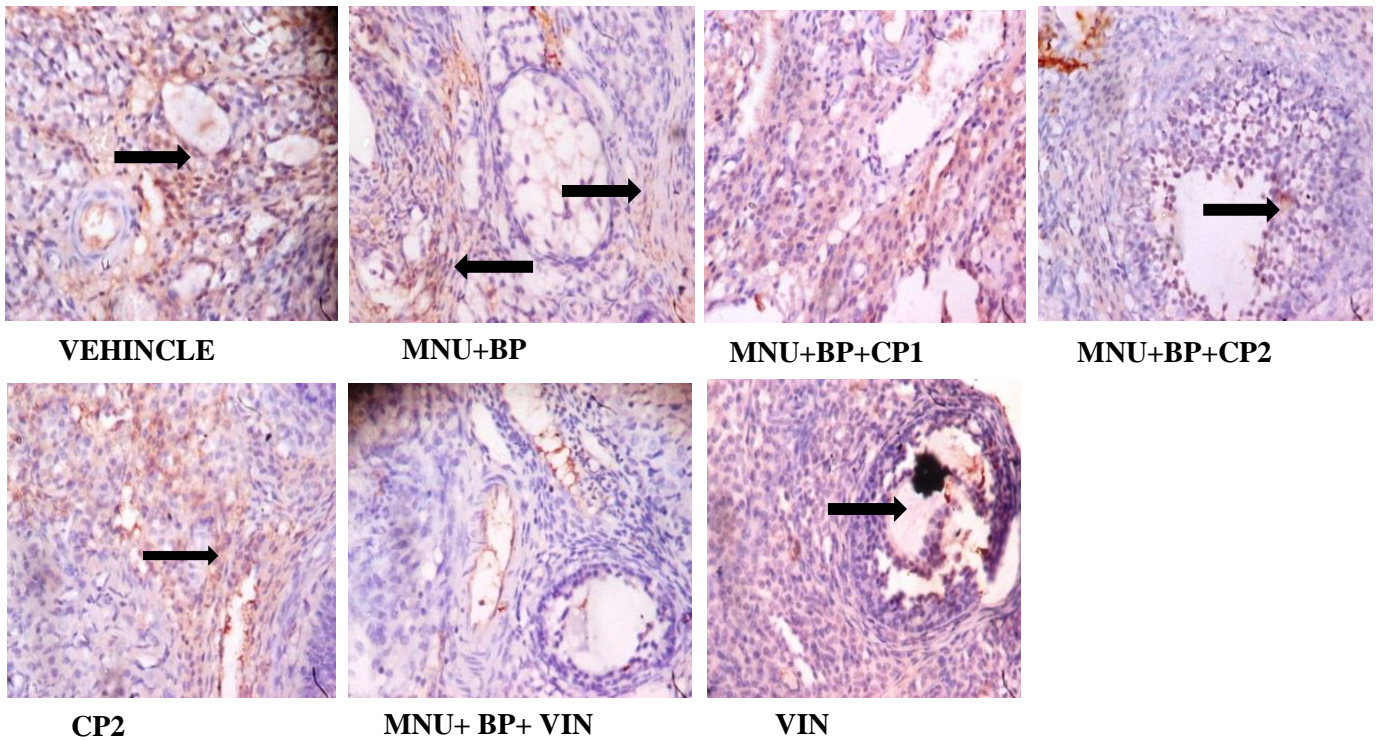


Figure 4.91: Immunohistochemical staining of prolactin level in the ovarian tissue of MNU and BP rats given chloroform fraction of *C. Portoricensis*. MNU= *N-nitroso-N-methylurea*; BP= Benzo[a]pyrene; CP= *C. portoricensis*; VIN= Vincasar. CP 1 =50 mg/kg and CP 2= 100 mg/kg. * = p less than .05 in contrast to vehicle. ** = p less than .05 in contrast to untreated group. Values (mean±SDev) are based on 5-8 rats per group. The white arrows showing expression of prolactin.

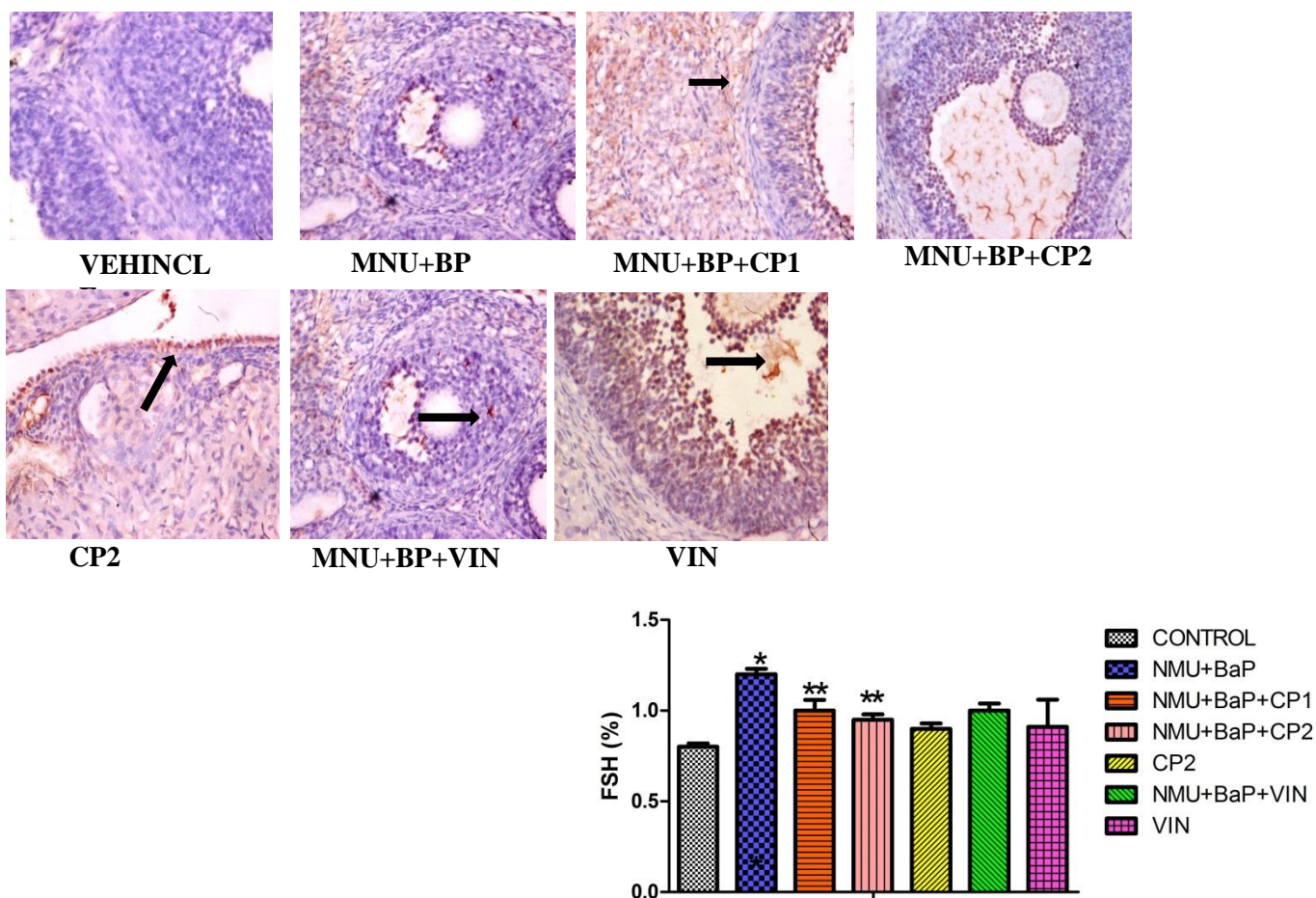


Figure 4.92: Immunohistochemical staining of follicle stimulating hormone (FSH) levels in the ovarian tissue of MNU and BP rats given chloroform fraction of *C. Portoricensis*. MNU= *N-nitroso-N-methylurea*; BP= Benzo[a]pyrene; CP= *C. portoricensis*; VIN= Vincasar. CP 1 =50 mg/kg and CP 2= 100 mg/kg. * = p less than .05 in contrast to vehicle. ** = p less than .05 in contrast to untreated group. Values (mean±SDev) are based on 5-8 rats per group. The white arrows showing expression of follicle stimulating hormones.

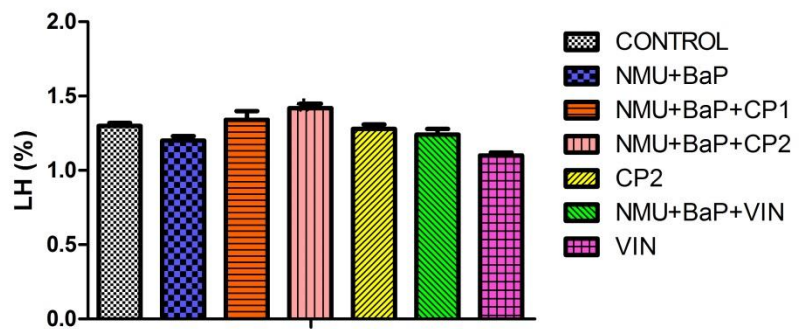
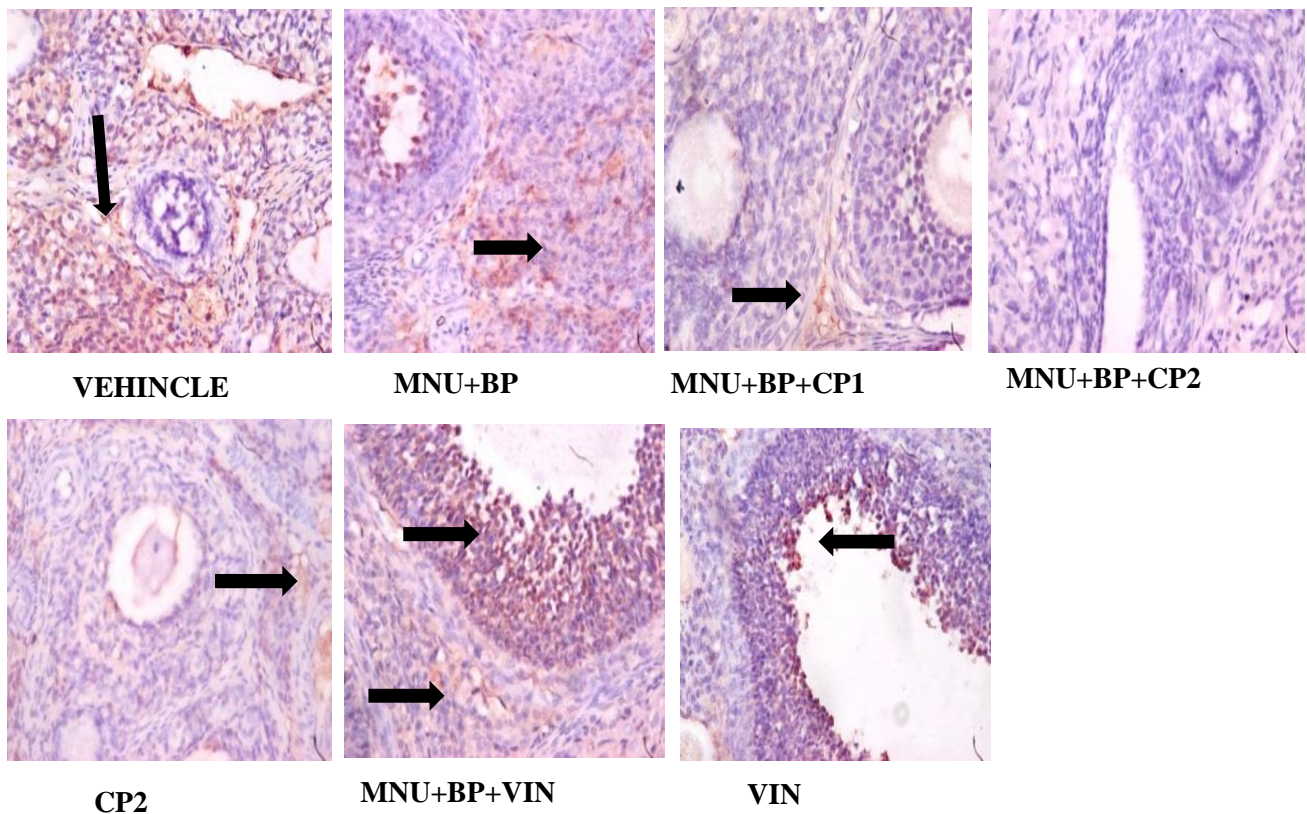


Figure 4.93: Immunohistochemical staining of luteinizing hormone (LH) levels in the ovarian tissue of MNU and BP rats given chloroform fraction of *C. Portoricensis*. MNU= *N-nitroso-N-methylurea*; BP= Benzo[a]pyrene; CP= *C. portoricensis*; VIN= Vincasar. CP 1 =50 mg/kg and CP 2= 100 mg/kg. The white arrows showing expression of luteinizing hormones.

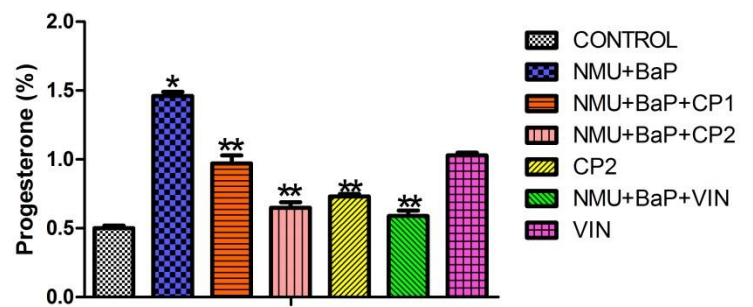
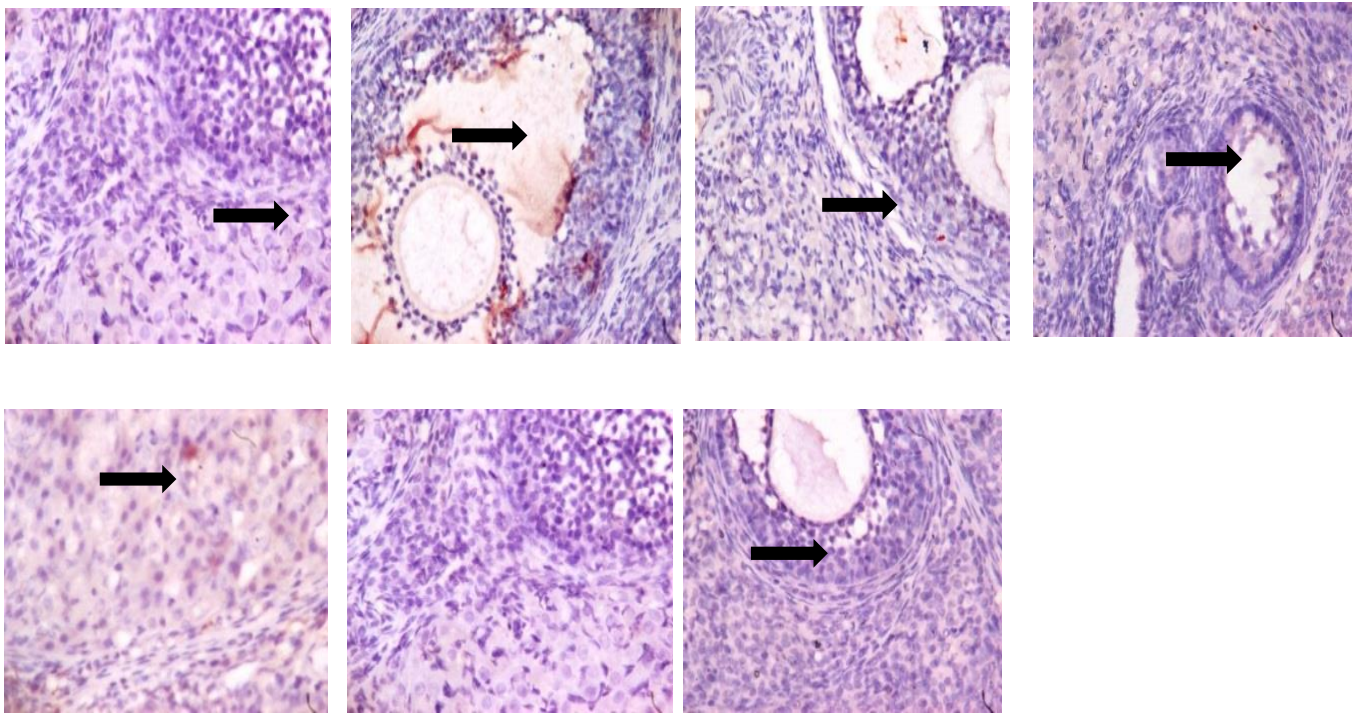


Figure 4.94: Immunohistochemical staining of progesterone levels in the ovarian tissue of MNU and BP rats given chloroform fraction of *C. Portoricensis*. MNU= *N-nitroso-N-methylurea*; BP= Benzo[a]pyrene; CP= *C. portoricensis*; VIN= Vincasar. CP 1 =50 mg/kg and CP 2= 100 mg/kg. * = p less than .05 in contrast to vehicle. ** = p less than .05 in contrast to untreated group. Values (mean±SDev) are based on 5-8 rats per group. The white arrows showing expression of progesterone hormone.

The cyto-architecture of ovarian tissues was examined in figure 4.94. The vehicle ovary tissues disclosed usual connective tissues with normal theca cells layer, while MNU and BP treatment causes fibrosis and vascular congestion in the ovarian stroma, as well as damaged cells. However, co-treatment with chloroform fraction of CP attenuated MNU and BP altered ovarian tissues cyto-architecture when compared to vehicles.

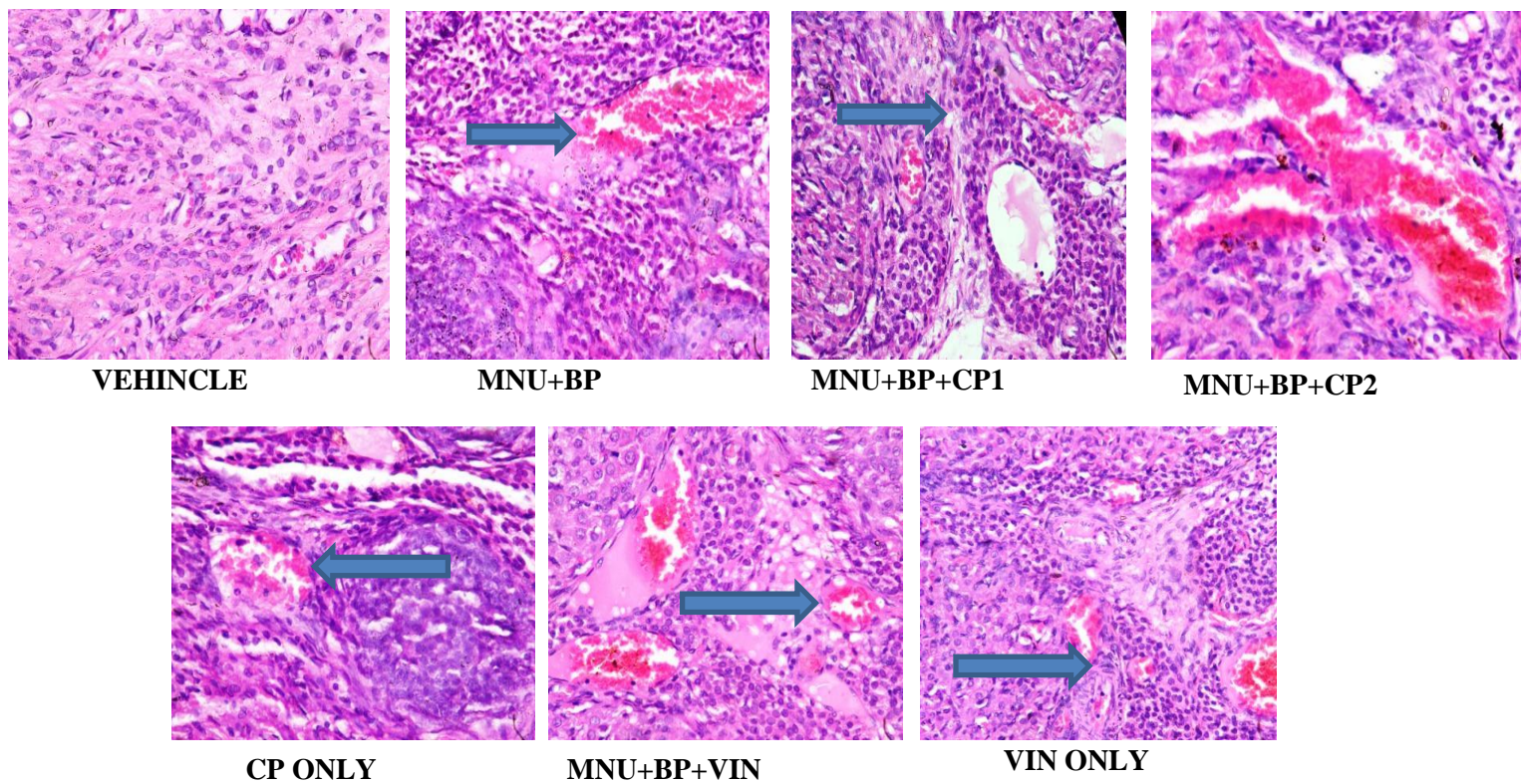


Figure 4.95: Ovarian cyto-architecture of MNU and BP rats given chloroform fraction of *C. Portoricensis* (M X 400). MNU= *N-nitroso-N-methylurea*; BP= Benzo[a]pyrene; CP= *C. portoricensis*; VIN= Vincasar. CP 1 =50 mg/kg and CP 2= 100 mg/kg body weight.

Administration of MNU and BP drastically reduced uterine caspase-3 while BCL-2 activity was strongly elevated when compared to vehicles. However, caspase-3 and BCL-2 were impressively regulated following co-treatments with chloroform fraction of CP at both doses.

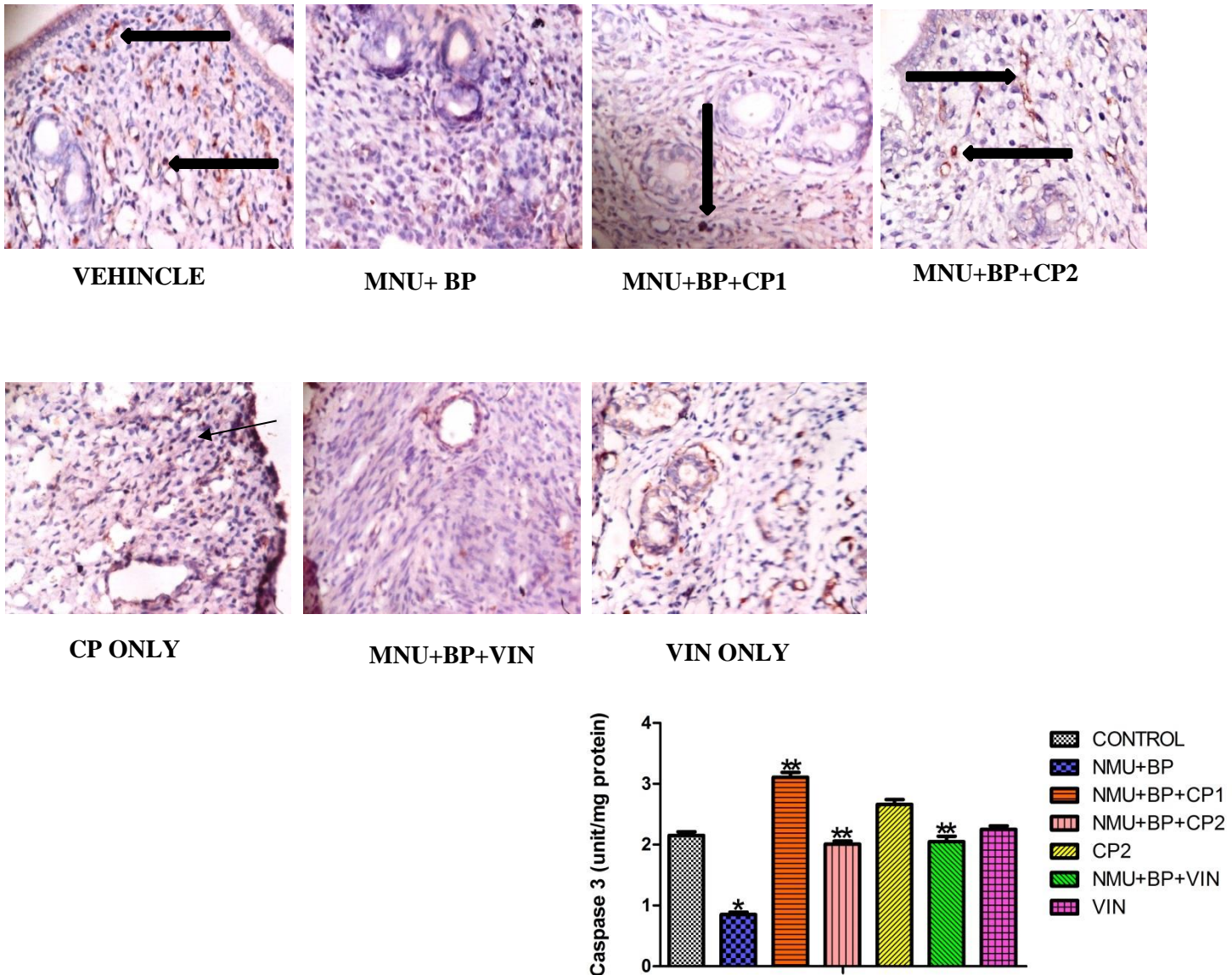


Figure 4.96: Immunohistochemical staining of Caspase-3 expression in the uterine tissue of MNU and BP rats given chloroform fraction of *C. Portoricensis*. MNU= *N*-nitroso-*N*-methylurea; BP= Benzo[a]pyrene; CP= *C. portoricensis*; VIN= Vincasar. CP 1 =50 mg/kg and CP 2= 100 mg/kg. * = p less than .05 in contrast to vehicle. ** = p less than .05 in contrast to untreated group. Values (mean±SDev) are based on 5-8 rats per group. The white arrows showing expression of caspase-3.

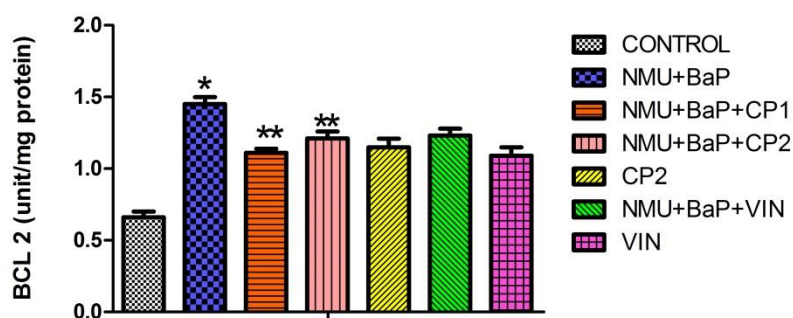
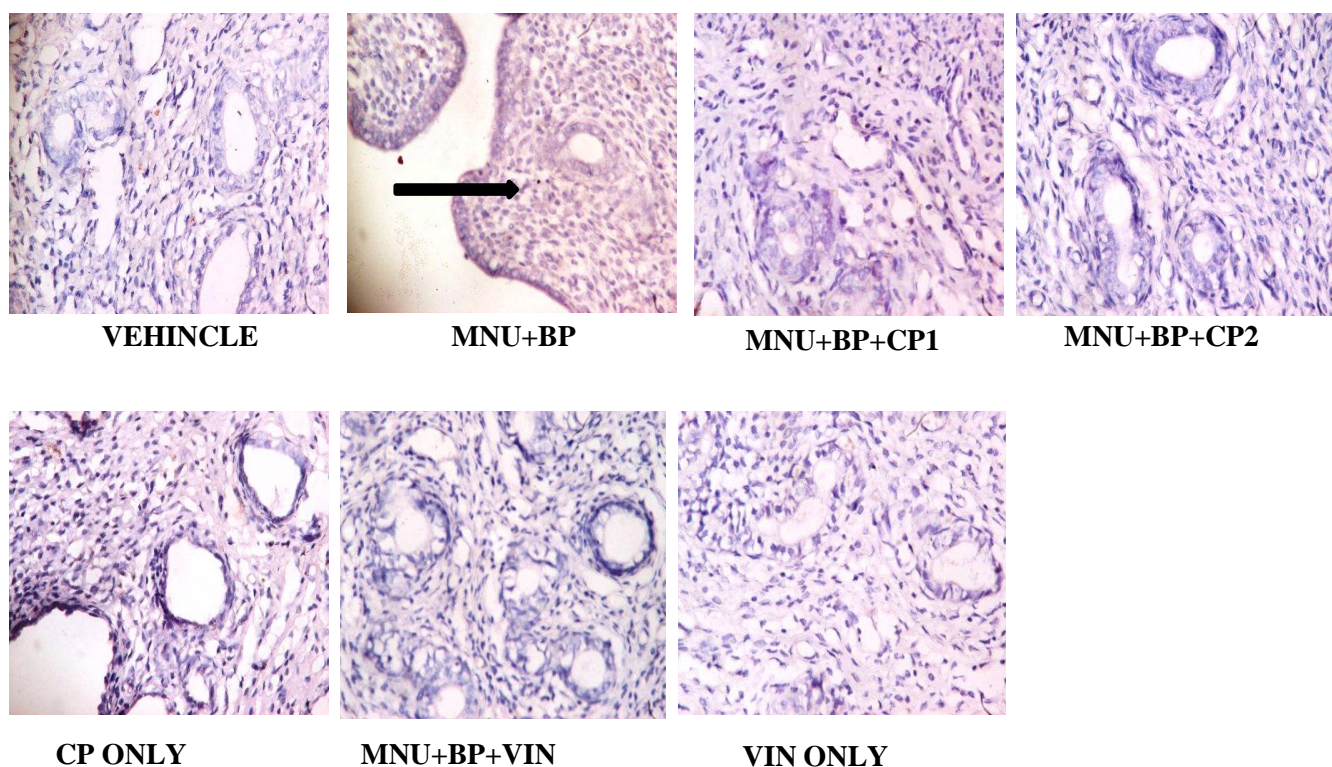


Figure 4.97: Immunohistochemical staining of BCL-2 expression in the uterine tissue of MNU and BP rats given chloroform fraction of *C. Portoricensis*. MNU= *N*-nitroso-*N*-methylurea; BP= Benzo[a]pyrene; CP= *C. portoricensis*; VIN= Vincasar. CP 1 =50 mg/kg and CP 2= 100 mg/kg. * = p less than .05 in contrast to vehinicle. ** = p less than .05 in contrast to untreated group. Values (mean±SDev) are based on 5-8 rats per group. The white arrows showing expression of BCL-2.

Uterine prolactin, FSH, LH, and progesterone levels were drastically increased in MNU and BP-treated groups (figures 4.97 - 4.100). However, following co-administration with chloroform fraction of CP, elevated prolactin, FSH, LH, and progesterone were significantly (p less than .05) reduced at both CP doses.

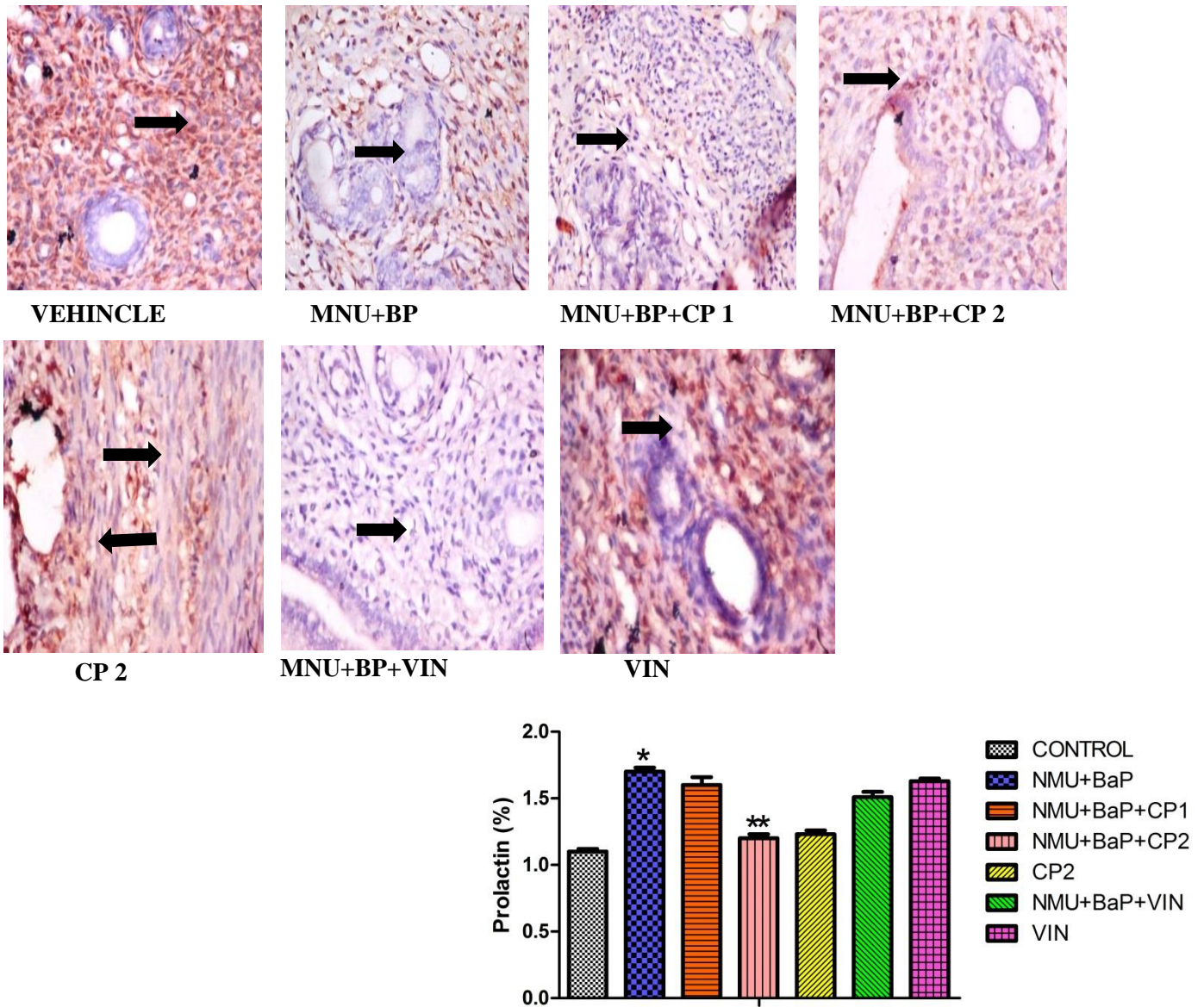


Figure 4.98: Immunohistochemical staining of prolactin hormone levels in the uterine tissue of MNU and BP rats given chloroform fraction of *C. Portoricensis*. MNU= *N-nitroso-N-methylurea*; BP= Benzo[a]pyrene; CP= *C. portoricensis*; VIN= Vincasar. CP 1 =50 mg/kg and CP 2= 100 mg/kg. * = p less than .05 in contrast to vehinCLE. ** = p less than .05 in contrast to untreated group. Values (mean±SDev) are based on 5-8 rats per group. The white arrows showing expression of prolactin hormone.

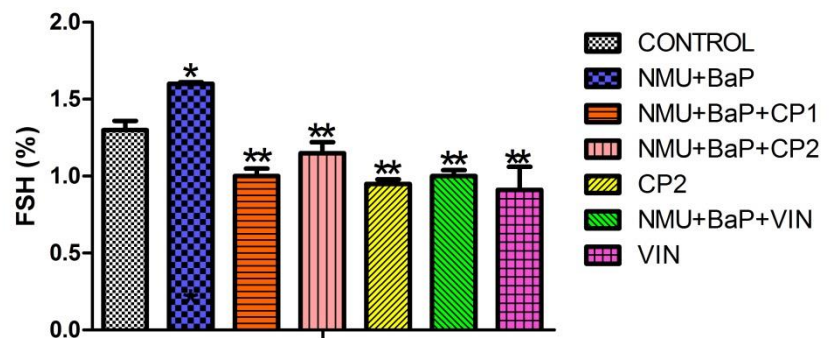
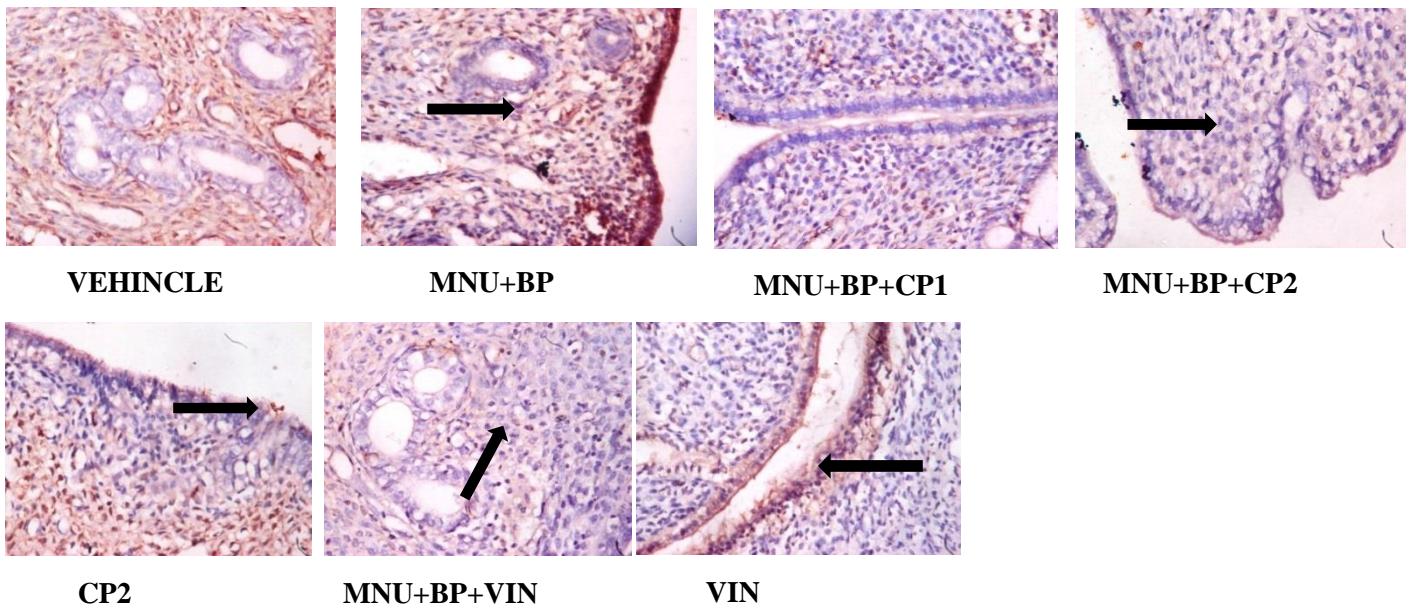


Figure 4.99: Immunohistochemical staining of follicle stimulating hormone (FSH) levels in the uterine tissue of MNU and BP rats given chloroform fraction of *C. Portoricensis*. MNU= *N-nitroso-N-methylurea*; BP= Benzo[a]pyrene; CP= *C. portoricensis*; VIN= Vincasar. CP 1 =50 mg/kg and CP 2= 100 mg/kg. * = p less than .05 in contrast to vehinacle. ** = p less than .05 in contrast to untreated group. Values (mean±SDev) are based on 5-8 rats per group. The white arrows showing expression of follicle stimulating hormone.

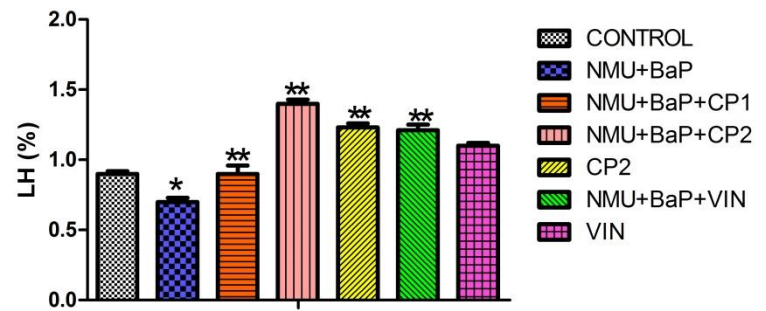
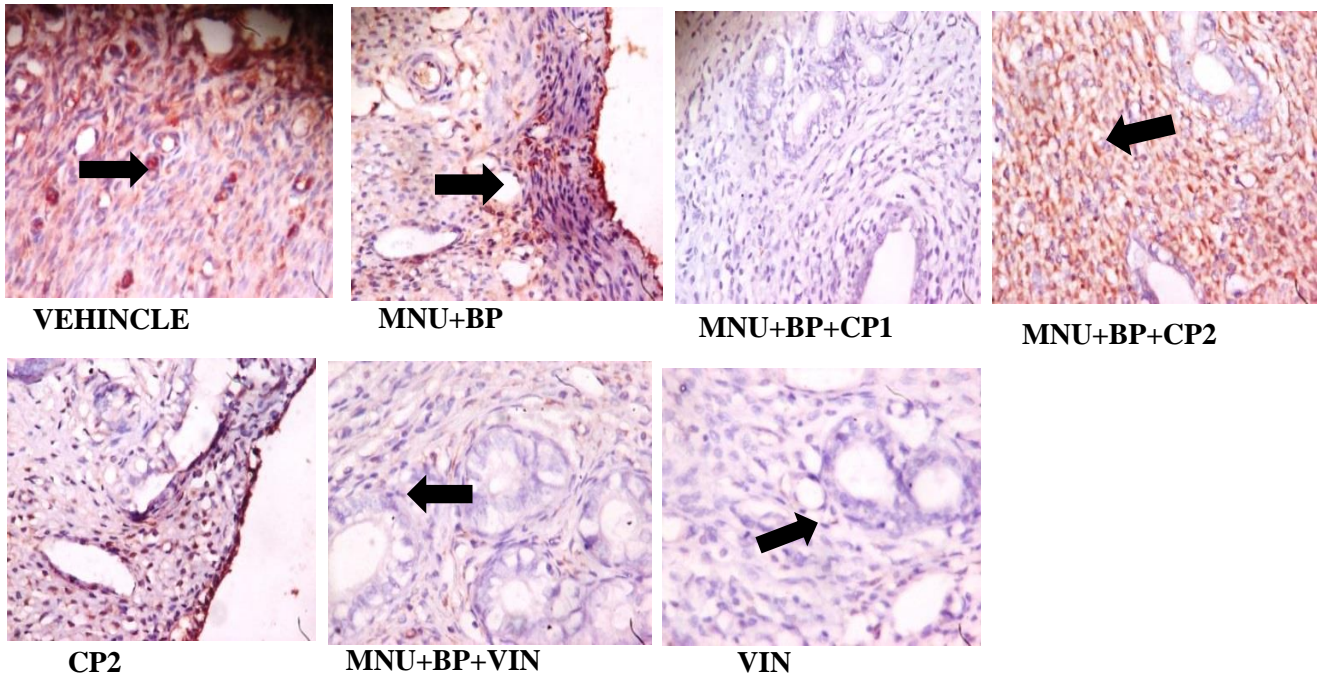


Figure 4.100: Immunohistochemical staining of lutenizing hormone (LH) levels in the uterine tissue of MNU and BP rats given chloroform fraction of *C. Portoricensis*. MNU= *N-nitroso-N-methylurea*; BP= *Benzo[a]pyrene*; CP= *C. portoricensis*; VIN= *Vincasar*. CP 1 =50 mg/kg and CP 2= 100 mg/kg. * = p less than .05 in contrast to vehinicle. ** = p less than .05 in contrast to untreated group. Values (mean±SDev) are based on 5-8 rats per group. The white arrows showing expression of lutenizing hormone.

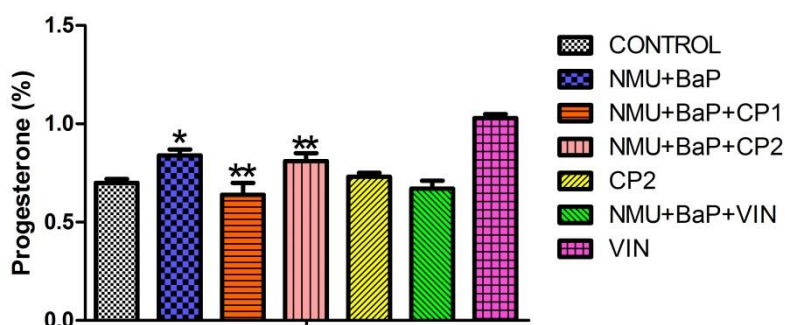
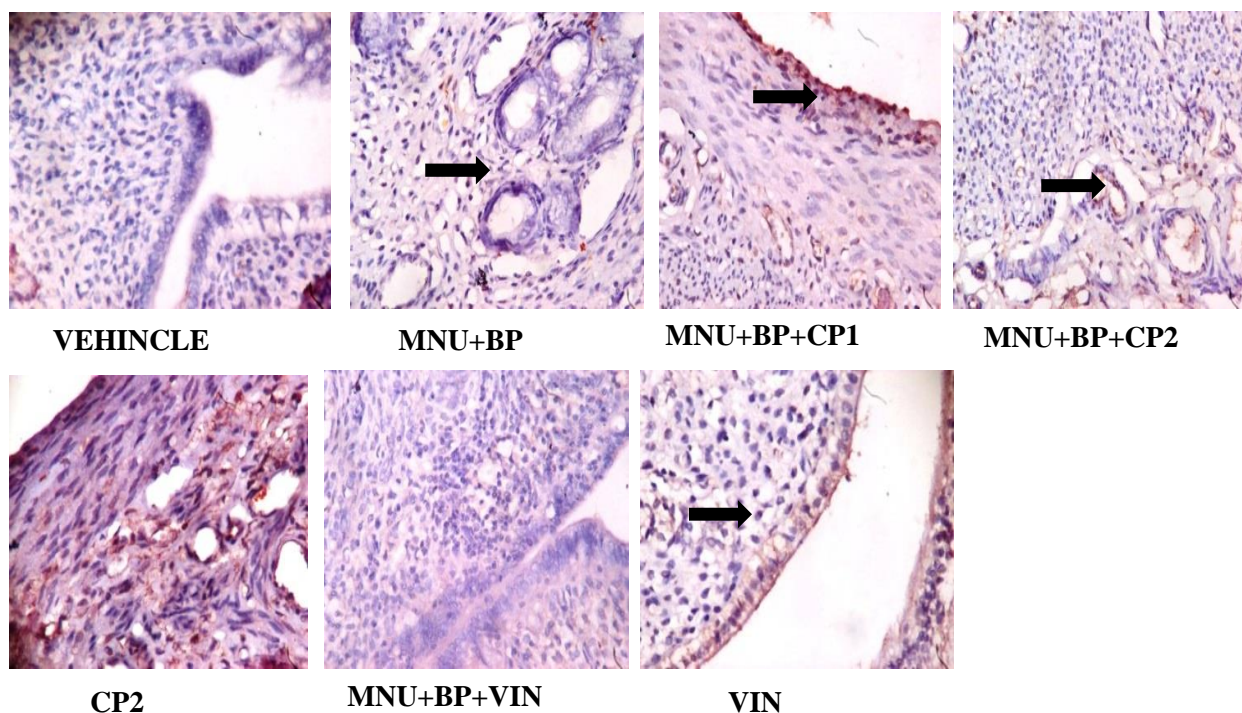


Figure 4.101: Immunohistochemical staining of progesterone hormone levels in the uterine tissue of MNU and BP rats given chloroform fraction of *C. Portoricensis*. MNU= *N-nitroso-N-methylurea*; BP= Benzo[a]pyrene; CP= *C. portoricensis*; VIN= Vincasar. CP 1 =50 mg/kg and CP 2= 100 mg/kg. * = p less than .05 in contrast to vehinacle. ** = p less than .05 in contrast to untreated group. Values (mean±SDev) are based on 5-8 rats per group. The white arrows showing expression of progesterone hormone.

The cyto-architecture of the uterus was investigated in figure 4.101. The uterine cyto-architecture emerges usual in the vehicle while MNU and BP treatment divulged extremely permeated endometrial glands with reddened swollen inflamed stroma cells. Co-treatment with chloroform fraction of CP ameliorated MNU and BP altered uterine tissues cyto-architecture when compared to vehicle group.

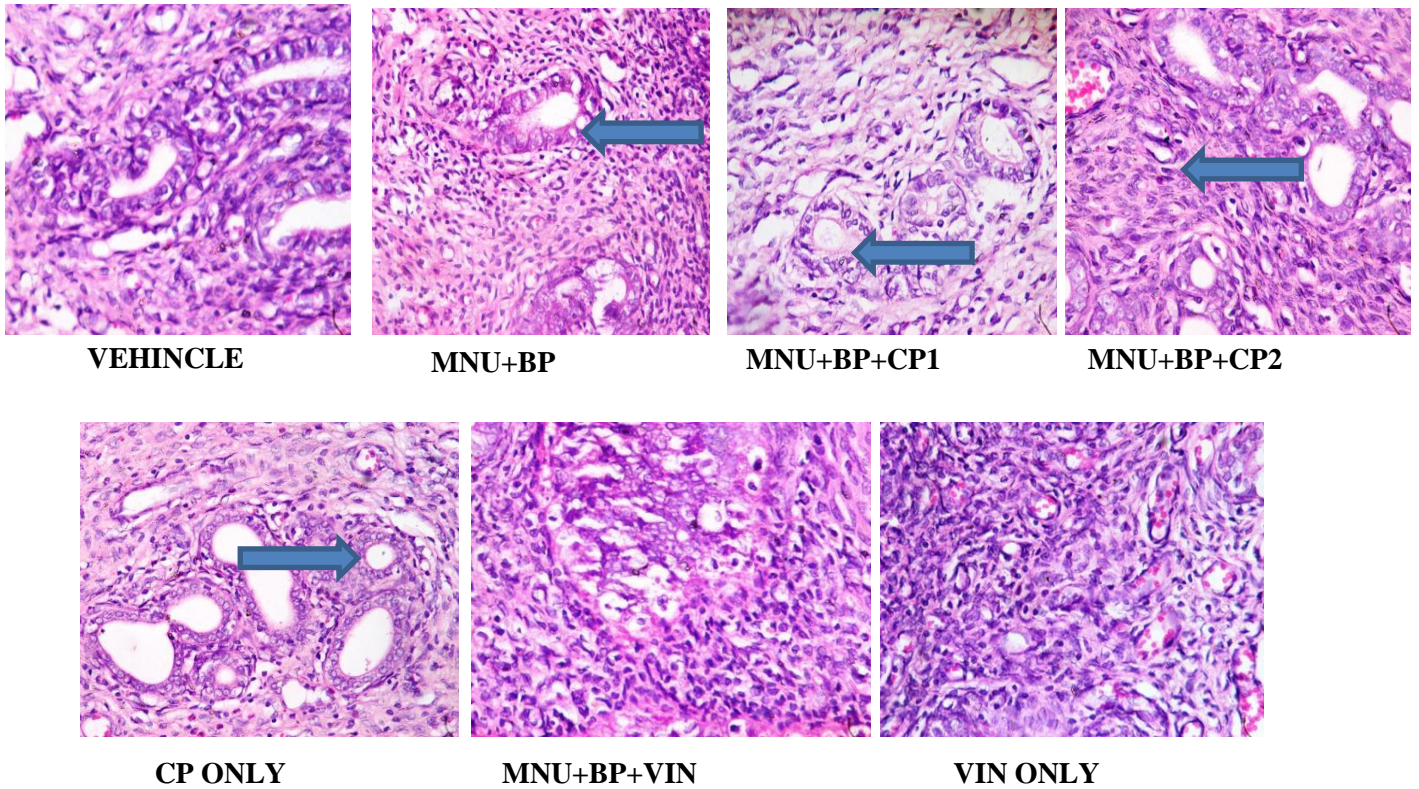


Figure 4.102: Uterine cyto-architecture tissues of MNU and BP given chloroform fraction of CP (M X 400). MNU= *N-nitroso-N-methylurea*; BP= Benzo[a]pyrene; CP= *C. portoricensis*; VIN= Vincasar. CP 1 =50 mg/kg, CP 2= 100 mg/kg.

The GC-MS spectral results and data base search identified ten (10) major compound from the chloroform fraction of *C. portoricensis*. Out of the compounds identified, GC-MS result revealed compound 2 (hexadecanoic acid methyl ester) as the major constituents while compound 9 (1-undecene,11-nitro-) as the least of the compounds identified.

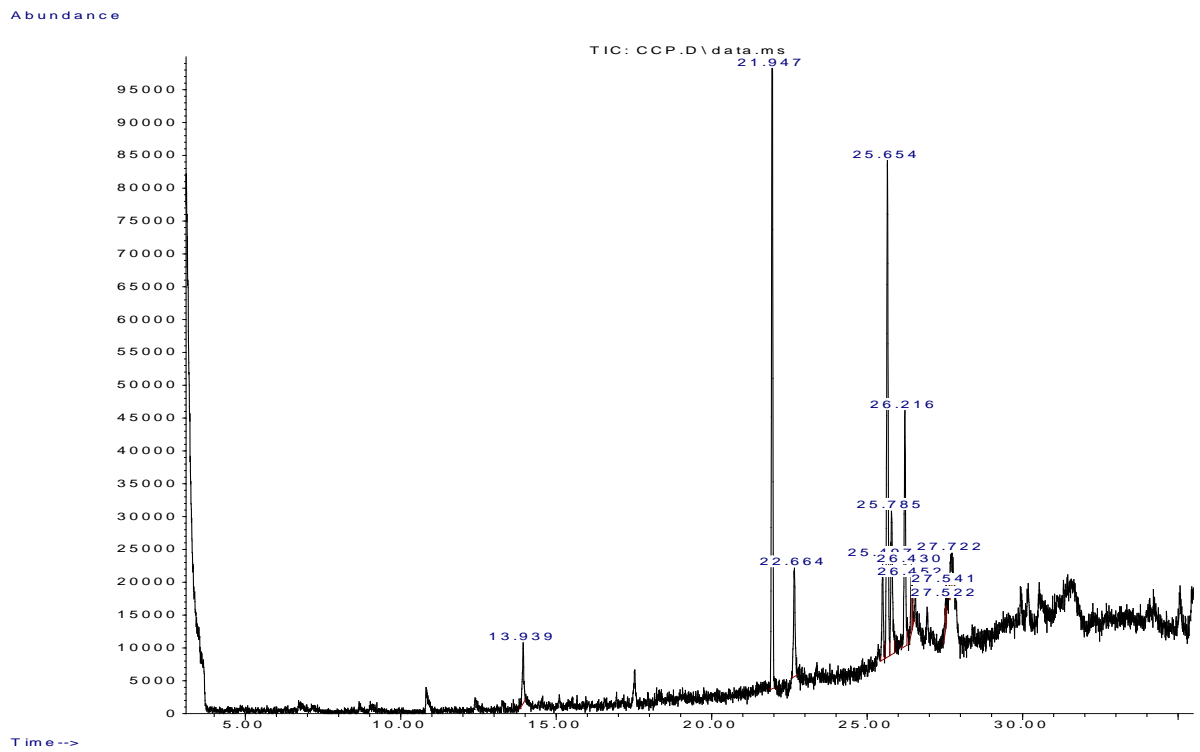


Figure 4.103: Finger printing of *C. portoricensis* (chloroform fraction) by GC-MS

Table 4.9: Identified Compounds from *C. portoricensis* (chloroform fraction)

GC Peak No	Compounds	Retention Time	Amount %
1	Hexadecyl pentyl ether	13.941	3.10
2	Hexadecanoic acid methyl ester	21.946	32.17
3	Tetradecanoic acid	22.662	6.25
4	1,8,11-Heptadecatriene	25.500	4.63
5	6-octadecenoic acid methyl ester	25.654	25.60
6	1,19-Eicosadiene	25.786	9.05
7	Z-7-tetradecenoic acid	26.215	11.51
8	13-tetradecenal	26.433	2.77
9	1-undecene,11-nitro-	26.450	1.10
10	Squalene	27.720	2.29

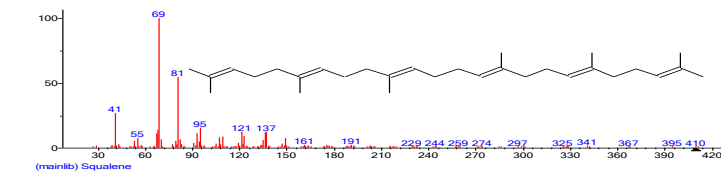
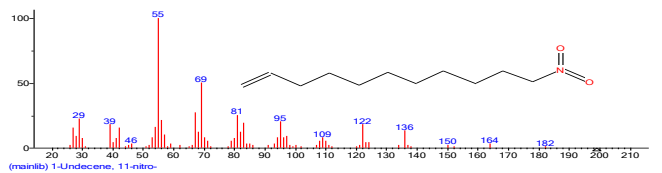
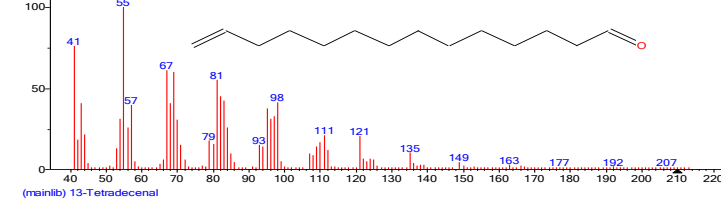
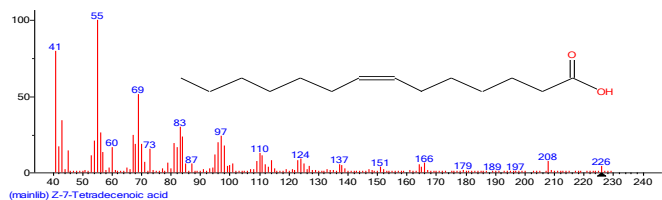
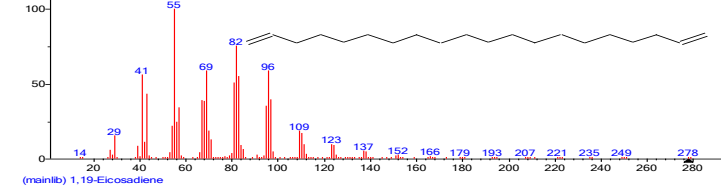
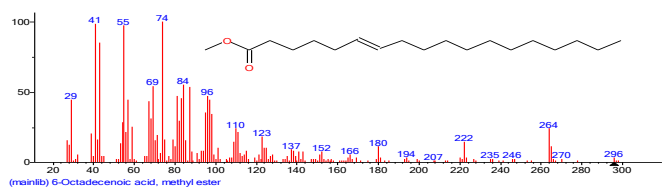
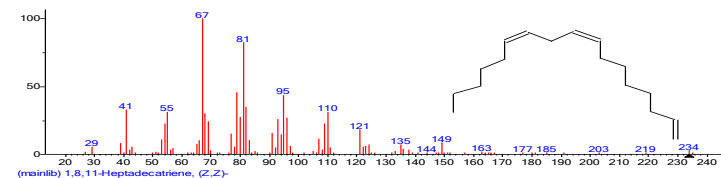
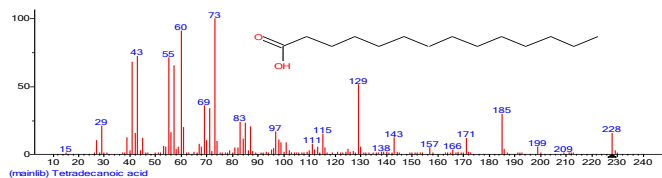
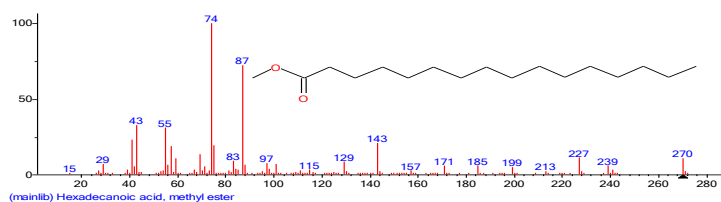
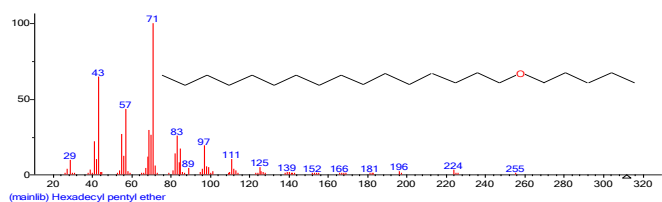


Figure 4.104: Chromatogram of *C. portoricensis* (chloroform fraction) by GCMS

4.4: Assessment of Antiproliferative, Antioxidative and Apoptotic Effects of Chloroform Fraction of *C. portoricensis* in MCF-7 cells

As indicated in Table 4.10 , chloroform fraction of CP significantly decreased cell viability and survival at 72 hours by 87.5% at 100 µg/ml similar to the effect of the standard drug Vincasar (87.6 %) relative to the Vehincles.

TABLE 4.10: EFFECT OF CHLOROFORM FRACTION OF *C. portoricensis* AND VINCASAR ON CELL GROWTH INHIBITION IN MCF-7 CELLS

CP		VIN	
Conc (µg/mL)	Growth Inhibition(%)	Conc (µg/mL)	Growth Inhibition
5	1.7*	5	49.0
25	28.6*	25	52.3
50	49.2*	50	87.6
100	87.5*	100	87.6

*= concentration-dependent increase in growth inhibition (%)

CP= *C. portoricensis*; VIN= Vincasar.

Figures 4.104, 4.105 and 4.106 showed chloroform fraction of CP influences and encouraged apoptosis to take place evidenced by increased in caspase-9,-3 and BaX activities in CP treated cell-lines relative to vehicle.

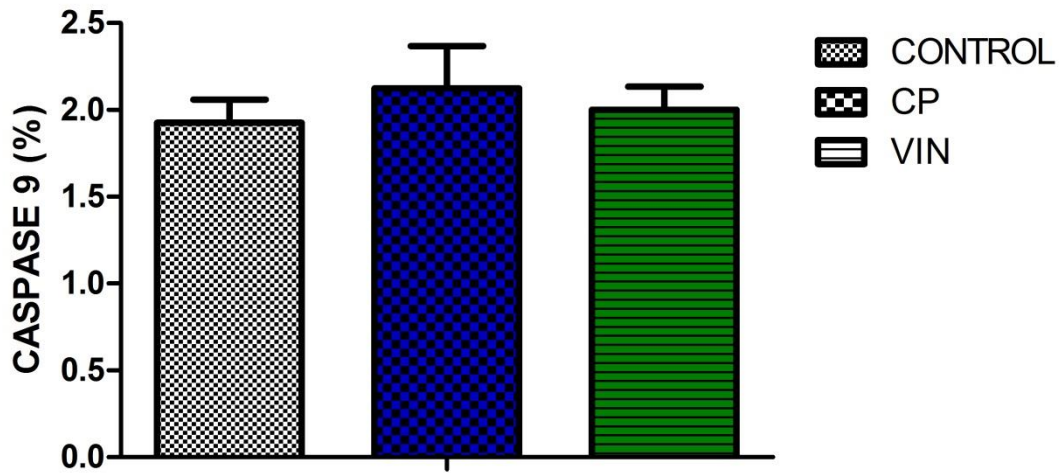


Figure 4.105: Effects of chloroform fraction of *C. portoricensis* on Caspase-9 activity on MCF-7 cell lysate *in vitro*. CP= *C. portoricensis*; VIN= Vincasar. Values are the mean \pm SDev of triplicate determination of the experiment.

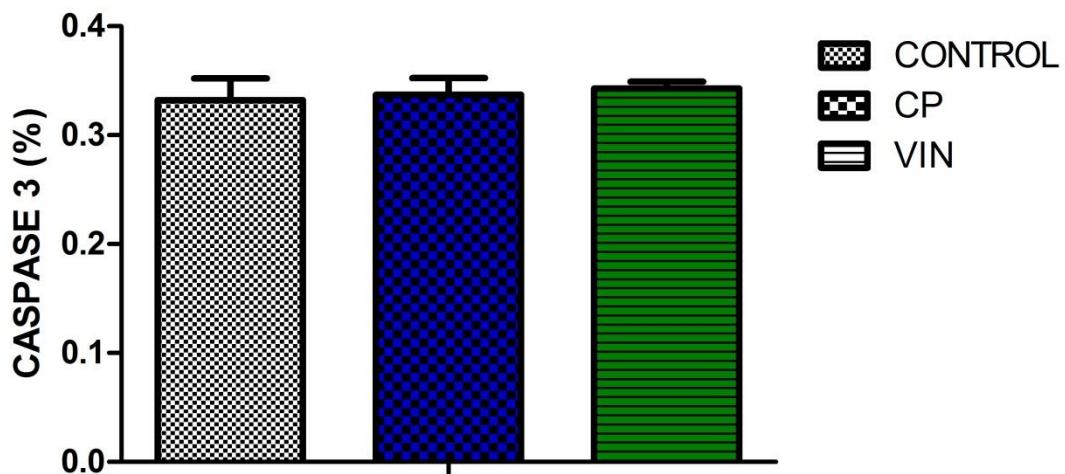


Figure 4.106 : Effects of chloroform fraction of *C. portoricensis* on Caspase-3 levels on MCF-7 cell lysate *in vitro*. VIN= Vincasar; CP= *C. portoricensis*. Values are the mean \pm SDev of triplicate determination of the experiment.

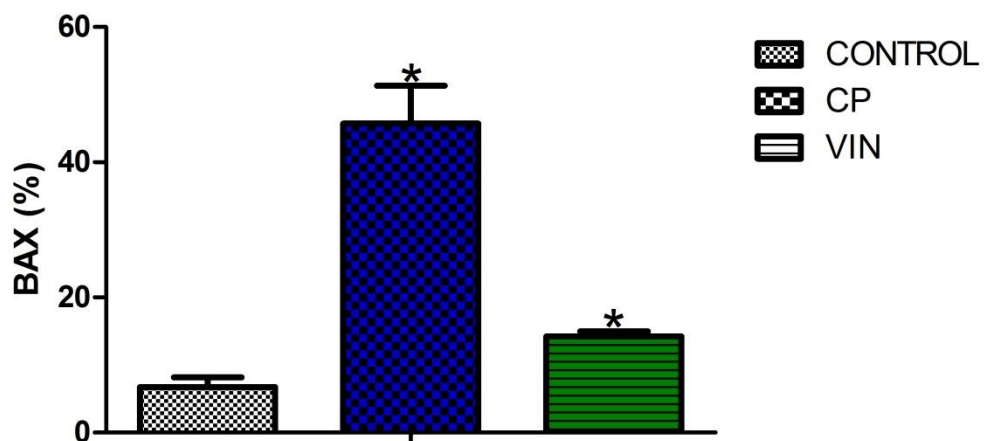


Figure 4.107: Effects of chloroform fraction of *C. portoricensis* on BAX activity on MCF-7 cell lysate *in vitro*. VIN= Vincasar; CP= *C. portoricensis*. Values are the mean \pm SDev of triplicate determination of the experiment. * pless than .05 in contrast to vehinle cell lysate.

Inflammatory markers IL-1 β and MPO was suppressed by CP treatment similar to standard drug vincasar when compared to vehicle (figures 4.107 and 4.109). In the same manner, CP and vincasar treatment suppressed oxidative stress (LPO) marker (figure 4.108). Also, SOD and Catalase activities was significantly elevated in CP and vincasar treated cells relative to vehicle groups (figures 4.110 and 4.111).

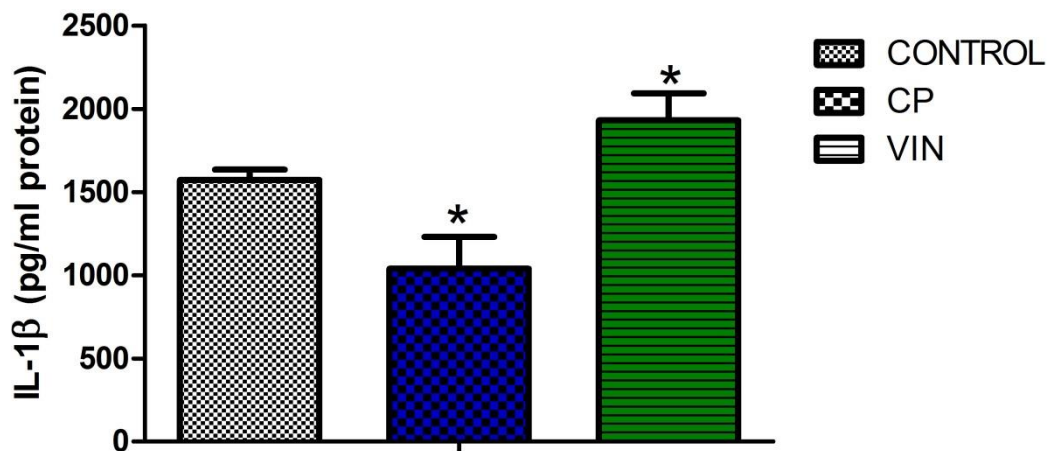


Figure 4.108: Effects of chloroform fraction of *C. portoricensis* on levels of interleukin-1 β (IL-1 β) on MCF-7 cell lysate *in vitro*. VIN= Vincasar; CP= *C. portoricensis*. Values are the mean \pm SDev of triplicate determination of the experiment. * pless than .05 in contrast to vehincle cell lysate.

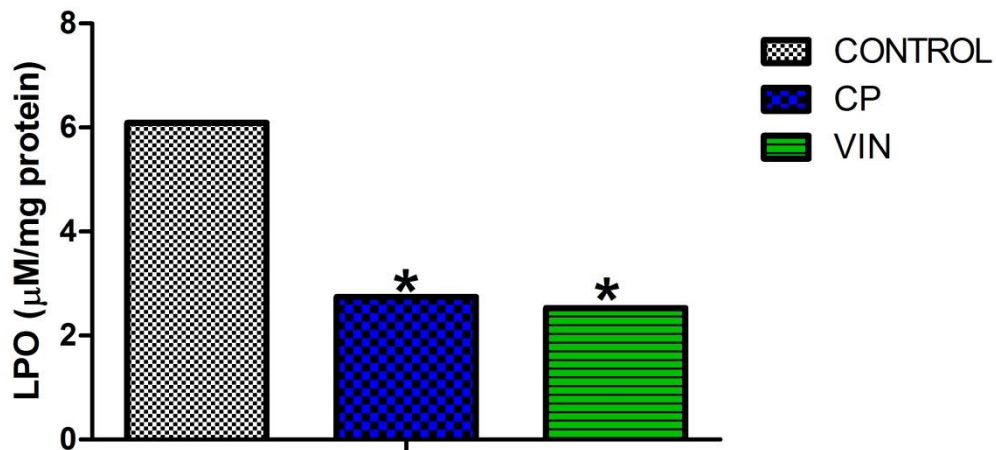


Figure 4.109: Effects of chloroform fraction of *C. portoricensis* on malondialdehyde (LPO) levels on MCF-7 cell lysate *in vitro*. VIN= Vincasar; CP= *C. portoricensis*. Values are the mean \pm SDev of triplicate determination of the experiment. * pless than .05 in contrast to vehinle cell lysate.

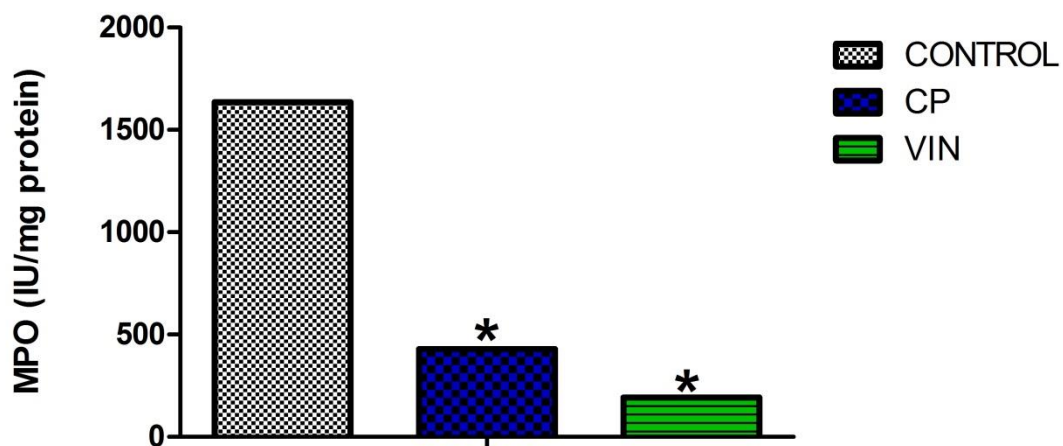


Figure 4.110: Effects of chloroform fraction of *C. portoricensis* on myeloperoxidase (MPO) activities on MCF-7 cell lysate *in vitro*. VIN= Vincasar; CP= *C. portoricensis*. Values are the mean \pm SDev of triplicate determination of the experiment. * pless than .05 in contrast to vehinle cell lysate.

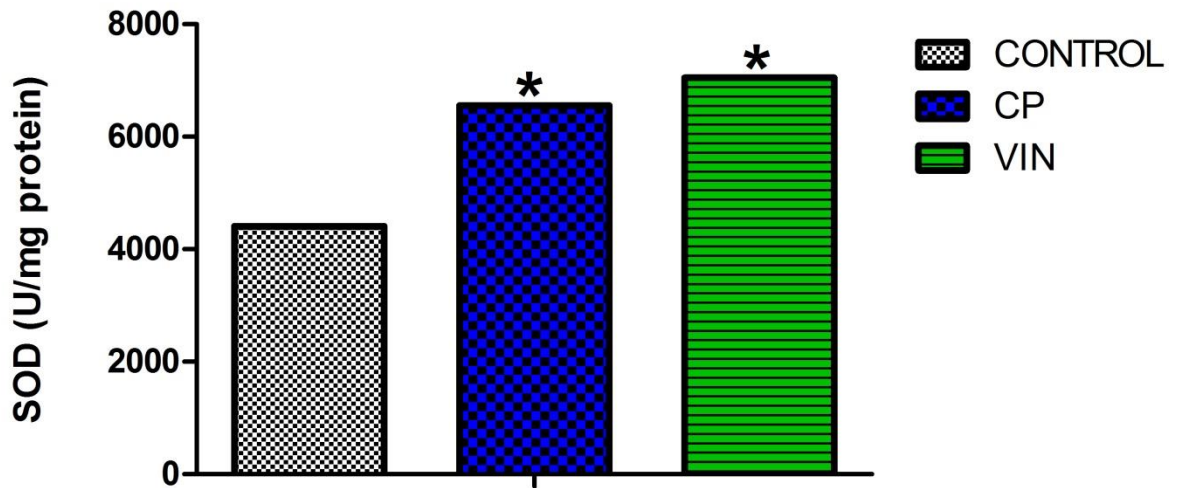


Figure 4.111: Effects of chloroform fraction of *C. portoricensis* on superoxide dismutase (SOD) activities on MCF-7 cell lysate *in vitro*. VIN= Vincasar; CP= *C. portoricensis*. Values are the mean \pm SDev of triplicate determination of the experiment. * pless than .05 in contrast to vehinle cell lysate.

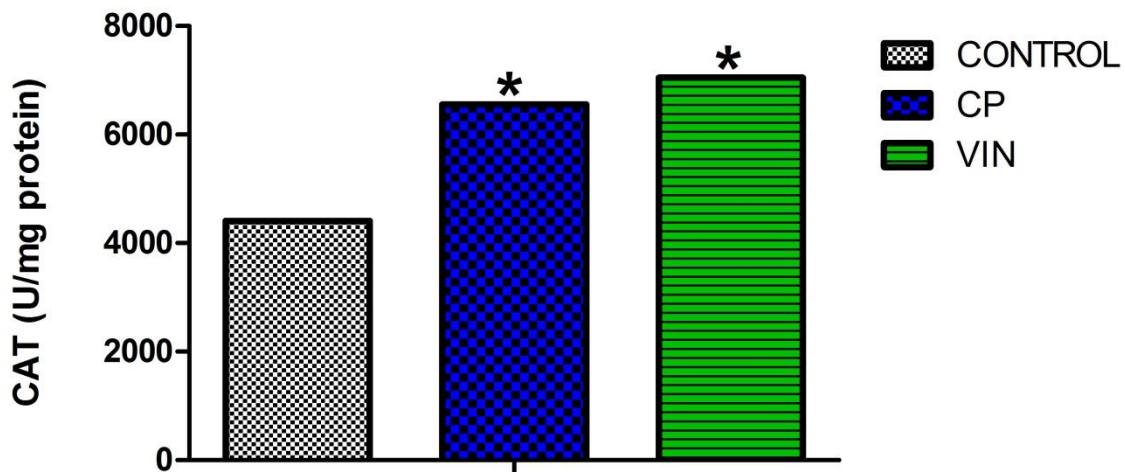


Figure 4.112: Effects of chloroform fraction of *C. portoricensis* on Catalase (CAT) activities on MCF-7 cell lysate *in vitro*. VIN= Vincasar; CP= *C. portoricensis*. Values are the mean \pm SDev of triplicate determination of the experiment. * pless than .05 in contrast to vehinle cell lysate.

4.5: Possible Curative Effects of *C. portoricensis* (chloroform fraction) on *N-nitroso-N-methylurea* and Benzo[a]pyrene-induced Mammary Toxicity in Wistar Rats

The body weight gained [MNU+BP-treated rats] was slightly reduced by **5%** in relation to vehicle group (Table 4.11). On the contrary, MNU and BP increased the weight and organo-somatic weight of mammary tissues in the groups by 3 folds and 2-folds, respectively. Post-treatment with chloroform fraction of CP restored the tissue weight and organosomatic weight near normal vehicle values.

TABLE 4.11: BODY WEIGHT CHANGES OF WISTAR RATS ON EXPOSURE TO MNU AND BP GIVEN CHLOROFORM FRACTION OF *C. portoricensis* AND VINCASAR

Treatment	Original Body mass	Terminal Body mass	Body mass Gained (g)	Mammary Weight (g)	Organ-body Weight (a)
VEHICLE	63.55±6.02	150.83±5.25	87.28±5.70	0.36±0.07	0.24±0.05
MNU+BP	83.43±6.66	164.08±8.28	80.65±8.14	1.46±0.40*	92±0.04*
MNU+BP+CP	79.51±5.89	157.67±22.22	78.16±6.8	11.00±0.21**	0.55±0.07**
MNU+BP+VIN	61.48±6.94	160.78±25.38	99.30±32.31	1.22±0.37	0.68±0.03**

MNU= *N-nitroso-N-methylurea*; BP= Benzo[a]pyrene; CP= *C. portoricensis* (100 mg/kg); VIN= Vincasar, a= % body weight. * = pless than .05 in contrast to vehincle. ** = pless than .05 in contrast to untreated group. Values (mean±SDev) are based on 5-8 rats per group.

The data from figure 4.112 – figure 4.114 on liver functions parameters (ALT, AST and BIL) clearly demonstrate a slight increased in ALT, AST and T-Bil by 4%, 1% and 16% in groups given MNU and BP. Post treatment with chloroform fraction of CP ameliorated the serum ALT and T-Bil level without affecting the AST activity.

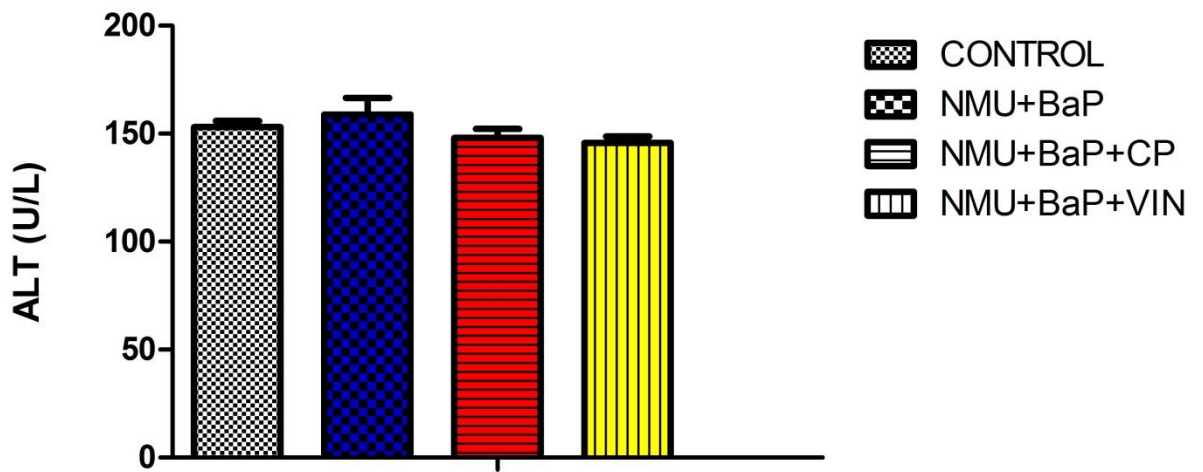


Figure 4.113: Effect of chloroform fraction of *C. portoricensis* (CP) on alanine-aminotransferases (ALT) activities in MNU and BP -treated rats. MNU= *N-nitroso-N-methylurea*; BP= Benzo[a]pyrene; CP= *C. portoricensis* (100mg/kg); VIN= Vincasar. Values (mean±SDev) are based on 5-8 rats per group.

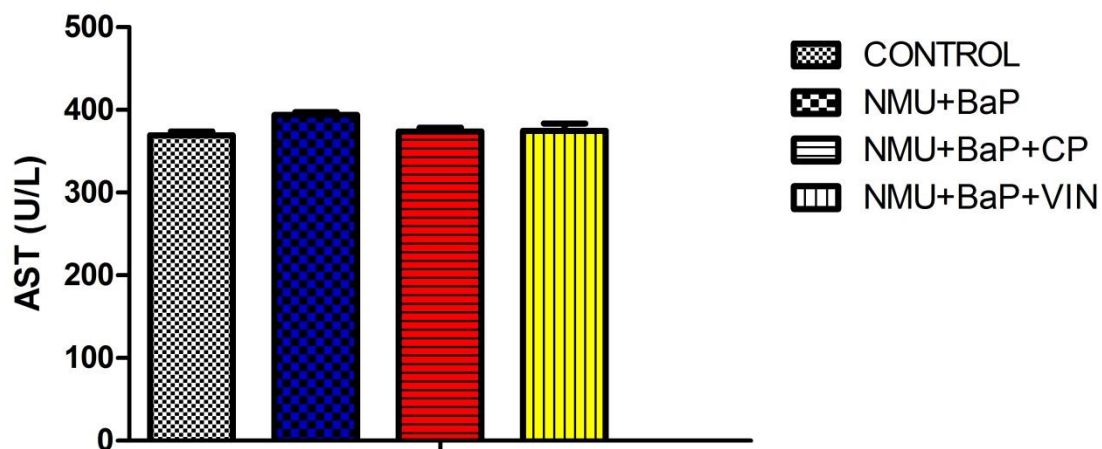


Figure 1.114: Effect of chloroform fraction of *C. portoricensis* (CP) on aspartate-aminotransferases (AST) activities in MNU and BP -treated rats. MNU= *N-nitroso-N-methylurea*; BP= Benzo[a]pyrene; CP= *C. portoricensis* (100 mg/kg); VIN= Vincasar. Values (mean±SDev) are based on 5-8 rats per group.

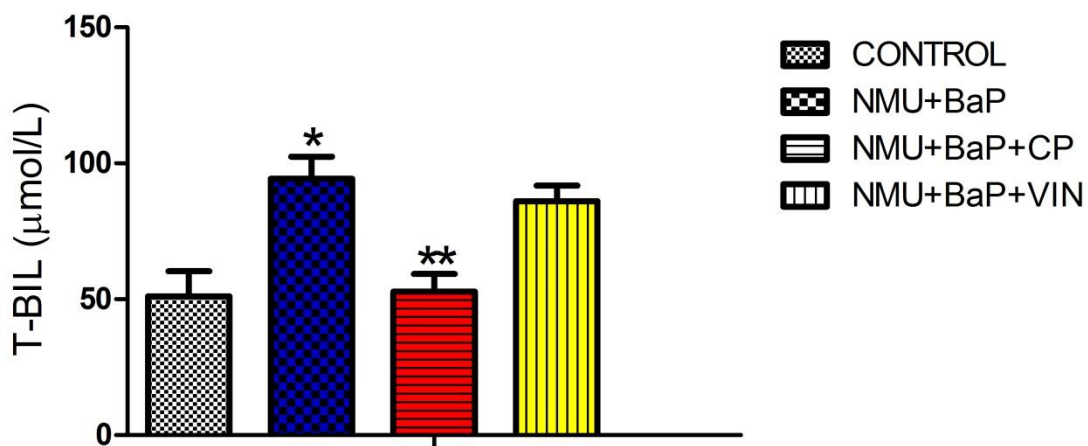


Figure 4.115: Effect of chloroform fraction of *C. portoricensis* (CP) on total bilirubin levels (T-BIL) in MNU and BP-treated rats. MNU= *N-nitroso-N-methylurea*; BP= Benzo[a]pyrene; CP= *C. portoricensis* (100 mg/kg); VIN= Vincasar. * = less than .05 in contrast to vehicle. ** = less than .05 in contrast to untreated group. Values (mean±SDev) are based on 5-8 rats per group.

Mammary SOD, GST and CAT activities decreased after MNU and BP treatment. However, CP post treatment restored the tissue SOD, GST and CAT significantly (Figures 4.115 - 4.117). MNU and BP treatment specifically decreased SOD, GST and CAT by 62%, 59% and 54% respectively relative to vehicle group.

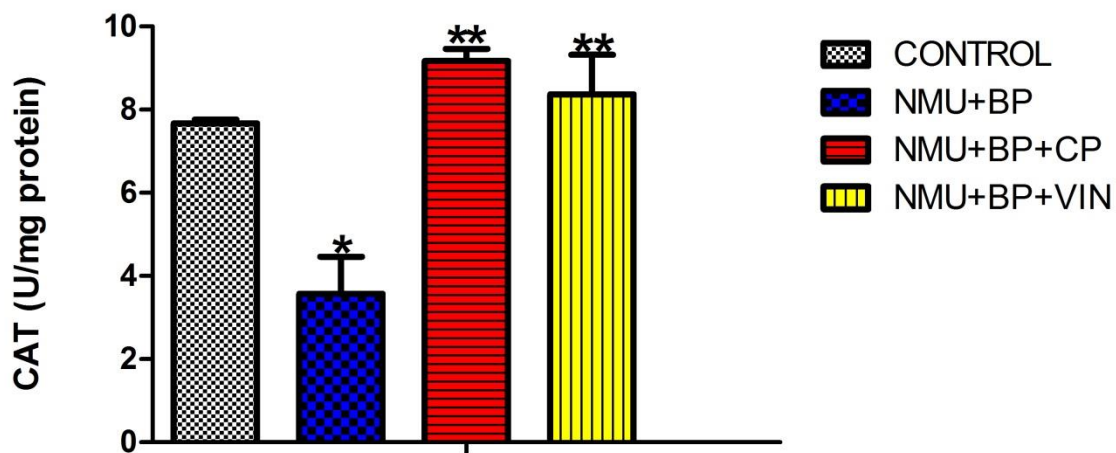


Figure 4.116: Effect of chloroform fraction of *C. portoricensis* (CP) on Catalase (CAT) activities in MNU and BP -treated rats. MNU= *N*-nitroso-*N*-methylurea; BP= Benzo[a]pyrene; CP= *C. portoricensis* (100 mg/kg); VIN= Vincasar. * = pless than .05 in contrast to vehinle. ** = pless than .05 in contrast to untreated group. Values (mean±SDev) are based on 5-8 rats per group.

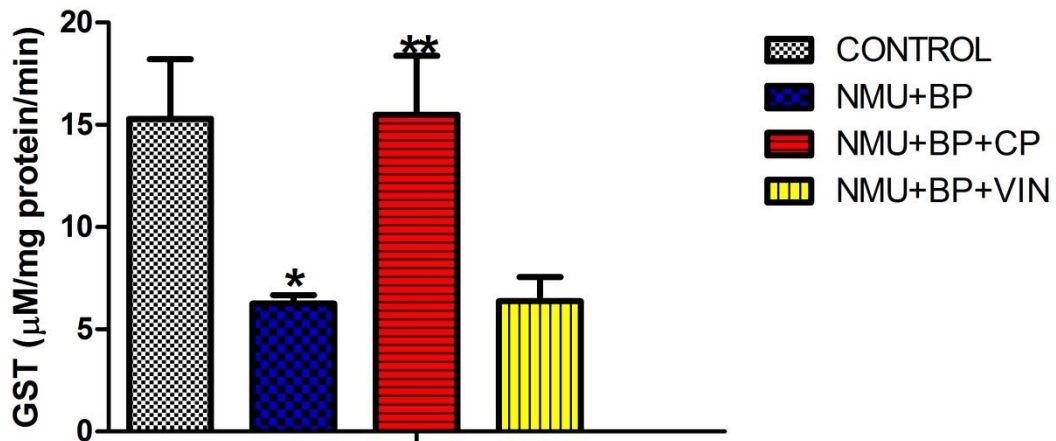


Figure 4.117: Effect of chloroform fraction of *C. portoricensis* (CP) on glutathione-S-transferases (GST) activities in MNU and BP-treated rats. MNU= *N-nitroso-N-methylurea*; BP= Benzo[a]pyrene; CP= *C. portoricensis* (100 mg/kg); VIN= Vincasar. * = p less than .05 in contrast to vehicle. ** = p less than .05 in contrast to untreated group. Values (mean±SDev) are based on 5-8 rats per group.

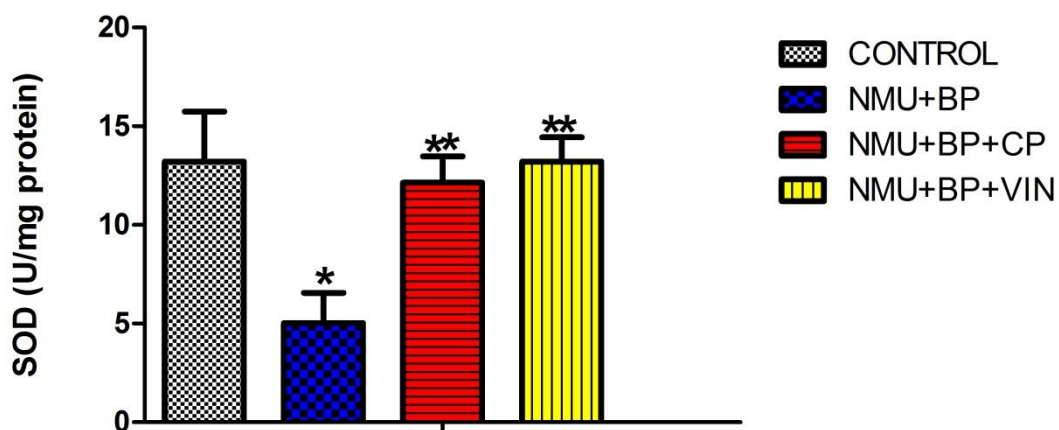


Figure 4.118: Effect of chloroform fraction of *C. portoricensis* (CP) on superoxide dismutase (SOD) activities in MNU and BP -treated rats. MNU= *N-nitroso-N-methylurea*; BP= Benzo[a]pyrene; CP= *C. portoricensis* (100 mg/kg); VIN= Vincasar. * = pless than .05 in contrast to vehicple. ** = pless than .05 in contrast to untreated group. Values (mean±SDev) are based on 5-8 rats per group.

The levels of GSH, TSH and GPx activity following MNU and BP administration slightly reduced when compared to the vehincles. While post CP treatement increased GSH, TSH and GPx activity but not significantly expressed. (Figures 4.118 - 4.120).

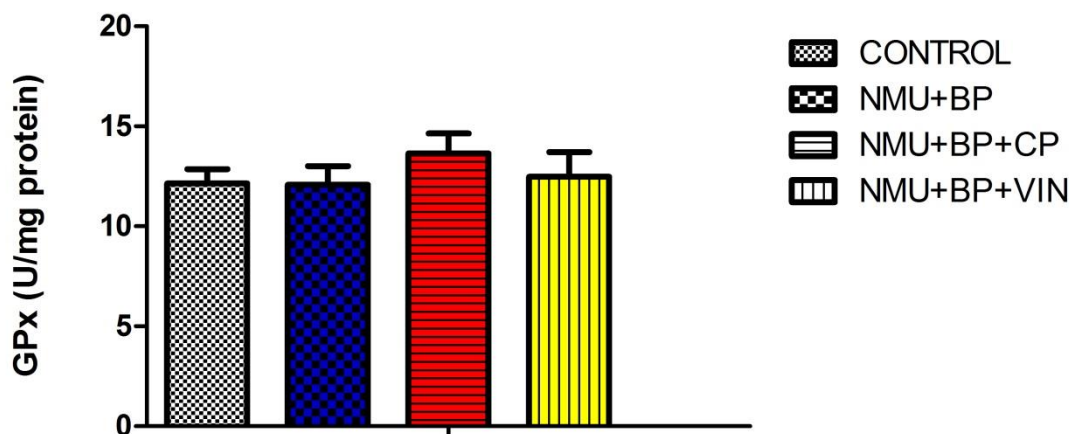


Figure 4.119: Effect of chloroform fraction of *C. portoricensis* (CP) on glutathione peroxidase (GPx) activities in MNU and BP-treated rats. MNU= *N-nitroso-N-methylurea*; BP= Benzo[a]pyrene; CP= *C. portoricensis* (100 mg/kg); VIN= Vincasar. Values (mean±SDev) are based on 5-8 rats per group.

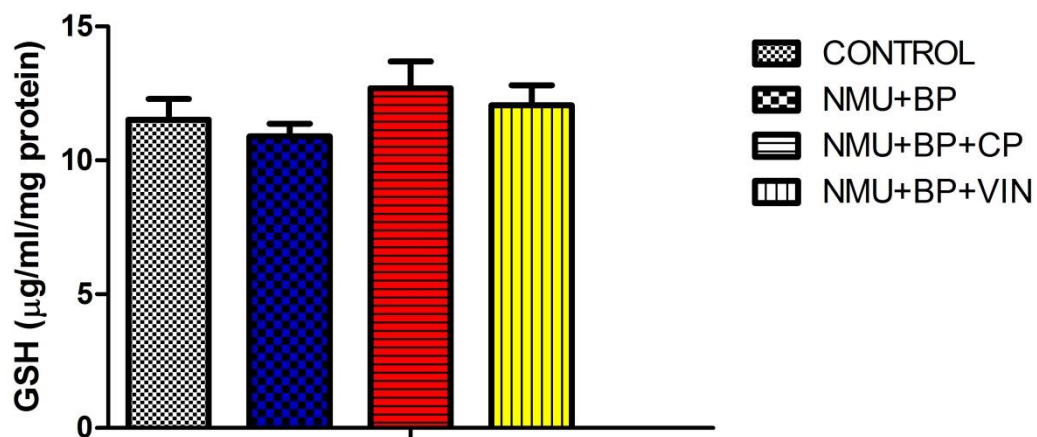


Figure 4.120: Effect of chloroform fraction of *C. portoricensis* (CP) on reduced glutathione (GSH) levels in MNU and BP-treated rats. MNU= *N-nitroso-N-methylurea*; BP= Benzo[a]pyrene; CP= *C. portoricensis* (100 mg/kg); VIN= Vincasar. Values (mean±SDev) are based on 5-8 rats per group.

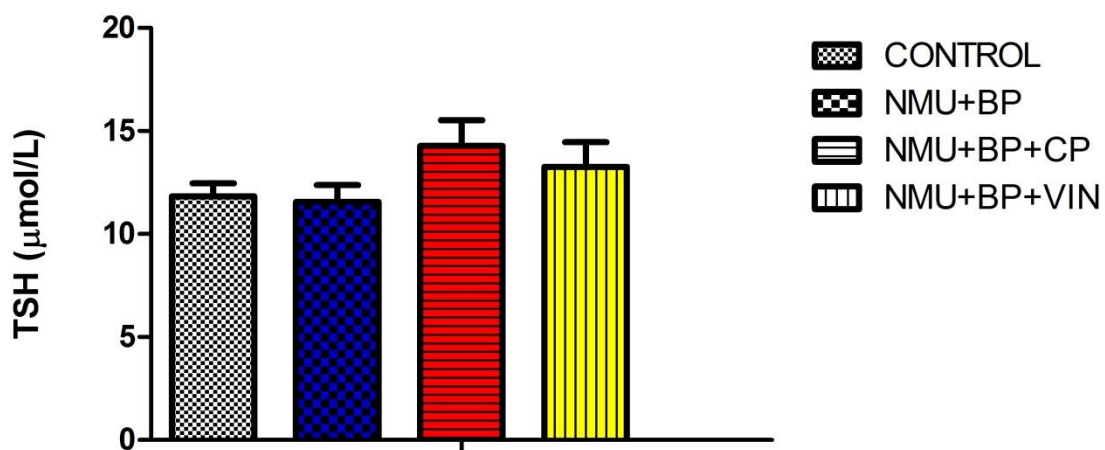


Figure 4.121: Effect of chloroform fraction of *C. portoricensis* (CP) on total sulphhydryl (TSH) levels in MNU and BP-treated rats. MNU= *N-nitroso-N-methylurea*; BP= Benzo[a]pyrene; CP= *C. portoricensis* (100 mg/kg); VIN= Vincasar. Values (mean±SDev) are based on 5-8 rats per group.

MNU and BP administration results showed a considerable increase in LPO, NO, and MPO activity in serum and mammary tissue. However, post treatment with chloroform fraction of CP reduced the levels of LPO, NO and MPO activity (figures 4.121 - 4.123).

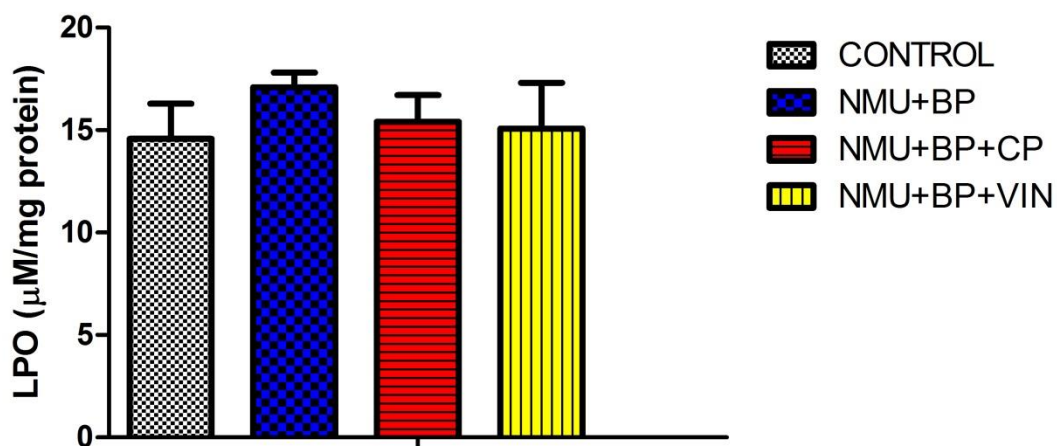


Figure 4.122: Effect of chloroform fraction of *C. portoricensis* (CP) on malondialdehyde (LPO) levels in MNU and BP-treated rats. MNU= *N-nitroso-N-methylurea*; BP= Benzo[a]pyrene; CP= *C. portoricensis* (100 mg/kg); VIN= Vincasar. Values (mean±SDev) are based on 5-8 rats per group.

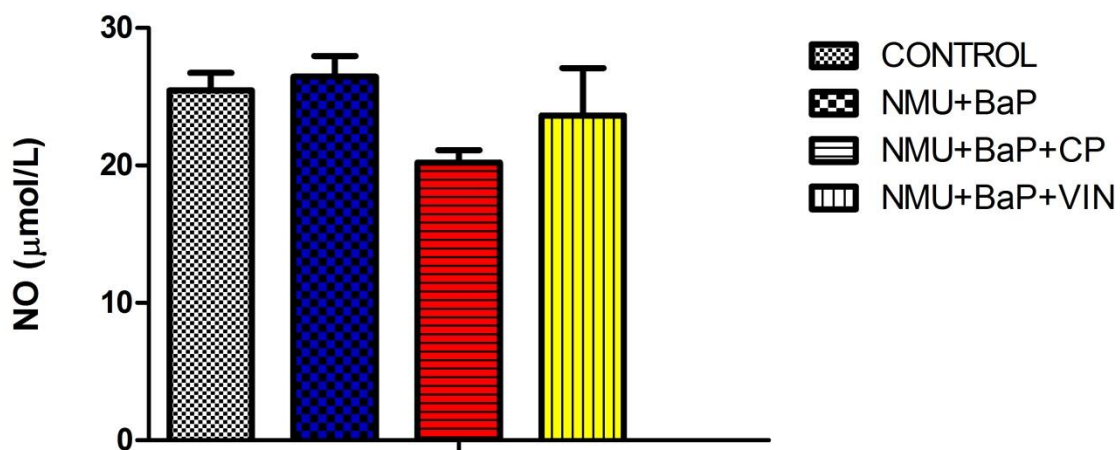


Figure 4.123: Effect of chloroform fraction of *C. portoricensis* (CP) on nitric oxide (NO) levels in MNU and BP-treated rats. MNU= *N*-nitroso-*N*-methylurea; BP= Benzo[a]pyrene; CP= *C. portoricensis* (100 mg/kg); VIN= Vincasar. Values (mean \pm SDev) are based on 5-8 rats per group.

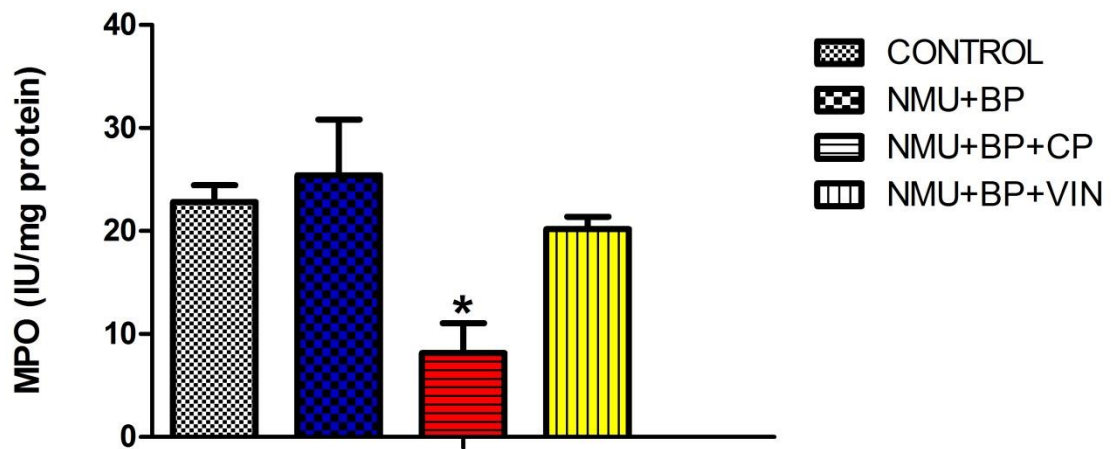


Figure 4.124: Effect of chloroform fraction of *C. portoricensis* (CP) on myeloperoxidase (MPO) activities in MNU and BP-treated rats. MNU= *N-nitroso-N-methylurea*; BP= Benzo[a]pyrene; CP= *C. portoricensis* (100 mg/kg); VIN= Vincasar. * = pless than .05 in contrast to vehinclc. Values (mean±SDev) are based on 5-8 rats per group.

The mammary tissues from MNU and BP administered group showed extensive NF- κ B and iNOS protein expression (Figures 4.124- 4.125), and CP treatment exhibited considerable inhibition of iNOS and NF- κ B expression (Figures 4.124- 4.125).

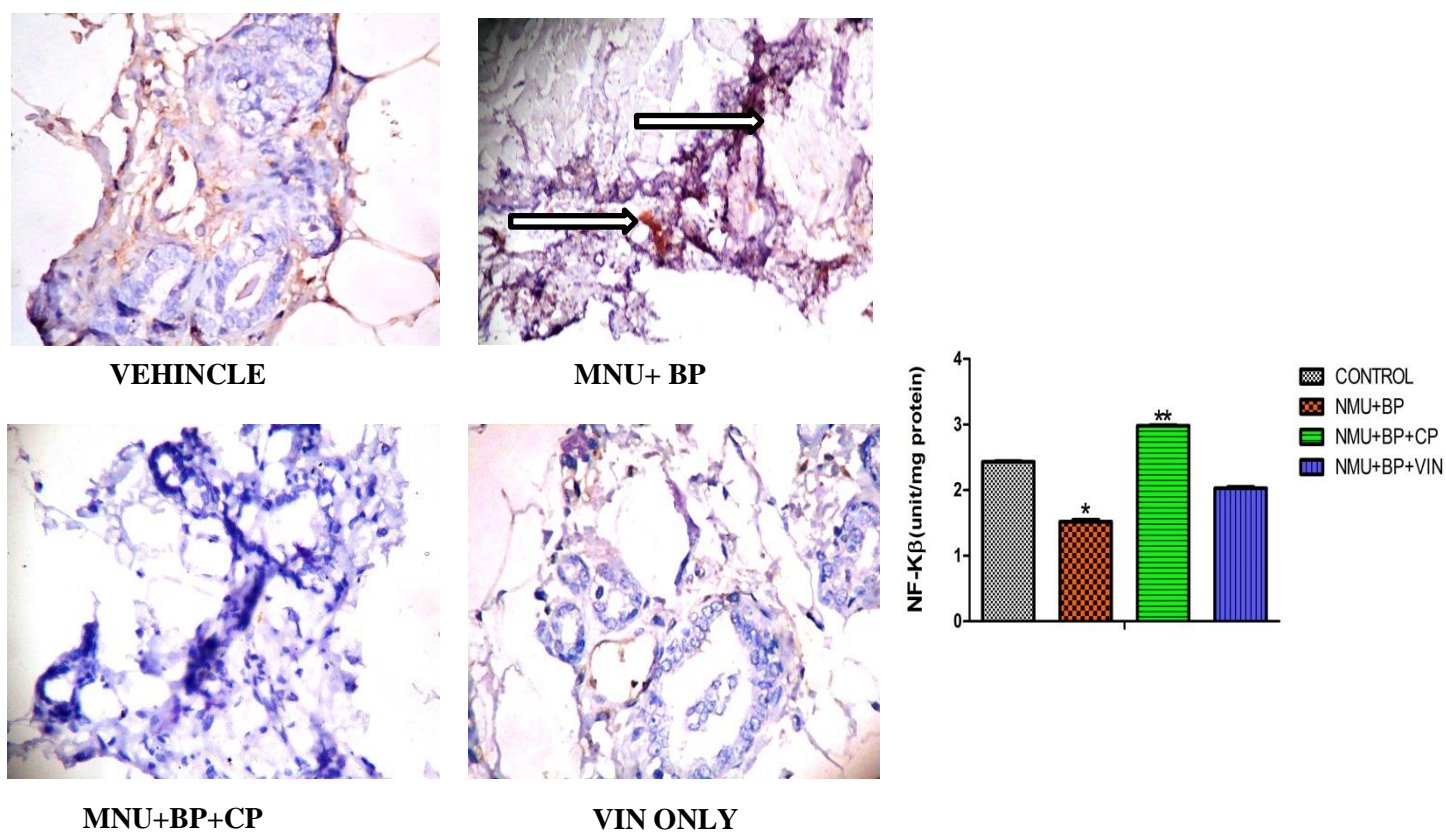


Figure 4.125: Effect of chloroform fraction of *C. portoricensis* (CP) on Nuclear factor kappa B (NF-kB) activity in MNU and BP-treated rats. MNU= *N-nitroso-N-methylurea*; BP= Benzo[a]pyrene; CP= *C. portoricensis* (100 mg/kg); VIN= Vincasar. * = pless than .05 in contrast to vehinle. ** = pless than .05 in contrast to untreated group. Values (mean±SDev) are based on 5-8 rats per group. The white arrows showing expression of NF-kB.

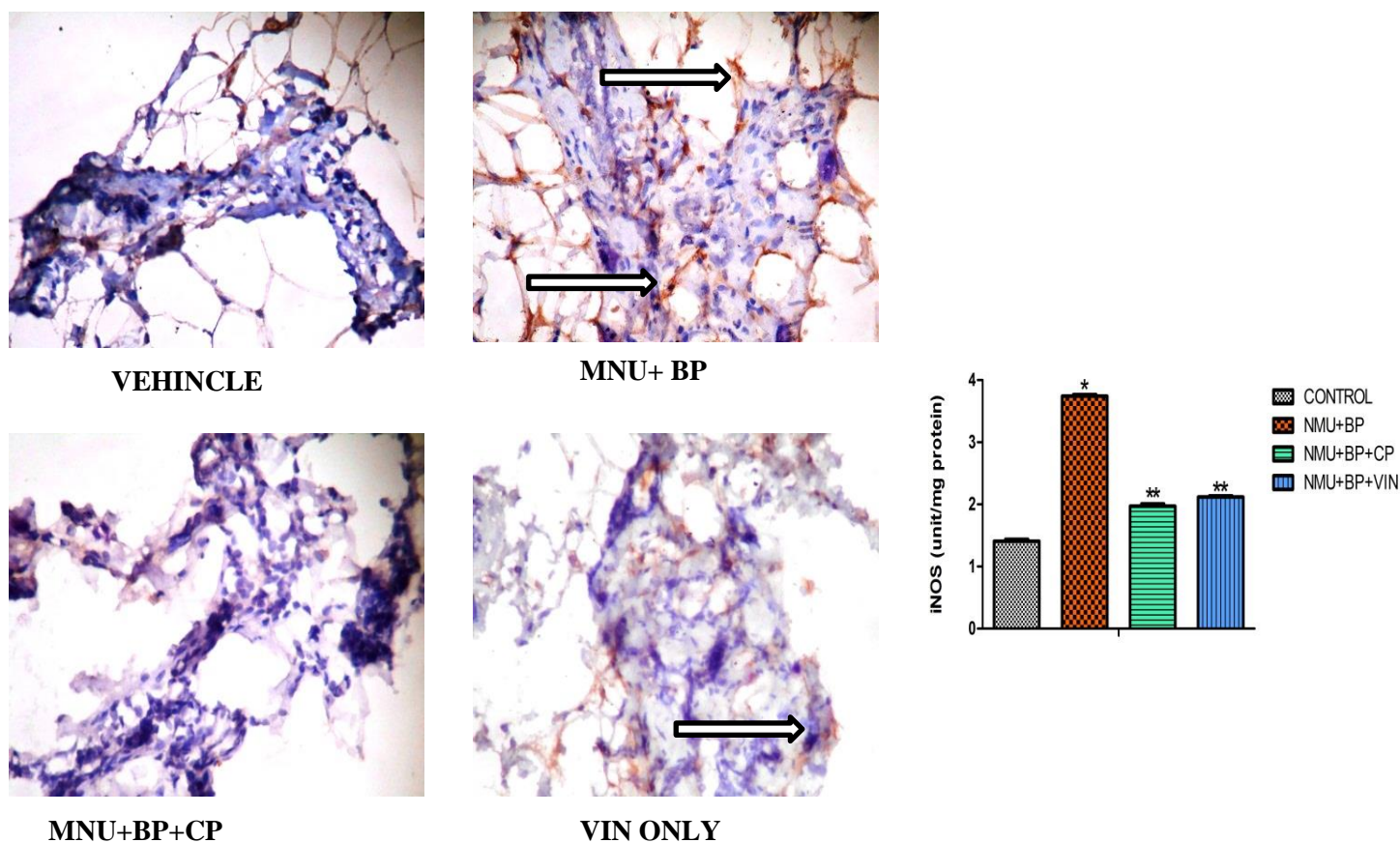


Figure 4.126: Effect of chloroform fraction of *C. portoricensis* (CP) on inducible nitric oxide synthase (iNOS) activity in MNU and BP-treated rats. MNU= *N*-nitroso-*N*-methylurea; BP= Benzo[a]pyrene; CP= *C. portoricensis* (100 mg/kg); VIN= Vincasar. * = p less than .05 in contrast to vehicle. ** = p less than .05 in contrast to untreated group. Values (mean±SDev) are based on 5-8 rats per group. The white arrows showing expression of iNOS.

To evaluate the amount of cell death in mammary tumor specimens, immunohistochemistry was performed. Apoptotic cells were highly uncommon in the tumors of MNU and BP vehicle rats. However, in the CP + MNU and BP groups, a substantial increase in the apoptotic cell population was observed (Figure 4.126). Bax, p53, Caspase-3 expression was extremely low in MNU and BP treated rats (figures 4.126- figure 4.128). However, in the mammary tissues collected from the CP and VIN treatment groups, there was a significant rise in Bax, p53, and caspase-3 expression.

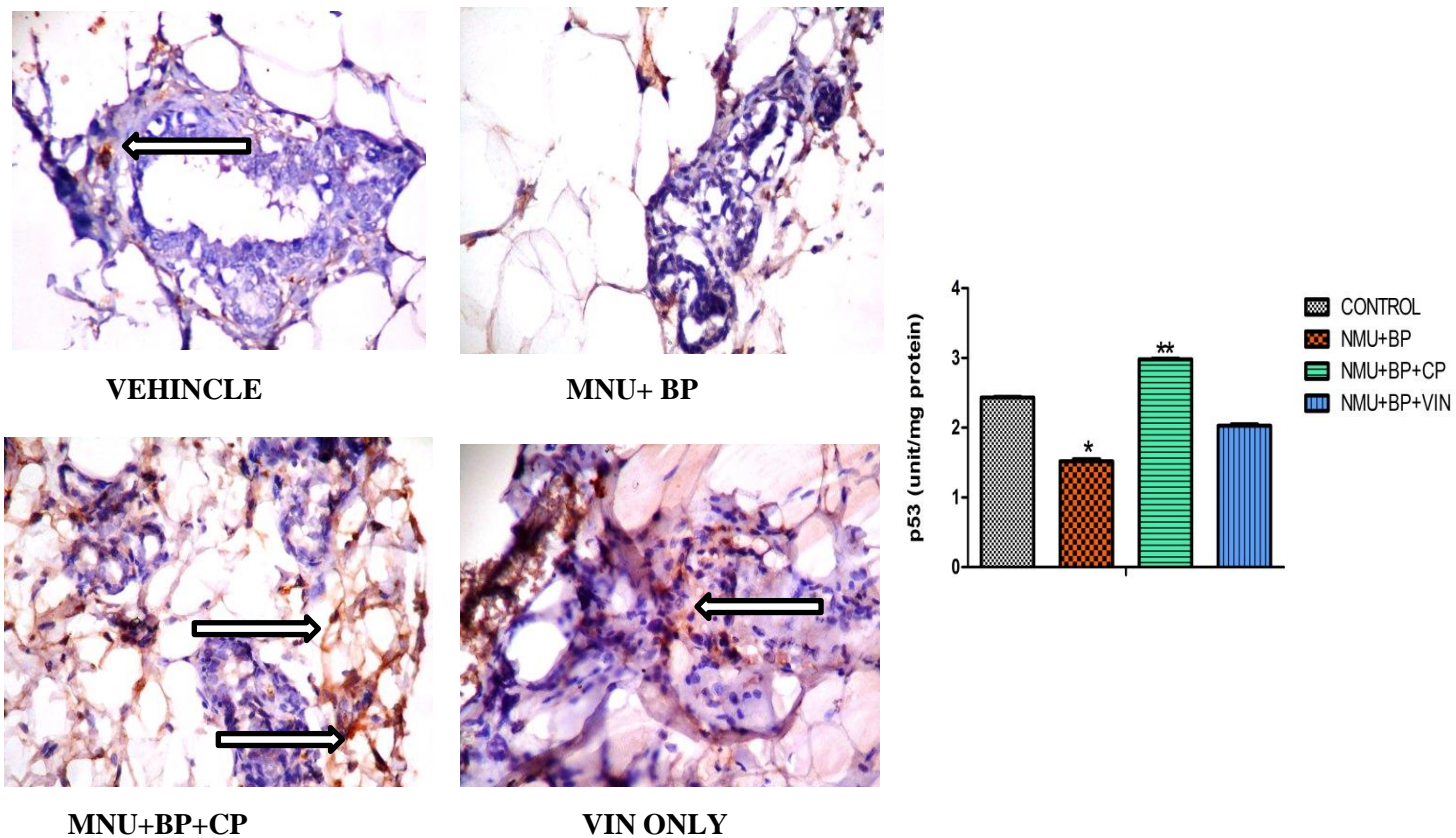


Figure 4.127: Effect of chloroform fraction of *C. portoricensis* (CP) on p53 activity in MNU and BP-treated rats. MNU= *N*-nitroso-*N*-methylurea; BP= Benzo[a]pyrene; CP= *C. portoricensis* (100 mg/kg); VIN= Vincasar. * = pless than .05 in contrast to vehicle. ** = pless than .05 in contrast to untreated group. Values (mean±SDev) are based on 5-8 rats per group. The white arrows showing expression of p53.

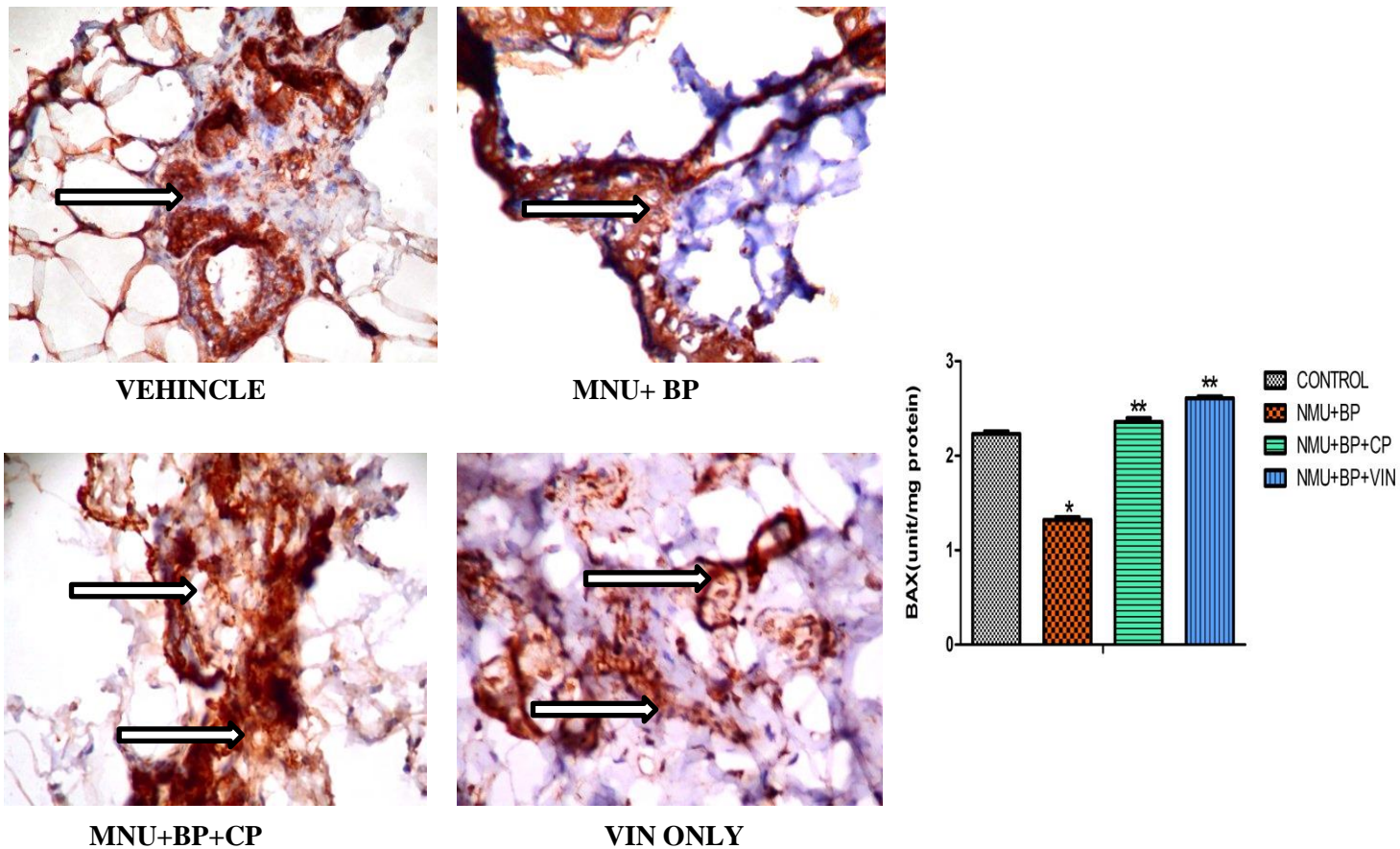


Figure 4.128: Effect of chloroform fraction of *C. portoricensis* (CP) on Bcl-2 Associated X-protein (BAX) activity in MNU and BP-treated rats. MNU= *N*-nitroso-*N*-methylurea; BP= Benzo[a]pyrene; CP= *C. portoricensis* (100 mg/kg); VIN= Vincasar. * = less than .05 in contrast to vehicle. ** = less than .05 in contrast to untreated group. Values (mean±SDev) are based on 5-8 rats per group. The white arrows showing expression of BAX.

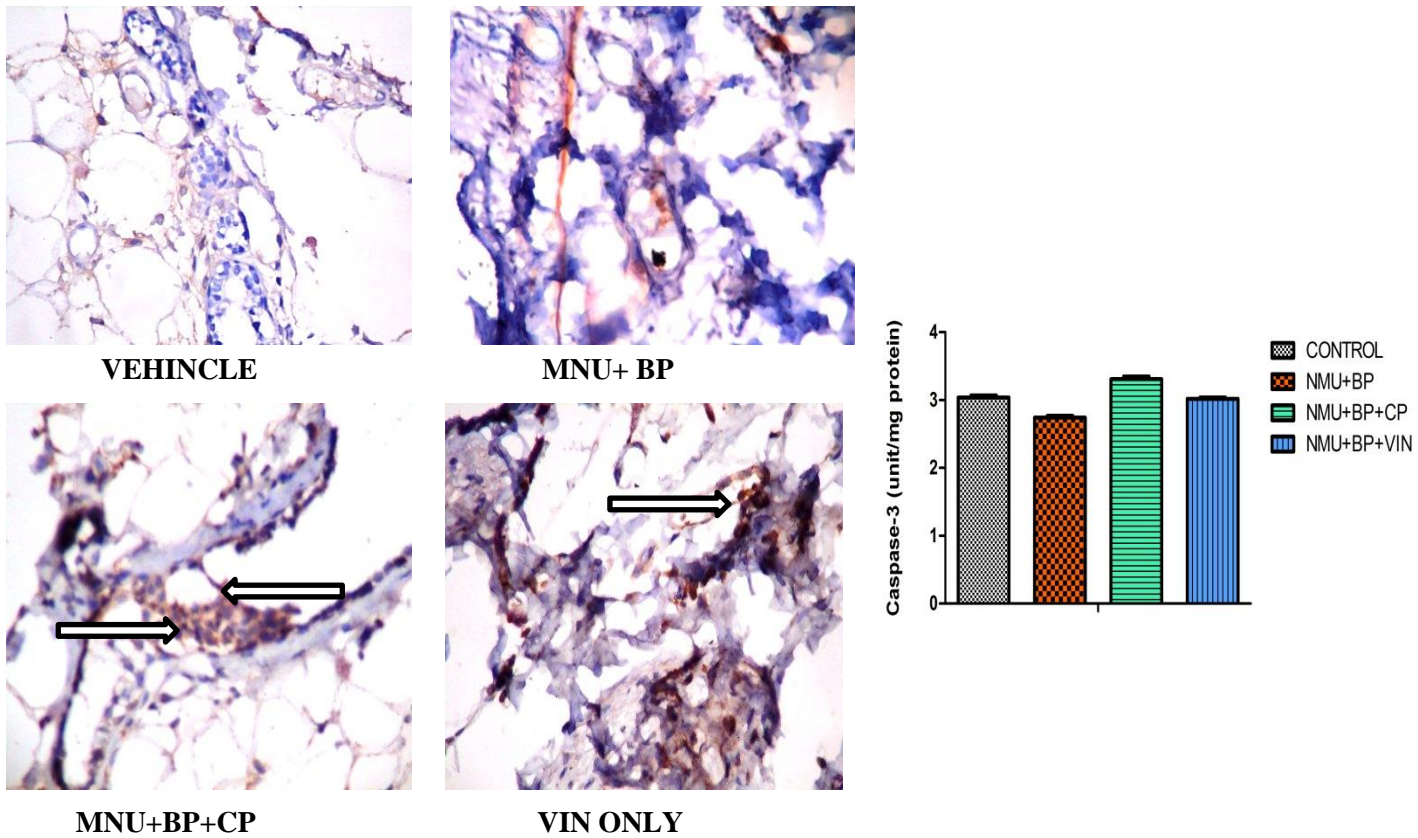
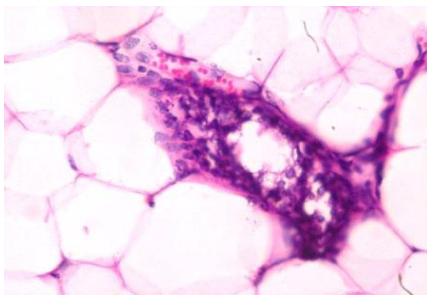
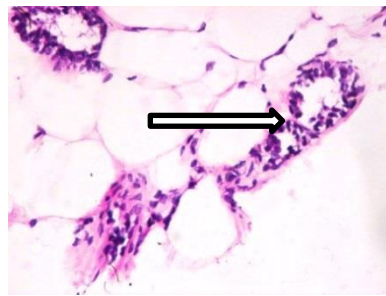


Figure 4.129: Effect of chloroform fraction of *C. portoricensis* (CP) on Caspase-3 activity in MNU and BP-treated rats. MNU= *N*-nitroso-*N*-methylurea; BP= Benzo[a]pyrene; CP= *C. portoricensis* (100 mg/kg); VIN= Vincasar. Values (mean±SDev) are based on 5-8 rats per group. The white arrows showing expression of caspase-3.

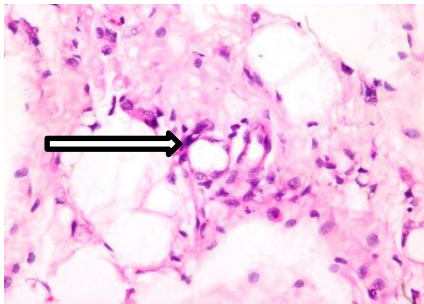
The mass tumor was identified in both the mammary gland and the neck tissue, as shown by malignant cells and pyknotic nuclei with a high nucleocytoplasmic ratio in the mammary gland (Figure 4.129). After 10 weeks of MNU and BP-treatment, the presence of mammary tumor accompanied by neck metastasis evidenced by massive neck tumor was confirmed by histological evaluation (Figure 4.130). In addition, the neck tissue showed severe metastatic cancer of the mammary glandular tissues (Figure 4.131 and figure 4.132). However, 2 weeks post treatment with chloroform fraction of CP reversed the tumorigenic effects of MNU and BP treatment.



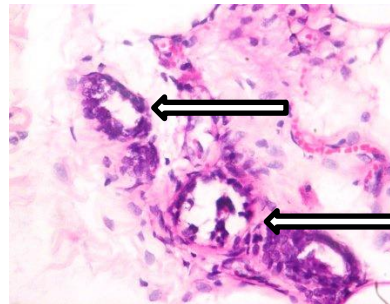
VEHICLE



MNU+ BP

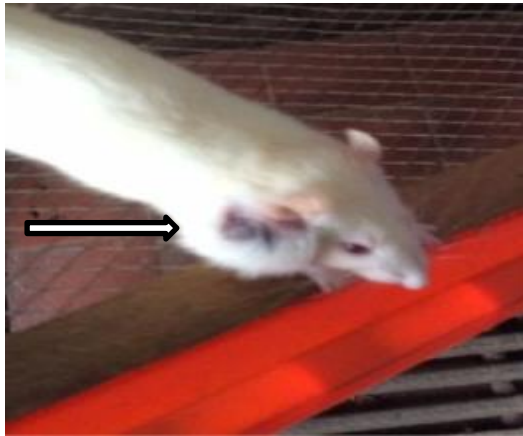


MNU+BP+CP

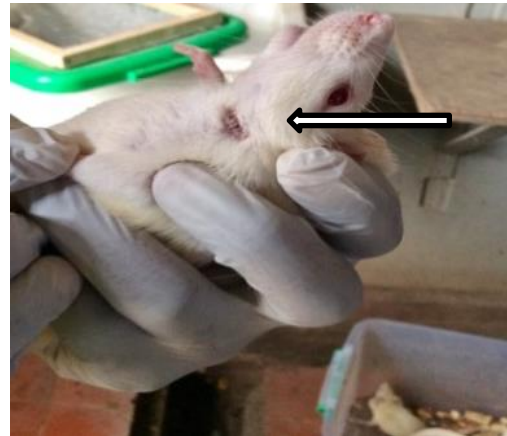


VIN ONLY

Figure 4.130: Photomicrograph of mammary gland tissues in MNU and BP rats given chloroform fraction of *C. portoricensis* (M X 400). MNU= *N-nitroso-N-methylurea*; BP= Benzo[a]pyrene; CP= *C. portoricensis* (100 mg/kg); VIN= Vincasar.



BEFORE CP



AFTER

Figure 4.131: Pictorial section of experimental animal bearing neck tumor before and after CP treatment.

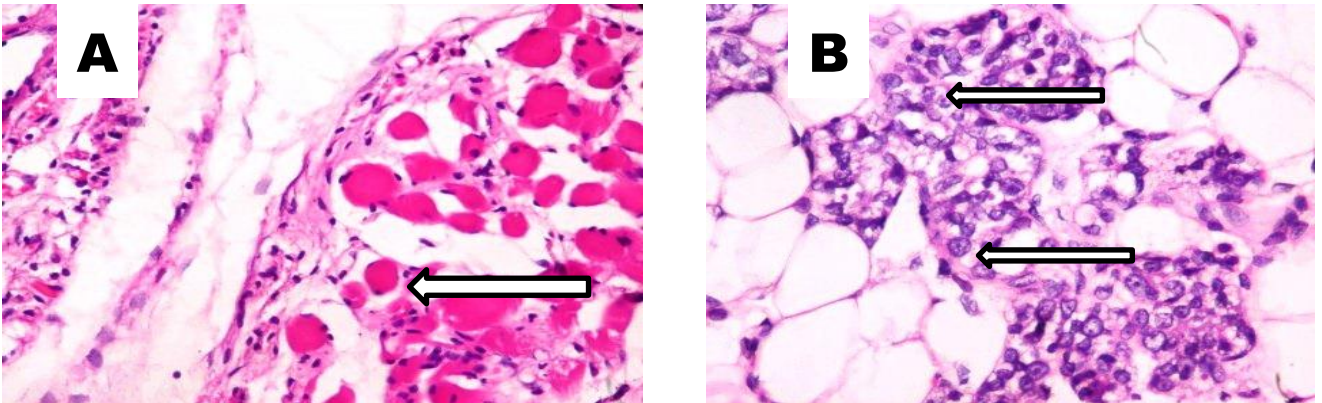
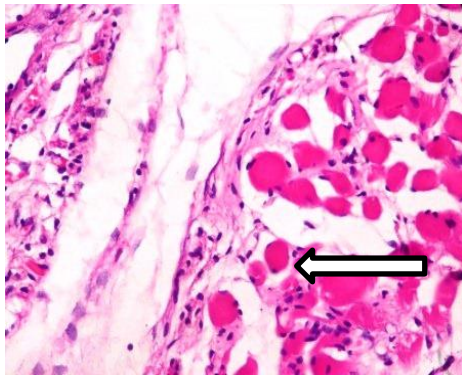
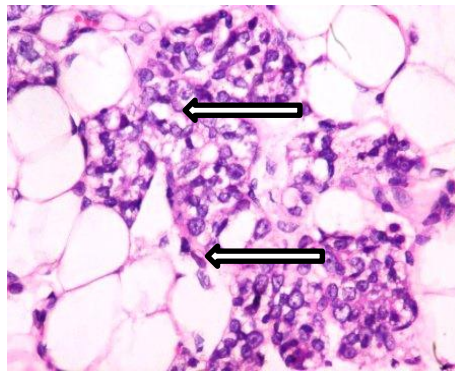


Figure 4.132: A - Photomicrograph of a neck tissue section stained with Haematoxylin and Eosin showing normal skin and muscularis tissues (white arrow) as well as normal adipose tissues.

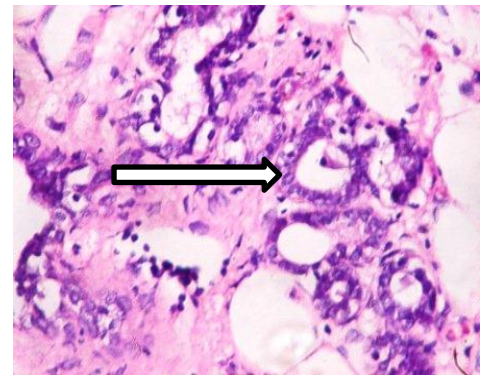
B - Photomicrograph of a Neck tissue section stained by Haematoxylin and Eosin showing severe metastatic cancerous mammary glandular tissues (white arrow).



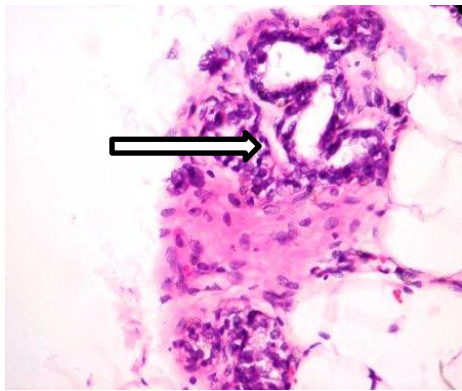
VEHICLE



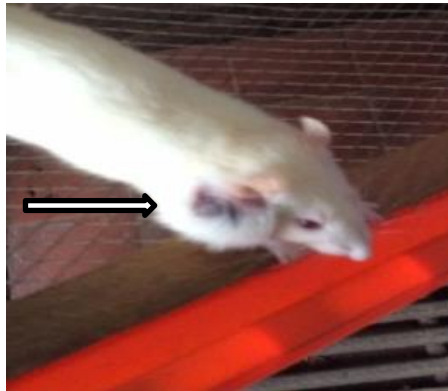
MNU+ BP



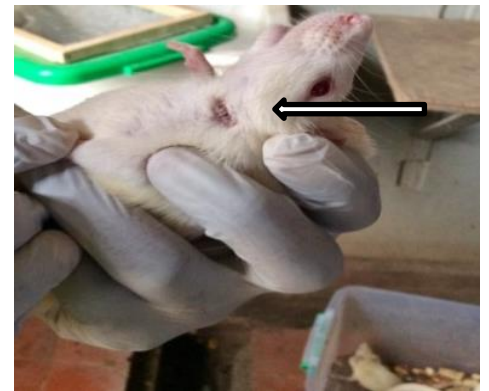
MNU+BP+CP



MNU+BP+VIN



BEFORE CP



AFTER CP

Figure 4.133: Photomicrograph of neck tumor in MNU and BP rats given chloroform fraction of CP (M X 400). MNU= *N*-nitroso-*N*-methylurea; BP= Benzo[a]pyrene; CP= *C. portoricensis* (100 mg/kg); VIN= Vincasar.

CHAPTER FIVE

5.1 DISCUSSION

Several studies have documented increased mortality rate due to BC (Rafieian-kopaei *et al.*, 2017). However, researchers have made progress in developing better options on effective and safer drugs towards cancer therapy (Brar *et al.*, 2018; Remani, 2019; Tai, 2020). Safer anticancer agents are ceaselessly being identified and evolved from natural plants which have been reported to be effective and less toxic. Plant extracts and phytoconstituents have been found to exhibit powerful anti-proliferative effects *in vitro* and *in vivo* studies (Harlev *et al.*, 2012; Pieme *et al.*, 2014; Etti *et al.*, 2017; Mate *et al.*, 2017; Jang *et al.*, 2019; Stephane *et al.*, 2019; Webb and Kukard, 2020). The effects of CP root bark formulations *in vitro* and in animals were studied to aid in the hunt for safer anticancer treatments. The CP has been reported to be used as a treatment for a variety of ailments. Using biochemical and immunohistochemical results, this study demonstrated that the root bark of CP possess anti-tumor effects against NMU and BP induced-mammary, uterine, and ovarine toxicities in experimental rats. The advancement of disease has been connected to a reduction in animal overall health as measured by body weight loss and death rate (Harguindey *et al.*, 2008). CP's capacity to restore body weight loss in the NMU and BP-treated groups demonstrated its protective impact. However, as compared to normal control rats, vincristine-treated animals had significantly lower body weights.

Protective effect of methanol extract of *Calliandra portoricensis* on serum parameters, antioxidants status, and hormone receptors in *N*-methyl-*N*-nitrosourea-administered rats.

The CP methanolic root extract reduced NMU-induced cell damage in the breast, uterus, as well as ovary of experimental animals, according to this study. This study showed a relationship between NMU administration and oxidative stress (Oishi *et al.*, 2017). Excess supply of oxidants, as well as weakening of the antioxidant defense system,

leads to an imbalance between pro-oxidants and antioxidants, resulting in oxidative stress. (Adaramoye *et al.*, 2016; Ou-yang *et al.*, 2019). However, because every molecule returns to its reduced state upon oxidation, a standard quantity of ROS is required for normal cellular activities (Scheibmeir *et al.*, 2005; Alehaideb *et al.*, 2020). Following administration of NMU in experimental rats, excessive generation of ROS ensued especially in female reproductive organs, this may be link to fertility problem (Knickle *et al.*, 2018; Alehaideb *et al.*, 2020) . NMU administration led to a significant increase in MDA levels in the breast, uterine, and ovarian tissues, as well as a decrease in the activities of SOD, CAT, TSH, and GSH. The fall in enzymatic and non-enzymatic antioxidant defense system as well as elevation in malondialdehyde levels is a clear testimony of oxidative stress which further corroborates previous findings on NMU-induced carcinogenesis (Pugalendhi *et al.*, 2011; Choi *et al.*, 2014) . GST and GPx activities were also severely damaged as a result of NMU administration. Treatment with CP, on the other hand, resulted in a considerable restoration of the oxidative stress indicators. Interestingly, with larger doses of CP, the markers of oxidative stress, particularly CAT and SOD activity, worsened, although GSH and TSH levels significantly improved in a dose-dependent manner, this is probably due to depletion in SOD and CAT activities as the first line defense antioxidant enzymes against the attacks of the generated free radicals. Furthermore, mammary, uterine and ovarian MPO and NO was elevated in NMU-administered groups. CP was found to drastically decrease MPO levels in mammary, uterine, and ovarian tissues at various doses, with no significant changes in uterine or ovarian NO levels.

In 90% of BCs, receptors for estrogen, progesterone , and epidermal growth factor are expressed (Rahman *et al.*, 2016; Burton *et al.*, 2019). In the same manner, estrogen, progesterone and prolactin are importantly involved in mammary gland development (You *et al.*, 2017; Silihe *et al.*, 2017). The expression of progesterone receptor and estrogen receptor requires certain amount of estrogen for its activations, thus, separating the effects of these hormones from its receptors will be difficult (Goss, 2014; Eaton *et al.*, 1999). The results show that receptors for estrogen, progesterone receptor, and epidermal growth factor receptor 2 activities are elevated in NMU groups, whereas CP treatments at all doses dramatically down-regulated estrogen receptor, progesterone receptor, and epidermal growth factor receptor activities across CP and vincristine treated groups.

Assessment of the most potent fraction of root bark of *Calliandra portoricensis* in vitro using antioxidants methods.

Free radical accumulation has been linked to diseases such as cancer, diabetes, heart disease, and neurological problems in several studies. At high concentrations, however, free radicals can be hazardous to the body and damage all major components of cells, including DNA, proteins, and cell membranes. The damage to cells caused by free radicals, especially the damage to DNA, may play a role in the development of cancer and other health conditions (Harguindey *et al.*, 2008; Lewis *et al.*, 2010; Naskar *et al.*, 2011; Seo and Park, 2020). A free radical is defined as an atom of unstable or unpaired electron. This unstable radical can be stabilized by pairing with electrons from biological macromolecules such as lipids, DNA, and proteins thereby resulting to damage of these macromolecules (Lin *et al.*, 2020; Lin *et al.*, 2015). This free radical cell damage is achievable when the cellular antioxidant defence system is weakened. Generally, all biological system is endowed with innate antioxidant defence mechanisms that protects the cells from free radical attack and remove damaged molecules. However, these mechanisms can be ineffective as a result of frequent assaults by free radicals (Naskar *et al.*, 2011; Rahman *et al.*, 2015).

Antioxidants are known to prevent free radical attacks and preserve damaged cells by supplying electrons to free radical violated cells (Etti *et al.*, 2017). Antioxidants not only protect cells from free radical damage, but they also convert excessive radicals into scrapage and thereafter ejected from the system. The major antioxidant enzymes directly involved in the neutralization of excess free radicals in the body are: superoxide dismutase, catalase, glutathione peroxidase and glutathione reductase (Taylor *et al.*, 2010). The free radicals steal electrons from the antioxidant molecules in order to complete their electron complement, which causes those molecules to suffer damage. They serve as a natural "off" switch for the free radicals by making this sacrifice (Rahman *et al.*, 2015). However, non-enzymatic antioxidants function by halting the chain reactions of these free radicals. Several non-enzymatic antioxidants include glutathione, vitamin C, vitamin e, plant polyphenols, and carotenoids among others.

The DPPH antioxidative approach is extensively used to assess the antioxidant capacity of medicinal plants (Balasundram, 2006). By adding the extract in a concentration-dependent way, the violet purple color in the DPPH assay is decreased to yellow color

diphenylpicryl hydrazine (Kedare and Singh, 2011; Kehinde *et al.*, 2016). Because of the short time involved in the analysis, this approach has been widely utilized to examine antioxidant activity (Aslan *et al.*, 2013; Otto and Sicinski, 2017). Tables 3 and 4 demonstrate that when catechin was compared to the six CP extracts tested for antioxidative capacities, the chloroform fraction of CP had the strongest DPPH antioxidative activity, mopping up DPPH radical in a concentration-dependent manner. Similarly, when comparing standard and chloroform fractions of CP, the chloroform fraction of CP showed the strongest reducing activity in scavenging ABTS cation radical in a concentration-dependent way. As a result, the chloroform fraction of CP displayed similar antioxidative activity when compared to standard catechin. The ability of CP extracts to mop up free radicals is most likely related to their hydrogen donating ability (Donaires, 2015; Saraiva *et al.*, 2020).

Chemopreventive effects of chloroform extract of *Calliandra portoricensis* on serum biochemicals, hormone profiles, antioxidants status, apoptotic, and inflammatory biomarkers in *N*-methyl-*N*-nitrosourea and benzo(a)pyrene-induced rats.

The potential proliferation associated with NMU-induced mammary gland tumours using BP as a promoter in regular mammary gland tissue was also investigated. Findings from this study showed that animals receiving NMU and BP exhibited significant reductions in body weight gain. However, chloroform fraction of CP at a low dose showed progressive weight gain, which implies that CP improves and supports positive energy metabolism. Conversely, mammary gland tumours may interfere with the coordinated metabolic network in the animal, resulting in rapid weight loss and tissue wasting evidenced by the organo-somatic weight differences of the mammary tissue as well as in vincristine treated-rats (Glory and Thiruvengadam, 2012; Bishayee *et al.*, 2016; Kubatka *et al.*, 2019). MDA is commonly used to assess the amount of free radical-induced lipid peroxidation. Results from this study revealed chloroform fraction of CP reduced the production of MDA in all the tissues (mammary, uterus and ovary) of the experimental animals. These data further supports and stipulates the antioxidant capacity of chloroform fraction of CP in rats carcinoma. The drastic elevation in malondialdehyde levels in all the tissues result into complementary reduction in enzymatic and non-enzymatic defense mechanism which further corroborates previous reports (Length, 2012; You *et al.*, 2017). Precisely, drastic depletion in catalase, reduced glutathione, total sulphhydryl, superoxide dismutase, glutathione peroxidase and

glutathione-S-transferase activities was detected in NMU and BP-administered rats in all the tissues indicating a compromised antioxidant defense system.

BC is assumed to be caused by chronic inflammation, which has long been thought to have a role in the initiation and development of the disease. (Balkwill and Mantovani, 2001; Visser *et al.*, 2005; Calogero *et al.*, 2007; Schetter *et al.*, 2010). Numerous studies show a link between BC, inflammation, and infertility. (Donaires, 2015; Pei *et al.*, 2015). Inflammation is frequently linked to the onset and spread of cancer. Inflammations is known to recruit immune cells which release cytokines and chemokines to the site of inflammation (Coussens and Werb, 2002; Visser *et al.*, 2005). Furthermore, tumours may facilitates components of inflammatory process to stimulate angiogenesis, inhibit apoptosis, and promote proliferation and metastasis (Balkwill and Mantovani, 2001; Naskar *et al.*, 2011). Results from this study demonstrates elevation in nitric oxide, malondialdehyde, and myeloperoxidase activity in NMU and BP-treated groups. Similarly, interleukins (IL-1beta and IL-6) were drastically upregulated in groups treated with NMU and BP. This corroborate Donaires, (2015) and Manral *et al.*, (2016), reports who found that interleukin overexpression promotes cancerous characteristics in Notch-3 generating progenitor cells from human ductal BC and normal mammary tissue. In addition, cells that are genomically altered and harmful to the body can be eliminated through apoptosis.

Generally, it has been documented that too little apoptosis or too much apoptosis could impose a high threat to cells resulting into cancer and neurodegeneration (Harguindey *et al.*, 2008; Schetter *et al.*, 2010; Seo and Park, 2020). The results form this study showed depletion in apoptotic activities evidenced by down-regulation in BAX, Caspases-3, -9, and p53 in NMU and BP exposed groups. In the NMU and BP-administered groups, however, there was an increase in BCL-2 expression. Similarly, drastic over expression in β -catenin activity as well as up regulation in COX-2, and iNOS activities was seen in NMU and BP-treated groups. Mandal *et al.*, (2017) discovered that cyclooxygenase-2 is involved in tumorigenesis and apoptosis in human cancers, and these data back up their findings. Co-treatment with chloroform fraction of CP intrestingly ameilorated NMU and BP altered apoptotic and inflammatory activites in the experimental animals.

BC has been connected to a variety of etiological factors, including hormonal factors, family history, lactation, and obesity, among others (Younglai *et al.*, 2005; Troisi *et al.*,

2007). However, many of these established risk factors are associated to hormones most importantly estrogens (Akingbemi and Hardy, 2001; Giwercman, 2011). Early menarche as well as late menopause in women have been reported to expose the body to estrogen for longer periods of time, increasing the risk of developing BC (Arntzen *et al.*, 1998; Vatten *et al.*, 2002). The importance of a high concentration of endogenous estradiol in BC incidence has also been highlighted by growing evidence, it shows the link between a woman's BC risk and the levels of estrogen and progesterone produced by her ovaries (Yin *et al.*, 2019). In the NMU and BP-treated groups, we found elevated amounts of prolactin, progesterone, follicle stimulating hormones, and lutenizing hormones in the ovarian, uterine, and mammary glands. This findings further corroborates reports by Fowler *et al.*, (2012) and Hauser *et al.*, (2015). Whereas, co-treatment with CP interestingly mitigated NMU and BP altered sex hormones levels.

Further research on the root bark of the chloroform fraction of CP shows for the first time that CP has a notable prospective curative effect in a chemically-induced mammary tumorigenesis model, as well as in BC cells *in vitro*. Our findings show that daily oral intake of CP can drastically slow the progression of mammary tumors in rats. When compared to a negative control group, consuming CP daily for two weeks reduced breast tumor incidence, neck metastasis, and burden, as demonstrated by a reduction in the number of tumors in animals having tumors, as well as tumor volume and weight (NMU and BP). You *et al.*, (2017); Lin *et al.*, (2017) and Tuli *et al.*, (2019) found that neem oil was cytotoxic to BC cells and prevented dimethylbenz(a)anthracene-induced BC in high-fat/sucrose-fed *Wistar* rats. Furthermore, we observed a slight increase in liver toxicity parameters (ALT, AST and T-BIL levels) in groups induced with NMU and BP compared to control groups and subsequently restored near control level upon post-treatment with CP. These results corroborates previous findings by Adaramoye *et al.*, (2017) and clearly indicates chloroform fraction of CP restored and protects liver integrity .

Anti-proliferative, antioxidative, and apoptotic effects of chloroform fraction of *Calliandra portoricensis* on MCF-7 cell line and cell lysates.

Given that CP (chloroform fraction) co-treatment effectively reduced NMU and BP-induced tumor development and accession of various proliferative and pro-apoptotic proteins in an *in vivo* tumor investigation, the anti-proliferative impact of CP on human

ER-positive breast adenocarcinoma (MCF-7) cells was presented in Table 9. The findings revealed that exposing BC cells to CP for 72 hours inhibited their proliferation in a dose-dependent way. The apoptosis of BC cells was considerably boosted after treatment with 100 µg/ml CP. This suggests that receptors for estrogen play a role in CP's cytotoxicity-inducing mechanism. When compared to Control, the cell viability and survival rate at 100 µg/ml CP was fully reduced by 87.5%, equal to the standard treatment Vincristine (87.6%), implying that CP inhibit BC cell growth by triggering apoptosis (Table 9). As a result, apoptosis induction is considered as a strategy for cancer control. We also found that CP inhibits IL-1beta production as well as oxidative stress indicators MPO and LPO, along with activation of anti-oxidant proteins and apoptotic activity. SOD, CAT; BAX, caspase-3, -9 activities *in vitro* using MCF-7 cell lysate. These results further supports our previous findings from *in vivo* study.

Curative effects of chloroform fraction of *Calliandra portoricensis* on antioxidant parameters, apoptotic, and inflammatory indices in *N*-methyl-*N*-nitrosourea and benzo(a)pyrene-induced rats

Findings from this study revealed that one of the possible mechanisms of anti-tumorigenic and anti-proliferative action of CP chloroform fraction *in vivo* and *in vitro* is reducing activities of generated free radicals. Exposure to chemical carcinogens such as *N*-methyl-*N*-nitrosourea and 7,12-dimethylbenz(a)thracene produces free radicals, or reactive oxygen species, according to numerous studies (Kedare and Singh, 2011; Pe *et al.*, 2012; Opdahl *et al.*, 2012). As a result, maintaining a balance between oxidants and antioxidants is critical for appropriate body system physiological performance. When the body's ability to regulate free radicals is overwhelmed, a situation known as oxidative stress develops. As a result, free radicals may be able to permeate lipids, proteins, or DNA, causing a wide range of human diseases, such as cancer (Lobo *et al.*, 2010; Farombi and Owoeye, 2011). On this point, the antioxidant potential of CP's chloroform fraction was assessed using two methods: (1) SOD, GPx, GSH, TSH, GST, and CAT (antioxidant enzyme activities); and (2) MDA, MPO, NO, and LPO (biochemicals). Following NMU and BP treatment, there was a considerable drop in the enzyme activity of SOD, GST, and CAT, as well as a modest decrease in the activity of GPx, GSH, and TSH levels in the mammary tissues. The enzymatic activation was completely induced after treatment with chloroform fraction of CP, just as it was in the control group and with the standard drug. Also, NMU and BP significantly increased

MDA, MPO and NO levels both in the serum and mammary tissues but these increases were completely blocked by post treatment with CP. These results indicate a strong capacity of chloroform fraction of CP on anti-oxidative stress, which further corroborates with previous reports by Adaramoye *et al.*, (2017).

The disruption of homeostatic molecular signaling pathways by carcinogens resulting into tumour formation due to physiological alterations in the cells is known as tumorigenesis (Zhou *et al.*, 2014; Li *et al.*, 2019). According to Siegel and colleagues, NMU and BP administration generates severe oxidative stress in the mammary gland, which triggers the release of a number of transcriptional regulators and enhances the production of genes involved in cell proliferation, induce apoptosis, and infiltration (Ouyang *et al.*, 2012). NF- κ B is a transcription factor that is activated in response to a range of stimuli (Lang *et al.*, 2007; Perkins and Barre, 2007; Shah *et al.*, 2014). When NF- κ B is activated, genes involved in cell death resistance, cell growth and longevity, vasculature, invasion, and inflammation are produced, all of which contribute to tumor formation. (Letai, 2016; Kowalczyk *et al.*, 2019; Song *et al.*, 2020). NF- κ B activity is stimulated in ER-negative BC, according to several investigations (Rayet and Ge, 1999; Li *et al.*, 2012). In our current findings, we demonstrated significant reduction in NF- κ B expression in the tumor of chloroform fraction of CP treated rats. This is in consistent with previous report by Mandal and Bishayee, (2015). Furthermore, NMU and BP drastically down-regulates BAX, p53, and caspase-3 activities after inducing mammary gland tumors.

The down-regulated expression of these proteins was shown to be normalized after treatment with CP (chloroform fraction). In a number of studies, iNOS has been linked to a worse prognosis in women with BC by increasing tumor aggressivity, and it has also been linked to the origin of malignancy. Overexpression of iNOS has thus been discovered in a variety of cancers. iNOS overexpression, on the other hand, was detected in roughly 15% of affected individuals, and since then has become a key indicator of chemoresistance and short survival in women with BC (Zhou *et al.*, 2014). The aberrant activation of the iNOS and NF- κ B pathways is connected to tumorigenesis, medication resistance, and carcinoma development (Cao and Karin, 2003). Our findings from this study showed that post-treatment with CP completely down-regulated iNOS expression. The high quantities of anthocyanin and polyphenols in CP extract likely

contributed to these decreases probably through cancer cell removal by modification of signaling pathways, inhibition of cell cycle events, and apoptosis induction. Polyphenols also regulate the activities of enzymes involved in tumor cell proliferation (Rahman *et al.*, 2015). Our findings imply that CP has anti-inflammatory properties in BC models.

A mammary gland tumor tissue histological analysis revealed severe cancerous epithelium with piknotic nucleus and dense nucleocytoplasm. The uterus exhibited a highly infiltrated endometrial gland with inflamed stroma cells in the NMU and BP-treated groups, while the ovarian cyto-structure revealed stiff ovarian tissue as well as arterial constriction with degraded cells. However, treatments with chloroform fraction of CP mitigated and reversed the carcinogenic effect of both NMU and BP. The histopathological findings further corroborate the biochemical data and previous findings.

CHAPTER SIX

SUMMARY, CONCLUSION AND RECOMMENDATIONS

6.1 SUMMARY

It can be deduced from the sequence of experiments conducted in this study that:

1. Administration of methanol crude extract of CP reduces inflammation and oxidative stress caused by *N-nitroso-N-methylurea*. Data from this study suggests methanol crude extract of CP at all doses attenuated estrogen receptor, progesterone receptor and epidermal growth factor receptor-2 activities in a dose-dependent manner.
2. The chloroform fraction of CP exhibited the best capacity to neutralize ABTS and DPPH radicals when compared to other extracts. CP extracts, according to the research, exhibit proton-donating characteristics that could work as free radical inhibitors or scavengers, possibly acting as primary antioxidants.
3. Co-administration of chloroform fraction of CP restored the altered antioxidant status, up-regulated pro-apoptotic proteins, down-regulated inflammatory markers and reproductive hormones respectively in MNU and BP-groups.
4. Chloroform fraction of CP inhibited cell viability and survival rate at 100 µg/ml CP by 87.5% similar to standard drug Vincasar.

5. Post-treatment with chloroform fraction of CP completely induced the enzymatic activation, attenuated liver marker enzymes similar to vehicle and standard drug in MNU and BP-administered rats.
6. Following CP treatment, MNU and BP-induced tumor development and expression of various pro-proliferative and anti-apoptotic proteins were considerably reduced.

6.2 CONCLUSION

Conclusively, administration of *N*-nitrosourea-*N*-methyl and benzo(a)pyrene caused depletion in antioxidant status, and apoptotic proteins; elevated hormones, inflammatory indices, and hormone receptors as well as causing disruption of cytoarchitecture of the mammary, ovary and uterus tissues. However, CP extracts protect the mammary gland, uterus and ovary evidenced by decrease in reproductive hormones and its receptors activities, down-regulated inflammatory markers, elevated antioxidants activities as well as induction of apoptosis.

6.3 RECOMMENDATIONS

I hereby recommend from this findings that:

1. Early diagnosis of breast cancer should be encouraged as early detection and treatment could halt progression.
2. Traditionally, *C. portoricensis* can be processed as herbal mixture for managing breast diseases and other related diseases.
3. The active compound responsible for anti-proliferative effect of *C. portoricensis* should be investigated.

6.4 CONTRIBUTIONS TO KNOWLEDGE

1. The findings from this study added to the scientific knowledge by confirming the protective effects of *C. portoricensis* in animal studies and *in vitro* models.
2. Free radical scavenging activity revealed that chloroform fraction of CP as the most potent with highest reducing potential by scavenging DPPH and ABTS cation radical in a concentration-dependent manner.
3. The chloroform fraction of CP inhibits anti-apoptotic proteins, inflammatory markers, oxidative stress, and reproductive hormones, as well as activating pro-apoptotic proteins, chemopreventing MNU and BP-induced carcinogenesis.

4. The CP may be used to manage mammary, uterine and ovarian toxicity.
5. Co-administration of MNU and BP showed severe metastatic cancerous mammary glandular tissues, a model that may be useful in cancer biology.
6. A first-of-its-kind finding is that posttreatment with CP mitigates the damaging effects of MNU and BP-induced tumorigenesis in experimental animals.

REFERENCES

- Acosta-casique, A., Rodríguez-rodríguez, S., Moreno, D. A., Ferreres, F., Flores-zg4c3alonso, J. C., Delgado-lópez, M. G., Pérez-santos, M., & Anaya-ruiz, M. 2018. *Bursera copallifera* Extracts Have Cytotoxic and Migration-Inhibitory Effects in Breast Cancer Cell Lines. *Integrative Cancer Therapies* 17(3): 654-664. <https://doi.org/10.1177/1534735418766416>.
- Adaramoye, O. A., Kehinde, A. O., Adefisan, A., Adeyemi, O., Oyinlola, I., & Akanni, O. O. 2016. Ameliorative effects of kolaviron, a biflavonoid fraction from *Garcinia kola* seed, on hepato-renal toxicity of anti-tuberculosis drugs in wistar rats. *Tokai Journal of Experimental and Clinical Medicine*, 41(1).
- Adaramoye, O., Erguen, B., Nitzsche, B., Michael, H., Jung, K., & Rabien, A. 2017. Punicalagin , a polyphenol from pomegranate fruit , induces growth inhibition and apoptosis in human PC-3 and LNCaP cells. *Chemico-Biological Interactions* 274, 1–7. <https://doi.org/10.1016/j.cbi.2017.07.009>
- Adaramoye, O., Erguen, B., Oyebode, O., & Nitzsche, B. 2015. Antioxidant , antiangiogenic and antiproliferative activities of root methanol extract of *C. portoricensis* in human prostate cancer cells. *Journal of Integrative Medicine*, 13(3), 185–193.
- Adefisan, A., Owumi, S., & Adaramoye, O. 2019. Root bark extract of *C. portoricensis* (Jacq .) Benth . chemoprevents N - methyl- N -nitroso-urea-induced mammary

- gland toxicity in rats. *Journal of Ethnopharmacology*. 233, 22–33. <https://doi.org/10.1016/j.jep.2018.12.027>
- Agunu, A., Abdurahman, E. M., Shok, M., & Yusuf, S. A. 2005. Analgesic activity of the roots and leaves extracts of *C. portoricensis*. *Fitoterapia*, 76(2257), 442–445. <https://doi.org/10.1016/j.fitote.2005.03.008>
- Aguwa, C. N., & Lawal, A. M. 1988. Pharmacologic studies on the active principles of *Calliandra portoticensis* leaf extracts. *Journal of Ethnopharmacology*. 22(1):63–71. doi: 10.1016/0378-8741(88)90231-0. PMID: 3352286.
- Akingbemi, B. T., & Hardy, M. P. 2001. Oestrogenic and antiandrogenic chemicals in the environment : effects on male reproductive health. 391–403.
- Akram, M., Iqbal, M., Daniyal, M., & Khan, A. U. 2017. Awareness and current knowledge of BC. *Biological Research*, 1–23. <https://doi.org/10.1186/s40659-017-0140-9>
- Al-Hajj, M., Wicha, M. S., Benito-Hernandez, A., Morrison, S. J., & Clarke, M. F. 2003. Prospective identification of tumorigenic breast cancer cells. *Proceedings of the National Academy of Sciences of the United States of America*, 100(7), 3983–3988. <https://doi.org/10.1073/pnas.0530291100>
- Alehaideb, Z., Alghamdi, S., Yahya, W. Bin, Al-eidi, H., Alharbi, M., Alaujan, M., Albaz, A., Tukruni, M., Nehdi, A., Abdulla, M., & Matou-nasri, S. 2020. Anti-Proliferative and Pro-Apoptotic Effects of *Calligonum comosum* (L ’ Her .) Methanolic Extract in Human Triple-Negative MDA-MB-231 Breast Cancer Cells. *Journal of Evidence-Based Integrative Medicine*, 25, 1–13. <https://doi.org/10.1177/2515690X20978391>
- Amujoyegbe, O. O., Agbedahunsi, J. M., & AkaMNU, M. A. 2014. Antisickling Properties of Two *Calliandra* Species : *C . portoricensis* and *C . haematocephala* (Fabaceae). *European Journal of Medicinal Plants*, 4(2), 206–219.
- Anderson, K. N., Schwab, R. B., & Martinez, M. E. 2014. Reproductive risk factors and BC subtypes : a review of the literature. *Breast Cancer Research and Treatment*, 144(1): 1–10. <https://doi.org/10.1007/s10549-014-2852-7>

- Arntzen, K. J., Kjollesdal, A. M., Halgunset, J., & Vatten, L. 1998. TNF , IL-1 , IL-6 , IL-8 and soluble TNF receptors in relation to chorioamnionitis and premature labor. *Journal of Perinatal Medicine*, 26(1): 17–26.
- Arzi, L., Hoshyar, R., Jafarzadeh, N., & Riazi, G. 2020. Anti-metastatic properties of a potent herbal combination in cell and mice models of triple negative breast cancer. *Life Sciences*, 243, 117245. <https://doi.org/10.1016/j.lfs.2019.117245>
- Aslan, Z., Kolay, E., & Ag, Y. 2013. Free radical scavenging activity , total phenolic content , total antioxidant status , and total oxidant status of endemic *Thermopsis turcica*. *Saudi Journal of Biological Sciences*, 235–239. <https://doi.org/10.1016/j.sjbs.2013.02.003>
- Attari, F., Arefian, E., Keighobadi, F., Abdollahi, M., & Farimani, M. M. 2020. Inhibitory effect of flavonoid xanthomicrol on triple-negative breast tumor via regulation of cancer-associated microRNAs. *Physiotherapy Research*, 1–16. <https://doi.org/10.1002/ptr.6940>
- Bagheri, M., Fazli, M., Saeednia, S., Kor, A., & Ahmadiankia, N. 2018. Pomegranate peel extract inhibits expression of β -catenin, epithelial mesenchymal transition, and metastasis in triple negative breast cancer cells. *Cellular and Molecular Biology*. 64(7), 86–91. <https://doi.org/10.14715/cmb/2018.64.7.15>
- Balasundram, N. 2006. Food Chemistry Phenolic compounds in plants and agri-industrial by-products : Antioxidant activity , occurrence , and potential uses. *Journal of Food Chemistry*, 99, 191–203. <https://doi.org/10.1016/j.foodchem.2005.07.042>
- Balkwill, F., & Mantovani, A. 2001. Inflammation and cancer : back to Virchow ? *The Lancet*, 357, 539–545.
- Benson, J. R., & Jatoi, I. 2012. The global breast cancer burden. *Future Oncology*. 8(6):697-702. doi: 10.2217/fon.12.61. PMID: 22764767.
- Béranger, R., Hoffmann, P., Christin-maitre, S., & Bonnetterre, V. 2012. Occupational exposures to chemicals as a possible etiology in premature ovarian failure : A critical analysis of the literature. *Reproductive Toxicology*, 33(3), 269–279. <https://doi.org/10.1016/j.reprotox.2012.01.002>

- Bhardwaj, J. K. 2015. Influence of Toxic Chemicals on Female Reproduction : A Review Cell Biology : Research & Therapy Influence of Toxic Chemicals on Female Reproduction : A Review. *Cell Biology Research and Therapy*. <https://doi.org/10.4172/2324-9293.1000110>
- Borges, K., Rocha, F., & I, C. N. O. 2019. Effect of Arrabidaea chica extract against chemically induced BC in animal model 1. *Acta Cirurgica Brasileira*, 34(10).
- Borkovic, S., Krizmanic, I., & Gavric, J. 2017. Comparative study of oxidative stress parameters and acetylcholinesterase activity in the liver of Pelophylax esculentus complex frogs. *Saudi Journal of Biological Sciences*. 51–58. <https://doi.org/10.1016/j.sjbs.2015.09.003>
- Bowers, L. W., Lineberger, C. G., Ford, N. A., Rossi, E. L., Punjala, A., Camp, K. K., Kimler, B. K., Fabian, C. J., & Hursting, S. D. 2019. The flaxseed lignan secoisolariciresinol diglucoside decreases local inflammation , suppresses NFκB signaling , and inhibits mammary tumor growth. *Breast Cancer Research and Treatment*, 173(3), 545–557. <https://doi.org/10.1007/s10549-018-5021-6>
- Brar, J., Fultang, N., Askey, K., & Tettamanzi, M. C. 2018. Full Length Research Paper A novel anti-triple negative BC compound isolated from medicinal herb Myrothamnus flabellifolius. *Journal of Medicinal Plant Research*. 12(1), 7–14. <https://doi.org/10.5897/JMPR2017.6518>
- Bray, F., McCarron, P., & Parkin, D. M. 2004. The changing global patterns of female BC incidence and mortality. *Breast Cancer Research : Breast Cancer Research*, 6(6), 229–239. <https://doi.org/10.1186/bcr932>
- Burton, L. J., Hawsawi, O., Sweeney, J., Id, N. B., Hudson, T., & Id, V. O. 2019. CCAAT-displacement protein / cut homeobox transcription factor (CUX1) represses estrogen receptor-alpha (ER- α) in triple-negative BC cells and can be antagonized by muscadine grape skin extract (MSKE). *PLOS ONE*. 1–17.
- Calogero, R. A., Cordero, F., Forni, G., & Cavallo, F. 2007. Review Inflammation and BC Inflammatory component of mammary carcinogenesis in ErbB2 transgenic mice. *Breast Cancer Research*. 9(4):211. <https://doi.org/10.1186/bcr1745>
- Cao, Y., & Karin, M. 2003. NF- κ B in Mammary Gland Development and Breast

Cancer. *Journal of Mammary Gland Biology and Neoplasia* 8(2).

- Cedolini, C., Bertozzi, S., Londero, A. P., Bernardi, S., Seriau, L., Concina, S., Cattin, F., & Risaliti, A. 2014. Type of BC Diagnosis , Screening , and Survival. *Clinical Breast Cancer*, 14(4), 235–240. <https://doi.org/10.1016/j.clbc.2014.02.004>
- Chakravarthi, S., Thani, P. M., Low, D., Yang, W., Husin, L. T., & Lee, N. 2010. Role of immunohistochemistry and apoptosis as investigative tools in assessing the prognosis of patients with prostate tumours. *The American Journal of Pathology* 391–393. <https://doi.org/10.3892/etm>
- Choi, J., Psarommatis, B., Gao, Y. R., Zheng, Y., Handelsman, D. J., & Simanainen, U. 2014. The role of androgens in experimental rodent mammary carcinogenesis. *Breast Cancer Research*. 1–12.
- Coussens, L. M., & Werb, Z. 2002. Inflammation and cancer. *Nature*. 420(6917):860-7. doi: 10.1038/nature01322..
- Craig, Z. R., & Wang, W. 2011. Endocrine-disrupting chemicals in ovarian function: Effects on steroidogenesis, metabolism and nuclear receptor signaling. *Reproduction* 142(5): 633-646. <https://doi.org/10.1530/REP-11-0136>
- Crespo, E., Maci, M., N, M. M., Vives, F., Guerrero, J. M., & Acun, O. 2018. Melatonin inhibits expression of the inducible NO synthase II in liver and lung and prevents endotoxemia in lipopolysaccharide-induced multiple organ dysfunction syndrome in rats. *FASEB Journal* 13(12):1537-46.
- Dai, X., Yin, C., Zhang, Y., Guo, G., Zhao, C., & Wang, O. 2018. Osthole inhibits triple negative BC cells by suppressing STAT3. *Journal of Experimental and Clinical Cancer Research* 1–11.
- Dawnay, A. B. S., Hirstl, A. D., Perry, D. E., & Chambers, R. E. 1991. A critical assessment of current analytical methods for the routine assay of serum total protein and recommendations for their improvement. *Ann Clin Biochem*. 28 (Pt 6):556-67.556–567.
- De Coster, S., & Van Larebeke, N. 2012. Endocrine-disrupting chemicals: Associated disorders and mechanisms of action. *Journal of Environmental and Public Health*.

<https://doi.org/10.1155/2012/713696>

- Desantis, C., Ma, J., Bryan, L., & Jemal, A. 2014. Breast Cancer Statistics. <https://doi.org/10.3322/caac.21203>.
- Diamanti-Kandarakis, E., Bourguignon, J. P., Giudice, L. C., Hauser, R., Prins, G. S., Soto, A. M., Zoeller, R. T., & Gore, A. C. 2009. Endocrine-disrupting chemicals: An Endocrine Society scientific statement. *Endocrine Reviews*, 30(4), 293–342. <https://doi.org/10.1210/er.2009-0002>
- Diermeier-Daucher S., Ortman O., Buchholz S., Brockhoff G. 2012. Trifunctional antibody ertumaxomab Non-immunological effects on Her2 receptor activity and downstream signaling. *mAbs.*; 4:614–622. doi: 10.4161/mabs.21003.
- Dimitrios T. 2005. Methods of quantitative analysis of the nitric oxide metabolites nitrite and nitrate in human biological fluids. *Free Radical Research*, 39(8): 797–815.
- Donaires, R. 2015. Protective Effect of Piper aduncum Capsule on DMBA- induced breast cancer in Rats. *Breast Cancer (Auckl)* 9, 41–48. <https://doi.org/10.4137/BCBCR.S24420.RECEIVED>
- Eaton, N. E., Reeves, G. K., Appleby, P. N., & Key, T. J. 1999. Endogenous sex hormones and prostate cancer : a quantitative review of prospective studies. *Meta-Analysis* 80, 930–934.
- El-kaream, S. A. A. 2019. Biochemical and biophysical study of chemopreventive and chemotherapeutic anti-tumor potential of some Egyptian plant extracts. *Biochemistry and Biophysics Reports*, 100637. <https://doi.org/10.1016/j.bbrep.2019.100637>
- Elvis-offiah, U. B., Bafor, E. E., Eze, G. I., & Igbinumwen, O. 2016. *In vivo* investigation of female reproductive functions and parameters in nonpregnant mice models and mass spectrometric analysis of the methanol leaf extract of Emilia Coccinea (Sims) G Dons. *Physiological Reports*, 4, 1–17. <https://doi.org/10.14814/phy2.13047>
- Etten, V., & The, H. 2005. Cancer and ageing : a nexus at several levels. *Nature*

Review Cancer, 5(8) 4180–4185.

- Etti, I. C., Abdullah, R., Kadir, A., Hashim, M., Yeap, S. K., Imam, M. U., Ramli, F., Malami, I., Lam, K. L., Etti, U., Waziri, P., & Rahman, M. 2017. The molecular mechanism of the anticancer effect of Artonin E in MDA-MB 231 triple negative breast cancer cells. *PLOS ONE* 1–20.
- Farombi, E. O., & Owoeye, O. 2011. Antioxidative and Chemopreventive Properties of *Vernonia amygdalina* and *Garcinia biflavonoid*. *International research of Environmental and Public Health* 2533–2555. <https://doi.org/10.3390/ijerph8062533>
- Fatima, I., El-ayachi, I., Taotao, L., Lillo, M. A., Krutilina, R., Seagroves, N., Radaszkiewicz, T. W., Hutnan, M., Bryja, V., Krum, A., Rivas, F., & Miranda-carboni, G. A. 2017. The natural compound Jatrophone interferes with Wnt / β -catenin signaling and inhibits proliferation and EMT in human triple- negative breast cancer. 1–18.
- Faustino-rocha, A. I., Ferreira, R., Oliveira, P. A., Gama, A., Ginja, M., & Ferreira, R. 2015. N -Methyl- N -nitrosourea as a mammary carcinogenic agent. <https://doi.org/10.1007/s13277-015-3973-2>
- Fowler, P. A., Bellingham, M., Sinclair, K. D., Evans, N. P., Pocar, P., Fischer, B., Schaedlich, K., Schmidt, J., Amezaga, M. R., Bhattacharya, S., Rhind, S. M., & Shaughnessy, P. J. O. 2012. Molecular and Cellular Endocrinology Impact of endocrine-disrupting compounds (EDCs) on female reproductive health. *Molecular and Cellular Endocrinology*, 355(2), 231–239. <https://doi.org/10.1016/j.mce.2011.10.021>
- Gallego-ortega, S. R. O. D., & Ormandy, C. J. 2014. The mammary cellular hierarchy and breast cancer. *Journal of endocrine-related cancer* 4301–4324. <https://doi.org/10.1007/s00018-014-1674-4>
- Gaskins, A. J., & Mínguez-Alarcón, L. 2018. Female exposure to endocrine disrupting chemicals and fecundity. *Current Opinion in Obstetrics and Gynecology*, 29(4), 202–211. <https://doi.org/10.1097/GCO.0000000000000373>.Female
- Gbadamosi, I. T. 2012. Evaluation of Antibacterial Activity of Six Ethnobotanicals

- Used in the Treatment of Infectious Diseases in Nigeria. *Botany Research International*, 5(4), 83–89. <https://doi.org/10.5829/idosi.bri.2012.5.4.22>
- Giudice, L. C. 2004. Infertility and Environmental Chemicals — Is There a Connection? *Integrative Medicine*, 11–13.
- Giwercman, A. 2011. Estrogens and phytoestrogens in male infertility. *Current Opinion in Urology*, 2(26), 519-26 <https://doi.org/10.1097/MOU.0b013e32834b7e7c>
- Glory, M. D., & Thiruvengadam, D. 2012. Potential chemopreventive role of chrysin against N -nitrosodiethylamine-induced hepatocellular carcinoma in rats. *Biomedicine & Preventive Nutrition*, 2(2), 106–112. <https://doi.org/10.1016/j.bionut.2011.06.022>
- Goss, P. E. (2014). Mammary carcinoma model and its effects on the uterus. 133(1), 137–144. <https://doi.org/10.1007/s10549-011-1724-7>.Anti-tumor
- Gray, J. M., Rasanayagam, S., Engel, C., & Rizzo, J. 2017. State of the evidence 2017: an update on the connection between BC and the environment. *Environmental Health*, 1–61. <https://doi.org/10.1186/s12940-017-0287-4>
- Hamed, S., Zahra, J., Arash, S., Momeni, F., Mokhtari, M., Sadri, J., Majid, N., & Mirzaei, H. 2017.. BC diagnosis : Imaging techniques and biochemical markers. *Journal of Cellular Biochemistry* 118 (12).
- Harguindey, S., Orive, G., Arranz, J. L., & Anitua, E. 2008. An integral approach to the etiopathogenesis of human neurodegenerative diseases (HNDDs) and cancer . Possible therapeutic consequences within the frame of the trophic factor withdrawal syndrome (TFWS). *Neuropsychiatric Disease and Treatment* 4(6), 1073–1087.
- Harlev, E., Nevo, E., Lansky, E. P., Ofir, R., & Bishayee, A. 2012. Anticancer Potential of Aloes : Antioxidant , Antiproliferative , and Immunostimulatory Attributes. *Planta Medica* 78(9) 843–852.
- Hauser, R., Skakkebaek, N. E., Hass, U., Toppari, J., Juul, A., Andersson, A. M., Kortenkamp, A., Heindel, J. J., & Trasande, L. 2015. Male Reproductive

- Disorders , Diseases , and Costs of European Union. *The Journal of Clinical Endocrinology and Metabolism* 100(4) –1277. <https://doi.org/10.1210/jc.2014-4325>
- Hsu, R., Hsu, Y., Chen, S., Fu, C., Yu, J., Chang, F., Chen, Y., Liu, J., Ho, J., & Yu, C. 2015. The triterpenoids of *Hibiscus syriacus* induce apoptosis and inhibit cell migration in BC cells. *BMC Complimentary Medicine and Therapy*, 1–9. <https://doi.org/10.1186/s12906-015-0592-9>
- Hunt, P. A., Sathyanarayana, S., Fowler, P. A., & Trasande, L. 2016. Female Reproductive Disorders, Diseases, and Costs of Exposure to Endocrine Disrupting Chemicals in the European Union. *Journal of Clinical Endocrinology and Metabolism* 1562–1570. <https://doi.org/10.1210/jc.2015-2873>
- Huo, X., Chen, D., He, Y., Zhu, W., Zhou, W., & Zhang, J. 2015. Bisphenol-a and female infertility: A possible role of gene-environment interactions. *International Journal of Environmental Research and Public Health*, 12(9), 11101–11116. <https://doi.org/10.3390/ijerph120911101>
- Illiano, M., Sapio, L., Salzillo, A., Capasso, L., Caiafa, I., Chiosi, E., Spina, A., & Naviglio, S. 2018. Forskolin improves sensitivity to doxorubicin of triple negative BC cells via Protein Kinase A-mediated ERK1 / 2 inhibition. *Biochemical Pharmacology*, 152, 104–113. <https://doi.org/10.1016/j.bcp.2018.03.023>
- Jaglanian, A. 2020. Rosemary Extract Inhibits Proliferation , Survival , Akt , and mTOR Signaling in Triple-Negative BC Cells. *International Journal of Molecular Science* 21(3): 810.
- Jang, H., Ko, H., Song, K., & Kim, Y. S. 2019. A Sesquiterpenoid from *Farfarae Flos* Induces Apoptosis of MDA-MB-231 Human BC Cells through Inhibition of JAK – STAT3 Signaling. *Biomolecules* 9(7): 28.
- Jemal, A., Center, M. M., DeSantis, C., & Ward, E. M. 2010. Global patterns of cancer incidence and mortality rates and trends. *Cancer Epidemiology, Biomarkers & Prevention: A Publication of the American Association for Cancer Research, Cosponsored by the American Society of Preventive Oncology. Cancer Epidemiology Biomarkers and Prevention* 19(8), 1893–1907.

<https://doi.org/10.1158/1055-9965.EPI-10-0437>

- Jones, S. E. 2008. Comprehensive review Metastatic BC : The Treatment Challenge. *Clinical Breast Cancer*, 8(3), 224–233. <https://doi.org/10.3816/CBC.2008.n.025>
- Kai, P., Zainira, W., & Z, W. 2018. Potential Benefits of *Annona muricata* in Combating Cancer : A Review. *Malaysia Journal of Medical Sciences* 25(1), 5–15.
- Kantarjian H., Stein A., Gokbuget N., Fielding A.K., Schuh A.C., Ribera J.M., Wei A., Dombret H., Foà R., & Bassan R. 2017. Blinatumomab versus chemotherapy for advanced acute lymphoblastic leukemia. *N. Engl. J. Med.*; 376:836–847. doi: 10.1056/NEJMoa1609783.
- Kedare, S. B., & Singh, R. P. 2011. Genesis and development of DPPH method of antioxidant assay. 48(August), 412–422. <https://doi.org/10.1007/s13197-011-0251-1>
- Kehinde, A., Adefisan, A., Adebayo, O., & Adaramoye, O. 2016. Biflavonoid fraction from *Garcinia kola* seed ameliorates hormonal imbalance and testicular oxidative damage by anti-tuberculosis drugs in Wistar rats. *Journal of Basic and Clinical Physiology and Pharmacology*, 27(4). <https://doi.org/10.1515/jbcpp-2015-0063>
- Kempen, C. L. T. Van, Ruiters, D. J., Muijen, G. N. P. Van, & Coussens, L. M. 2003. The tumor microenvironment : a critical determinant of neoplastic evolution. *European Journal of Cell Biology* 548, 539–548.
- Kerdelhu, B., Forest, C., & Coumoul, X. 2016. ScienceDirect Dimethyl-Benz (a) anthracene : A mammary carcinogen and a neuroendocrine disruptor. 3, 49–55. <https://doi.org/10.1016/j.biopen.2016.09.003>
- Khalki, L. El, Maire, V., & Dubois, T. 2020. Berberine Impairs the Survival of Triple Negative BC Cells : Cellular and Molecular Analyses. *Biomolecules* 25(3) 506.
- Kim, J. H., Stansbury, K. H., Walker, N. J., Trush, M. A., Strickland, P. T., & Sutter, T. R. 1998. Metabolism of benzo [a] pyrene and benzo [a] pyrene-7 , 8-diol by human cytochrome P450 1B1. *Carcinogenesis* 19(10), 1847–1853.
- Kim, J. Y., Dao, T. T. P., Song, K., Park, S. B., Jang, H., Park, M. K., Gan, S. U., &

- Kim, Y. S. 2018. *Annona muricata* Leaf Extract Triggered Intrinsic Apoptotic Pathway to Attenuate Cancerous Features of Triple Negative BC MDA-MB-231 Cells. *Evidenced-Based Complimentary and Alternative Medicine* <https://doi.org/10.1155/2018/7972916>
- Knez, J. 2013. Endocrine-disrupting chemicals and male reproductive health. *Reproductive BioMedicine Online*, 26(5), 440–448. <https://doi.org/10.1016/j.rbmo.2013.02.005>
- Knickle, A., Fernando, W., Greenshields, A. L., Vasantha, H. P., & Hoskin, D. W. 2018. Myricetin-induced apoptosis of triple-negative BC cells is mediated by the iron-dependent generation of reactive oxygen species from hydrogen peroxide. *Food and Chemical Toxicology*. <https://doi.org/10.1016/j.fct.2018.05.005>
- Kowalczyk, T., Sitarek, P., Skała, E., & Toma, M. 2019. Induction of apoptosis by in vitro and in vivo plant extracts derived from *Menyanthes trifoliata* L . in human cancer cells. *Cytotechnology* 9, 165–180.
- Kurubanjerdjit, N. 2020. Gene Reports Identifying the regulation mechanism of phytochemicals on triple negative BC ' s biological network. *Gene Reports*, 100656. <https://doi.org/10.1016/j.genrep.2020.100656>
- Lang, S. J., Schmiech, M., Hafner, S., Paetz, C., Werner, K., Gaafary, M. El, Schmidt, C. Q., Syrovets, T., & Simmet, T. 2020. Chryso-splenol d , a Flavonol from *Artemisia annua* , Induces ERK1 / 2-Mediated Apoptosis in Triple Negative Human BC Cells. *International Journal of Molecular Science*, 21(11): 4090.
- Lantz, P. M., Ph, D., Hawley, S. T., Ph, D., Morrow, M., Schwartz, K., & Katz, S. J. 2007. Symptom Experience and Quality of Life of Women Following BC Treatment. *Journal of Women's Health*, 16(9): 1348-61. <https://doi.org/10.1089/jwh.2006.0255>
- Length, F. 2012. Effects of *C. portoricensis* extracts on the lipid profile of wistar rats challenged with venom of carpet viper. *Journal of Medicine and Medical Sciences*, 3(10), 674–678.
- Lenoir, V., Jonage-canonico, M. B. Y. De, Perrin, M., Martin, A., Scholler, R., & Kerdelhué, B. 2005. Research article Preventive and curative effect of melatonin

- on mammary carcinogenesis induced by dimethylbenz [a] anthracene in the female Sprague – Dawley rat. *Breast Cancer Research*, 7(4), 470–476. <https://doi.org/10.1186/bcr1031>
- Lewis, P. A., Hardy, J., Martins, L. M., & Wood, N. W. 2010. Cancer and Neurodegeneration : Between the Devil and the Deep Blue Sea. *PLOS Genetics*, 6(12). <https://doi.org/10.1371/journal.pgen.1001257>
- Li, C., Tsang, S., Tsai, C., Tsai, H., Chyuan, J., & Hsu, H. 2012. Momordica charantia Extract Induces Apoptosis in Human Cancer Cells through Caspase- and Mitochondria-Dependent Pathways. *Cancers* 12(8): 2064 <https://doi.org/10.1155/2012/261971>
- Li, J., Liu, X., Chen, H., Sun, Z., Chen, H., Wang, L., Sun, X., & Li, X. 2019. Multi-targeting chemoprevention of Chinese herb formula Yanghe Huayan decoction on experimentally induced mammary tumorigenesis. *BMC-Based Complementary and Alternative Medicine*, 1: 1–15.
- Lin, D. A. N., Kuang, G. E., Wan, J., Zhang, X., Li, H., Gong, X. I. A., & Li, H. 2017. Luteolin suppresses the metastasis of triple-negative BC by reversing epithelial-to-mesenchymal transition via downregulation of β -catenin expression. 895–902. <https://doi.org/10.3892/or.2016.5311>
- Lin, P., Chiang, Y., Shieh, T., & Chen, H. 2020. Dietary Compound Isoliquiritigenin , an Antioxidant from Licorice , Suppresses Triple-Negative Breast Tumor Growth via Apoptotic Death Program Activation in Cell and Xenograft Animal Models. *Antioxidants*, 9(3): 228.
- Lin, W., & Tan, T. 1994. The role of gastric muscle relaxation in cytoprotection induced by San-huang-xie-xin-tang in rats. *Journal of Ethnopharmacology*, 44, 171–179.
- Lin, Y., Collier, A. C., Liu, W., Berry, M. J., & Panee, J. 2015. HHS Public Access. 22(11), 1440–1445. <https://doi.org/10.1002/ptr.2439>.The
- Lobo, V., Patil, A., Phatak, A., & Chandra, N. 2010. Free radicals , antioxidants and functional foods : Impact on human health. *Pharmacognosy Review*, 4(8): 118-26. <https://doi.org/10.4103/0973-7847.70902>

- Louis, G. M. B., Barr, D. B., Kannan, K., Chen, Z., & Kim, S. 2016. Paternal exposures to environmental chemicals and time- to-pregnancy: overview of results from the LIFE study. *Andrology*, 4(4): 638-648.
- Luccio-camelo, D. C., & Prins, G. S. 2011. Journal of Steroid Biochemistry and Molecular Biology Disruption of androgen receptor signaling in males by environmental chemicals. *Journal of Steroid Biochemistry and Molecular Biology*, 127(1–2), 74–82.
- Ma, Y., He, X., Qi, K., Wang, T., Qi, Y., Cui, L., Wang, F., & Song, M. 2019. Effects of environmental contaminants on fertility and reproductive health. *Journal of Environmental Sciences (China)*, 77, 210–217.
- Mamounas E.P., Anderson S.J., Dignam J.J., Bear H.D., Julian T.B., Geyer C.E., Taghian A., Wickerham D.L., Wolmark N. 2012. Predictors of locoregional recurrence after neoadjuvant chemotherapy: results from combined analysis of National Surgical Adjuvant Breast and Bowel Project B-18 and B-27. *Journal of Clinical Oncology*, 30: 3960–3966.
- Mandal, A., & Bishayee, A. 2015. *Trianthema portulacastrum* Linn . Displays Anti-Inflammatory Responses during Chemically Induced Rat Mammary Tumorigenesis through Simultaneous and Differential Regulation of NF- κ B and Nrf2 Signaling Pathways. *International Journal of Molecular Sciences*, 2426–2445. <https://doi.org/10.3390/ijms16022426>
- Manral, C., Roy, S., Singh, M., Gautam, S., Yadav, R. K., Rawat, J. K., Devi, U., Ansari, N., Saedan, A. S., & Kaithwas, G. 2016. Effect of β -sitosterol against methyl nitrosourea-induced mammary gland carcinoma in albino rats. *BMC Complementary and Alternative Medicine*, 1–10. <https://doi.org/10.1186/s12906-016-1243-5>
- Menezes, S., Leita, G. G., Reis, A. S., Tereza, C., & Mensor, L. L. 2001. Screening of Brazilian Plant Extracts for Antioxidant Activity by the Use of DPPH Free Radical Method. *Physiotherapy Research*, 130, 127–130.
- Mileo, A. M., Nisticò, P., & Miccadei, S. 2019. Polyphenols : Immunomodulatory and Therapeutic Implication in Colorectal Cancer. *Frontiers in Immunology*, 10:729.

<https://doi.org/10.3389/fimmu.2019.00729>

- Misra, H. P., & Fridovich, I. 1972. The Role of Superoxide Anion in the Epinephrine and a Simple Assay for Superoxide Dismutase * Autoxidation of. *Journal of Biological Chemistry*, 247(10), 3170–3175. [https://doi.org/10.1016/S0021-9258\(19\)45228-9](https://doi.org/10.1016/S0021-9258(19)45228-9)
- Miyagawa, S., Sato, M., & Iguchi, T. 2011. Journal of Steroid Biochemistry and Molecular Biology Molecular mechanisms of induction of persistent changes by estrogenic chemicals on female reproductive tracts and external genitalia &. *Journal of Steroid Biochemistry and Molecular Biology*, 127(1–2), 51–57. <https://doi.org/10.1016/j.jsbmb.2011.03.009>
- Narayanan, B. A., Condon, M. S., Bosland, M. C., Narayanan, N. K., & Reddy, B. S. 2003. Suppression of N -Methyl- N -nitrosourea / Testosterone-induced Rat Prostate Cancer Growth by Celecoxib : Effects on Cyclooxygenase-2 , Cell Cycle Regulation , and Apoptosis Mechanism (s) 1. 9, 3503–3513.
- Naskar, S., Mazumder, U. K., Pramanik, G., Gupta, M., Kumar, R. B. S., Bala, A., & Islam, A. 2011. Evaluation of antihyperglycemic activity of *Cocos nucifera* Linn . on streptozotocin induced type 2 diabetic rats. *Journal of Ethnopharmacology*, 138(3), 769–773. <https://doi.org/10.1016/j.jep.2011.10.021>
- Nassan, M. A., Soliman, M. M., Ismail, S. A., & El-shazly, S. 2018. Effect of *Taraxacum officinale* extract on PI3K / Akt pathway in DMBA-induced BC in albino rats. *Bioscience Reports*, 38(6): 1–11.
- Nvau, J. B., Alenezi, S., Ungogo, M. A., Alfayez, I. A. M., Koning, H. P. De, & Igoli, J. O. 2020. Antiparasitic and Cytotoxic Activity of Bokkosin , A Novel Diterpene-Substituted Chromanyl Benzoquinone From *C. portoricensis*. *Frontiers in Chemistry*, 1–12. <https://doi.org/10.3389/fchem.2020.574103>
- Oguegbulu, N. E., Abo, A. K., & Afieroho, O. E. 2020. Comparative Study of Antimicrobial Potentials of Leaf and Root Extracts of *C. portoricensis* (Jacq) - benth (Fabaceae) on Some Human Pathogens. 31(10), 141–151. <https://doi.org/10.9734/EJMP/2020/v31i1030290>
- Ogugu, S. E., Kehinde, A. J., James, B. I., & Paul, D. K. 2012. Assessment of

- cytotoxic effects of methanol extract of *C. portoricensis* using brine shrimp (*artemia salina*). *Macedonian Pharmaceutical Bulletin*,1(2), 257–260.
- Oishi, Y., Nambu, H., Yamamoto, D., & Yang, J. 2000. Cataractogenesis in Neonatal Sprague-Dawley Nitrosourea Rats. *Toxicology Pathology*, 280, 555–564.
- Onyeama, H. P., Igile, G. O., Mgbeje, B. I. A., Eteng, M. U., & Ebong, P. E. 2013. Evaluation of the biochemical and anti-snake venom effects of *C. portoricensis* extract fractions in wistar rat models challenged with venom of carpet viper (*Echis Ocellatus*). 3(6), 441–449.
- Orishadipe, A. T., Okogun, J. I., & Mishelia, E. 2010. Gas chromatography – mass spectrometry analysis of the hexane extract of *C. portoricensis* and its antimicrobial activity. 131–134.
- Otto, T., & Sicinski, P. 2017. HHS Public Access. 17(2), 93–115. <https://doi.org/10.1038/nrc.2016.138>.Cell
- Ou-yang, F., Tsai, I., Tang, J., Yen, C., & Cheng, Y. 2019. Antiproliferation for BC Cells by Ethyl Acetate Extract of *Nepenthes thorellii* x (*ventricosa* x *maxima*). *Interntional Journal of Molecular Science*, 20(130): 3238.
- Ouyang, L., Shi, Z., Zhao, S., Wang, F., Zhou, T., Liu, B., & Bao, J. 2012. Programmed cell death pathways in cancer : a review of apoptosis , autophagy and programmed necrosis. *Cell Proliferation*, 45(6): 487–498. <https://doi.org/10.1111/j.1365-2184.2012.00845.x>
- Oyebode OT, Owumi SE, Oyelere AK, Olorunsogo OO. 2019. *C. portoricensis* Benth exhibits anticancer effects via alteration of Bax/Bcl-2 ratio and growth arrest in prostate LNCaP cells. *Journal of Ethnopharmacology*, 233:64-72. doi: 10.1016/j.jep.2018.12.020.
- Parodi, D. A., Greenfield, M., Evans, C., Chichura, A., Alpaugh, A., Williams, J., Cyrus, K. C., & Martin, M. B. 2017. Alteration of Mammary Gland Development and Gene Expression by In Utero Exposure to Cadmium. *International Journal of Molecular Science*. <https://doi.org/10.3390/ijms18091939>
- Patel, S., Zhou, C., Rattan, S., & Flaws, J. A. 2015. Effects of endocrine-disrupting

- chemicals on the ovary. *Biology of Reproduction*, 93(1), 1–9.
<https://doi.org/10.1095/biolreprod.115.130336>
- Pathways, N. S., Mandal, A., Bhatia, D., & Bishayee, A. 2017. Anti-Inflammatory Mechanism Involved in Pomegranate-Mediated Prevention of BC : *Nutrients*, 9(5): 436. <https://doi.org/10.3390/nu9050436>
- Pe, E., Mu, E., Go, I., Ha, I., & Peter, A. 2012. Evaluation of the Effects of *C. portoricensis* Extracts on Oxidative Stress Enzymes in Wistar Rats Challenged with Venom of *Echis Ocellatus*. *Journal of Applied Pharmaceutical Science*, 02(06),199–202. <https://doi.org/10.7324/JAPS.2012.2623>
- Perkins, N. D., & Barre, B. 2007. A cell cycle regulatory network Vehincling NF- j B subunit activity and function. *The MBO Journal*, 26(23), 4841–4855. <https://doi.org/10.1038/sj.emboj.7601899>
- Pieme, C. A., Kumar, S. G., Dongmo, M. S., Moukette, B. M., Boyoum, F. F., Ngogang, J. Y., & Saxena, A. K. 2014. Antiproliferative activity and induction of apoptosis by *Annona muricata* (Annonaceae) extract on human cancer cells. *BMC Complimentary Alternative Medicine*, 1–10.
- Prakash, P., Sheshu, P., & Kapewangolo, P. 2019. *Bulbine frutescens* phytochemical inhibits notch signaling pathway and induces apoptosis in triple negative and luminal BC cells. *Life Sciences*, 234, 116783. <https://doi.org/10.1016/j.lfs.2019.116783>
- Pratheeshkumar, P., Sreekala, C., Zhang, Z., Budhraj, A., Ding, S., Son, Y., Wang, X., Hitron, A., Hyun-jung, K., Wang, L., & Lee, J. 2016. HHS Public Access. 12(10), 1159–1184.
- Pugalendhi, P., Manoharan, S., Suresh, K., & Nadu, T. 2011. Genistein and daidzein , in combination , protect cellular integrity during 7 , 12-dimethylbenz [a] anthracene (DMBA) induced mammary carcinogenesis in sprague-dawley rat. *African Journal of Traditional Complementary Alternative Medicine*, 8 (2): 91-97 8, 91–97.
- Rafieian-kopaei, M., Movahedi, M., Plants, M., & Movahedi, M. 2017. Electronic Physician (ISSN : 2008-5842). 3838–3844.

- Rahman, M., Islam, B., Biswas, M., & Alam, A. H. M. K. 2015. In vitro antioxidant and free radical scavenging activity of different parts of *Tabebuia pallida* growing in Bangladesh. *BMC Research Notes*, 1–9. <https://doi.org/10.1186/s13104-015-1618-6>
- Rahman, N. A., Yazan, L. S., Wibowo, A., Ahmat, N., Foo, J. B., & Tor, Y. S. 2016. Induction of apoptosis and G₂ / M arrest by ampelopsin E from *Dryobalanops* towards triple negative BC cells, *BMC Complementary and Alternative Medicine*, 1–9. <https://doi.org/10.1186/s12906-016-1328-1>
- Raj, A., Mayberry, J. F., & Podas, T. 2003. Occupation and gastric cancer. *Postgraduate Medical Journal*, 79(931): 252–259.
- Rayet, Â., & Ge, Â. 1999. Aberrant rel / nfkb genes and activity in human cancer. *Oncogenes*, 18(49): 6938–6947.
- Remani, P. 2019. Cytotoxicity Profiling of *Annona Squamosa* in Cancer Cell Lines. *Asian Pacific Journal of Cancer Prevention*, 20(9): 2831–2840.
- Sánchez, C. 1951. Determination of serum proteins by means of the biuret reaction.
- Sanguinetti, A., Santini, D., Bonafè, M., Taffurelli, M., & Avenia, N. 2015. Interleukin-6 and pro inflammatory status in the breast tumor microenvironment. *World Journal of Surgical Oncology*. 4–9. <https://doi.org/10.1186/s12957-015-0529-2>
- Saraiva, N., Costa, G., Reis, C., Almeida, N., & Fernandes, A. S. 2020. Anti-Migratory and Pro-Apoptotic Properties of Parvifloron D on Triple-Negative BC Cells. *Biomolecules*, 10(1): 158.
- Scheibmeir, H. D., Christensen, K., Whitaker, S. H., Jegaethesan, J., Clancy, R., & Pierce, J. D. 2005. A review of free radicals and antioxidants for critical care nurses. *Oxidative Medicine and Cellular Longevity*, 24–28. <https://doi.org/10.1016/j.iccn.2004.07.007>
- Schetter, A. J., Heegaard, N. H. H., & Harris, C. C. 2010. Inflammation and cancer : interweaving microRNA , free radical , cytokine and p53 pathways. *Carcinogenesis*, 31(1), 37–49. <https://doi.org/10.1093/carcin/bgp272>

- Schuster S.J., Bartlett N.L., Assouline S., Yoon S.S., Bosch F., Sehn L.H., Cheah C.J., Shadman M., Gregory G.P., Ku M. 2019. Mosunetuzumab induces complete remissions in poor prognosis non-Hodgkin lymphoma patients, including those who are resistant to or relapsing after chimeric antigen receptor T-cell (CAR-T) therapies, and is active in treatment through multiple lines; Proceedings of the 2019 ASH Annual Meeting; Orlando, FL, USA; Abstract 6.
- Schwarz, D., Kisselev, P., Cascorbi, I., Schunck, W., & Roots, I. 2001. Differential metabolism of benzo [a] pyrene and benzo [a] pyrene-7 , 8-dihydrodiol by human CYP1A1 variants. *Carcinogenesis*, 22(3), 453–459.
- Scully, O. J., Bay, B., Yip, G., & Yu, Y. 2012. BC Metastasis. Non Coding RNA *Research Journal*, 320, 311–320.
- Seo, A. N., Lee, H. J., Kim, E. J., Jang, M. H., Kim, Y. J., Kim, J. H., Kim, S., Ryu, H. S., Park, I. A., Im, S., Gong, G., Jung, K. H., Kim, H. J., & Park, S. Y. 2016. Expression of BC stem cell markers as predictors of prognosis and response to trastuzumab in HER2 - positive BC. April, 1–8. <https://doi.org/10.1038/bjc.2016.101>
- Seo, J., & Park, M. 2020. Molecular crosstalk between cancer and neurodegenerative diseases. *Cellular and Molecular Life Sciences*, 77(14), 2659–2680. <https://doi.org/10.1007/s00018-019-03428-3>
- Shah, A. S. V, Lee, K. K., Mcallister, D. A., Hunter, A., Nair, H., Whiteley, W., Langrish, J. P., Newby, D. E., & Mills, N. L. 2014. Short term exposure to air pollution and stroke : systematic review and meta-analysis. <https://doi.org/10.1136/bmj.h1295>
- Shehata, M., Teschendorff, A., Sharp, G., Novcic, N., Russell, I. A., Avril, S., Prater, M., Eirew, P., Caldas, C., Watson, C. J., & Stingl, J. 2012. Phenotypic and functional characterisation of the luminal cell hierarchy of the mammary gland. *Breast Cancer Research*, 14(5), R134. <https://doi.org/10.1186/bcr3334>
- Shindikar, A., Singh, A., Nobre, M., & Kirolikar, S. 2016. Curcumin and Resveratrol as Promising Natural Remedies with Nanomedicine Approach for the Effective Treatment of Triple Negative BC. *Journal of Oncology*.

- Siemuri, E. O., Akintunde, J. K., & Salemcity, A. J. 2015. Effects of sub-acute methanol extract treatment of *C. portoricensis* root bark on antioxidant defence capacity in an experimental rat model. *BMC Complementary Medicine and Therapy*, 26(4), 375–382. <https://doi.org/10.1515/jbcpp-2013-0151>
- Sifakis, S., Androutsopoulos, V. P., Tsatsakis, A. M., & Spandidos, D. A. 2017. Human exposure to endocrine disrupting chemicals: effects on the male and female reproductive systems. *Environmental Toxicology and Pharmacology*, 51, 56–70. <https://doi.org/10.1016/j.etap.2017.02.024>
- Silihe, K. K., Winter, E., Awounfack, C. F., Bishayee, A., Desai, N. N., Jr, M., Michel, T., Tankeu, F. N., Ndinteh, D. T., Riwom, S. H., Njamen, D., & Creczynski-pasa, T. B. 2017. *Ficus umbellata* Vahl . (Moraceae) Stem Bark Extracts Exert Antitumor Activities In Vitro and In Vivo. <https://doi.org/10.3390/ijms18061073>
- Sims, A. H., Howell, A., Howell, S. J., & Clarke, R. B. 2007. Origins of BC subtypes and therapeutic implications. *Nature Clinical Practice Oncology*, 4(9): 515-25. <https://doi.org/10.1038/ncponc0908>
- Singh, D. P., Verma, S., & Prabha, R. 2018. Journal of Plant Biochemistry & Investigations on Antioxidant Potential of Phenolic Acids and Flavonoids : The Common Phytochemical Ingredients in Plants. 6(3). <https://doi.org/10.4172/2329-9029.1000219>
- Sledge, G. W., Mamounas, E. P., Health, F., Hortobagyi, G. N., & Burstein, H. J. 2014. Past , Present , and Future Challenges in BC Treatment. *Journal of Clinical Oncology*, 32(19), 1979–1986.
- Smarr, M. M., Kannan, K., & Buck Louis, G. M. 2016. Endocrine disrupting chemicals and endometriosis. *Fertility and Sterility*, 106(4), 959–966. <https://doi.org/10.1016/j.fertnstert.2016.06.034>
- Song, L., Chen, X., Mi, L., Liu, C., Zhu, S., Yang, T., Luo, X., Zhang, Q., Lu, H., & Liang, X. 2020. Icaritin-induced inhibition of SIRT6 / NF- κ B triggers redox mediated apoptosis and enhances anti-tumor immunity in triple-negative Breast Cancer. *Cancer Science*, 111(11): 4242-4256. <https://doi.org/10.1111/cas.14648>
- Stein A.S., Larson R.A., Schuh A.C., Stevenson W., Lech-Maranda E., Tran Q.,

- Zimmerman Z., Kormany W., Topp M.S. 2018. Exposure-adjusted adverse events comparing blinatumomab with chemotherapy in advanced acute lymphoblastic leukemia. *Blood Advance*, 2:1522–1531.
- Stuff, J. E., Goh, E. T., Barrera, S. L., Bondy, M. L., & Forman, M. R. 2009. Construction of an N-nitroso database for assessing dietary intake. *Journal of Food Composition and Analysis*, 2005–2010. <https://doi.org/10.1016/j.jfca.2009.01.008>
- Sun, Y., Zhao, Z., Yang, Z., Xu, F., Lu, H., Zhu, Z., & Shi, W. 2017. Risk Factors and Preventions of Breast Cancer. *International Journal of Biological Science*, 13(11): 1387-1397. <https://doi.org/10.7150/ijbs.21635>
- Taka, E., Mendonca, P., Messeha, S. S., & Soliman, K. F. A. 2021. The Anticancer Effects of Flavonoids through miRNAs Modulations in Triple-Negative BC. *Nutrients*, 13(4): 1212.
- Taylor, P., Cambridge, C., & Jacob, J. 2006. A review of: “ BENZOPYRENES By M . R . Osborne and N . T . 1–2. <https://doi.org/10.1080/10406639208048430>
- Taylor, P., Malhotra, G. K., Zhao, X., Band, H., & Band, V. 2010. Histological , molecular and functional subtypes of BCs. *Cancer Biology and Therapy*, 10(10): 955-960. <https://doi.org/10.4161/cbt.10.10.13879>
- Tiwari, J., & Rai, G. 2016. In vitro investigation of anti-microbial and anti- helmintic activity of extract obtained from flowers of the shrub *Calliandra haematocephala*. *Journal of Medicinal Plant Studies*, 4(4), 192–195.
- Troisi, R., Innes, K. E., Roberts, J. M., & Hoover, R. N. 2007. Preeclampsia and maternal BC risk by offspring gender : do elevated androgen concentrations play a role ? *PLOS ONE*, 688–690. <https://doi.org/10.1038/sj.bjc.6603921>
- Trush, M. A. 1994. Myeloperoxidase as a biomarker of skin irritation and inflammation. *Food and Chemical Toxicology*, 32(2), 143–147.
- Tueche, A. B., Zingue, S., Tchoupang, E. N., Gueyo, T. N., Joël, A., Yaya, G., Njuh, A. N., Ntsa, D. M., & Njamen, D. 2018. Abyssinone V-4 ' Methyl Ether Isolated from *Erythrina droogmansiana* (Leguminosae) Inhibits Cell Growth and

- Mammary Glands Hyperplasia Induced in Swiss Mice by the 7, 12-Dimethylbenz (a) anthracene. *Evidenced Based Complementary and Alternative Medicine*. <https://doi.org/10.1155/2018/7959068>
- Tuli, H. S., Tuorkey, M. J., Thakral, F., Sak, K., Kumar, M., Sharma, A. K., Sharma, U., Jain, A., Aggarwal, V., & Bishayee, A. 2019. Molecular Mechanisms of Action of Genistein in Cancer : Recent Advances. *Frontiersin Pharmacology*, 1–16. <https://doi.org/10.3389/fphar.2019.01336>
- Umthong, S., Phuwapraisirisan, P., Puthong, S., & Chanchao, C. 2011. In vitro antiproliferative activity of partially purified *Trigona laeviceps* propolis from Thailand on human cancer cell lines. *BMC Complementary and Alternative Medicine*, 11(1), 37. <https://doi.org/10.1186/1472-6882-11-37>
- Unger-saldaña, K. 2014. Cancer in developing countries. *World Journal of Clinical Oncology*, 5(3), 465–478. <https://doi.org/10.5306/wjco.v5.i3.465>
- Uri, D. 2014. Lactate Dehydrogenase Like Crystallin : A Potentially Protective Shield for Indian Spiny-Tailed Lizard (*Uromastix hardwickii*) Lens Against Environmental Stress ? *Biomedical and Pharmaceutical Sciences*, 33(2).
- Utage, B. G., Patole, M. S., & Vasudeo, P. 2018. *Prosopis juliflora* (Sw .), DC induces apoptosis and cell cycle arrest in triple negative BC cells : in vitro and in vivo investigations. *Oncotarget*, 9(54), 30304–30323.
- Vander, M., & Wyns, C. 2018. Fertility and infertility :Definition and epidemiology. *ClinicalBiochemistry*.<https://doi.org/10.1016/j.clinbiochem.2018.03.012>
- Varghese, E., Samuel, S. M., Abotaleb, M., Cheema, S., Mamtani, R., & Büsselberg, D. 2018. The “ Yin and Yang ” of Natural Compounds in Anticancer Therapy of Triple-Negative BCs. *Cancers*, 12(8): 2252. <https://doi.org/10.3390/cancers10100346>
- Vatten, L. J., Mæhle, B. O., Nilsen, T. I. L., Tretli, S., Hsieh, C., Trichopoulos, D., & Stuver, S. O. 2002. Birth weight as a predictor of BC : a case – Vehinle study in Norway. *The British Journal of Nutrition*, 89–91.
- Visser, K. E. De, Korets, L. V., & Coussens, L. M. 2005. De novo carcinogenesis

- promoted by chronic inflammation is B lymphocyte dependent. *Cancer Cells*, 7(5): 411–423. <https://doi.org/10.1016/j.ccr.2005.04.014>
- Wang, L. 2017. Early Diagnosis of BC. *Sensors*, 17(7): 1572 <https://doi.org/10.3390/s17071572>
- Waterborg, J. H., & Matthew, H. R. 1984. Chapter 1 The Burton Assay for DNA. *Sensors*, 1–3.
- Webb, M. J., & Kukard, C. 2020. A Review of Natural Therapies Potentially Relevant in Triple Negative BC Aimed at Targeting Cancer Cell Vulnerabilities. <https://doi.org/10.1177/1534735420975861>
- Weber, D., Zhang, M., Zhuang, P., Zhang, Y., Wheat, J., Currie, G., & Al-eisawi, Z. 2014. The efficacy of betulinic acid in triple-negative BC. *SAGE Open Medicine*, <https://doi.org/10.1177/2050312114551974>
- Weigelt, B., Geyer, F. C., & Reis-filho, J. S. 2010. Histological types of BC : How special are they? *Molecular Oncology*, 4(3), 192–208. <https://doi.org/10.1016/j.molonc.2010.04.004>
- Westwood, A. 1991. The analysis of bilirubin in serum.
- Whitsett, T., Carpenter, M., & Lamartiniere, C. A. 2006. Mammary cancer in rats. 11, 1–11. <https://doi.org/10.1186/1477-3163-5-15>
- Yaacob, N. S., Yankuzo, H. M., Devaraj, S., & Ka, J. 2015. Anti-Tumor Action , Clinical Biochemistry Profile and Phytochemical Constituents of a Pharmacologically Active Fraction of *S. crispus* in MNU-Induced Rat Mammary Tumour Model. *PLOS ONE*, 1–20. <https://doi.org/10.1371/journal.pone.0126426>
- Ye, X., Skjaerven, R., Basso, O., Baird, D. D., Eggesbo, M., Aurora, L., Uicab, C., Haug, K., & Longnecker, M. P. 2010. In utero exposure to tobacco smoke and subsequent reduced fertility in females. 25(11), 2901–2906. <https://doi.org/10.1093/humrep/deq235>
- Yoshizawa, K., Kinoshita, Y., Emoto, Y., Kimura, A., Uehara, N., Yuri, T., Shikata, N., & Tsubura, A. 2013. N -Methyl- N -nitrosourea-induced Renal Tumors in Rats : Immunohistochemical Comparison to Human Wilms Tumors. 141–148.

<https://doi.org/10.1293/tox.26.141>

- You, Z., Sun, J., Xie, F., Chen, Z., Zhang, S., Chen, H., Liu, F., Li, L., Chen, G., Song, Y., Xuan, Y., Zheng, G., & Xin, Y. 2017. Modulatory Effect of Fermented Papaya Extracts on Mammary Gland Hyperplasia Induced by Estrogen and Progesterone in Female Rats. *Oxidative Medicine and Cellular Longevity*.
- Younglai, E. V., Holloway, A. C., & Foster, W. G. 2005. Environmental and occupational factors affecting fertility and IVF success. *Human Reproduction Update*, 11(1), 43–57. <https://doi.org/10.1093/humupd/dmh055>
- Zama, A. M., & Uzumcu, M. 2010. Epigenetic effects of endocrine-disrupting chemicals on female reproduction: An ovarian perspective. *Frontiers in Neuroendocrinology*, 31(4), 420–439. <https://doi.org/10.1016/j.yfrne.2010.06.003>
- Zhou, Q., Yin, W., Du, Y., & Lu, J. 2014. For or against Adjuvant Trastuzumab for pT1a-bN0M0 BC Patients with HER2-Positive Tumors: A Meta-Analysis of Published Literatures. 9(1), 8–11. <https://doi.org/10.1371/journal.pone.0083646>
- Zingue, Stephane, Njuh, A. N., Tueche, A. B., Tamsa, J., Tchoupan, E. N., Kakene, S. D., Trésor, M., Sipping, K., & Njamen, D. 2018. *In Vitro* Cytotoxicity and *In Vivo* Antimammary Tumor Effects of the Hydroethanolic Extract of *Acacia seyal* (Mimosaceae) Stem Bark. *Biomedicine Research International*. <https://doi.org/10.1155/2018/2024602>
- Zingue, Stephane, Silihe, K. K., Bourfane, I. F., Boukar, A., Tueche, A. B., Njuh, A. N., & Njamen, D. 2019. Potential of Regular Consumption of Cameroonian Neem (*Azadirachta indica* L.) Oil for Prevention of the 7, 12-Dimethylbenz (a) anthracene-Induced BC in High-Fat / Sucrose-Fed Wistar Rats. <https://doi.org/10.1155/2019/2031460>
- Zingue, Stéphane, Tchoumtchoua, J., Ntsa, D. M., Sandjo, L. P., Cisilotto, J., Beatrice, C., Nde, M., Winter, E., Awounfack, C. F., Ndinteh, D. T., Clyne, C., Njamen, D., Halabalaki, M., & Creczynski-pasa, T. B. 2016. Estrogenic and cytotoxic potentials of compounds isolated from *Millettia macrophylla* Benth (Fabaceae): towards a better understanding of its underlying mechanisms. 1–17. <https://doi.org/10.1186/s12906-016-1385-5>

Ziv-Gal, A., & Flaws, J. A. 2016. Evidence for bisphenol A-induced female infertility: a review (2007–2016). *Fertility and Sterility*, 106(4), 827–856. <https://doi.org/10.1016/j.fertnstert.2016.06.027>

APPENDICES

Appendix 1

3.3 Weighed DPPH (39.4mg), dissolved in methanol and filled to 100 mL with methanol.

Appendix 2

3.4 In the dark, ABTS (0.054 g) was weighed and dissolved in dH₂O (15 mL). Also weighed and dissolved in 15mL dH₂O was 0.0099 g of potassium persulphate.

Appendix 3

3.5.1 Buffer (phosphate buffer-100 mmol/L, pH 7.4, L-Aspartate – 100mmol/L, α -oxoglutarate-2 mmol/L), 2,4-dinitrophenylhydrazine-2 mmol/L, Sodium hydroxide- 0.4 mol/L.

Appendix 4

3.5.2 Buffer (phosphate buffer-100 mmol/L, pH 7.4, L-Alanine – 100mmol/L, α -oxoglutarate-2 mmol/L), 2,4-dinitrophenylhydrazine-2 mmol/L, Sodium hydroxide- 0.4 mol/L.

Appendix 5

3.5.3 R1 – constitutes sulphanilic acid (29 mmol/L) and hydrochloric acid (0.17 μ L); R2- constitutes sodium nitrite (38.5 mmol/l); R3- constitutes caffeine (0.26 mol/L) and sodium benzoate (0.52 mol/L); R4- constitutes tartrate (0.93mol/L) and sodium hydroxide (1.9 μ L)

Appendix 6

3.5.4 (a) LDH Substrate Mix- Reconstitute in 1 mL of water.

(b) 1.25 mM NADH standard- Reconstitute in 400 μ L of water

(c) LDH Positive Vehicle- Reconstitute in 200 μ L of LDH assay buffer before use.

Appendix 7

3.6.1 NaCl solution (0.9% normal saline)

Dissolution of 2.7 g of NaCl in dH₂O (little amount) was filled to 300 mL capacity with dH₂O.

NaOH (0.2M)

Dissolution of 8 g of NaOH in dH₂O (little amount) was filled to a litre capacity with dH₂O.

1. Biuret Reagent

In 500 mL of 0.2 M NaOH, copper sulphate, CuSO₄.5H₂O (3 g) and sodium-potassium tartrate, C₄H₄KNaO₆ (5 g) were dissolved. To the mixture, KI (5 g) was added and then filled with 0.2 M NaOH to make it 1 mL capacity.

2. Stock Bovine Serum Albumin (BSA) Solution

To make a stock solution of 1 mg/mL, BSA (0.1g) was dissolved in a normal saline (little quantity) and filled to 100 mL capacity.

Appendix 8

3.6.2 Trichloroacetic Acid (30% of TCA)

DH₂O was used to dissolve TCA and make up to 30ml capacity with dH₂O.

- 1. Thiobarbituric Acid (0.075% of TBA in 0.1M HCL)**
- To make this, TBA (0.225 g) was dissolved in HCL (0.1 M) and dilute to 30 mL capacity with dH₂O.
- 3. Tris-KCL (0.15 M, pH 7.4)**

KCL (1.12 g) and Tris base (2.36 g) were dissolved in dH₂O and used to make a 100 mL solution. After then, the pH was raised to 7.4.

Appendix 9

3.6.3 Carbonate buffer (0.05M, pH 10.2)

In 900 mL of dH₂O, Na₂CO₃.10H₂O (14.3 g) and NaHCO₃ (4.2 g) were dissolved. After adjusting the pH to 10.2, 1000 mL of distilled water was added.

Epinephrine (0.3M)

Epinephrine (0.0137 g) was dissolved in dH₂O (200 mL) and filled to capacity with same. Before use, the solution was newly made.

Appendix 10

3.6.4 Phosphate buffer (0.05 M, pH 7.4)

K₂HP04 (0.696 g) and KH₂P04 (0.265 g) dissolved in dH₂O (90 mL) and filled to 100 mL capacity at pH 7.4

Hydrogen peroxide (19mM)

This was made by dissolving 30 % H₂O₂ in 50 mL phosphate buffer and filling to 100 mL with the same solution.

Appendix 11

3.6.5 1-Chloro-2,4-dinitrobenzene (CDNB)

3.37 mg of CDNB was dissolved in one 1mL of ethanol to make 20 mM CDNB.

Reduced Glutathione (0.1M)

30.73 mg of GSH was dissolved in 1mL of phosphate buffer to make this.

Phosphate buffer (0.1 M; pH 6.5)

K₂HPO₄ (4.96 g) and KH₂PO₄ (9.73 g) were diluted with distilled water and filled to a capacity of 1000 mL, with a pH of 6.5.

Appendix 12

3.6.6 Sodium azide (NaN₃; 10mM)

Dissolve NaN₃ (0.0325 g) in dH₂O (50 mL) for the preparation.

Reduced glutathione (GSH 4 mM)

0.0123 g of GSH was weighed and dissolved in phosphate buffer to make this (10 mL).

Hydrogen peroxide (H₂O₂; 2.5 mM)

0.028 mL H₂O₂ was added to 100 mL distilled water for the preparation.

Trichloroacetic acid (10%)

2g trichloroacetic acid in 20 mL distilled water was used to make this mixture.

Dipotassium Hydrogen orthophosphate K₂HPO₄ (0.3 M)

This was produced by mixing K₂HPO₄ (5.23 g) in dH₂O (100 mL capacity).

Ellman's reagent

Ellman's reagent (0.04 g) was dissolved in phosphate buffer (100 mL) to make this.

Phosphate buffer

This was made by adding K₂HPO₄ (0.992 g) and KH₂PO₄ (1.946 g) in dH₂O (200 mL capacity) and with a pH of 7.4.

Appendix 13

3.6.7 Glutathione Working Standard

Phosphate buffer (0.1M; 100 mL; pH 7.4) was used to dissolved 40 g of GSH.

1. Phosphate Buffer (0.1M; pH 7.4)

- a. $\text{Na}_2\text{HPO}_4 \cdot 2\text{H}_2\text{O}$ (7.1628 g; mol. Wt. 358.22) was dissolved in dH_2O (200 mL capacity) to make $\text{Na}_2\text{HPO}_4 \cdot 2\text{H}_2\text{O}$ (0.1M; mol. Wt. 358.22).
 - b. $\text{NaH}_2\text{PO}_4 \cdot 2\text{H}_2\text{O}$ (1.5603 g; mol. Wt. 156.03) was dissolved in dH_2O (100 mL capacity) to make 0.1M $\text{NaH}_2\text{PO}_4 \cdot 2\text{H}_2\text{O}$ (mol. Wt. 156.03).
2. Finally, by combining solutions (a) and (b) and setting the pH to 7.4, 0.1M phosphate buffer was created.

Ellman's Reagent [5,5'-dithiobis-(-2-nitrobenzoic acid) DTNB]

A total of 40 mg of DTNB was dissolved in 0.1M phosphate buffer and filled to a capacity of 100 mL.

Precipitating Solution

4 % sulphosalicylic acid was obtained by dissolution of 4 g of sulphosalicylic acid in dH_2O of 100 mL capacity ($\text{C}_7\text{H}_6\text{O}_6\text{S} \cdot 2\text{H}_2\text{O}$, Mol Wt. 254.22).

Appendix 14

3.6.8 0.1% N-(1-naphthyl) ethylenediamine dihydrochloride

In a small amount of water, 0.1g of 0.1 % N-(1-naphthyl) ethylenediamine dihydrochloride was mixed with dH_2O and filled to 100mL capacity.

1. 5% Phosphoric Acid

To 95 mL of distilled water, 5 mL concentrated phosphoric acid was added.

2. 1% Sulphanilamide

In 100 mL of 5% phosphoric acid, 1 g of sulphanilimide was dissolved. Greiss reagent was made by combining equal parts of solutions 1 and 3. (1:1).

3. 20 mmol/L Sodium Nitrite

In a small amount of water, 13.8 mg of sodium nitrite (NaNO_2) was dissolved and made up to 100mL.

Appendix 15

3.6.9 O-dianisidine

O-dianisidine dihydrochloride (0.0167 g) was mixed in phosphate buffer (100 mL capacity) for the preparation.

Phosphate Buffer (0.1 M; pH 7.4)

K₂HPO₄ (486 mg) and KH₂PO₄ (973 mg) were dissolved in dH₂O and filled to a capacity of 100 mL for the preparation.

Appendix 16

3.8 (a) 10% Trichloroacetic Acid (TCA)

TCA (10 g) was dissolved in distilled water and used to make a 1000 ml solution.

(b) 5% TCA

TCA (5 g) was dissolved in distilled water and used to make a total of 100 ml.

(c) DPA Reagent

150 mg diphenylamine was dissolved in mixture of 10 mL glacial acetic acid, 150 µL concentrated H₂SO₄ and 50 µl of acetaldehyde solution. 150 mg diphenylamine was dissolved in a solution of 10 mL glacial acetic acid, 150 µL concentrated H₂SO₄, and 50 µL acetaldehyde